AROMATIC CARBOXAMIDES AS NON-STEROIDAL INHIBITORS OF CYP17 FOR THE TREATMENT OF PROSTATE CANCER

by

Ahmet Köseoğlu

B.S., Chemistry, Boğaziçi University, 2005

M.S., Chemistry, Boğaziçi University, 2007

Submitted to the Institute for Graduate Studies in
Science and Engineering in partial fulfillment of
the requirements for the degree of
Doctor of Philosophy

Graduate Program in Chemistry

Bogazici University

2015

ACKNOWLEDGEMENTS

I would like to express my gratitude to my supervisor and mentor Assoc. Prof. A. Ersin Acar for his encouragement, guidance, and patience throughout my study. I am grateful to him for giving me the opportunity to do cancer research in his lab where one can employ their research ideas freely and independently. I am also thankful to him for his endless support over these years, not exclusively in the field of research.

I would like to thank Prof. İlknur Doğan, Prof. Selim Küsefoğlu, Prof. İ. Halil Kavaklı, and Assist. Prof. Fırat İlker for reviewing my thesis and Prof. Gürkan Hızal for his support during my study.

I am grateful to Assoc. Prof. İ. Halil Kavaklı and Prof. Metin Turkay for providing us with this project. I would also like to thank their group members for doing biological tests and performing computational runs.

I would like to thank Turan Gul for his friendship, hood partnership and inspiring energy and optimism while doing research. Collaborating with him accelerated my work and helped me delve into research.

I would like to thank Sezgin, Selda, Tuba, Ayşenur, Duygu, Halenur, Kamil, Aylin, Sedef, Vildan, Deniz, Şeyma, Christoph, Merve, Tuğçe, İbrahim and all other people who helped me a lot for synthesis and made it possible for me to move my research forward. I would also like to thank Myrat, Turgay, Seda, Elif, Nergiz, Aydın, Şükrü, Özgün, Cem, Gökçe, Nurdan, İlknur, Erhan, Nariye, Engin, and Kanykey for their friendship and support.

I would like to express my missing, a great friend and a great chemist, Ali Hikmet Karayel, who suddenly passed away. He was very supportive and helpful to everyone.

I am grateful to all members of the chemistry department, my teachers who taught me chemistry, my dear friends and coworkers with whom I always enjoyed working with, and administrative and technical staff for their help and support.

Finally, I would like to thank my parents Kıymet and Erdan, my sister Emine and my brother Şevket for their love and support.

This research has been funded by Bogazici University Research Funds (BAP, Project No: 5085) and The Scientific and Technological Research Council of Turkey (TÜBİTAK, Project No: 109T431).

ABSTRACT

ALKYL SUBSTITUTED AROMATIC CARBOXAMIDES AS NON-STEROIDAL INHIBITORS OF CYP17 FOR THE TREATMENT OF PROSTATE CANCER

Cancer is the most common neoplasm of the prostate in developed countries. Since up to 80 % of Prostate Cancer (PCa) proliferation depends on androgens, most patients take hormone therapy as first choice of treatment. The PCa cell proliferation occurs due to binding of these androgens to androgen receptor (AR) that is overexpressed on PCa cells. Therefore, when the androgens are segregated from the tumor cells, the proliferation of PCa cell will stop. Although the androgens are secreted from three different sites, namely the testes, adrenal glands, and PCa cells, androgen production depends on catalysis by one enzyme, CYP17, which is also known as P450-C17. Being a pivotal enzyme in the biosynthetic route to steroidal hormones, CYP17 has a key role in the conversion of progesterone and pregnenolone to androstenedione and dehydroepiandrostenedione (DHEA) respectively, which constitute as the direct precursors of 5α-dihydrotestosterone (DHT) and testosterone (T). Although Abiraterone was launched as a potent steroidal CYP17 inhibitor, it interferes with other steroidogenic enzymes leading to side effects such as hypokalemia, hepatic dysfunction, oedema, and hypertension. Due to the potential side effects of steroidal CYP17 inhibitors resulting from inhibition of other steroid receptors, there is a certain need to develop nonsteroidal inhibitors. In this study, several derivatives of a nonsteroidal lead compound were designed and synthesized in order to optimize its interaction with CYP17 enzyme. Throughout optimization process, bioisosterism was utilized as a rational drug design approach. Quinoline moiety was chosen as center of interest as it was hypothesized that similar to other CYP17 inhibitors, it could bind well to iron of the heme group of CYP17 enzyme. In order to perform a structure-activity relationship (SAR) study, a systematic synthesis of *n*-butyl substituted 8-amnionquinolines was done. A library of final products was built by synthesizing several aromatic carboxamides via coupling aromatic amines with aromatic carboxylic acids.

ÖZET

PROSTAT KANSERİNE KARŞI STEROIDAL OLMAYAN CYP17 İNHİBİTÖRLERİ OLARAK AROMATİK KARBOKSAMİT TÜREVLERİ

Gelişmiş ülkelerde kanser, prostatın en yaygın görülen tümör türüdür. Prostat kanserinin yayılmasının % 80'i androjenlere bağlı olduğundan, çoğu hasta ilk seçenek olarak hormon tedavisini seçmektedir. Prostat kanserinin yayılmasının nedeni androjenlerin prostat kanserli hücrelerde çokça üretilen androjen reseptörüne bağlanmlarıdır. Dolaysıyla, androjenler tümörlü hücrelerden ayrılırsa prostat kanserinin yayılması duracaktır. Androjenlerin erbezleri, adrenal bezleri ve prostat kanser hücreleri olarak üç farklı bölgeden salınmalarına rağmen, androjen üretimi anahtar enzim olan P450-C17 olarak da bilinen CYP17' nin katalizine dayanmaktadır. Steroidal hormonların biyosentezinde merkezi bir öneme sahip olan bir enzim olarak CYP17, pregnenolon ve progesteronun, sırasıyla, DHT ve T öncül maddeleri olan androstendion ve DHEA' ya dönüştürlmesinde anahtar bir rol oynamaktadır. Abirateron potent steroid yapıda bir ilaç olarak çıkarılmasına rağmen steroidojenik diğer enzimlerle çakışarak hipokalemi, hepatik fonksiyon bozukluğu, ödem, ve hipertansiyon gibi yan etkilere yol açmaktadır. Steroid yapıdaki CYP17 inhibitörlerinin diğer steroid reseptörlerini inhibe etmesinden kaynaklanan potansiyel yan etkilerinden dolayı steroidal olmayan inhibitörlerin geliştirilmesine kesin bir ihtiyaç vardır. Bu çalışmada steroidal olmayan bir öncü bileşiğin CYP17 enzimine bağlanmasını optimize etmek için çeşitli türevleri tasarlanmış ve sentezlenmiştir. Optimizasyon süreci boyunca rasyonel ilaç tasarımı yaklaşımı olarak biyoizosterizmden faydalanılmıştır. Odak mekrezi olarak kinolin parçası seçilmiştir ki diğer CYP17 inhibitörlerine benzer şekilde kinolin de enzimin heme grubunun demir atomuna bağlanabileceği hipotez edilmiştir. Bir yap-aktivite ilişkisi (YAİ) çalışması gerçekleştirmek için n-bütil sübstitentli 8-aminokinolinlerin sentezi yapılmıştır. Aromatik aminler ve aromatik asitlerin kenetlenmesi yoluyla çeşitleri karboksamit türevleri sentezlenerek bir son ürün kütüphanesi oluşturulmuştur.

TABLE OF CONTENTS

LIST OF FIGURES

LIST OF TABLES

LIST OF ACRONYMS/ABBREVIATIONS

1D	One Dimensional
2D	Two Dimensional
3D	Three Dimensional
5α-R	5α-Reductase
ACTH	Adrenocortico-Tropic Hormone
ADT	Androgen Deprivation Therapy
AR	Androgen Receptor
ATR	Attenuated Total Reflectance
BCL-2	B-cell Lymphoma 2
BPH	Benign Prostatic Hyperplasia
BtOH	Hydroxybenzotriazole
CAB	Combined Androgen Blockade
COSY	Correlation SpectroscopY
CRH	Corticotropin-Releasing Hormone
CRPC	Castration Resistant Prostate Cancer
CT	X-Ray Computed Tomography
CYP	Cytochrome P-450
CYP11B1	Steroid 11β-Hydroxylase
CYP17	17 alpha-hydroxylase cytochrome P-450 ($P\text{-}450_{17\square}$)
CZ	Central Zone
DCM	Dichloromethane
DHEA	Dehydroepiandrostenedione
DHT	5α-dihydrotestosterone
DMF	N,N-Dimethylformamide
DMSO	Dimethyl Sulfoxide
DNA	Deoxyribonucleic acid
DOC	11-Deoxycorticosterone
EA	Ethyl Acetate
EDC	1-Ethyl-3-(3-dimethylaminopropyl)carbodiimide
ERK5	MAPK7 (Mitogen-Activated Protein Kinase 7)

ESI	Electrospray Ionization
et al.	Et Alii (and Others)
FT-IR	Fourier Transform-Infrared Spectroscopy
GnRH	Gonadotropin-Releasing Hormone
Gn	Gonadotropin
HEK 293T	Human Embryonic Kidney Cell Line
HIFU	High Intensity Focused Ultrasound
HRMS	High Resolution Mass Spectrometry
IC_{50}	Concentration at 50% Inhibition
Ki-67	Antigen KI-67
LDA	Lithium Diisopropylamide
LHRH	Luteinizing Hormone-Releasing Hormone
LNCaP	Lymph Node Carcinoma of the Prostate
MRI	Magnetic Resonance Imaging
NBS	N-Bromosuccinimide
NMR	Nuclear Magnetic Resonance
NOESY	Nuclear Overhauser Enhancement SpectroscopY
OS	Overall Survival
P450-C17	17 alpha-hydroxylase cytochrome (CYP17)
PCa	Prostate Cancer
PET	Positron Emisson Tomography
PSA	Prostate-Specific Antigen
PCI	Protein C Inhibitor
PZ	Peripheral Zone
RT	Room Temperature
SAR	Structure-Activity Relationship
SBDD	Structure Based Drug Design
SCC	Small Cell Carcinoma
T	Testosterone
TC_{50}	Concentration at % Toxicity
TFT	α, α, α-Trifluorotoluene
THF	Tetrahydrofuran
TLC	Thin Layer Chromatography

TMEDA	Tetramethyethylenediamine
TMS	Trimethylsilane
TNM	Tumor/Node/Metastasis
TUMT	Transurethral Microwave Thermotherapy
TUNA	Transurethral Needle Ablation of the Prostate
TURP	Transurethral resection of the prostate
US	Ultrasound Imaging
USA	United States of America

1. INTRODUCTION

1.1. Cancer

Cancer is the general name used for a group of more than 100 diseases in which abnormal cells uncontrollably grow, order and invade other tissues [1]. Normal body cells are needed to keep the body healthy by growing, dividing, and dying in a controlled way. Environmental factors, such as chemicals, viruses, tobacco smoke or too much sunlight damage the genetic material (DNA) of a single human cell, producing mutations that influence normal cell growth and division. In general, when DNA becomes damaged, either the cell undergoes apoptosis or detect the abnormalities and repair the DNA by itself. However, in cancer cells the impaired DNA is not repaired and new cells form unnecessarily by mitosis of the cell nucleus. Accordingly, the damaged DNA in the cell nucleus gets duplicated and the newly produced cells repeatedly carry the same damaged DNA. Damaged DNA can also be inherited, which is responsible for inherited cancers. The bulk of tissue formed by these extra cells is called a growth or a tumor.

Some cancers such as leukemia do not form tumors, however instead, the cancer cells contain the blood and blood-forming organs, and circulate through other tissues where they can grow. Not all tumors are carcinogenic. Cancer cells can spread over other parts of the body through the bloodstream and lymph systems where they start to grow and replace normal tissue. Such spreading mechanism is called *metastasis*. Benign tumors do not metastasize and are very rarely lethal.

Cancers can start in many different parts of the body and are usually named after the organ or type of cell in which they begin. For instance, prostate cancer is the kind of cancer which starts in the prostate. Even though the cancer has spread to another part of the body, it is still named after the place where it started. For example, if it has spread to the bone, it is called metastatic prostate cancer, not bone cancer. This is crucial, since different sorts of cancer can act very differently, e.g., prostate cancer and lung cancer are quite different

diseases. They grow and spread at different rates and react to different treatments. Hence people with cancer need treatment that aims at their particular kind of cancer.

Although cancer is not infectious, its occurrence rate is very high. Almost half of the men and one-third of the women in the USA develop cancer during their lifetimes. The risk of developing cancer can be decreased by making changes in lifestyles, e.g., by quitting smoking, reducing the time under the sun, physical activity, and a better diet [2]. The faster a cancer is diagnosed and treated, the better the chances are for survival.

Prostate cancer has many unique characteristics compared to other common cancer forms. For instance, there is not much information about the risk factors and the causes of prostate cancer. Age, ethnicity and genetic factors increase the risk of prostate cancer, although the effect of diets, exercise, sexual activity, smoking, or overweight have been reported significantly influence prostate cancer appearance [3]. Depletion of androgens is known to protect men from prostate cancer; on the other hand, increase in androgen level does not increase the risk compared to low level of androgens [4].

The treatment of prostate cancer has been troublesome in many cases. Contrary to breast cancer, e.g., genetic markers that could predict the aggressiveness of prostate cancer or bring guidance for the best treatment do not exist. Even though localized prostate cancer can be treated highly efficiently with radiation therapy or prostatectomy, prostate cancer continues to be the second highest cause of deaths in men in Western world. One of the reasons for this is the absence of effective treatment methods for aggressive and metastatic prostate cancer. Prostate cancer is highly sensitive to hormone levels; consequently, hormone ablation therapy is an extremely effective treatment, even for advanced prostate cancer. Unfortunately, hormonal therapy is by no means curative and generally within 24 months metastasized prostate cancer ends up at castration resistant prostate cancer (CRPC) stage [5].

Development of novel and more effective treatment methods can be accomplished if the molecular mechanisms behind prostate cancer initiation, progression, and the formation of resistance to treatments are understood better. Totally new approaches, e.g. immune and gene therapy, may also provide benefits in future.

1.2. Prostate Cancer

Prostate cancer is a disease of old men, with the median age of diagnosis being 71 [6]. The risk of getting prostate cancer during lifetime in the developed countries is 16%, which means that every sixth man will be diagnosed with prostate cancer.

1.2.1. The Prostate

The word prostate comes from the Greek word προστάτης, *prostates*, literally meaning "protector" or "guardian". The prostate is a compound tubuloalveolar exocrine gland that is found in the male reproductive system of the most mammals. It varies significantly among species in terms of anatomy, chemistry, and physiology. The prostate functions in humans as the unit that secretes 30% volume of the semen, which is a slightly alkaline fluid with a white or milky appearance. Secretions of the other contributing glands including the seminal vesicle fluid contribute to the alkalinity of the semen [7].

The size of healthy human prostate is described as a little larger than a walnut. In adult males, the weight of a prostate range between 7 and 16 grams, with a median weight of 11 grams [8]. It covers the urethra below the urinary bladder. It can be felt during physical examination of the rectal. The prostate can be classified in two ways: by lobe or by zone. The lobe classification is more frequently used in anatomy. Zone classification is more appropriate for pathology studies. The prostate has an internal fibromuscular band surrounding it rather than a capsule.

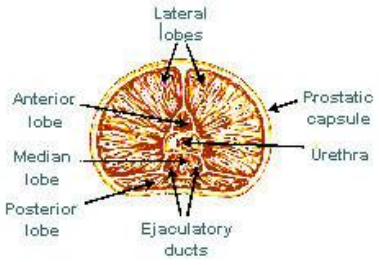

Figure 1.1. The structure of the prostate [9].

The anterior portion of the gland present at the frontal urethra is described by the anterior lobe. The anterior lobe forms part of the transitional zone. The median lobe is cone-shaped part of the gland present in the central zone within the urethra and the two ejaculatory ducts. The lateral lobes are right and left lobes that form the majority of the gland. The prosterior lobe roughly corresponds to peripheral zone. It is sometimes described as postero-medial part of the lateral lobes. During the digital rectal examination, the posterior lobe can be palpated through the rectum.

The prostate gland has four distinct glandular regions, two of which emerge from different parts of the prostatic urethra [10,11]:

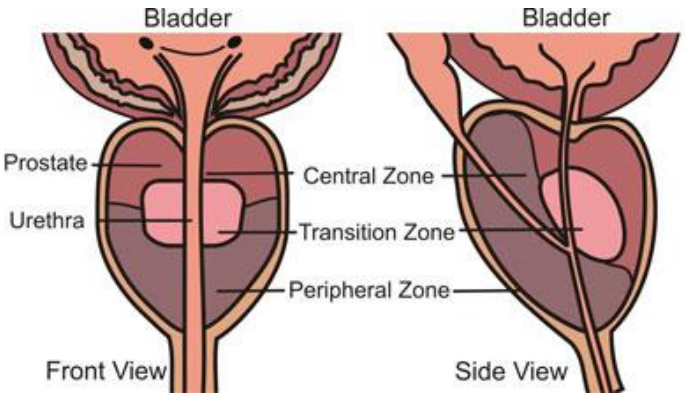

Figure 1.2. The zones of the prostate [12].

The peripheral zone (PZ) constitutes 70 % portion of the gland in young men. It is the sub-capsular portion of the posterior aspect of the prostate gland, surrounding the distal urethra. Around 75 % of prostate cancers originate from this portion of the gland.

The central zone (CZ) normally forms approximately 25 % fraction of the gland. The ejaculatory ducts are surrounded by this zone. Central zone tumors account for more than 2.5 % of the prostate cancers, although these cancers tend to be more aggressive.

The transition zone forms the 5 % fraction of the gland at puberty. It surrounds the proximal urethra. Around 20 % of prostate cancers originate from this region. It is the region of the prostate gland that grows throughout the life and it is the cause of the disease of benign prostatic enlargement.

The anterior fibromuscular zone (or stroma) constitutes approximately 5 % of the gland. This zone is usually composed of only muscle and fibrous tissue lacking glandular components.

The final anatomically discrete part of the prostate gland is the periurethral gland region. It forms less than 1 % of the total glandular prostate volume. It has a ductal network which represents a more proximal extension of the networks of the transition zone and peripheral zone areas.

The transmission of sperm from the ductus deferens into the male urethra occurs via the ejaculatory ducts present in the prostate gland during male ejaculation.

The prostatic secretions differ among species. Their composition is mainly simple sugars and they are slightly acidic. The protein content of the human prostatic secretions is 1% of the total mass and include prostate-specific antigen (PSA), proteolytic enzymes, beta-microseminoprotein, and prostatic acid phosphatase.

Prostate demands male hormones, namely testosterone (T) and dihydrotestosterone (DHT), in order to function regularly. The main male hormone T is produced mainly by the testicles. Adrenal glands also produce some male hormones in small amount. However, it is DHT that regulates the prostate.

1.2.2. Prostatic Disorders

The most frequent prostatic disorders are inflammatory or neoplastic (new tissue development) type: prostatitis, benign prostate hyperplasia (BPH), and prostate cancer (PCa) [1, 13].

Prostatitis is described as inflammation of the prostate and sometimes the area around it. The symptoms of the prostatitis depend on the type of infection. While some people experience symptoms that are similar to the ones in the infection of urinary tract, symptoms are often remain unnoticed. It is very important for the patient to be examined by a medical professional so that the type of prostatitis is determined and the patient is treated accordingly.

In acute prostatitis the symptoms are sudden and severe so that emergency medical care may be required. Acute prostatitis may result in urinary obstruction, and in some cases chills and fever. It is usually caused by bacteria that are found in the urine, usually from E. coli. Both leukocyte and PSA levels are high. Tetracyclines are fluoroquinolone antibiotics are successful in the treatment of the disease.

Chronic bacterial prostatitis has symptoms similar to acute prostatitis except it does not produce fever. Other symptoms include urinary frequency; burning during urination; painful ejaculation; and perineal, testicular, bladder and low back pain. The condition can occur episodically with remissions and flare-ups.

Chronic non-bacterial prostatitis make 95 % of all prostatitis diagnoses. Many different causes include myofascial pain syndrome, autoimmunological failing, and neurogenical inflammation. There are two types of chronic nonbacterial prostatitis: inflammatory and non-inflammatory. The treatment methods for either type include phytotherapy, psychotherapy, alpha blockers, physical therapy, nerve modulators, antihistamines, anxiolytics and more.

BPH is the noncancerous enlargement of prostate in older men, obstructing the urethra so that, urination becomes difficult. 25-40 percent % of men above 50 years old are diagnosed with BPH. Symptoms of the disease are mostly taking some time begin urinating and needing to urinate often. If prostate grows too large, urination becomes difficult and painful, and even impossible in extreme cases.

The treatment of BPH is done with medication or minimally invasive procedure. The prostate is removed by surgery in extreme cases. Transurethral needle ablation of the prostate (TUNA) and transurethral microwave thermotherapy (TUMT) are two of the methods applied as minimally invasive procedure. These procedure can be followed by placement of a temporary prostatic stent to allow voluntary urination without provoking irritative symptoms.

Transurethral resection of the prostate (TURP) is the regularly used surgery in such cases. In TURP, an instrument is placed inside the urethra to get rid of prostate tissue that applies pressure against the upper part of the urethra and hampering the urine flow. Elderly

men often frequently have *corpora amylacea* (amyloid) which is dense accumulation of calcified proteinaceous material in the ducts of the prostate. The amyloid may obstruct the lumens of the prostatic ducts and can underlie some BPH cases.

Urinary frequency resulting from the bladder can sometimes be confused with prostatic hyperplasia. From the statistical data it is suggested that a low fat and low meat diet as well as high in protein and vegetables can protect against BPH.

Life-style changes such as urinating in the sitting position improve the quality of urination. In this way, the amount of urine volume left in the bladder is reduced, the urinary flow rate increases, and voiding time decreases.

Cancer is the most common neoplasm of the prostate in developed countries. Regarding the diagnosis and the treatment of PCa many arguments exist especially in screening and the choice of therapy following the diagnosis. The disease's extraordinary biological heterogeneity presents complex difficulties during management. For example, one person may have an early stage cancer and not affected by the disease for the rest of his life, whereas a younger man may have an advanced stage disease and may die in 5 years. Therefore determining the patient profile remains very important for research. Also, the pathogenesis to PCa is intensely investigated so that new findings may be useful for the better treatment of the disease or even prevention of it [14].

1.2.3. Risk Factors and Prevention

Risk factor can be defined as anything that increase the probability of a person to develop a disease [15]. Different cancer types have different risk factors. Some of the risk factors, such as smoking, can be changed whereas, other such as family history or a person's age cannot. Risk factors doesn't always indicate a disease. Some people with a few risk factors may never get a cancer. On the other hand, others without any apparent risk factor may develop cancer.

The causes of prostate cancer are not completely understood but some risk factors have been found by researchers such as age, geography, race/ethnicity, gene changes, family history, obesity, diet, workplace exposures, smoking...etc.

The chance of having prostate cancer is very low below the age 40 but, it increases rapidly after the age 50. 6 in 10 men with prostate cancer is above the age of 65.

PCa occurrence rate is higher in Caribbean men of African ancestry than in man of other races. It also occurs less often in Asian and Hispanic/Latino men than non-Hispanic whites. There are no clear reasons for these ethnic and racial differences. PCa is also most common in northwestern Europe, North America, Australia and Caribbean islands. Its occurrence rate is lower in Asia, Africa, South America, and Central America. The reasons for geographical variation are not clear. Lifestyle difference such as diet between developed countries and others are likely to be important.

It seems that PCa runs in some families suggesting that there can be genetic factor in some cases. A man's risk of developing PCa gets more than double if he has a brother or father with PCa. If several relatives are affected with the disease, the risk is much higher, particularly their relatives were detected PCa at an early age.

Many inherited gene changes that seem to affect prostate cancer risk have been detected but, they are probably a small fraction of the overall cases. It has been recently found that some of the common gene changes are linked to the increased risk of prostate cancer. More studies need to be done in order to confirm this to see it will be useful to do tests for gene variants for predicting PCa risk.

The effect of diet in risk of developing PCa is not clear, but many factors have been studied. It has been found that the chance of getting PCa slightly increases in men who eat red meat or high-fat products. Also, these men are inclined to eat fewer fruits and vegetables. It is not clear to the doctors which of these factors are the causes of the disease. In some studies it has been suggested that calcium consumption, through food or supplements, may increase the risk of developing PCa.

Since the exact cause of PCa is unknown, it is currently impossible to prevent most cases of the disease. However, considering what is known about the disease so far, the risk of PCa can be lowered [16].

The effect of physical activity, body weight and diet are not quite clear but, there are some things one can do to reduce the risk of PCa such as eating variety of fruits and vegetables every day, being physically active, and preserving a healthy weight.

Some drugs may reduce the risk of PCa. 5-alpha reductase inhibitors Finasteride and Dutasteride are used to treat BPH. The studies so far have shown that it is not clear the benefits of these drugs can outweigh the risks for most men. Some research suggests that taking aspirin for a long period of time can reduce the risk of PCa but more studies are required for better conclusion.

1.2.4. Diagnosis of Prostate Cancer

Biopsy is the only test that can confirm the diagnosis of PCa. Biopsy involves removal of small pieces from the prostate for examination although less invasive tests can be applied prior to biopsy.

1.2.4.1. Prostate Imaging. The two main imaging techniques used to monitor prostate cancer are magnetic resonance imaging (MRI) and ultrasound (US). Transrectal ultrasound is used by urologists during biopsy and sometimes a hypoechoic site which reflect relatively less of the ultrasound directed at them can be seen.

Compared to ultrasound, MRI has better soft tissue resolution [17]. In low risk patients, MRI may help them choose active surveillance. In patients with intermediate risk, it may help determine the disease stage. In patients with high risk it can be helpful finding bone disease [18].

MRI is currently used for identifying prostate biopsy targets making use of MRI with US or MRI alone. In candidates with for active surveillance 33% of cancers were detected

by fusion MRI/US guided prostate biopsy whereas, 7% were detected by standard US guided biopsy [19].

In men who undergo robotic prostatectomy, prostate MRI is used for surgical planning. It has also been helpful to surgeons in deciding whether to resect or spare the neurovascular bundle, assessing the difficulty of surgery, determining return to urinary continence [20].

1.2.4.2. Biopsy. A biopsy is offered when there is a suspicion of cancer. Tissue samples are obtained via the rectum by a urologist or radiologist during a biopsy. Special hollow-core needles are inserted and removed by a biopsy gun in less than a second. Biopsies of prostate are done routinely and on an outpatient basis and usually does not require hospitalization. It was reported that 55% of men were discomfort during biopsy [21].

Then, to determine if there are prostate cancer cells or not, the tissue samples obtained from biopsy are examined under microscope and the microscopic features of any cancer found or Gleason score is evaluated. A trans membrane carboxypeptidase prostate specific membrane antigen exhibits folate hydroxylase activity. In PCa tissues, this protein is over expressed and is related to a high Gleason score [22].

1.2.4.3. Tumor Markers. The presence of PSA and tumor markers can be examined by staining tissue samples in order to determine the metastasized tumor cells [23]. Small cell carcinoma (SCC), a very rare PCa type, cannot be diagnosed using PSA [24]. Although SCC is very rare type of PCa, it is very serious and rapidly spreads to the other parts of the body. Therefore, researchers have been trying to determine the best screening methods for this type of PCa. Protein capturing by making use of immunized antibodies or immunoassays or chromatic separation methods using mass spectrometry are two of the methods for screening SCC. The test method include quantification of the biomarker PCI (Protein C inhibitor) with respect to the Gleason score. This test is both quick and sensitive and can detect diagnostic grey zone patients.

The BCL-2 (B-cell lymphoma 2) oncoprotein has been associated with androgen-independent PCa development because of its high level expression in androgen-independent tumors in the advanced stages of the disease. The connection between PCa progression and

BCL-2 expression was strengthened by the findings that BCL-2 is upregulated after ablation in PCa cell lines and in castrated-male rat model [25].

Ki-67 (Antigen KI-67) expression using immunohistochemistry maybe a significant patient outcome predictor for men with PCa [26].

ERK5, a protein that can be used as a marker, is present in both abnormally high levels of PCa and invasive cancer that has spread to the other parts of the body. It is also found in relapsed cancer following hormone therapy. It has been found that reducing the amount of ERK5 present in cancerous cells reduces their invasiveness.

1.2.4.4. Staging. Determining the stage of PCa is an important part of evaluating how far it has spread. It is useful to know the stage in defining prognosis and selecting therapies. The most common staging system is Tumor/Node/Metastasis (TNM) system, which is a four-stage system. TNM system include tumor size, the number of involved lymph nodes, and presence of any other metastasis [27].

It is very important that any staging system makes a distinction whether or not the disease is still confined to the prostate. In TNM system T1 and T2 types are classified as being confined to the prostate whereas T3 and T4 types as having spread to elsewhere. Several tests can be performed to look for evidence of spread. In case of early PCa with low risk of metastasis, CT (X-Ray Computed Tomography) scans, PET (Positron Emisson Tomography) scans, or bone scans are not recommended by medical specialty professional organizations. It would be more appropriate to apply these tests in cases when spread within pelvis is evaluated by CT scan, a bone scan to look for spread to the bones, and endorectal coin magnetic resonance imaging to evaluate the seminals and the prostatic capsule.

Following prostate biopsy, a pathologist examines the samples under the microscope and reports the grade of the tumor when a cancer is present. The difference between a tumor tissue and normal prostate tissue is reported by the grade, which also suggests how fast the tumor is likely grow.

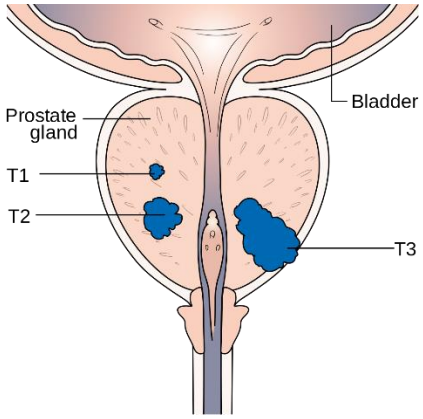

Figure 1.3. Staging of the prostate cancer [28].

The Gleason system grades tumor from 2 to 10, where most abnormalities are indicated by a Gleason score of 10. A number from 1 to 5 is assigned to the most common tumor and the second most common tumor observed under microscope. The Gleason score is the sum of these two numbers.

1.2.5. Management of Prostate Cancer

When managing prostate cancer the first decision is whether a treatment is needed or not. Low grade forms of PCa, especially in elderly men, grows so slowly that no treatment is necessary. Also, in case of person having serious health problems, the treatment will be unnecessary because, he will not have lived long enough for the symptoms of PCa to appear.

The stage of the disease indicated by the Gleason score and the PSA level determines which option is the best. General health, age, and a person's view about the side effects of a potential treatment are other important factors in determining the management option. Most of the treatment methods have significant side effects including urinary incontinence and erectile dysfunction that, center of focus of treatment discussions is a balance on the goals of the treatment with the risks of lifestyle alterations. In order to manage PCa, a combination therapy is often applied [29].

The guidelines for the treatment of a patient requires that the long-term life expectancy is well estimated. An 18-item questionnaire is often used to learn about how well the patient

is aware of the treatment options and their risks. Most of the patients who made a treatment choice or newly diagnosed cannot give a correct answers to more than half of the questions [30].

In the case of radiation therapy was chosen first but fails, the surgery becomes very technically challenging that it may not be advised. However, if radiation therapy is done after surgery fails, many complications may arise as well [31].

1.2.5.1. Surveillance. Active surveillance can be applied to those who were diagnosed with low-risk prostate cancer. The implication of the term is carefully observing the disease over the time and in case of any cancer signs, the treatment will be applied. Active surveillance should not be mixed with the term watchful waiting, an older term which does not imply any treatment method assuming that palliative treatment would be applied if a complicated, symptomatic disease develops.

In active surveillance, the tumor is monitored to observe any signs of growth or symptoms. During the monitoring process many PSA tests as well as physical examination of the prostate and many biopsies may be required. The purpose of surveillance is to avoid overtreatment of the patient, which may lead to serious, sometimes permanent side effects. A self-limited or slow growing disease would not cause any problems to the person. This method is not used for those with aggressive cancers, which may cause anxiety for people who think that every cancer is deadly or that they have a life-threatening cancer. PCa will not cause any harm for up to 75% of the patients before they die [32].

1.2.5.2. Aggressive Cancer. The treatment options for the aggressive type of PCa include surgery radiation therapy, high intensity focused ultrasound (HIFU), chemotherapy, cryosurgery, hormonal therapy, or some combination of therapies [33].

Although PSA test has decreased the detection age of the PCa, vast majority of the cases are still being diagnosed after age of 65, with 25% of the cases above 75 years [34]. Many elderly patients are treated with hormonal therapy or watchful waiting rather than radiation therapy or radical prostatectomy, even though using a life expectancy of 10 years

or lower is suggested. This pattern in practice can be related to several factors such as medical co-morbidity and patient preferences regarding the quality of life, as well as PCa specific risk factors such as PSA, Gleason score, and clinical stage.

Since the advances in treatment of other disease such as cardiovascular and pulmonary diseases has increased the life-expectancy, it is now more likely that elderly patients will live long enough to suffer the consequences of PCa. Therefore, the center of interest is now treatment modalities in surgery or radiation in elderly patient population with localized PCa.

When the cancer spreads beyond the prostate, the treatment options vary significantly. Therefore, a variety of nomograms are used to predict the probability of spread. For those patients who cancer remained in the prostate the treatment options offered by doctors include watchful waiting / active surveillance, brachytherapy, external beam radiation therapy, cryosurgery, HIFU, and surgery. If the disease spreads beyond the prostate, hormonal therapy and chemotherapy are used for treatment. Sometimes, in exceptional cases, early stage tumors are treated with hormonal therapy, and radiation therapy is used for advanced tumors. When the initial therapy fails resulting in the progress of cancer, cryotherapy, hormonal therapy, or chemotherapy can be applied.

1.2.5.3. Palliative Care. Palliative care includes treatment of symptoms of serious illnesses such as cancer and aims to improve the quality of life. One of the main goals of palliative care is to control symptoms rather than treating the cancer. In metastatic PCa, the patients have pain which can be treated using bisphosphonates, opioids, and palliative radiation therapy.

When there is spinal cord compression with metastasis to span, the treatment is done with steroids, radiation therapy, or surgery. Palliative care can also address to other symptoms such as fatigue, lymphedema in the penis or the scrotum, delirium, nausea, weight loss, and vomiting [35].

1.3. Hormonal Therapy as a Treatment for Prostate Cancer

Since up to 80 % of PCa proliferation depends on androgens, most patients take hormone therapy as first choice of treatment. So, when the androgens are segregated from the tumor cells, the proliferation of PCa cell will stop [36].

1.3.1. Androgens and Androgen Receptor

Hypothalamic-pituitary-gonadal-adrenal axes are responsible for the regulation of production of androgens. Many important functions of the body such as body temperature, blood pressure, and immune response are modulated by hypothalamus. The hypothalamus secretes several hormones which target pituitary through hypophyseal portal system. Examples to these hormones include gonadotropin-releasing hormone (GnRH, or luteinizing hormone-releasing hormone (LHRH)) and corticotropin-releasing hormone (CRH). The release of the adrenocortico-tropic hormone (ACTH) and gonadotropins is stimulated by CRH and GnRH, respectively. Therefore, after gonadotropin (Gn) and ACTH bind to the corresponding receptors, they prompt androgen production in testes and adrenal glands. The production of androgens is testes and adrenals are catalyzed by 17α-hydroxylase-17,20-lyase (CYP17) as well as other steroidogenic enzymes [36].

It is estimated that 90% of androgen production are from the testes and less than 10% from the adrenal glands. Furthermore, testosterone is generated *in situ* in testes and can be converted into DHT, which is the strongest androgen, by 5α-reductase (5α-R) catalysis, whereas adrenals produce only testosterone. Most of the circulation of testosterone is done by binding to albumin and globulin, while free unbound hormone is only 2%. When there is sufficient testosterone in plasma, production of GnRH and CRH are down regulated by a negative feedback mechanism. Since 5α-R is present also in the prostate, DHT can be produced from testosterone in this gland, too. Moreover, one of the major reasons PCa cells become castration-resistant is the *de novo* biosynthesis of androgens from adrenal steroids or even cholesterol [37].

The PCa cell proliferation occurs due to subsequent binding of these androgens to AR that is overexpressed on PCa cells. The AR belongs to the steroid and nuclear receptor

superfamily and its structure and function resemble to other steroid receptors such as mineralocorticoid receptors, estrogen receptors, and progesterone receptors. In the cytoplasm, AR receptor floats and acts as an intercellular transcription factor. Heat shock proteins are associated with unbound ARs. When androgens bind to AR, a series of sequential changes in conformation occur, disassociation, formation of dimers, and phosphorylation. Phosphorylation or dephosphorylation of ARs are essential events for agonism or antagonism [38]. The, subsequent translocation of these ARs into the nucleus is followed by binding to the androgen response element that is present in the promoter region of the target gene. When other transcriptional coregulators get involved, they stimulate the transcriptional machinery, initiating AR-regulated gene expression and resulting in the mitogenic effects in PCa cells. Involvement of different coregulators, such as coactivator or corepressor, has been shown to be a different type of switch for agonistic or antagonistic activity [39]. Apart from genomic effects, it has been shown that ARs also interact with cytosolic proteins of various different pathways in the prostate, resulting in the activation of kinase signaling cascades and changes in the calcium levels between the cells and therefore proliferation of PCa cells [40].

1.3.2. Targets for Androgen Stimulation

There are two approaches to prevent PCa cells benefit from androgen stimulation, using AR antagonists to block the AR and interrupting the biosynthesis of androgens, which is called androgen deprivation therapy (ADT). Although for the letter there are several nodes in the androgens secretion system, only some of them are useful targets. It is feasible to interrupt androgens secretion through interference with the hypothalamus-pituitary-testes axis. Androgen production from the testes can directly be cut by castration whereas, same effect can be observed by the application of GnRH analogs, by decreasing the secretion of Gn through either GnRH agonists or GnRH antagonists. However, it is necessary to leave the hypothalamus-pituitary-testes axis alone, since biosynthesis of mineralocorticoids and glucocorticoids are also controlled by ACTH. It is important to not to interfere with the production and the function of ACTH or CTH, otherwise, it would lead to severe side effects. Moreover, enzymes in the androgen biosynthesis pathway are important promising targets. The pivotal enzyme CYP17 is a key enzyme for the conversion of progestogens to androgens. The plasma testosterone level can be reduced to less than 1 ng / dL by inhibition

of CYP17 [41]. However, although 5α-R inhibitors are used to reduce intracellular prostatic DHT concentration for the treatment of benign prostatic hyperplasia, they are ineffective in PCa cells, since, as a precursor of DHT, T can also stimulate PCa cell proliferation.

1.3.3. Hormonal Therapy

1.3.3.1. Orchiectomy. It is reasonable to apply orchiectomy (castration) as a treatment method for PCa, since around 90% of the androgen production occurs in testes. Compared to other long-term therapies, it is a simple, inexpensive operation but, it is not everyone's choice due to permanent impotency as a consequence.

1.3.3.2. GnRH Analogues. In application of GnRH analogs, also known as "chemical castration", agonists and antagonists can both suppress Gn secretion therefore, prevent the androgen production in testes. Even though androgen production in testes is annihilated by GnRH analogs such as goserelin, leuprolide, and buserelin, they don't have any effect on adrenals. In spite of the fact that testosterone concentration in plasma is reduced to 50 ng/dL, androgen concentration in the prostate, either from adrenals or *de novo* synthesis in the tumor, is still high enough for proliferation of PCa cells. Side effects such as loss of bone mineral density and testicular atrophy are also observed as a result of application GnRH analogs [42, 43].

1.3.3.3. AR Antagonists. The fact that adrenal androgen production is not blocked by GnRH analogs, they are used in combination with AR antagonists. This current standard therapy is called combined androgen blockade (CAB) and has been shown to be more effective than AR antagonists alone. Compared to nonsteroidal AR antagonists, steroidal ones are less potent and also affect the production of some adrenal steroids. Therefore, nonsteroidal AR antagonists are mainly employed. CAB has been successfully applied to delay the progression of the disease and to improve overall survival.

However, some cases progresses into CRPC, which result from several reasons such as synthesis of androgens inside the tumor and ligand-independent activation of AR. Mixed agonistic and antagonistic activities were observed with early AR antagonists, like bicalutamide. Overexpression of AR and some other transcriptional factors can boost this

partial agonism, therefore resulting in resistance. Moreover, prolonged application of antiandrogens may lead to AR mutations such as W741C and T877A, reducing the capability of AR to recognize antagonists [44, 45] and glucocorticoids as agonists [46].

Thanks to the wonderful performance by the CYP17 inhibitor abiraterone acetate recently, CRPC has been shown to be still hormone dependent [41]. The second-generation AR antagonist enzalutamide (MDV3100), which has been launched in 2012, also confirmed this finding. Enzalutamide has higher AR affinity compared to other AR antagonists. It has no agonism even when there is overexpressed AR and FoxA1. Moreover, in more than half of the patients that are treated with enzalutamide, more than 50% of decrease in serum PSA level has been observed. Especially important is that overall survival (OS) has increased by 4.8 months [47].

1.4. CYP17 as a Target for Treatment of Prostate Cancer

1.4.1. CYP17 in Androgen Biosynthesis

Although the androgens are secreted from three different sites, namely the testes, adrenal glands, and PCa cells, androgen production depends on catalysis by one enzyme, CYP17, which is also known as P450-C17 [48].

Being a pivotal enzyme in the biosynthetic route to steroidal hormones, CYP17 has a key role in the conversion of progesterone and pregnenolone to androstenedione and DHEA respectively, which constitute as the direct precursors of DHT and T (Figure 1.4).

The formation of key intermediates even some backdoor pathways depends on CYP17. Therefore, when CYP17 is inhibited the androgen production is obstructed and the PCa proliferation is prevented. The effect of inhibition of CYP17 on PCa was first shown by the imidazole antifungal agent ketoconazole. The efficiency of CYP17 inhibition was shown by development of abiraterone which reduces the plasma T level to 1 ng / dL [41]. Moreover, it has also been shown that CRPC is still hormone dependent [41].

1.4.2. Abiraterone Acetate

Abiraterone is a steroidal drug that was begun to be developed in 1990s as strong inhibitor of CYP17 [49]. Compared to the natural substrate pregnenolone, abiraterone has an additional double bond and 3-pyridyl substituent which coordinates to the Fe atom of the heme of CYP17 (Figure 1.5).

Abiraterone blocks the active site of the enzyme resulting in a competitive inhibition. In 2011, the prodrug abiraterone acetate (Zytiga®) was launched as a potent and selective CYP17 inhibitor. Abiraterone is effective in inhibiting both activities of CYP17, 17α-hydroxylase and C17-20-lyase with similar IC_{50} values of 4 and 2.9 nM, respectively.

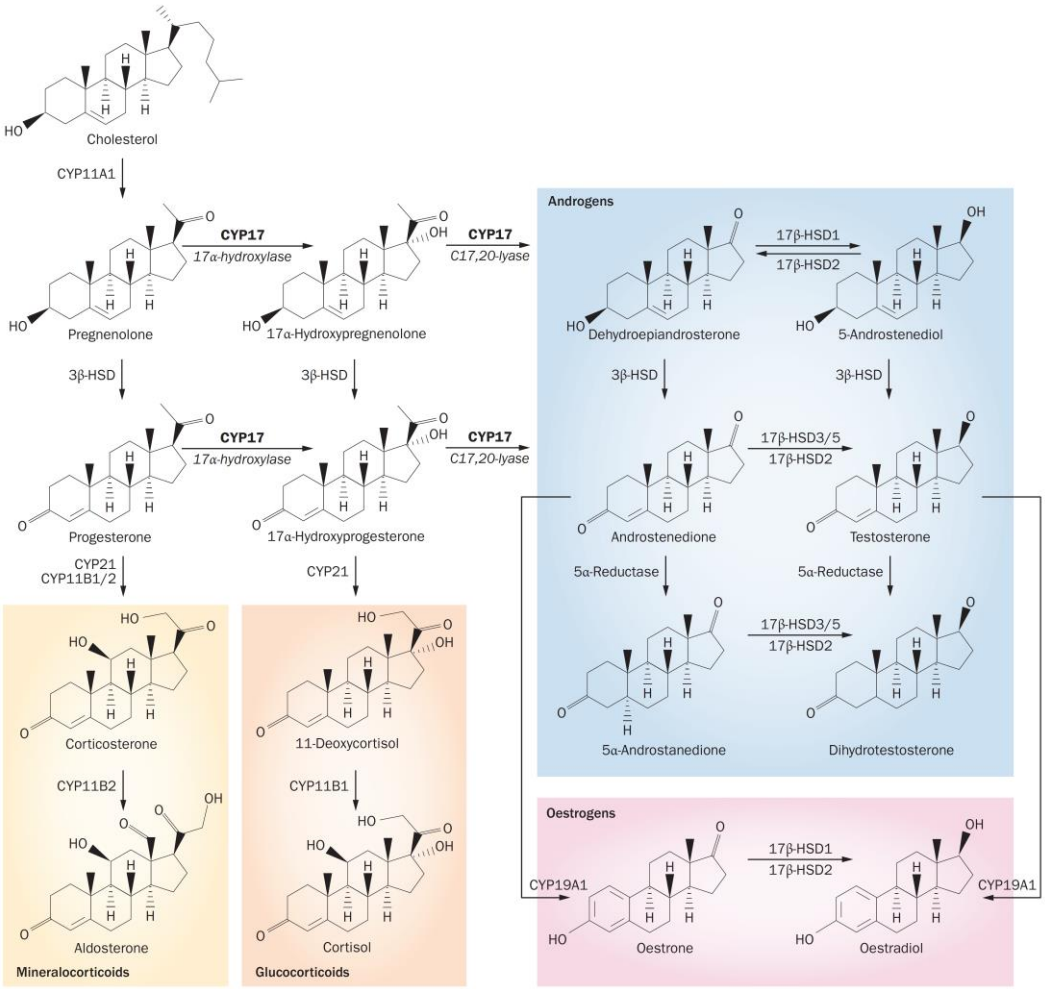

Figure 1.4. The role of CYP17 enzyme in the biosynthesis of steroidal hormones [48].

In LNCaP (lymph node carcinoma of the prostate) cells, abiraterone eliminates up to 80 % of the steady state AR. It also prevents AR mediated transactivation, which can contribute to antitumor effects. After application of abiraterone via the oral drug abiraterone acetate with a dose of 1000 mg per day, abiraterone is released so rapidly and completely that plasma maximum concentration of abiraterone (226 ± 178 ng / mL) is reached in 2h, whereas abiraterone acetate plasma concentration becomes undetectable. However, almost half of the abiraterone acetate is excreted as unchanged via feces, indication a poor gastrointestinal absorption.

It was observed that within 70 % of the patients that don't respond to Ketoconazole and Docetaxel, there is at least 50 % of decrease in PSA level, a major biomarker of CRPC. Moreover, after the treatment with abiraterone, counts of circulating tumor cells is reduced to 5 / 7.5 ml blood in half of the CRPC patients. Other improved symptoms include pathological fracture, pain, fatigue, and spinal cord compression. More important of all, overall survival is improved. In CRPC patients following Docetaxel treatment, abiraterone prolongs the median overall survival to 15.8 months with an improvement of 4.6 months in comparison to placebo.

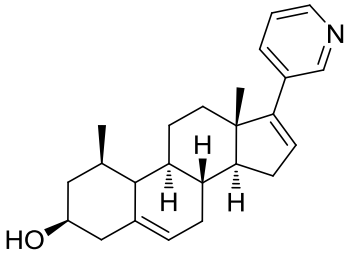

Figure 1.5. The structure of Abiraterone.

1.4.3. Promiscuity of Abiraterone and Its Side Effects

The use of the first CYP17 inhibitor ketoconazole has been discontinued due to the side effects such as adrenal insufficiency and hepatotoxicity, which result from its unselective inhibition of many other steroidogenic and hepatic CYP17 enzymes [48]. Compared to ketoconazole, abiraterone has definitely a better selectivity profiles *in vitro* but, it also interferes with other steroidogenic enzymes. Although abiraterone is well tolerated in

high doses such as 2000 mg per day, large clinical trials have shown that it also shows some severe adverse effects. Although, off target actions of abiraterone can be regarded as a contributor to the side effects, curative outcomes also occur, for example, due to inhibition of 3β-hydroxysteroid dehydrogenase.

Abiraterone inhibits many hepatic CYP enzymes moderately or potently such as CYP1A2, CYP2B6, CYP2C8, CYP2C19, CYP3A4, and CYP3A5 and this can be attributed to the observed hepatotoxicity. Since these enzymes are important for other biological functions and constitute a target for other drugs, careful surveillance and attention should be paid for those taking other drugs.

In patients taking abiraterone, the common symptoms of secondary mineralocorticoid excess include hypokalemia, hepatic dysfunction, oedema, and hypertension even in the case that prednisone is coapplied to suppress ACTH secretion. In a phase I study where abiraterone is the only drug employed, 11-deoxycorticosterone (DOC) plasma concentration increased to 10-fold, whereas downstream corticosterone plasma concentration was elevated 40-fold. These increases are assumed to be the result of promotion of ACTH secretion by 5-fold. However, inhibition of 17α-hydroxylase function of CYP17 might have also caused these increases in steroid levels. CYP17 is the vital enzyme for the biosynthesis of steroidal hormones and determines which hormone is to be synthesized by using its 17α-hydroxylase or C17-20-lyase function. Pregnenolone and progesterone are converted to the corresponding 17α-hydroxypregnenolone and 17α-hydroxyprogesterone respectively by 17α-hydroxylase function. These two progestogens are converted to DHEA and androstenedione by C17-20-lyase function, on the path to the more-potent androgens such as T and DHT. However, androstenedione and DHEA can be converted to 11-deoxycortiol by 3β-hydroxysteroid dehydrogenase and steroid 21-hydroxylase (CYP21) and then ultimately to cortisol by CYP11B1. Therefore, inhibition of C17-20-lyase function of CYP17 can totally block androgen production but, blocking 17α-hydroxylase function can result in the accumulation of pregnenolone and progesterone, leading to overproduction of mineralocorticoids.

1.4.4. Other Steroidal Inhibitors of CYP17

The design of steroidal inhibitors of CYP17 are based on the structures of natural substrates pregnenolone and progesterone [50]. In order to increase the interaction with the enzyme active site, the steroid core is modified especially at C17 position.

Galeterone (VN/124-1 or TOK-001) is one such novel antiandrogens that has been under development [51]. It has a special dual mechanism of action: it is an inhibitor of CYP17 and it also antagonizes AR [48].

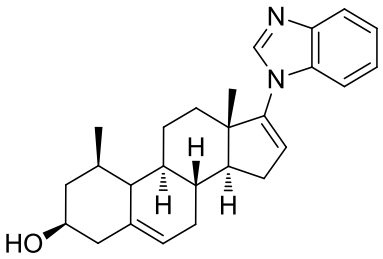

Figure 1.6. The structure of Galeterone.

Galeterone was reported to be 2.7 fold more potent against C17,20-lyase activity than abiraterone but, there is no information about its inhibitory effect against 17α-hydroxylase activity. All in all, galeterone is the only agent reported so far to be both CYP17 inhibitor and AR antagonist, even though some antagonistic effects of abiraterone have also been noted. Considering the similarity between the two agents, it is curious to see whether galeterone will delay or even prevent the resistance to CYP17 inhibition.

Other steroidal competitive inhibitors of CYP17 were designed by chemical modification of natural substrates pregnenolone and progesterone at C17 position [50]. Several groups with moderate to strong dipolar properties, such as hydroxyl and oxime, were introduced at C20 position. It was found that pregnenolone derivatives are more potent than progesterone derivatives, which is not surprising since pregnenolone is the preferred substrate of CYP17.

Introduction of heterocyclic moieties to modify molecules so that they will bind better to the active site of CYP17 enzyme has been a successful strategy in designing new CYP17

inhibitors. Large sets of active compounds have been discovered by modifying the C(17) position of the steroid core with an iron-coordinating heterocyclic group, especially nitrogen heterocycles. Several heterocycles such as pyrimidyl and azole derivatives have been used to obtain several derivatives with interesting properties [50].

Although potent steroidal drugs and drug candidates have been discovered so far, there is still much research to be done in order to discover more potent and more selective agents that will be effective against castration-resistant PCa.

1.4.5. Non-Steroidal Inhibitors of CYP17

Due to the potential side effects of steroidal CYP17 inhibitors resulting from inhibition of other steroid receptors, nonsteroidal inhibitors have attracted attention. Several non-steroidal CYP17 inhibitors have been synthesized so far.

Hartmann and *co*-workers have synthesized several non-steroidal CYP17 inhibitors with different selectivity profiles including dual CYP17/CYP11B2 inhibitors [52] and C17,20-lyase selective inhibitors [53]. The common structural property of these compounds is the presence of a heme-coordinating N-heterocycle which is responsible for effective binding of the compound to the enzyme. The validation of these compounds with *in-vivo* tests will determine if these compounds will be drug candidates.

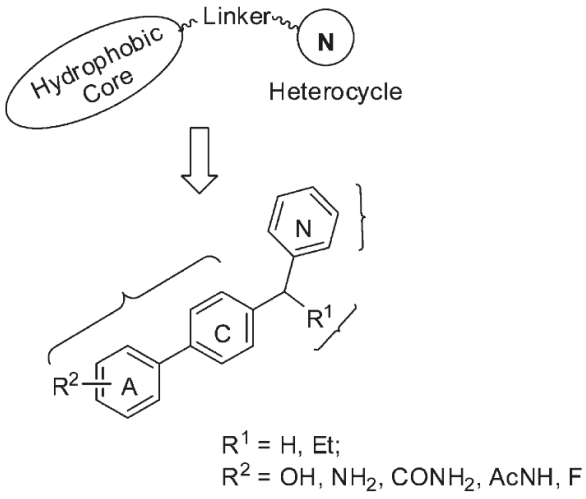

Figure 1.7. Some non-steroidal CYP17 inhibitors by Hartmann *et al.* [52].

Orteronel (TAK-700) is another non-steroidal CYP17 inhibitor which was being developed. It has five-fold selectivity for C17,20-lyase activity compared to 17α-hydroxylase activity with IC_{50} values 140 nm and 760 nm respectively, using an assay with Escherichia coli expressing recombinant CYP17 [48].

Although, Orteronel has superior 17α-hydroxylase/C17,20-lyase and CYP11B1 selectivity profiles compared to abiraterone, an increase in ACTH levels and a decrease in cortisol levels was observed indicating that, it renders less interference compared to abiraterone. However, after two phase III clinical trials orteronel did not show any improvement in overall survival rates which lead to voluntary termination of its development.

VT-464 is another orally available nonsteroidal inhibitor of CYP17 [48, 54]. The compound was found to be selective inhibitor for C17,20-lyase activity with IC_{50} = 69 nM compared to 17α-hydroxylase activity with IC_{50} = 670 nM. Recent preclinical models have shown that VT-464 is potent for prostate tumor models which are resistant to abiraterone or enzalutamide. VT-464 is currently going into phase 1/2 clinical development [55].

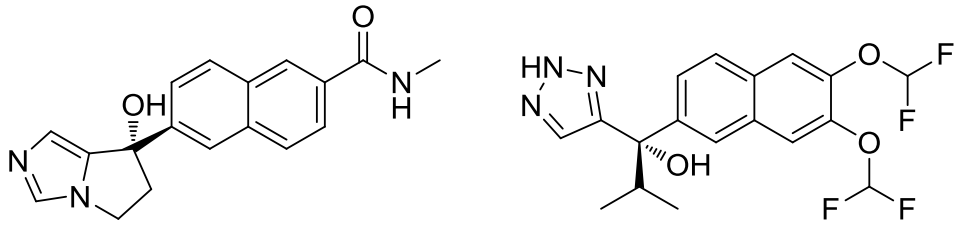

Orteronel VT-464

Figure 1.8. The structures of Orteronel and VT-464.

A lead compound was discovered by Armutlu *et al.* using *in silico* and experimental methods (Figure 1.8) [56]. The lead compound (IC_{50} = 35.65 μM) was shown to have no toxic effects on HeLa Cell line in 24h at IC_{50} concentration and can be used as a lead for discovery of more active nonsteroidal CYP17 inhibitors, which constitutes as the basis of this dissertation project as explained in details in Section 1.5.

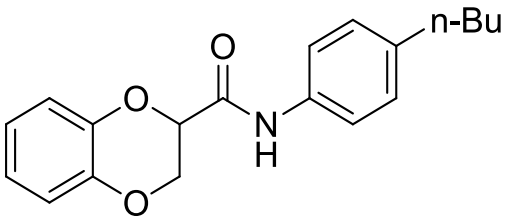

Figure 1.9. The structure of the lead compound.

1.4.6. Structures of CYP17 with Abiraterone, Galeterone, and Substrates

.

Drug development for PCa was hampered since the structural information about CYP17 was lacking. Although homology models of CYP17 was used with considerable success, the lack of the exact structural information was preventing better estimation of potential compounds. In 2012, the X-ray structures of CYP17 with abiraterone and galeterone were published [57].

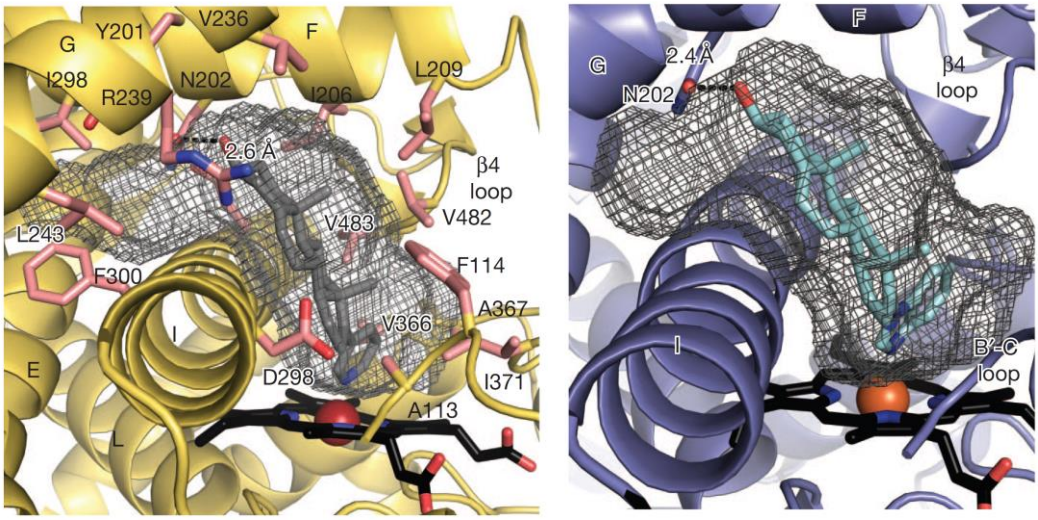

Figure 1.10. The X-ray structures of abiraterone (left) and galeterone (right) with CYP17 [57].

As it was estimated by homology models and spectral binding data, abiraterone and galeterone form coordinate covalent bond with the heme iron, by the nitrogen atoms on their heterocyclic moieties pyridine and benzimidazole, respectively. Their steroidal cores stand on the heme forming a 60º angle and directing between F and G helices. Their α-face leans

onto the hydrophobic pocket over the I-helix forming favorable hydrophobic interactions with G301, A302, and adjacent residues. Especially important is that 3β-OH groups of abiraterone and galeterone form hydrogen bond with N202 in the F helix, with H-bond lengths ~2.6 Å and ~2.4 Å, respectively.

In a follow-up study, the structures of four physiologically-relevant steroid substrates with CYP17 was published [58]. Similar to abiraterone and galeterone, all substrates were found to bind with 60º angle with respect to heme. The hydroxylase substrates pregnenolone and progesterone form hydrogen bond with Asn202, consistent with formation of 17α-hydroxy major metabolites. Also, 17α-hydroxyprogesterone is only observed farther from Fe atom whereas, 17α-hydroxypregnenolone is also observed closer, which might explain the substrate specificity of the following 17,20-lyase reaction. This observation combined with the spectroscopic evidence suggests that it is 17α-hydroxypregnenolone only that approaches and interacts with the proximal oxygen of the iron-peroxy intermediate, thus producing the key intermediate dehydroepiandrosterone for the synthesis of T and estrogen.

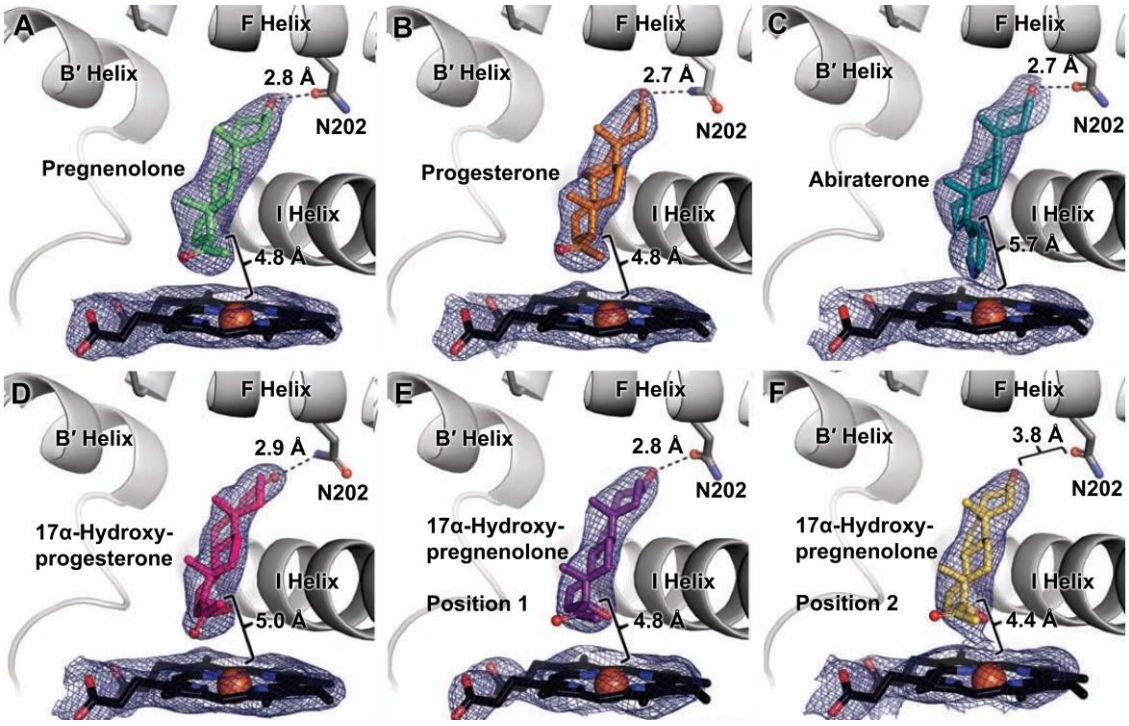

Figure 1.11. The X-ray structures of CYP17 with its natural substrates and abiraterone [58].

The structural information provided by these complexes can be a model for other inhibitors. It is important to provide such structural information to understand key reaction of human steroidogenesis. Therefore, it would be crucial to modify the physiological status in various diseases such as prostate and breast cancer, fertility, sexual development, blood pressure, and immune and stress responses.

1.5. Discovery of the Lead Compound as Inhibitor of CYP17

In search for nonsteroidal CYP17 inhibitors, structure-based drug design (SBDD) approach was successfully applied by using a model CYP17 enzyme [59]. The structure of CYP17 enzyme is similar to structures of other CYP enzymes, having a heme group with an iron atom on it and a hydrophobic region. Although the crystal structure of CYP17 was not known when the project started, a homology model was designed and its structure was improved by molecular dynamics simulations for use in docking studies.

After an initial virtual screening of ~2,000,000 compounds provided by Ambinter SARL, the top 23 compounds with best binding energy and docking energy were subjected to detailed docking analysis and subsequent biological tests [56].

By making use of calcium-phosphate precipitation method, vectors with human CYP17 (pKU-1) were transfected into HEK 293T, human embryonic kidney cell line [60]. The inhibitory effect of the candidate compounds were measure by Acetic Acid Release Assay based on the protocol by Grigoryev *et al.* using a ^{3}H labeled substrate 17α-hydroxypregnenolone [61]. For toxicity tests, HeLa cells were used without transfection and CellTiter-Glo® Luminescent Cell Viability Assay was performed.

The results of the computations and biological tests indicated two compounds, N15 (nonsteroidal) and S3 (steroidal), with IC_{50} values 35.65 μM and 46.30 μM, respectively (Figure 1.12). The docking conformation of the nonsteroidal hit N15 shows that its oxygen and nitrogen atoms are well oriented to the heme iron and the oxygen atom of threonine residue. There is strong hydrophobic interaction between butyl group of N15 and the residues 254 (glycine) and 255 (alanine) of the I-helix that help stabilize the compound in the active site of the enzyme.

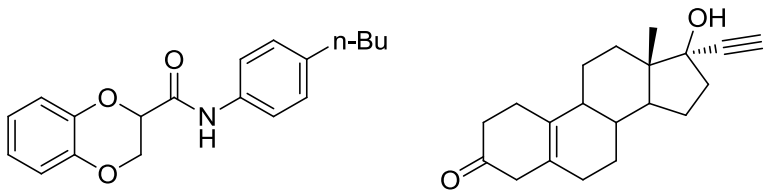

N15 **S3**

Figure 1.12. The structures of the two hit compounds N15 and S3.

The viability scores of N15 were found to be above its IC_{50} value. The TC_{50} values after 12h assay and 24 hour assay were very promising with 271 μM and 397 μM values, respectively. Therefore, N15 was chosen as the lead compound for optimization studies to increase inhibition and reduce toxicity.

1.6. Bioisosterism: A Rational Approach in Drug Design

1.6.1. Historical Background

Bioisoteres can be defined as groups or substituents with similar chemical or physical properties that induce similar biological effect with a lead compound [62-64]. This modification strategy has been successfully applied by pharmaceutical industry not only to discover therapeutically innovative drugs but also to derive commercially attractive *me-too* drugs.

Bioisosterism has its foundations in the concept isosterism, a term introduced by Langmuir in 1919 when studying chemical reactivity to define determined substances having atoms or groups with same number of valance electrons (Figure 1.13) [65, 66].

In 1925, Grimm developed Hydride Displacement Law which states that addition of hydride to an atom that belongs to one of groups 4A, 5A, 6A, 7A on the Periodic Table forms a pseudoatom having similar physical properties with the initial atom in the next column (Table 1.1) [67].

O^{2-} x F^{-} x Ne x Na^{+} x Mg^{2+}

ClO_4^{-} x SO_4^{2-} x PO_4^{3-}

N=N x C=O

CO_2 x NO_2

$N{=}N{=}N$ x $N{=}C{=}O^{-}$

Figure 1.13. Some examples to isosteres.

Erlenmeyer made an expansion of the concept by publishing series of papers in 1930s. Erlenmeyer demonstrated that antibodies didn't discriminate between phenyl and thienyl rings or -O-, -NH-, and -CH_2- present on some series of artificial antigens (Figure 1.14) [63].

Table 1.1. Grimm's Hydride Displacement Law

C	N	O	F	Ne	Na
	CH	NH	OH	FH	-
		CH_2	NH_2	OH_2	FH_2^{+}
			CH_3	NH_3	OH_3^{+}
				CH_4	NH_4^{+}

In 1950, Harris Friedman introduced the term "bioisostere" and made its definition as compounds having the same biological effect and made the distinction that isosteres are not necessarily bioisosteres. This notion implies that bioisosterism depends on the context and relies less on the physicochemical resemblance for biochemical mimicry [63].

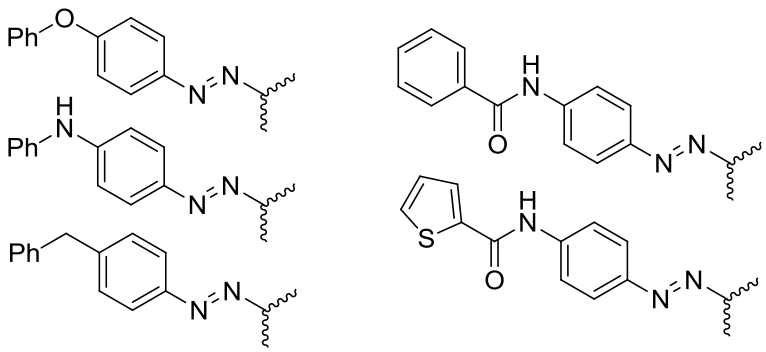

Figure 1.14. The artificial antibodies in Erlenmeyer's work.

1.6.2. Classical and Nonclassical Bioisosteres

Bioisosterism can be classified in two main categories according electronic and steric factors: classical bioisosteres and nonclassical bioisosteres.

Classical bioisosteres are basically the early depiction of the concept and cover plain structures, monovalent, divalent, trivalent atoms or groups, tetravalent atoms, and ring equivalents. Classical isosteres obey steric and electronic definition (Table 1.2).

Table 1.2. Classification of classical isosterism.

Classical Bioisosteres		
Monovalent Bioisosteres	Bivalent Bioisosteres	Trivalent Bioisosteres
D and H	C=C, C=N, C=O, C=S	R_3CH, R_3N
NH and OH	$-CH_2-$, -NH-, -O-, -S-	R_4C, R_4Si, R_4N^+
RSH and ROH	RCOR′, RCONHR′, RCOOR′, RCOSR′	alkene, imine
F, OH, NH_2, CH_3		-CH=CH-, -S-
Cl, Br, SH, and OH		-CH= and –N=C
C and Si		

Nonclassical bioisosteres are more subtle and sophisticated extension of the concept for biochemical mimicry. They are built upon functionality although they might considerably differ in electronic, steric, physicochemical, and topological representation (Table 1.3).

Table 1.3. Classification of nonclassical bioisosterism.

Nonclassical Bioisosteres	
Distinct structures, usually having different number of atoms, different electronic properties and steric effects Divided into two subgroups:	
Cyclic and noncyclic isosteres	Exchangeable functional group isosterism

2. OBJECTIVES

It is crucial to examine each group and individual atom on the lead compound and to predict their specific interactions with the enzyme in order to design more potent derivatives. As a general terminology to be used throughout this work the lead compound and its derivatives can be divided into two parts: right-hand side and left-hand side. The left-hand side of the lead compound is 2,3-dihydro-1,4-dioxine ring and the right-hand side is the phenyl unit which contains an *n*-butyl group on it. In between these two parts lies an amide group that connects them.

The left-hand side can be modified in several ways such as extending the aromaticity, replacing the C atoms with heteroatoms, and/or replacing the O atoms with other atoms. Aromatic rings may interact with the planar heme or with the aromatic side chains of the amino acids *via* π-π stacking interactions. Therefore extending the aromaticity can result in better binding. As it was stated before, N-heterocycles are known to make a good coordination with heme Fe atom. This property can be exploited by introducing nitrogen atoms on the left-hand side. Other heteroatoms such as O and S can also coordinate well with the heme Fe atom. For these purposes, left-hand side will be modified by replacing 2,3-dihydro-1,4-dioxine ring with derivatives of naphthalene, quinoline, isoquinoline, benzofuran, and benzothiophene derivatives. The heteroatoms of these heterocycles may well cooperate with O or N of the neighboring amide group when binding to heme Fe atom so that the compound can act as a bidentate ligand and bind better to it.

The right hand-side phenyl group can also be modified with N-heterocycles. Quinolines not only have extended aromaticity compared to phenyl ring but also bear a nitrogen atom capable of hydrogen bonding with the amino acids. Therefore, it is important not to be contended with modifying only the left-hand side with quinolines but also the right-hand side. Compared to naphthalene analogues, quinolines are easier to modify due to different kind of chemistries that can be applied so that, the butyl group can be introduced easily.

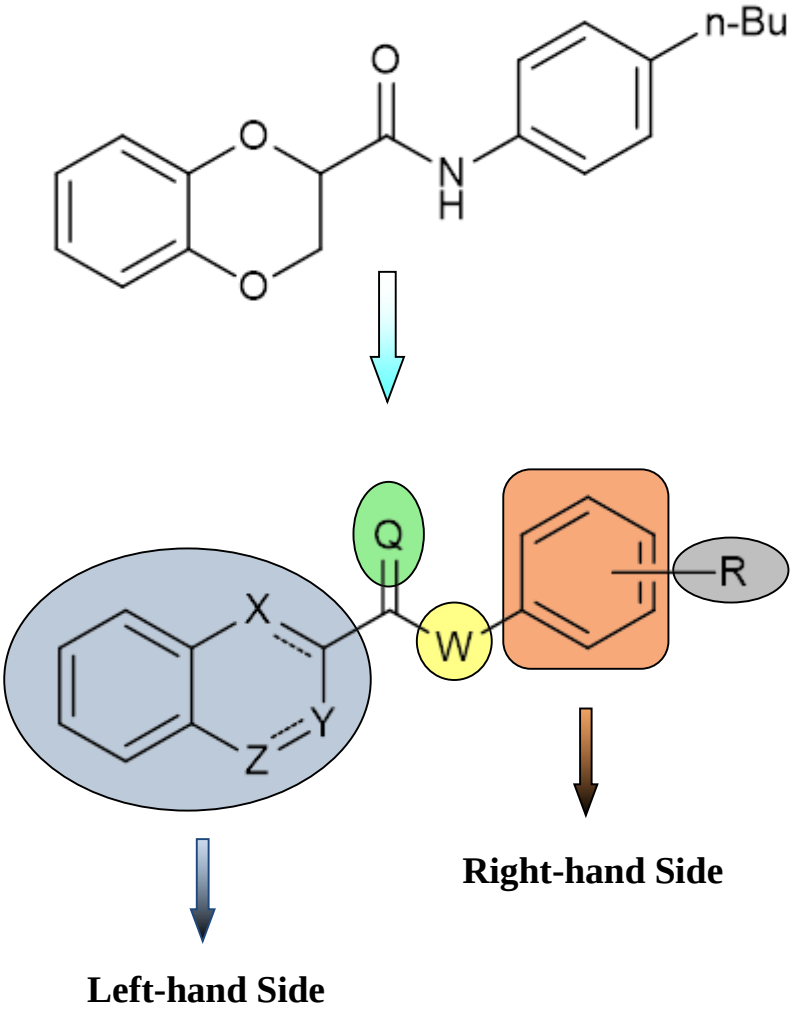

Where, X, Y, and Z : C, N, O

W : NH, O

Q : O, S

R : $C_1 – C_9$ alkyl or branching alkyl

Figure 2.1. Modification of the lead molecule by parts.

It is also possible to either retain or to modify the amide functionality of the lead compound. The amide functionality having a carbonyl oxygen and –NH- group is capable of acting as both H-donor and H-acceptor having a good capacity of making hydrogen bonds. Therefore, it might be good to retain the amide group as it is. However, its O atom can be replaced with S atom which might coordinate well to heme Fe atom. So, Q will be chosen as S and O atoms. It is possible to modify W with O atom but, the resulting functional group

will be an ester group which is known as metabolically unstable. Therefore, W will be retained as –NH- functionality.

Finally, *n*-butyl group attached at the right hand side of the lead compound can be modified to improve potency. Depending on the space requirements and the presence of hydrophobic side chains at the active site, *n*-butyl group can replaced with shorter, longer, or branching alkyl groups. Improved hydrophobic interaction may result in better binding of the ligand to the enzyme and/or better selectivity.

3. RESULTS AND DISCUSSION

In this work, the synthesis of new long chain alkyl substituted aromatic carboxamide derivatives as inhibitors of CYP17 are reported. Several potentially active quinoline derivatives were synthesized. For this purpose, *n*-butyl substituted 8-aminoquinolines were synthesized in a systematic way and subsequently coupled with naphthoic acid derivatives to obtain candidate final products.

The synthesis of all the final products were accomplished by coupling reactions of anilines and aromatic carboxylic acids (Figure 3.1). The first of the three methods applied for coupling reactions is activation of a carboxylic acid with PBr_3 followed by *in situ* addition of Et_3N and the aniline derivative (Method A). The second method used is reacting a carboxylic acid and an amine in the presence of 1-ethyl-3-(3-dimethylaminopropyl)carbodiimide (EDC) and hydroxybenzotriazole (BtOH) using DCM / DMF (dichloromethane / dimethylformamide) as solvent system at room temperature (RT) (Method B). The third and the final method involves the activation of the carboxylic acid by oxalyl chloride in α, α, α-trifluorotoluene (TFT) and catalytic amount of DMF and *in situ* addition of the resulting acid chloride to Et_3N / aniline derivative mixture (Method C).

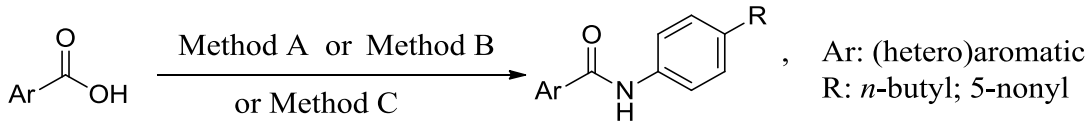

Method A: i) PBr_3, DCM, RT, 3h ii) Et_3N, R-aniline; Method B: BtOH, EDC, R-aniline, DCM / DMF. RT; Method C: i) $(COCl)_2$, TFT, DMF(cat.) ii) Et_3N, R-aniline, DCM, RT.

Figure 3.1. General coupling reaction schemes, reagents, and conditions.

The synthetic transformations were verified by ^{1}H-NMR, 2D-NMR spectroscopy techniques COSY (Correlation Spectroscopy) and NOESY (Nuclear Overhauser Enhancement Spectroscopy), ^{13}C-NMR, FT-IR (Fourier Transform-Infrared Spectroscopy) and HRMS (High Resolution Mass Spectrometry).

The potency was examined against several changes on the lead compound such as, increasing the flexibility by virtually breaking the C-O bonds of the 2,3-dihydro-1,4-dioxine ring, replacing the 2,3-dihydro-1,4-dioxine ring with other (hetero)aromatic rings, and increasing the alkyl chain length. The biological tests were performed by Kavakli Research Group at Koc University.

3.1. Systematic Synthesis of *n*-Butyl Substituted 8-Aminoquinolines

This part of the study is basically the presentation a systematic work on the synthesis of quinolines done in collaboration with Turan Gul and was published in a journal article [79].

The syntheses of 8-amino-3-butylquinoline and 8-amino-4-butylquinoline, nitration of 8-amino-2-butylquinoline, and separation and nitration of 5-butylquinoline and 7-butylquinoline were done by Turan Gul. The literature search, choice of reaction type and the method, design of synthetic schemes, initial trials of the model reactions, and performing the rest of the reactions constitute the content of the present dissertation.

A systematic study on the synthesis of 8-aminoquinoline derivatives with an *n*-butyl group at each alternate position of the quinoline ring was carried out (Figure 3.2). Skraup Reaction and its Doebner - von Miller variation were used to obtain most of the quinoline ring except for the 2- and 4-butyl-8-aminoquinolines where the commercially available methylquinoline derivatives were used as precursors.

As a general approach, Skraup Reaction and its Doebner - von Miller variation were used to obtain the quinoline ring except for the 2- and 4-butyl-8-aminoquinolines where the commercially available methyl quinoline derivatives were used as precursors.

3.1.1. Syntheses of 8-amino-2-butylquinoline and 8-amino-4-butylquinoline

Compounds **4** and **8** were synthesized starting from 2-methylquinoline and 4-methylquinoline respectively (Figures 3.3 and 3.4). When the methyl group is on the

positions 2- and 4- on the quinoline ring, its protons are acidic enough to be abstracted by a strong base and the resulting carbanion is prone to electrophilic attack.

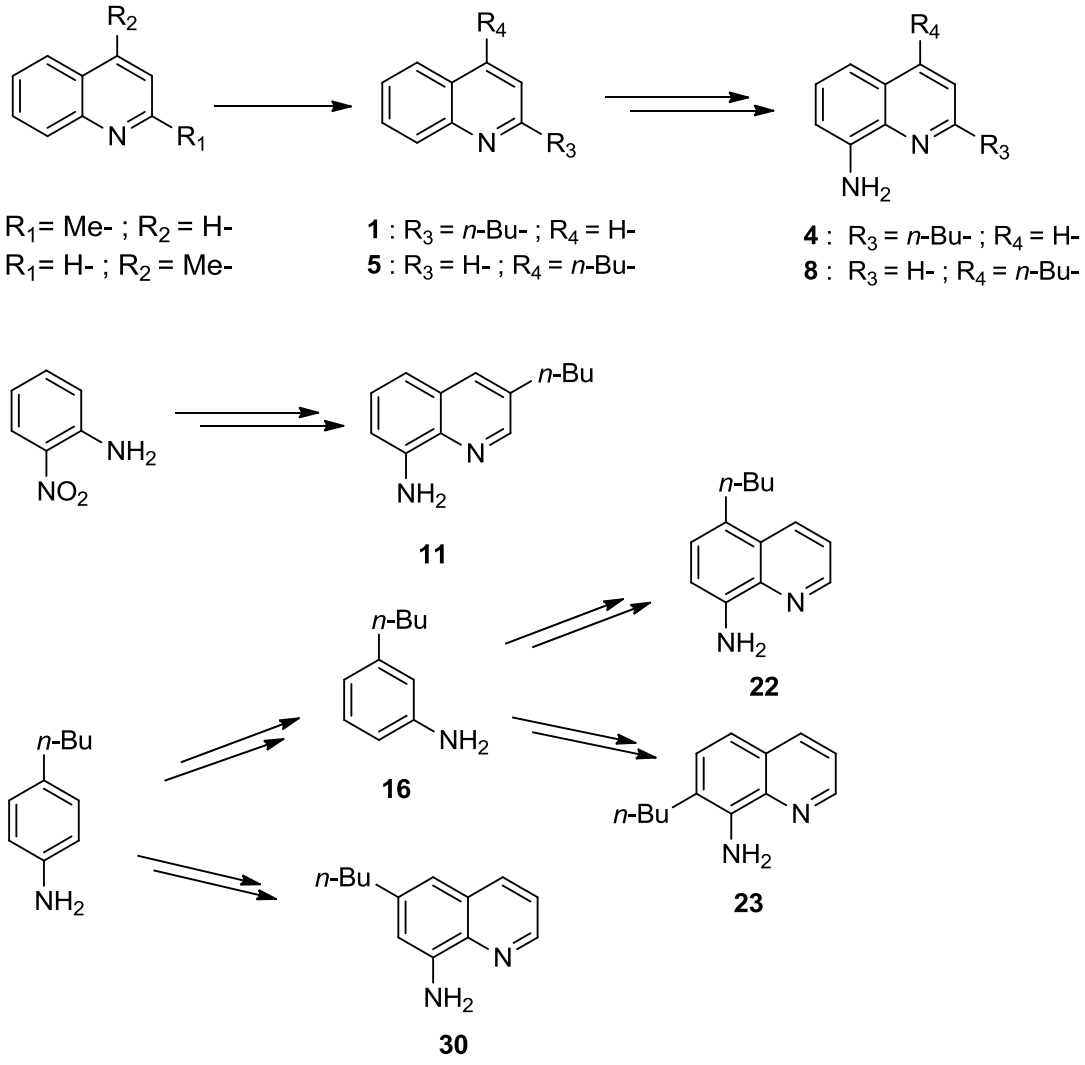

Figure 3.2. *n*-Butyl substituted 8-aminoquinolines and their precursors.

Thus, syntheses of 2-butylquinoline **1** and 4-butylquinoline **5** were accomplished by the chain extension of 2-methylquinoline (quinaldine) and 4-methylquinoline (lepidine) respectively, using LDA and 1-iodopropane. Nitration of **2** and **7** each gave both 8-nitro and 5-nitro isomers. After the separation of the isomers, the subsequent reduction of 2-butyl-8-nitroquinoline **2** and 4-butyl-8-nitroquinoline **6** by $SnCl_2.2H_2O$ / $NaBH_4$ gave **4** and **8**.

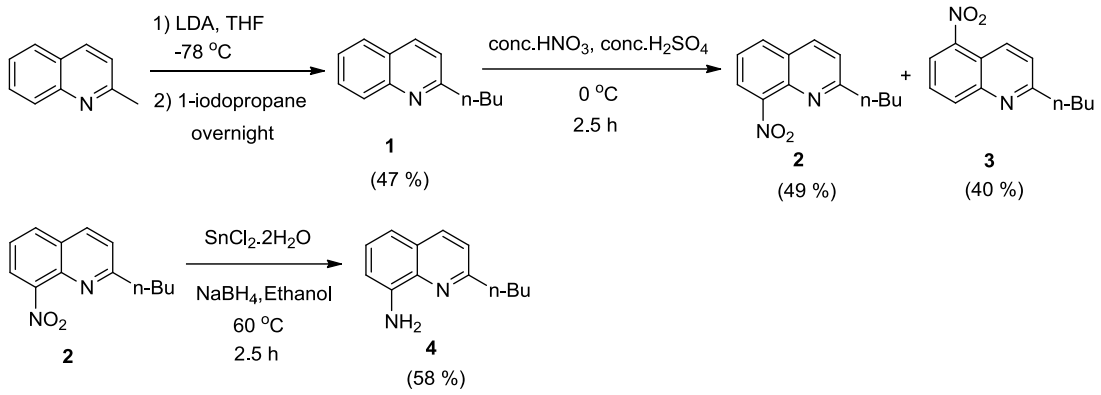

Figure 3.3. Synthesis of 8-amino-2-butylquinoline 4.

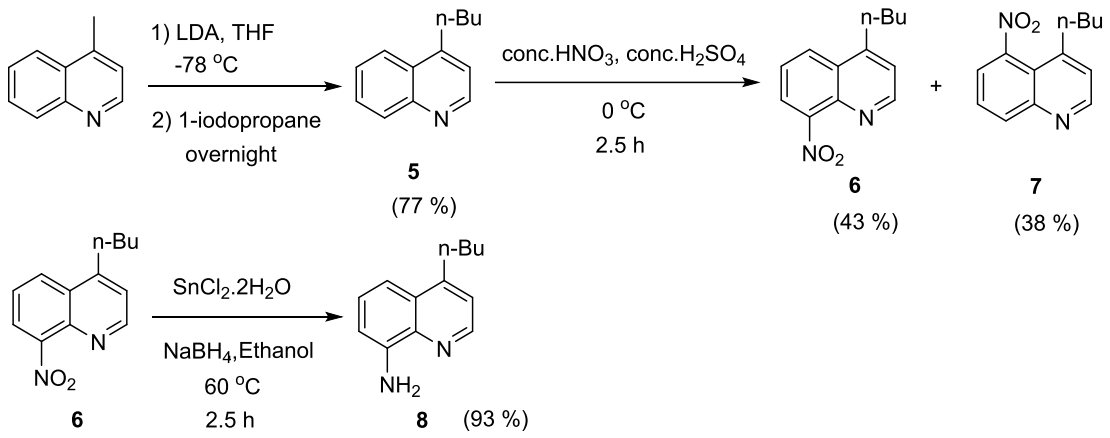

Figure 3.4. Synthesis of 8-amino-4-butylquinoline **8.**

In order to determine the exact positions of the amino groups on compounds **4** and **8** ^{1}H-NMR itself was not sufficient. So, 2D NOESY NMR experiments were carried out. The 3D structure of 5-amino-4-butylquinoline shows that one of the hydrogen atoms of the amino group is very close to the hydrogen atom of CH_2 group (Figure 3.5) [80].

If it was the 5-nitro compound that formed after the nitration, it would have led to 5-amino product and therefore forming this interaction between protons but, no such correlation were spotted in NOESY experiment (Figure 3.6).

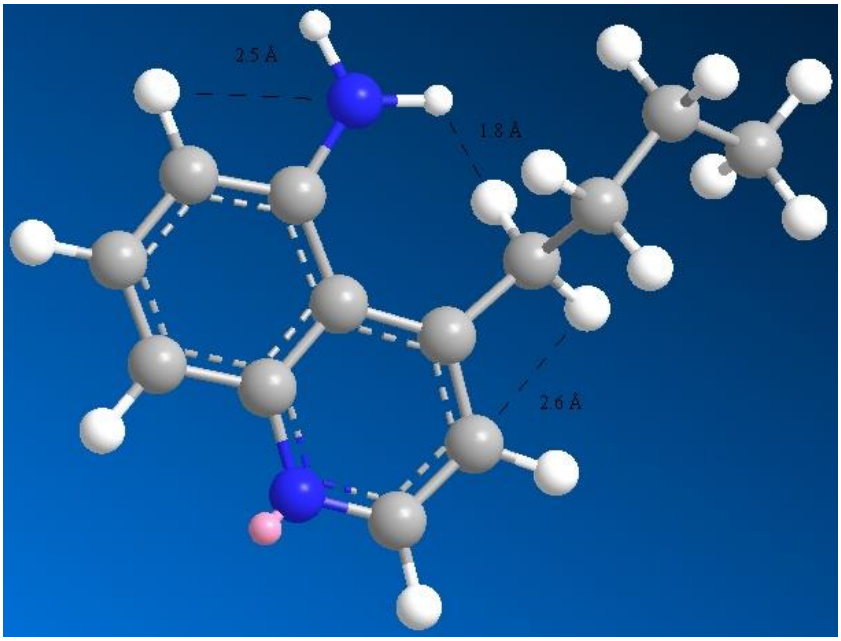

Figure 3.5. 3D structure of 4-butylquinolin-5-amine [80].

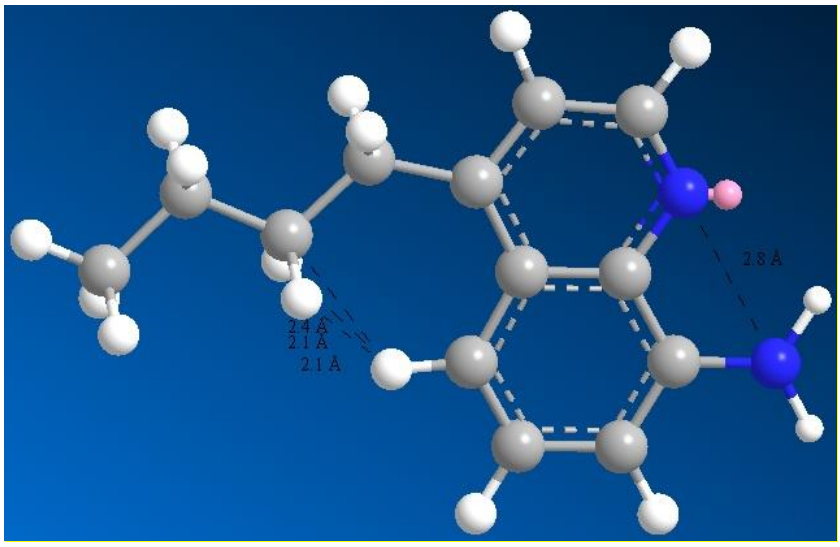

Figure 3.6. 3D structure of 4-butylquinolin-8-amine [80].

However, when the 3D structure of 8-amino-4-butylquinoline is examined it can be seen that one of the hydrogen atoms of the amine group interacts with the hydrogen atom on the C atom at the 6th position and this correlation was verified by the 2D NOESY NMR spectrum (Figure 3.7).

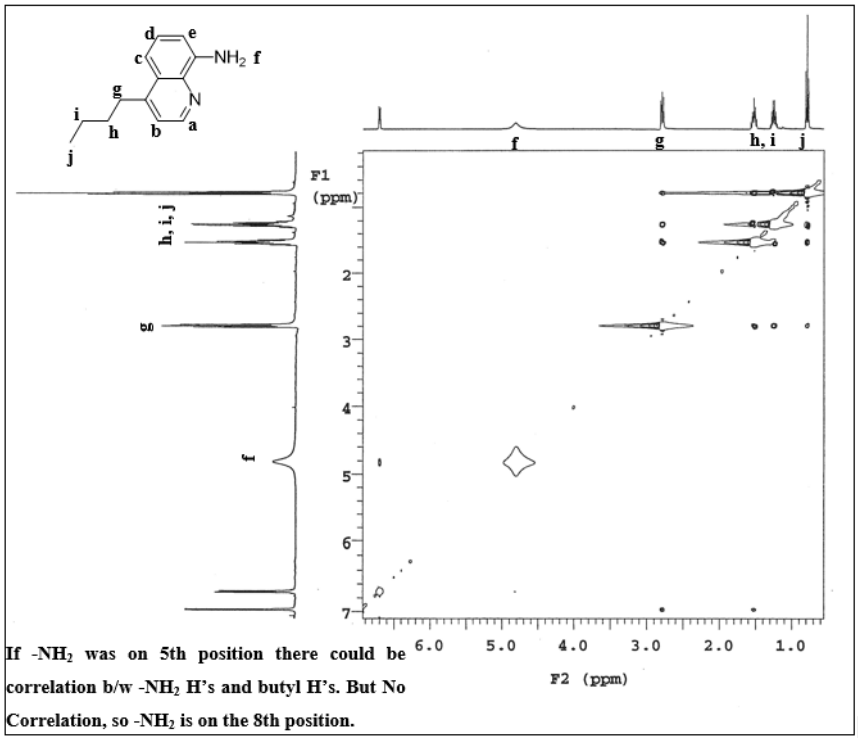

Figure 3.7. 2D NOESY NMR of 4-butylquinolin-8-amine.

3.1.2. Synthesis of 8-amino-3-butylquinoline

Compound 11 was synthesized starting from 2-methylenehexanal and 2-nitroaniline by Doebner – von Miller variation of Skraup Reaction (Figure 3.8). Both of the quinoline substituents, the nitro group and the butyl group, were simultaneously introduced during the ring formation.

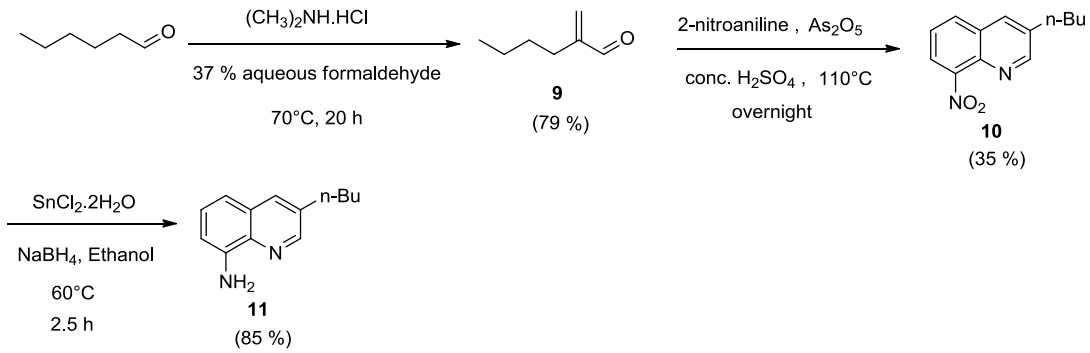

Figure 3.8. Synthesis of 8-amino-3-butylquinoline **11.**

Hexanal was treated with 37% anhydrous formaldehyde and dimethylamine hydrochloride to give 2-methylenehexanal **9**. The next step involved the cyclisation of **9** and 2-nitroaniline to obtain the 3-butyl-8-nitroquinoline **10**, which was then reduced by $SnCl_2/NaBH_4$ to give the desired product **11**.

3.1.3. Syntheses of 8-amino-5-butylquinoline and 8-amino-7-butylquinoline

The syntheses of **22** and **23** started by the cyclization of butyl anilines to corresponding butyl quinolines using the Skraup reaction, where the position of the butyl group on the aniline ring dictated its final position on the 8-aminoquinoline (Figure 3.9). The route to 8-amino-5-butylquinoline **22** and 8-amino-7-butylquinoline **23** begins with the multi-step synthesis of 3-butylaniline **16** from the commercially available 4-butylaniline. 4-Butylaniline was first protected by acetylation. After the standard nitration and the deprotection steps, the amino group of the 4-butyl-2-nitroaniline **14** was removed by forming the corresponding diazonium salt followed by *in situ* deazotization to give 1-butyl-3-nitrobenzene **15**. The reduction of **15** gave **16** which was then cyclised with glycerol using the Skraup reaction to give 7-butylquinoline **18** and 5-butylquinoline **17**. The crude products were subjected to column chromatography, but the products were inseparable. In order to elucidate the structures of **17** and **18**, a small portion of the mixture was separated by thin layer chromatography on silica plates. However, the next reaction was continued with the nitration step where the mixture of the two isomers **17** and **18** was used directly. The nitration reaction gave a mixture of 5-butyl-6-nitroquinoline **19**, 5-butyl-8-nitroquinoline **20**, and 7-butyl-8-nitroquinoline **21** which were successfully separated by column chromatography using silica and hexane/dichloromethane (3/1) mixture as the eluent. The subsequent reductions of **20** and **21** gave 8-amino-5-butylquinoline **22** and 8-amino-7-butylquinoline **23** respectively.

3.1.4. Synthesis of 8-amino-6-butylquinoline

The synthesis of **30** was initially designed as shown in Figure 3.10 where the 6-butylquinoline **24** was synthesized by Skraup method starting from 4-butylaniline. However, the nitration of 6-butylquinoline **24** did not give the desired 8-nitro isomer **30**. Instead, it lead to the exclusive formation of 6-butyl-5-nitroquinoline **25**.

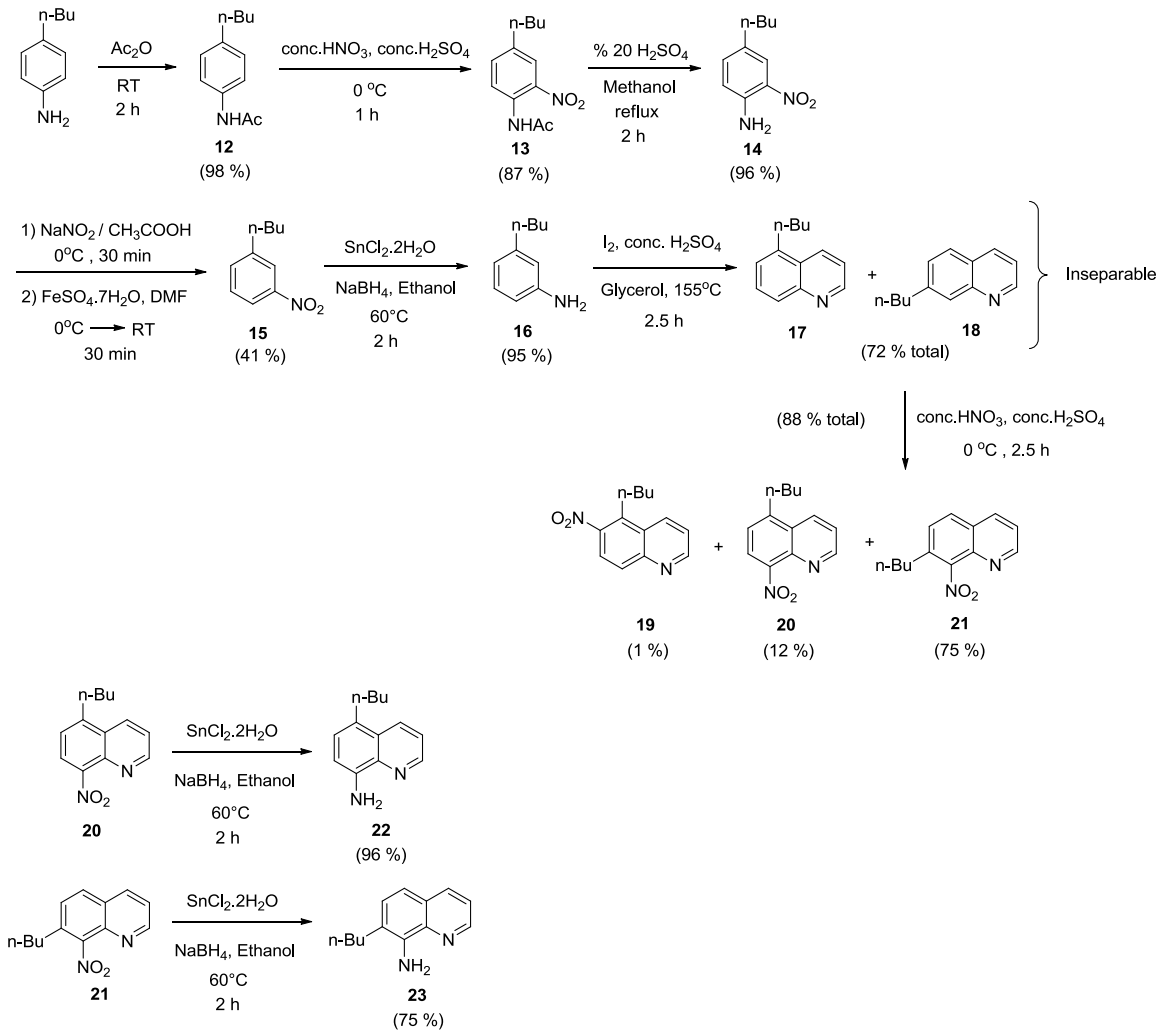

Figure 3.9. Syntheses of 8-amino-5-butylquinoline **22** and 8-amino-7-butylquinoline **23**.

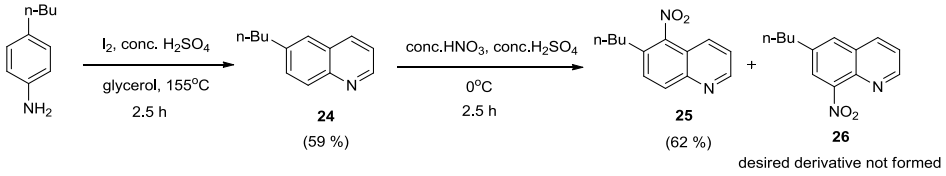

Figure 3.10. The tentative synthetic route to 6-butyl-8-nitroquinoline **26**.

Since the elucidation of the structure of **25** ^{1}H-NMR was insufficient, 2D COSY (Correlation Spectroscopy) NMR was also used. It was shown by 2D COSY NMR spectra that the isolated compound was **25** (Figure 3.11).

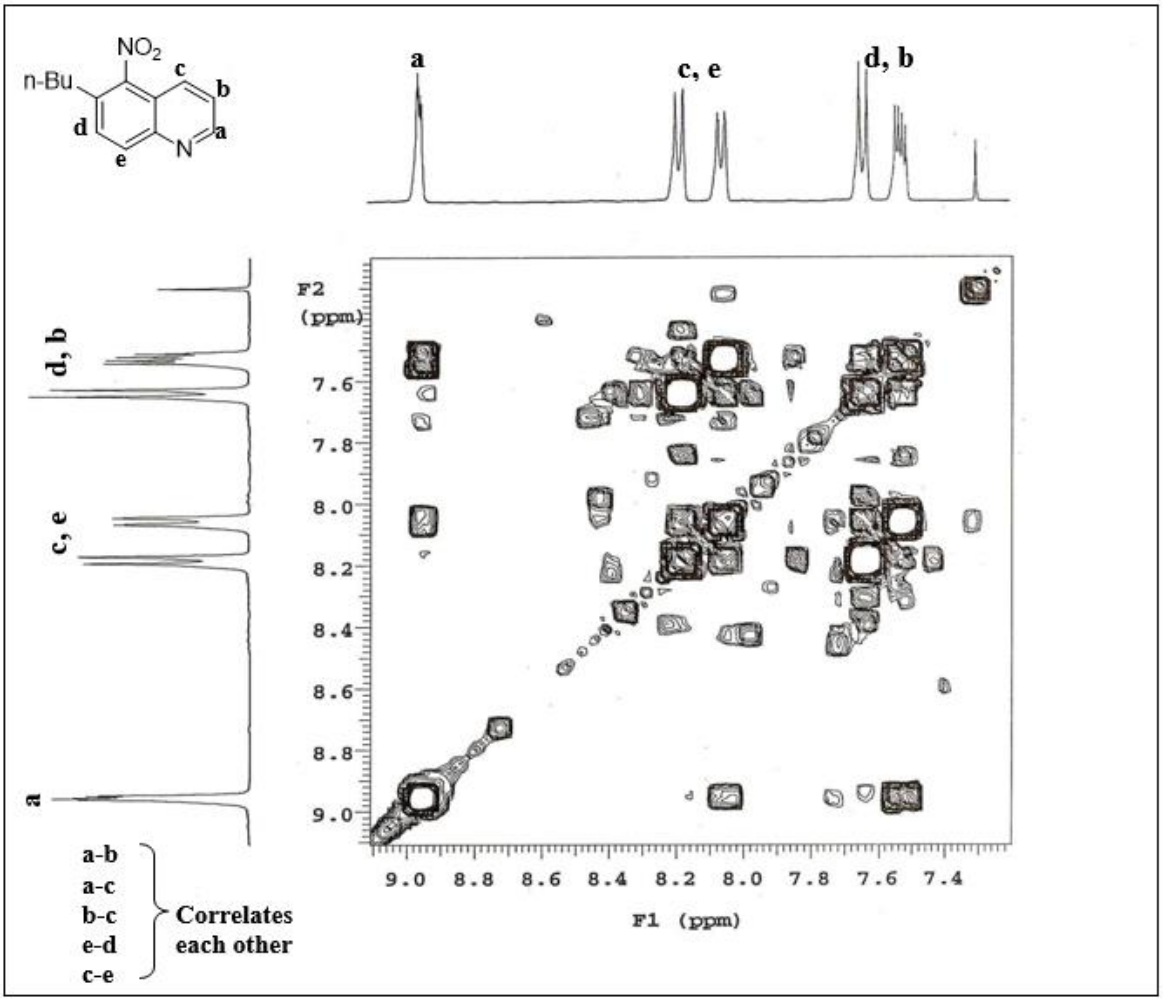

Figure 3.11. 2D COSY NMR spectrum of 6-butyl-5-nitroquinoline.

Therefore, a different strategy was used to produce 8-amino-6-butylquinoline **30** (Figure 3.12) [25]. Since, the 5th position of **24** is the most reactive for the electrophilic aromatic substitution reaction, it was first blocked by bromination with *N*-bromosuccinimide to give a mixture of 5-bromo-6-butylquinoline **27** and 5,8-dibromo-6-butylquinoline **28**.

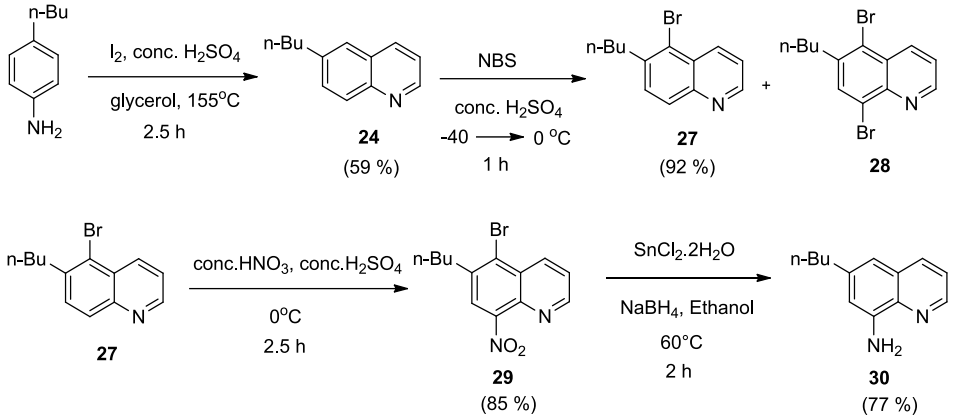

Figure 3.12. The successful synthetic route to 8-amino-6-butylquinoline **30**.

After the necessary separation, the nitration of **27** gave 5-bromo-6-butyl-8-nitroquinoline **29** as the only product. The standard reduction procedure with $SnCl_2.2H_2O/NaBH_4$ to reduce the nitro group to the amino group resulted in simultaneous removal of the bromine substituent to give the final product **30**. The structure of **30** was determined by 2D COSY experiment as shown by the 2D COSY NMR data (Figure 3.13).

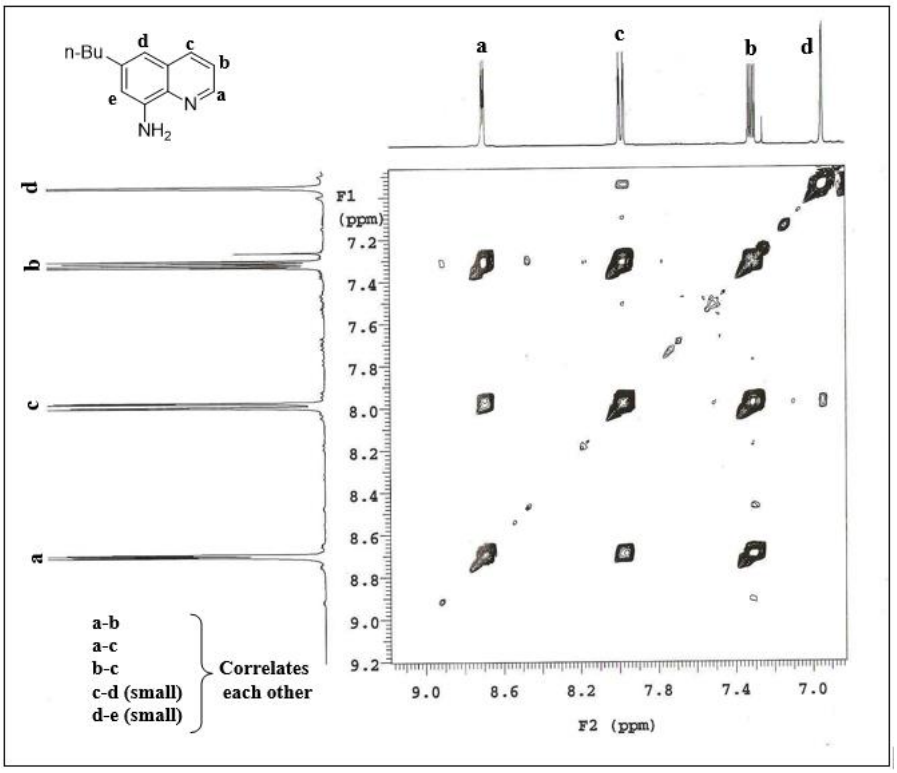

Figure 3.13. 2D COSY NMR of 6-butylquinolin-8-amine.

In summary, we presented the syntheses of 8-aminoquinolines with an *n*-butyl group at all possible positions. The methods employed in this work can be used to introduce a variety of alkyl groups to the core aminoquinoline ring. The systematic syntheses of such compounds might be useful in building libraries of compounds with potential biological activity. In the following steps, these *n*-butyl substituted quinolines were used as precursors to potentially active final products.

3.2. Syntheses of N-(2-butylquinolin-8-yl)-2-naphthamide Derivatives

After *n*-butyl substituted quinolines were synthesized they were coupled with naphthoic acid derivatives to obtain candidate compounds. The coupling reactions of 8-amino-2-butylquinolines are described in this work whereas, the coupling reactions of 8-amino-3-butylquinoline, 8-amino-4-butylquinoline, and 8-amino-6-butylquinoline were described in Turan Gul's thesis [80].

For the coupling reactions of the 8-amino-2-butylquinolines with naphthoic acids, first the naphthoic acid derivatives were activated by reacting with PBr_3 in CH_2Cl_2 in dry conditions at room temperature for 3h to obtain naphthoyl bromide derivatives. Next, Et_3N was added to the reaction mixture followed by addition of 8-amino-2-butylquinoline in CH_2Cl_2 (Figure 3.14).

The reaction mixture was stirred at room temperature for additional 3h. After removal of the solvent *in vacuo*, extraction with water / ethyl acetate, and column chromatography using a suitable eluent the final products were obtained. All the final products were characterized by ^{1}H-NMR and ^{13}C-NMR.

3.3. Syntheses of 2-Benzofuran and 2-Benzothiophene Left-Hand Side Derivatives

We proposed that benzofuran and benzothiophene derivatives can bind even better to the heme Fe atom through their O and S atoms. Therefore, benzofuran and benzothiophene derivatives with different alkyl chain lengths were synthesized using coupling method A and their activities were tested (Table 3.1).

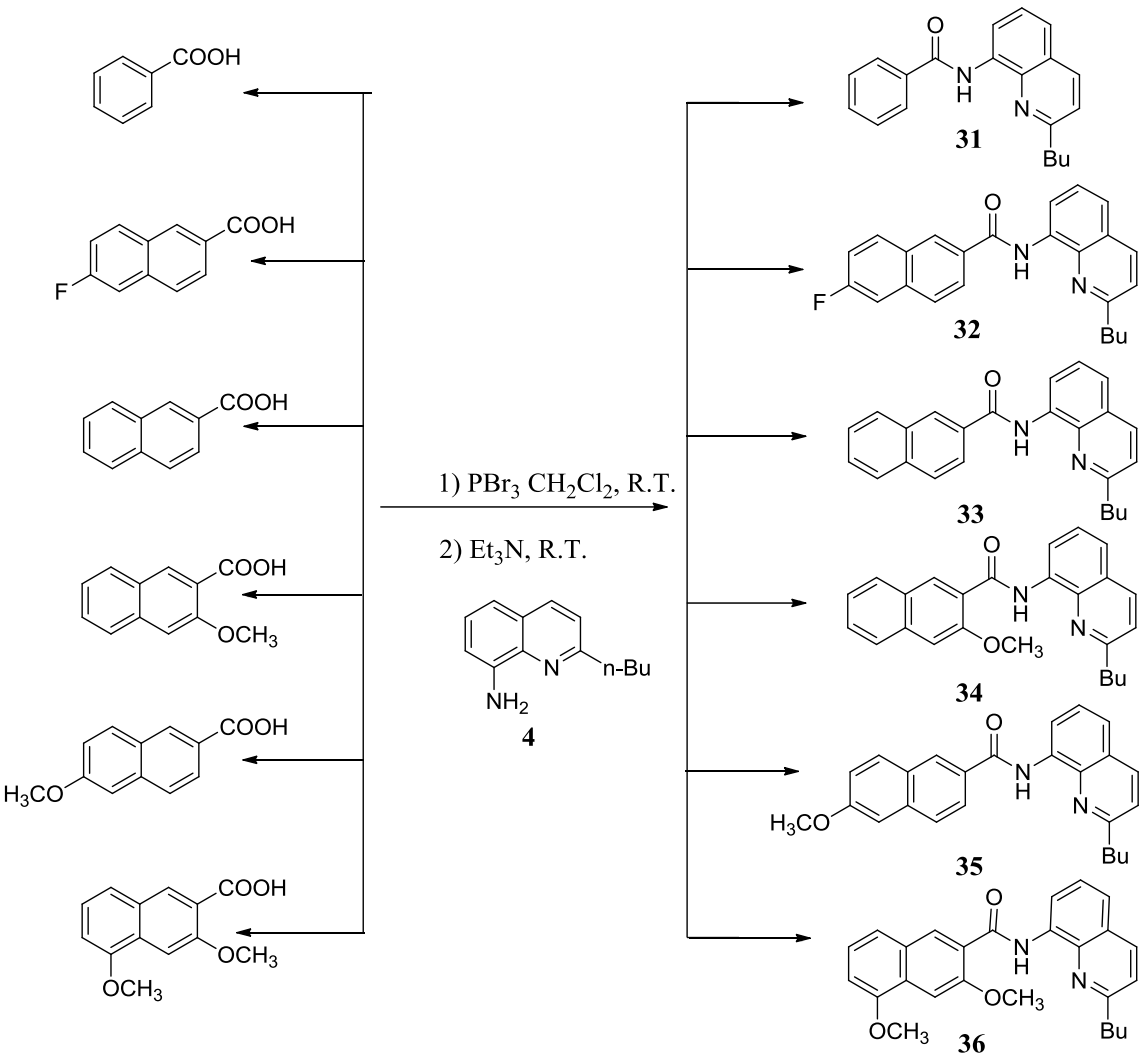

Figure 3.14. The coupling reactions of 8-amino-2-butylquinoline with several naphthoic acid derivatives.

The benzothiophene derivatives are found to be potent with % inhibition values similar to benzofuran derivatives. The benzothiophene derivative **40** was found to have same % inhibition value (56.4 %) with the benzofuran analogue **37**. The IC_{50} values of **40** and **37** were then calculated and **40** was found to be more potent than **37**, with the IC_{50} values 15.4 μM and 25.5 μM, respectively. Increasing the alkyl chain length results in an increase in potency within both groups except *n*-pentyl derivative **38** being less potent than *n*-butyl derivative **37**.

Table 3.1. Benzothiophene and benzofuran derivatives with various alkyl chains.

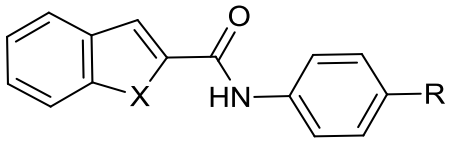

Compound	X	R	% inhibition (5μM)	IC_{50} (μM)	Synthetic method
37	O	*n*-butyl	56.4	25.5	A
38	O	*n*-pentyl	51.2		A
39	O	*n*-heptyl	59.1		C
40	S	*n*-butyl	56.4	15.4	A
41	S	*n*-hexyl	59.6		A

3.4. Synthesis of Derivatives Obtained by Replacing Left-Hand Side with Various Aromatic Groups

Bioisosteric transformations were performed by virtually breaking bonds on the lead compound to modify flexibility, so as to increase the potency (Figure 3.15). The bonds of the 2,3-dihydrobenzodioxine ring of the lead compound were virtually broken to get compounds **42** and **43**.

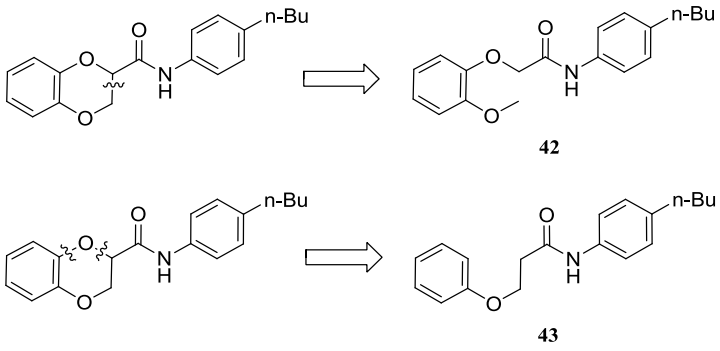

Figure 3.15. Bioisosteric transformations performed on the lead compound.

Other derivatives of the lead compound were designed by replacing 2,3-dihydrobenzodioxine ring with several other aromatic groups including phenyl, naphthyl, biphenyl, quinoline and isoquinoline rings (Table 3.2). The design, the synthesis and the characterization of compound **46** were done by Selda Erkoc and experimental details can be found in her PhD thesis [59].

Table 3.2. Rigid and flexible derivatives of the lead compound.

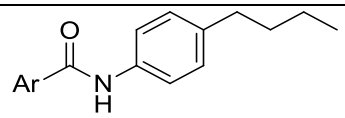

Compound	Ar	% inhibition (5μM)	IC_{50} (μM)	Synthetic method
42	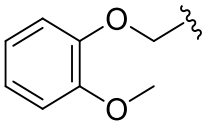	34.7	9.1	C
43	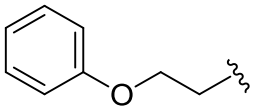	54.2		C
44	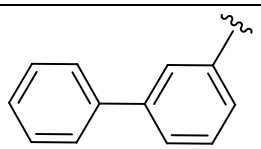	nd		C
45	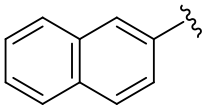	nd		A
46	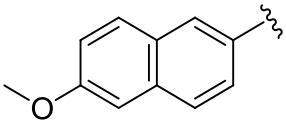	50.2	27.1	DCC/ DMAP coupling
47	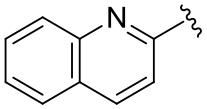	nd		C
48	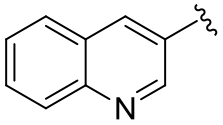	nd		A
49	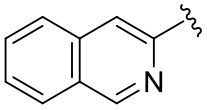	nd		C
50	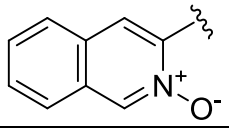	50.6		mcpba DCM RT

After compound **49** was synthesized, some of it was converted to its N-oxide derivative **50** by stirring it with mcpba in dry DCM overnight.

Most of these derivatives were found to be inactive except 6-methoxynaphthyl derivative **46** (% 50.2; IC_{50}: 27.1 μM) and isoquinoline-N-oxide derivative **50** (% inhib. 50.6 at 5 μM).

3.5. Synthesis of (R)- and (S)- Stereoisomers of the Lead Compound

During discovery phase of the lead compound, the library screened consisted of commercially available compounds only. The lead compound was available only in racemate form. Therefore, a racemic mixture was used during biological testing and the IC_{50} value actually belongs to the racemic mixture of the lead compound. In the development phase of the project, we realized the presence of the chiral center and also the need to synthesize (R)- and (S)- enantiomers separately (Figure 3.16).

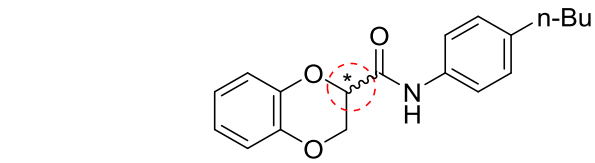

The lead compound : racemate

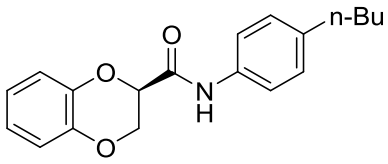

51

(R)- enantiomer

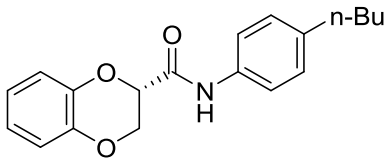

52

(S)- enantiomer

Figure 3.16. The structures of the lead compound racemate, (R)- enantiomer, and (S)- enantiomer.

Although there are examples in literature in which the enantiomers have very close potency, there are also many cases in which one enantiomer was found to be much more

potent than the other (Figure 3.17) [81]. In other cases, one enantiomer made the drug whereas the other was toxic [82].

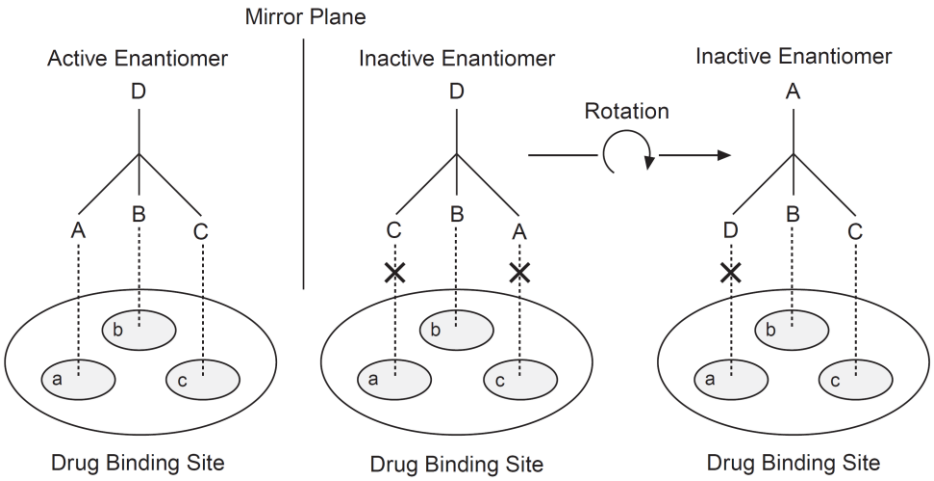

Figure 3.17. The active enantiomer interacts perfectly with the binding site whereas, the inactive enantiomer cannot be aligned in a way to match its all 3 sites [81].

A significant disadvantage of testing two enantiomers together can be that enantiomers may be taking part in a competitive inhibition against each other so that the potency of the more potent enantiomer might have been misinterpreted [83]. The so called IC_{50} value of the lead compound, which is 37.7 μM, actually belongs to the racemate and one of the enantiomers might indeed have a better IC_{50} value.

All in all, (R)- and (S)- enantiomers of the lead compound were synthesized by coupling the corresponding commercially available chiral acids with 4-butylaniline using Method C. Neither of the enantiomers were found to be potent in a preliminary screening done at 2.5 μM. More biological testing needs to be done at higher concentrations since the IC_{50} value of the racemate is 37.7 μM.

3.6. Miscellaneous Derivatives of the Lead Compound

Various other derivatives of the lead compound were designed and synthesized by making bioisosteric replacements. Upon nonclassical bioisosteric replacement on the left

hand side of the lead compound, **45** was obtained (Figure 3.18). Given a seemingly promising result of preliminary biological testing of **45**, it was chosen as our center of interest and a few derivatives of it were synthesized.

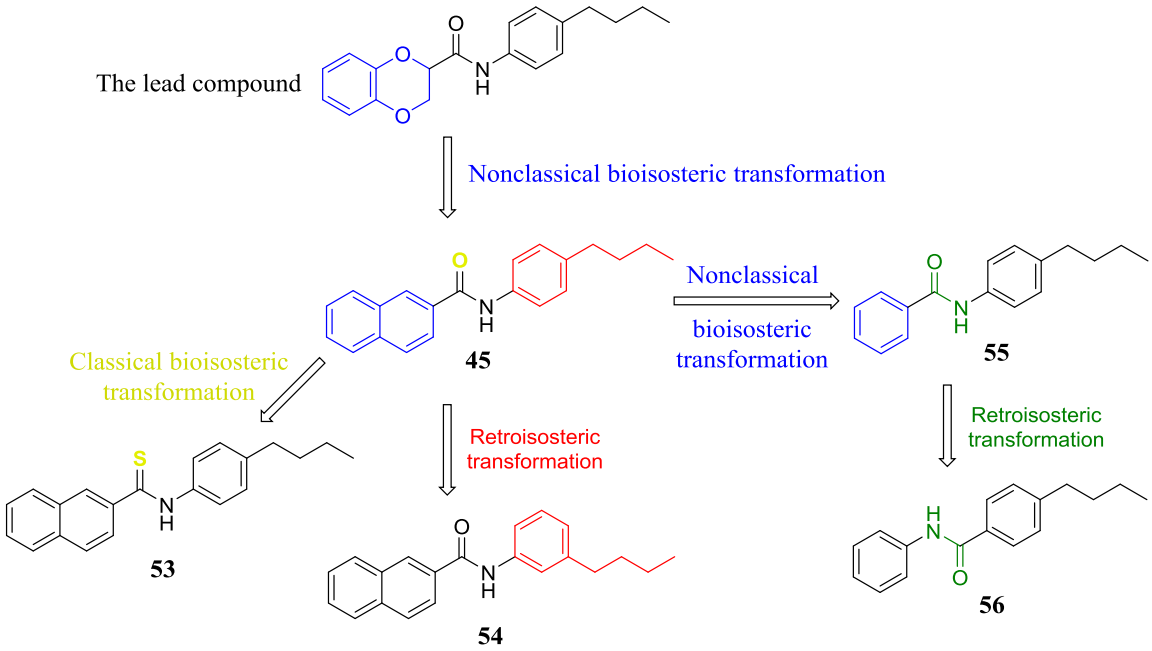

Figure 3.18. Miscellaneous derivatives of the lead compound designed by making bioisosteric replacements.

The oxygen atom of the carbonyl group on **45** was replaced with a classical bioisostere, sulfur atom, since we hypothesized that it could bind to iron atom of the heme group better than oxygen (Figure 3.18). The synthetic transformation of **45** to **53** was done by refluxing it with Lawesson's reagent in toluene under dry conditions (Figure 3.19).

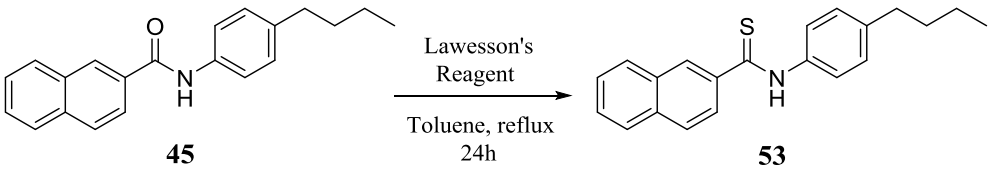

Figure 3.19. Synthesis of **53** via conversion of O to S using Lawesson's reagent.

The position of the butyl group on the phenyl ring at the right hand side of **45** was questioned by synthesizing its constitutional isomer **54** (Figure 3.18). This approach of switching or inversion of the position of a functional group is called *retroisosterism*, which was successfully applied in several cases as reported in literature [84-86]. Although 3-butylaniline was commercially unavailable, we had already synthesized it as an intermediate in the route to 5- and 7- butylquinolines (**16**; Section 3.1.3; Figure 3.9). It was now coupled with 4-butylaniline using Method A to obtain **54** (Figure 3.20).

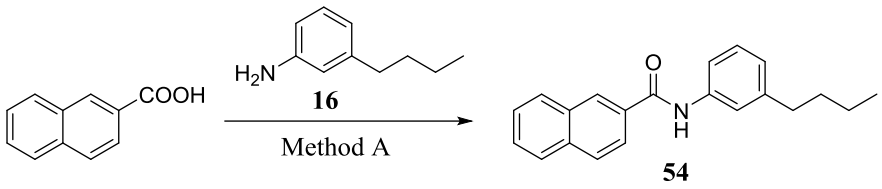

Figure 3.20. Synthesis of **54** from 2-naphthoic acid and **16** by method A.

Another derivative of **45** was designed by a nonclassical bioisosteric replacement of naphthyl group by phenyl group to obtain **55**. Compound **55** was synthesized from benzoic acid and 4-butylaniline by using Method B (Figure 3.21).

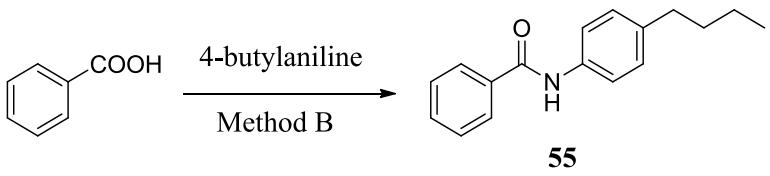

Figure 3.21. Synthesis of **55** from benzoic acid and aniline by method C.

Although naphthyl and phenyl groups are similar in terms of electronics and both capable of making favorable interactions with aromatic amino acid residues via π-stacking, they differ a lot in size which can be important in terms of space requirements in the active site of the enzyme. Being the smaller molecule of the two, molecule **55** can orient itself more easily and bind better in the active site of the enzyme. A derivative of **55** was designed by retroisosteric transformation on the amide functional group to obtain molecule **56**. The synthesis of **56** was done by coupling reaction of benzoic acid and 4-butylaniline using Method A (Figure 3.22).

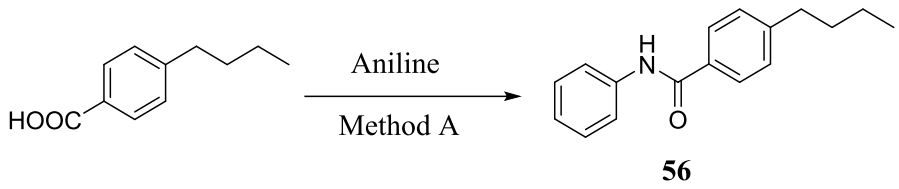

56

Figure 3.22. Synthesis of **56** from 4-butylbenzoic acid and aniline by method A.

The biological screening results of compounds **53-56** and the synthetic method used for the coupling reaction of their precursor carboxylic acids and anilines are summarized on Table 3.3. Upon preliminary screening at 5 μM concentrations, all the derivatives were found to be inactive except **55** which had 23.8 % inhibition.

Table 3.3. Miscellaneous derivatives of the lead compound, biological test results, and synthetic methods.

Compound	Structure	% inhibition (5 μM)	Synthetic method
53	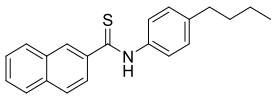	nd	Lawesson's Reagent
54	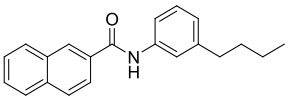	nd	A
55	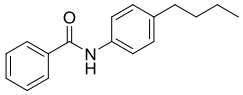	23.8	B
56	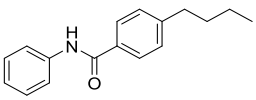	nd	A

3.7. Attempts to Synthesize O(8)-Heterocycle Substituted Derivatives of Compound 42 and N-Heterocycle Substituted Derivatives of Compound 45

Once **42** and **45** were identified as more active derivatives of the lead compound, their variations were the new targets (Figure 3.23). In order to improve the interaction of the lead

molecule derivatives, they would be further derivatized by N-heterocycles which can coordinate to Fe atom of the heme group of the enzyme. Syntheses of aromatic nitrogen-heterocycle derivatives of **42** substituted at O(8) position and aromatic nitrogen-heterocycle derivatives of **45** substituted at amide nitrogen were attempted.

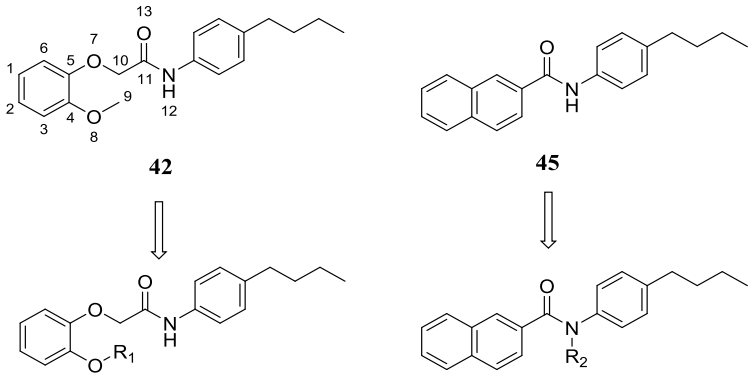

Figure 3.23. The new derivatives that were aimed to be synthesized.

The first group of compounds in interest were heteroaromatic ether derivatives of **42** that were estimated to bind to the heme Fe atom more effectively. The retrosynthetic analysis is shown in Figure 3.24.

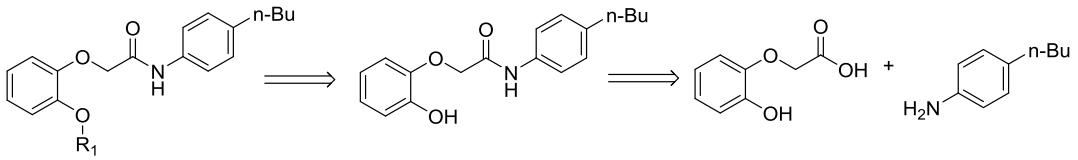

Figure 3.24. The retrosynthetic analysis for heteroaromatic ether derivatives of 42.

The synthesis started with acetyl protection of 2-(2-acetoxyphenoxy)acetic acid (Figure 3.25). Next, the phenoxy protected acid **57** was coupled with 4-butylaniline using Method B. However, the NMR analysis of the final product showed that it did not have the acetyl-group and the sequence resulted in O(8) methyl deprotected derivative of **42**. Regardless, the resulting deprotected product **58** was kept for biological tests.

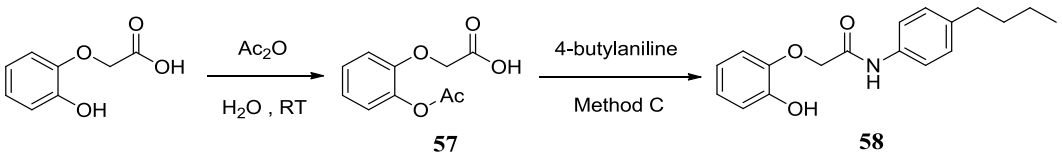

Figure 3.25. Synthesis of O(8) methyl deprotected derivative of **42**.

Therefore a different method was applied for the synthesis of aryl ethers (Figure 3.26). First, the disodium salt of the acid was prepared. However, the subsequent coupling reaction was not successful as the starting material was recovered.

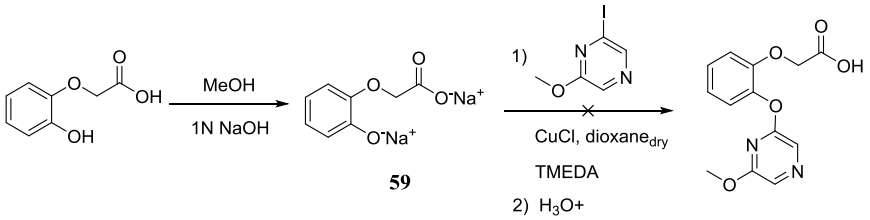

Figure 3.26. The alternative synthetic route to aryl ethers.

A second group of compounds in interest were N- heteroaromatic substituted derivatives of **45** (Figure 3.27). It was estimated that the resulting compounds would bind to Fe atom of the heme of CYP17 enzyme by the heteroatom of their heteroaromatic rings. The coupling reactions of compounds **45** with nitrogen and sulfur containing heteroaryl halides were attempted.

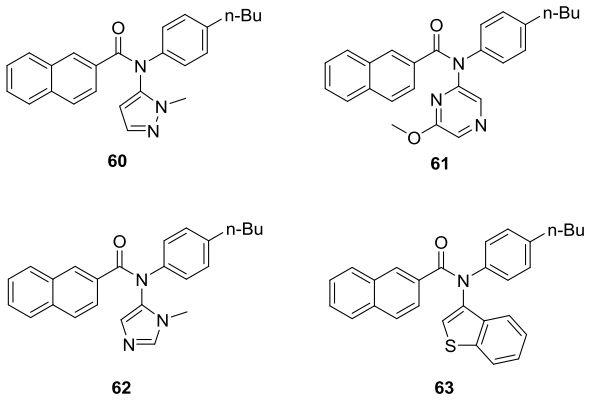

Figure 3.27. Proposed structures of the new candidates with heteroaromatic rings.

The syntheses of candidate drug molecules **60** and **61** were designed according to two different the literature methods [87, 88]. However, none of the reactions were successful. (Figure 3.28).

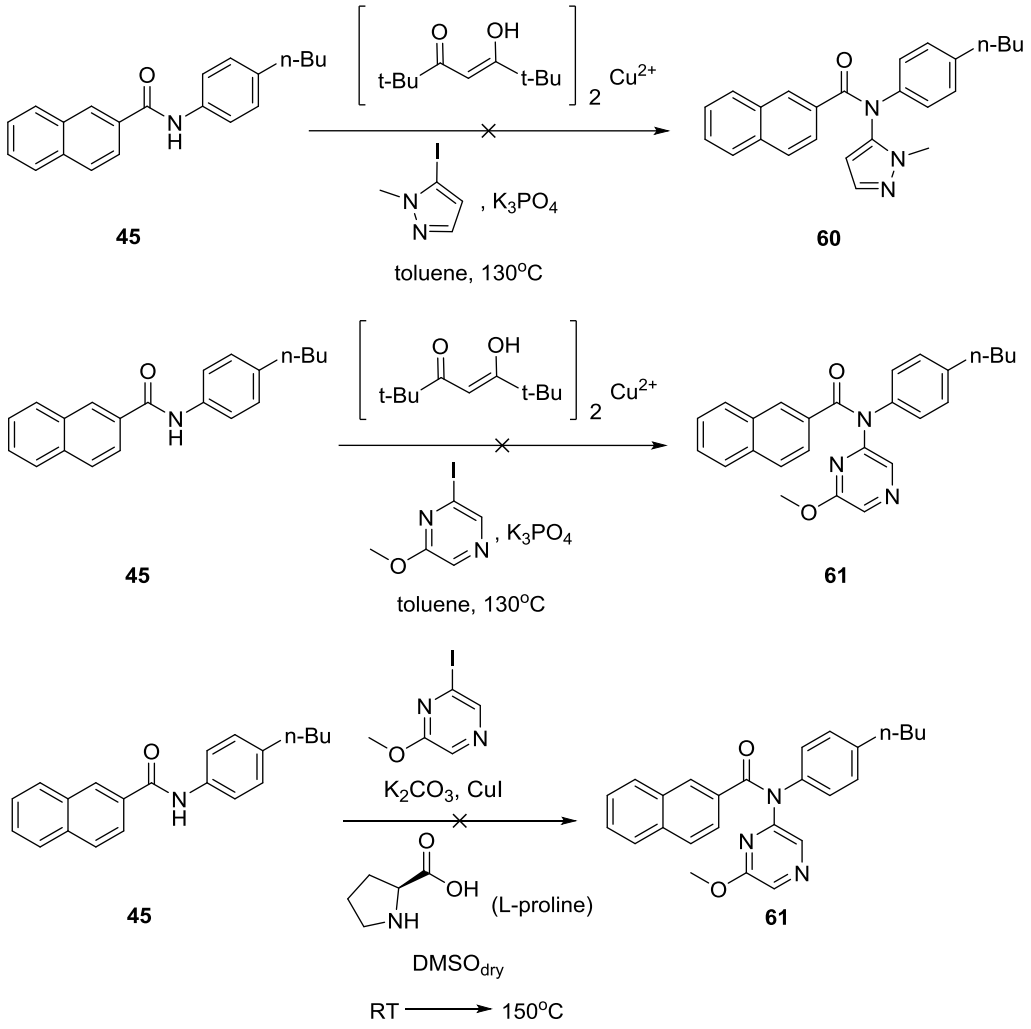

Figure 3.28. Attempted syntheses of candidate drug molecules 60 and 61. All the trials failed to obtain the desired products.

After these unsuccessful attempts (Route A; Figure 3.29), a different route was planned through retrosynthetic analysis (Route B; Figure 3.29). The synthesis of these molecules were to be tried according to Route B.

Initial trial for the Buchwald-Hartwig coupling of 4-butylaniline and 2-iodo-6-methoxypyrazine was done according to the literature procedure however unsuccessfully (Figure 3.30) [89]. More trials needs to be performed for this reaction.

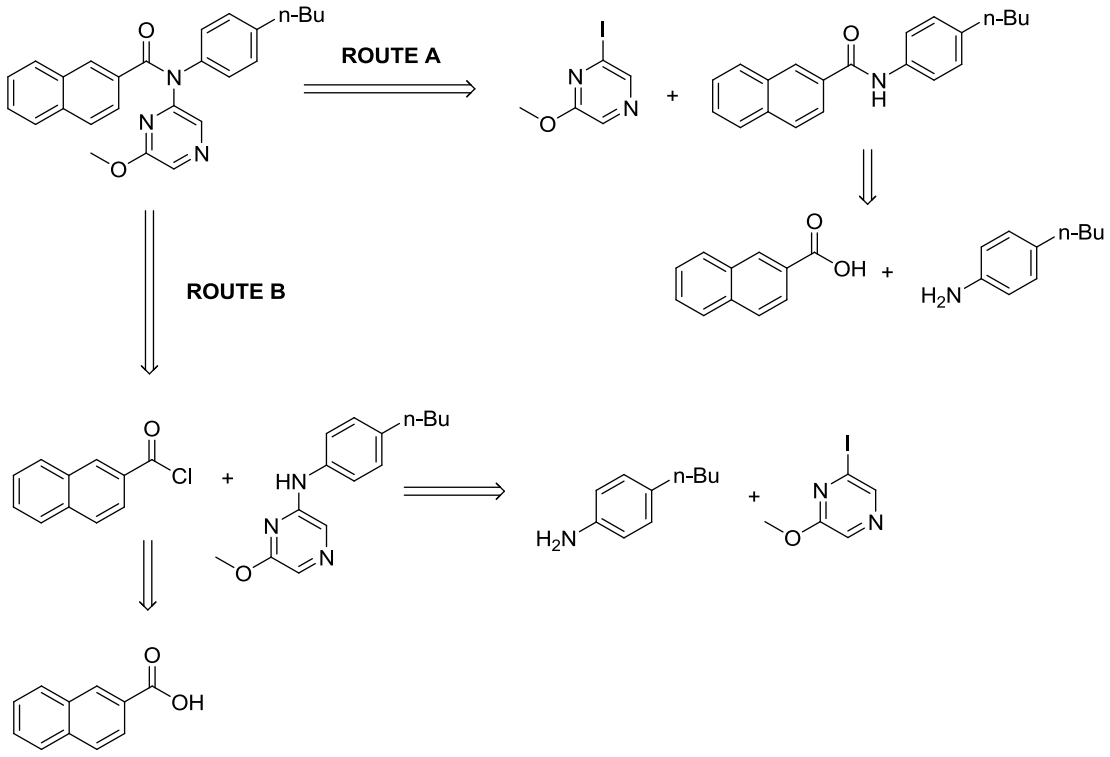

Figure 3.29. The retrosynthetic analysis for synthesis of **61** with Route A and Route B.

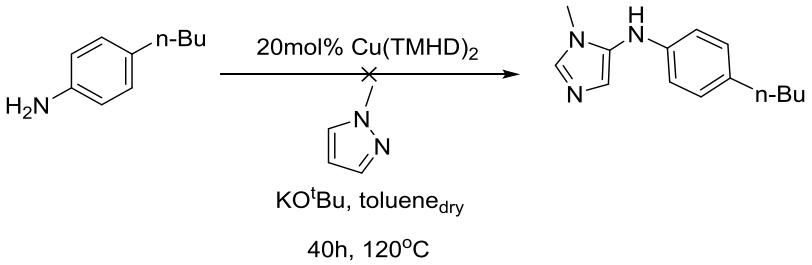

Figure 3.30. The unsuccessful Buchwald–Hartwig reaction of 4-butylaniline and 2-iodo-6-methoxypyrazine.

3.8. Synthesis of Isoquinoline Derivatives as Quinoline Bioisosteres

Once biological test results of quinoline derivatives turned out to be negative (Section 3.3), we proposed that isoquinoline derivatives can bind better to CYP17. The negative results of quinolines can be attributed to lack of binding of the quinoline ring through its N atom to the Fe atom of the heme of CYP17 due to steric hindrance. As quinoline ring approaches to the Fe atom, after a certain distance it becomes too close that the forces between H(8) of quinoline ring and heme N atoms become repulsive, therefore preventing the binding to the Fe atom (Figure 3.31). In case of isoquinoline however, there would be no such steric hindrance.

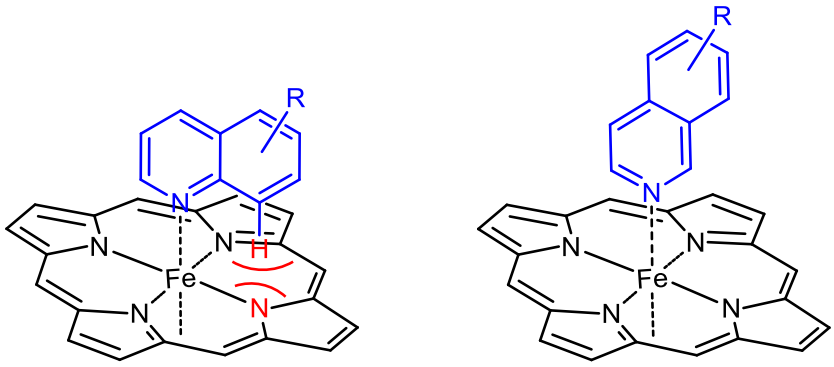

Figure 3.31. Proposed interactions of quinoline and isoquinoline moieties with the heme of CYP17.

Moreover, the similarity between the proposed binding mode of isoquinoline derivatives (Figure 3.31) and the binding mode of the existing CYP17 inhibitor abiraterone through the N atom of its pyridine ring (Figure 3.32) makes isoquinoline derivatives excellent potential candidates.

Therefore, by using some commercially available isoquinoline carboxylic acids and amines already in hand, a small series of isoquinoline carboxamide derivatives were proposed and synthesized for a preliminary testing of the design concept. All of these isoquinoline derivatives were synthesized by EDC coupling (Method B) and their structures

are tabulated on Table 3.4. The biological tests for these compounds will be carried out in the future.

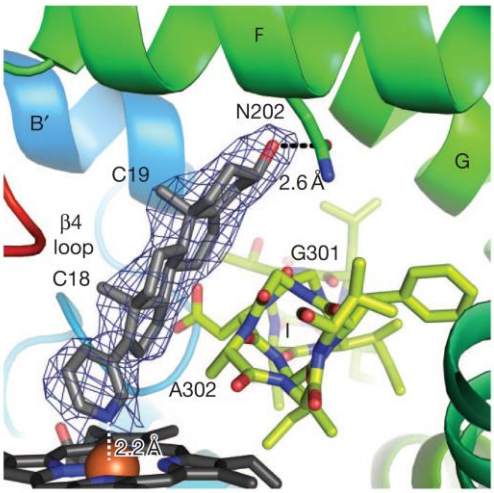

Figure 3.32. The binding mode of abiraterone through the N atom of its pyridine ring [57].

Table 3.4. The structures of isoquinoline derivatives proposed and synthesized.

Compound	Structure
64	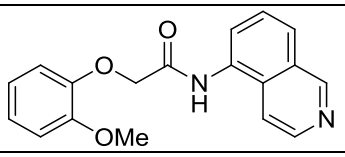
65	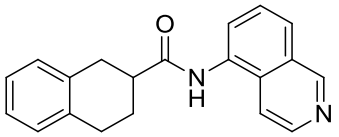
66	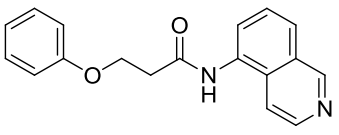
67	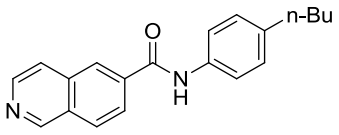
68	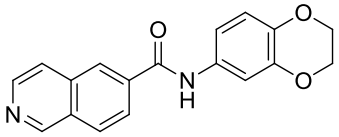

4. EXPERIMENTAL

4.1. Methods and Materials

The starting materials and reagents were purchased from Aldrich, Alfa Aesar, and Merck. Dry solvents were generally prepared by drying over activated molecular sieves and occasionally obtained from ScimatCo Purification System. Cryostat was used to cool reaction mixtures down to -78°C. Analytical Chromatography was performed on silica gel 60 F254 TLC (Thin Layer Chromatography) plates.

4.2. Instrumentation

Melting points were determined on Stuart SMP11 melting point apparatus (Bibby Scientific Limited, Staffordshire, UK). Fourier Transform Infrared Spectroscopy (FTIR) characterizations were performed on a Thermo Nicolet 380 FT-IR equipped with Smart Orbit diamond ATR (Attenuated Total Reflectance) accessory. ^{1}H-NMR and ^{13}C-NMR spectra were recorded on Varian 400 MHz NMR spectrometer (Varian Associates, Palo Alto, CA, USA) at the Advanced Technologies Research and Development Center at Bogazici University using TMS (Trimethylsilane) as internal standard. Correlations were established using 1H-1HCOSY and 2D NOESY experiments. High resolution mass spectra (HRMS) were obtained by using electrospray ionization (ESI) with Micro-Tof; m/z values are reported.

4.3. Synthesis of *n*-Butyl Substituted 8-Aminoquinolines

4.3.1. 2-butylquinoline (1) [90]

In order to prepare the LDA solution, in a 25 mL flask equipped with a magnetic stirrer, diisopropylamine (1.83 mL, 13.1 mmol) was dissolved in 12 mL dry THF (tetrahydrofuran) under N_2 at -78 °C. To this solution, 2.5 M *n*-buLi in hexane (5.68 mL, 14.2 mmol) was added and the mixture was warmed to 0 °C in 30 min. Then, the mixture was cooled to -78 °C. In order to form the carbanion, 40 mL dry THF was put into a 250 mL round bottom

flask with a magnetic stirrer. To this solution, quinaldine (1.49 mL, 11 mmol) was added under N_2 at -78 °C. The prepared LDA solution was added to this solution at -78 °C. The color of the solution changed to dark orange. This mixture was kept at -78 °C for 2.5 h. Iodopropane (1.39 mL, 14.2 mmol) was then added drop wise to this mixture at -78 °C under N_2 and this mixture was kept at -78° C for 3 h. The resulting mixture was allowed to warm up to room temperature overnight. The color of the solution turned to light orange. The reaction was then quenched with saturated 20 mL NH_4Cl and extracted with 3 x 50 mL ethyl acetate. The combined organic layers were washed with water and brine, dried over anhydrous Na_2SO_4 and concentrated under reduced pressure. The product was further purified by column chromatography using silica gel as the packing material and ethyl acetate as the mobile phase. After evaporation of the solvent, a yellow viscous liquid was obtained, 0.96 g (47%); **FTIR** (v, cm^{-1}): 3056, 2955, 2928, 1618, 1600, 1503, 1465, 1426, 1310, 1116, 824, 754; **^{1}H-NMR** ($CDCl_3$), δ**:** 0.76 (t, 3H, *J* = 7.6 Hz), 1.24 (m, 2H), 1.60 (m, 2H), 2.76 (t, 2H, *J* = 7.6 Hz), 6.94 (d, 1H, *J* = 8.8 Hz), 7.18 (t, 1H, *J* = 7.6, 7.2 Hz), 7.40 (d, 1H, *J* = 8.0 Hz), 7.44 (d, 1H, *J* = 8.8 Hz), 7.68 (d, 1H, *J* = 8.4 Hz), 7.92 (d, 1H, *J* = 8.8 Hz) ppm; **^{13}C-NMR** ($CDCl_3$), δ:13.82, 22.49, 31.88, 38.80, 121.08, 125.36, 126.54, 127.27, 128.72, 129.01, 135.82, 147.82, 162.70 ppm; **HRMS** (ESI): (m/z) calcd. for $C_{13}H_{16}N$ $[M+H]^+$: 186.1283, found: 186.1257.

4.3.2. 2-butyl-8-nitroquinoline (2) [91]

To an ice bath cooled solution of 2-butylquinoline **1** (0.556 g, 3 mmol) in 1.25 mL conc. H_2SO_4, was added drop wise 1 mL of conc. H_2SO_4 / conc. HNO_3 mixture (3:1). Reaction was maintained at 0 ^oC, stirred and monitored by TLC until all the quinoline had been consumed (2.5 h). Mixture was diluted with 10 mL water and NaOH(s) was added until the pH reached 10-11. Solution was extracted with 3 x 50 mL CH_2Cl_2, dried over anhydrous Na_2SO_4, filtered and evaporated. Nitration of 2-butylquinoline **1** resulted in 2-butyl-8-nitroquinoline **2** and 2-butyl-5-nitroquinoline **3**. In order to separate 2-butyl-8-nitroquinoline **2**, a column was prepared using silica gel and CH_2Cl_2 as the eluent phase. 2-butyl-8-nitroquinoline **2** was concentrated under reduced pressure to afford a yellowish solid, 0.34 g (49%), mp not determined, decomposes upon heating; **FTIR** (v, cm^{-1}): 2957, 2929, 2871, 1602, 1527, 1499, 1465, 1430, 1357, 1312, 870, 795, 761; **^{1}H-NMR** ($CDCl_3$), δ: 0.94 (t, 3H, *J* = 7.2 Hz), 1.39 (m, 2H), 1.78 (m, 2H), 2.97 (t, 2H, *J* = 8.0 Hz), 7.39 (d, 1H, *J* = 8.8 Hz),

7.50 (t, 1H, *J* = 8.0, 7.6 Hz), 7.91 (dd, 1H, *J* = 7.2, 1.2 Hz), 7.95 (dd, 1H, *J* = 8.4, 1.2 Hz), 8.09 (d, 1H, *J* = 8.8 Hz) ppm; **^{13}C-NMR** ($CDCl_3$), δ: 13.87, 22.45, 31.07, 38.83, 123.01, 123.20, 124.13, 127.57, 131.26, 135.66, 139.17, 148.00, 165.84 ppm; **HRMS** (ESI): (m/z) calcd. for $C_{13}H_{15}N_2O_2$ $[M+H]^+$: 231.1134, found: 231.1124.

4.3.3. 8-amino-2-butylquinoline (4) [92]

The experiment was carried out under N_2 atmosphere. 2-butyl-8-nitroquinoline **2** (1.38 g, 6.1 mmol) was dissolved in 10 mL ethanol. Stannous chloride dihydrate (2.73 g, 10.8 mmol) was added to this solution. The color of the solution turned to yellow-orange. This mixture was refluxed at 60 °C for 1.5 h. $NaBH_4$ (0.065 mg, 0.61 mmol) was dissolved in 2 mL ethanol and then injected into the reaction mixture. The resulting mixture was refluxed for an additional hour. The reaction mixture was made alkaline with 5-6 mL 40% aq. NaOH. The color of the mixture changed to gray. Reaction mixture was extracted with 3 x 50 mL ethyl acetate, dried over anhydrous Na_2SO_4, filtered and concentrated under reduced pressure to afford the desired product, 0.14 g (58%). **FTIR** (v, cm^{-1}): 3296, 2955, 2922, 2852, 1682, 1568, 1520, 1494, 1463, 1456, 1434, 1377, 1311, 1260, 1082, 834, 798, 749; **^{1}H-NMR** ($CDCl_3$), δ: 1.01 (t, 3H, *J* = 7.6 Hz), 1.48 (m, 2H), 1.85 (m, 2H), 2.98 (t, 2H, *J* = 8.0 Hz), 5.02 (bs, 2H), 6.91 (dd, 1H, *J* = 7.6, 1.2 Hz), 7.13 (dd, 1H, *J* = 7.6, 1.2 Hz), 7.24 (d, 1H, *J* = 8.4 Hz), 7.28 (d, 1H, *J* = 7.6 Hz), 7.95 (d, 1H, *J* = 8.0 Hz) ppm; **^{13}C-NMR** ($CDCl_3$), δ: 12.99, 21.52, 30.68, 37.55, 108.94, 114.82, 120.60, 125.23, 126.03, 134.94, 136.80, 142.48, 159.04 ppm; **HRMS** (ESI): (m/z) calcd. for $C_{13}H_{17}N_2$ $[M+H]^+$: 201.1392, found: 201.1283.

4.3.4. 2-methylenehexanal (9) [93]

A mixture of hexanal (12 mL, 0.10 mol), dimethylamine hydrochloride (9.85 g, 0.12 mol) and 37% aq. formaldehyde (9 mL, 0.12 mol) were stirred at 70 °C for 20 h. The aqueous phase was separated and extracted with 3 x 60 mL diethyl ether. The combined organic phases were dried over $CaCl_2$ and solvent was evaporated under reduced pressure. The product was purified by distillation at 70 °C / 40 mmHg to afford the pure colorless oil, 8.90 g (79%); **FTIR** (v, cm^{-1}): 3367, 2956, 2931, 2872, 1712, 1592, 1465, 1379, 1093, 960, 731; **^{1}H-NMR** ($CDCl_3$), δ: 0.97 (t, 3H), 1.23 (m, 2H), 1.37 (m, 2H), 2.18 (t, 2H), 5.91 (s, 1H),

6.17 (s, 1H), 9.45 (s, 1H) ppm; **HRMS** (ESI): (m/z) calcd. for $C_7H_{12}O$ $[M+H]^+$: 113.0966, found: 113.0968.

4.3.5. 3-butyl-8-nitroquinoline (10) [94]

This compound was prepared according to the literature procedure [94]. The experimental procedure and the spectroscopic data for this compound can be found in Turan Gul's M.Sc. Thesis [80].

4.3.6. 8-amino-3-butylquinoline (11)

This compound was prepared according to the literature procedure [95]. The experimental procedure and the spectroscopic data for this compound can be found in Turan Gul's M.Sc. Thesis [80].

4.3.7. 4-butylquinoline (5)

The same procedure as **1** was used. The spectroscopic data for this compound can be found in Turan Gul's M.Sc. Thesis [80].

4.3.8. 4-butyl-8-nitroquinoline (6)

The procedure of this experiment is the same as **2.** The spectroscopic data for this compound can be found in Turan Gul's M.Sc. Thesis [80].

4.3.9. 8-amino-4-butylquinoline (8)

The procedure of this experiment is the same as **4 .** The spectroscopic data for this compound can be found in Turan Gul's M.Sc. Thesis [80].

4.3.10. N-(4-butylphenyl)acetamide (12) [96]

In a 50 mL round bottom flask, 4-butylaniline (4.47 g, 30 mmol) and 9 mL water were added and stirred vigorously. To this reaction mixture, acetic anhydride (4.59 g, 45 mmol) was added. The reaction mixture was stirred at room temperature for 2 h. During this time, a precipitate was observed. The precipitate was filtered and washed with several portions of water and dried under vacuum to give the desired product as khaki solid, 5.21 g (91%), mp 77-80 ºC; **FTIR** (v, cm^{-1}): 3250(d), 3186, 3120, 3065, 2954, 2924, 2854, 1660, 1602, 1551, 1510, 1409, 1368, 1320, 1265, 830, 812, 762; **^{1}H-NMR** ($CDCl_3$), δ: 0.91 (t, 3H, *J* = 7.3 Hz), 1.33 (m, 2H), 1.56 (m, 2H), 2.16 (s, 3H), 2.56 (t, 2H, *J* = 7.6 Hz), 7.12 (d, 2H, *J* = 8.4 Hz), 7.19 (bs, 1H), 7.37 (d, 2H, *J* = 8.4 Hz) ppm; **^{13}C-NMR** ($CDCl_3$), δ: 13.92, 22.26, 24.50, 33.62, 35.03, 120.01, 128.84, 135.44, 139.05, 168.25 ppm; **HRMS** (ESI): (m/z) calcd. for $C_{12}H_{18}NO$ $[M+H]^+$: 192.1388, found: 192.1381.

4.3.11. N-(4-butyl-2-nitrophenyl)acetamide (13) [97]

12 (5.16 g, 26.98 mmol) was dissolved in 6 mL glacial acetic acid. The solution was warmed gently in order to dissolve all the solid material. Then the solution was cooled in an ice-bath. To this solution, 7.5 mL conc. H_2SO_4 was added drop wise at 5 ºC. Then the nitrating mixture (3 mL conc. HNO_3 and 3 mL conc. H_2SO_4) was added in small portions. After the addition of nitrating mixture was finished, the reaction mixture was stirred at room temperature for 50 min. Then, the viscous reaction mixture was poured into a mixture of 50 mL water 10 g ice. The resulting precipitate was filtered, washed with ice cold water, and dried under vacuum to give crude product. The crude product was purified with silica gel and CH_2Cl_2 as the eluent to give the pure product as a yellow solid, 6.18 g (97%), mp 46 ºC; **FTIR** (v, cm^{-1}): 3359, 2953, 2927, 2868, 2852, 1698, 1623, 1575, 1510, 1466, 1364, 1331, 1311, 1267, 1253, 1198, 1105, 1037, 854, 680, 581, 524; **^{1}H-NMR** ($CDCl_3$), δ: 0.93 (t, 3H, *J* = 7.3 Hz), 1.35 (m, 2H), 1.60 (m, 2H), 2.27 (s, 3H), 2.63 (t, 2H, *J* = 7.6 Hz), 7.46 (dd, 1H, *J* = 8.6, 1.8 Hz), 7.99 (d, 1H, *J* = 1.8 Hz), 8.62 (d, 1H, *J* = 8.6 Hz), 10.21 (bs, 1H) ppm; **^{13}C-NMR** ($CDCl_3$), δ: 13.85, 22.14, 25.57, 33.10, 34.55, 122.19, 124.87, 132.53, 136.24, 138.55, 168.96 ppm; **HRMS** (ESI): (m/z) calcd. for $C_{12}H_{16}N_2O_3Na$ $[M+Na]^+$: 259.1059, found: 259.1071.

4.3.12. 4-butyl-2-nitroaniline (14) [97]

13 (1.84 g, 7.8 mmol) was refluxed in 40 mL methanol and 40 mL 20 % H_2SO_4 for 2 h. Then, the reaction mixture was cooled to room temperature and made weakly alkaline by slowly adding a 5% aqueous $NaHCO_3$. The resulting solution was extracted with 2 x 50 mL diethyl ether. The ether layers were combined, washed with water, dried over anhydrous Na_2SO_4, filtered and concentrated under reduced pressure. The pure orange liquid product was obtained, 1.45 g (96 %), mp 259 ºC; **FTIR** (v, cm^{-1}): 3490, 3370, 2956, 2928, 2858, 1634, 1590, 1515, 1466, 1410, 1337, 1246, 1190, 1168, 1094, 824, 767; **^{1}H-NMR** ($CDCl_3$), δ: 0.92 (t, 3H, *J* = 7.3 Hz), 1.33 (m, 2H), 1.55 (m, 2H), 2.52 (t, 2H, *J* = 7.6 Hz), 5.94 (bs, 2H), 6.73 (d, 1H, *J* = 8.5 Hz), 7.19 (dd, 1H, *J* = 8.5, 2.0 Hz), 7.90 (d, 1H, *J* = 1.6 Hz) ppm; **^{13}C-NMR** ($CDCl_3$), δ: 13.87, 22.12, 33.26, 34.17, 118.76, 124.71, 131.79, 136.55, 142.91 ppm; **HRMS** (ESI): (m/z) calcd. for $C_{10}H_{15}N_2O_2$ $[M+H]^+$: 195.1134, found: 195.1131.

4.3.13. 1-butyl-3-nitrobenzene (15) [98]

In a 50 mL round bottom flask, **14** (0.767 g, 3.25 mmol) was dissolved in 15 mL acetic acid. To this solution, 6.5 g ice was added and the resulting suspension was cooled to 0 ºC. A solution of sodium nitrite (0.246 g, 3.58 mmol) in water (1 mL) was added drop wise and the reaction mixture was stirred at 0 °C for 30 min. The resulting clear solution of the diazo-salt was added drop wise to a solution of $FeSO_4.7H_2O$ (0.904 g, 3.25 mmol) in DMF (11 mL) pre-cooled to 0°C. The reaction mixture was allowed to warm to room temperature and stirred for additional 30 min, diluted with water (100 mL) and the product was extracted into dichloromethane (3 x 40 mL). The organic phase was washed with a 10% aqueous NaOH (3 x 30 mL), dried (Na_2SO_4), and evaporated. In order to remove DMF, the product was again extracted with water / diethyl ether (10:1) mixture and combined organic phases were evaporated. The resulting crude product was purified through a column chromatography using silica gel and hexane as eluent phase. Solvent was evaporated to afford a yellowish liquid, 264 mg (41%); **FTIR** (v, cm^{-1}): 2958, 2931, 2861, 1524, 1348, 1098, 1086, 804, 790, 731, 685, 672; **^{1}H-NMR** ($CDCl_3$), δ: 0.94 (t, 3H, *J* = 7.2 Hz), 1.38 (m, 2H), 1.63 (m, 2H), 2.71 (t, 2H, *J* = 7.6 Hz), 7.44 (dd, 1H, *J* = 8.4, 1.2 Hz), 7.49 (d, 1H, *J* = 7.2 Hz), 8.02 (d, 1H, *J* = 1.2 Hz), 8.04 (bs, 1H) ppm; **^{13}C-NMR** ($CDCl_3$), δ: 12.81, 21.18, 32.20, 34.25,

119.83, 122.17, 128.04, 133.72, 143.81, 147.35 ppm; **HRMS** (ESI): (m/z) calcd. for $C_{10}H_{14}NO_2$ $[M+H]^+$: 180.1025, found: 180.1022.

4.3.14. 3-butylaniline (16)

The procedure of this experiment is the same as **4**. Yellow liquid (95%); **FTIR** (v, cm^{-1}): 3306, 2955, 2928, 2858, 1677, 1605, 1591, 1488, 1441, 1377, 1311, 1260, 1167, 1105, 776, 696; **^{1}H-NMR** ($CDCl_3$), δ: 0.93 (t, 3H, *J* = 7.6 Hz), 1.37 (m, 2H), 1.58 (m, 2H), 2.53 (t, 2H, *J* = 7.6 Hz), 3.36 (bs, *2*H), 6.52 (d, 1H, *J* = 8.0 Hz), 6.54 (s, 1H), 6.60 (d, 1H, *J* = 7.6 Hz), 7.07 (t, 1H, *J* = 7.6 Hz) ppm; **^{13}C-NMR** ($CDCl_3$), δ: 13.96, 22.41, 33.52, 35.64, 112.59, 115.38, 118.98, 129.11, 144.22, 146.12 ppm; **HRMS** (ESI): (m/z) calcd. for $C_{10}H_{16}N$ $[M+H]^+$: 150.1283, found: 150.1278.

4.3.15. 5-butylquinoline (17) and 7-butylquinoline (18) [95]

In a 100 mL 3-necked round-bottom flask was placed **16** (7.69 g, 51.5 mmol), glycerol (5.7 mL, 78 mmol) and iodine (0.24 g, 1.9 mmol). The reaction mixture was stirred and 8 mL conc. H_2SO_4 was added down the condenser. Reaction soon commenced, the temperature raised to 100-105 °C. Flask was heated gradually, with stirring, in a silicone bath to 140 °C; the reaction proceeded with the evolution of sulfur dioxide and some iodine vapor. Heating at 170 °C was continued for 2.5 h. Reaction was monitored by TLC. When the reaction was complete, it was cooled and made alkaline by using 5 *N* aq. NaOH. The resulting mixture was extracted using dichloromethane (3 x 100 mL), dried over anhydrous Na_2SO_4 and filtered. Solvent was removed on a rotary evaporator. The crude products were subjected to column chromatography using silica and different solvent mixtures but the vast majority of the products were inseparable. In order to identify the structures of 5-butylquinoline **17** and 7-butylquinoline **18**, a small amount of mixture was separated by analytical chromatography on silica TLC plates. The amount of 5-butylquinoline **17** was just enough to get ^{1}H-NMR. Since it was difficult to separate isomers, the mixture of products was nitrated at the next step, 6.82 g (72%); regioisomeric ratio 1:4.

4.3.16. 5-butylquinoline (17)

^{1}H-NMR ($CDCl_3$), δ: 0.85 (t, 3H, *J* = 7.6 Hz), 1.33 (m, 2H), 1.58 (m, 2H), 2.92 (t, 2H, *J* = 7.6 Hz), 7,25 (d, 1H, *J* = 6.8 Hz), 7.28 (t, 1H, *J* = 8.0, 4.0 Hz), 7.50 (dd, 1H, *J* = 8.4, 6.8 Hz), 7.87 (d, 1H, *J* = 8.8 Hz), 8.23 (dd, 1H, *J* = 8.0, 1.6 Hz), 8.78 (dd, 1H, *J* = 4.0, 1.6 Hz) ppm; **HRMS** (ESI): (m/z) calcd. for $C_{13}H_{16}N$ $[M+H]^+$: 186.1283, found: 186.1263.

4.3.17. 7-butylquinoline (18)

FTIR (v, cm^{-1}): 3049, 2955, 2928, 2858, 1625, 1596, 1501, 1450, 1317, 833, 769, 730, 614, 477; **^{1}H-NMR** ($CDCl_3$), δ: 0.94 (t, 3H, *J* = 7.2 Hz), 1.39 (m, 2H), 1.70 (m, 2H), 2.82 (t, 2H, *J* = 7.6 Hz), 7,32 (dd, 1H, *J*= 8.4, 4.4 Hz), 7.38 (dd, 1H, *J* = 8.4, 1.6 Hz), 7.71 (d, 1H, *J* = 8.4 Hz), 7.88 (s, 1H), 8.09 (dd, 1H, *J* = 8.0, 1.2 Hz), 8.67 (dd, 1H, *J* = 4.0, 1.6 Hz) ppm; **^{13}C-NMR** ($CDCl_3$), δ: 13.92, 22.29, 33.14, 35.80, 120.29, 126.55, 127.44, 127.73, 128.21, 135.78, 144.70, 148.43, 150.23 ppm; **HRMS** (ESI): (m/z) calcd. for $C_{13}H_{16}N$ $[M+H]^+$: 186.1283, found: 186.1263.

4.3.18. Nitration of 5-butylquinoline (17) and 7-butylquinoline (18) Mixture

This experiment was carried out by Turan Gul. To a mixture of **17** and **18** (6.82 g, 36.81 mmol) in 15.5 mL conc. H_2SO_4, cooled in an iced bath was added drop wise 12.5 mL of conc. H_2SO_4 / conc. HNO_3 mixture (3:1). Reaction was maintained at 0 ^oC, stirred rapidly and monitored by TLC until all the quinoline was consumed (2.5 h). Mixture was diluted with 50 mL water and NaOH(s) was added until pH 10-11. Solution was extracted with 3 x 100 mL CH_2Cl_2, dried over anhydrous Na_2SO_4, filtered and evaporated. Nitration of **17** and **18** resulted in 5-butyl-8-nitroquinoline **20**, 5-butyl-6-nitroquinoline **19**, and 7-butyl-8-nitroquinoline **21**. In order to separate the mixture of isomers, column was prepared using silica gel and dichloromethane / hexane (3:1) as the eluent phase. 5-butyl-8-nitroquinoline **20**, 1.13 g (13%); 5-butyl-6-nitroquinoline **19**, 0.1 g (1.2%); 7-butyl-8-nitroquinoline **21**, 7.45 g (86%); overall nitration yield: 90%.

4.3.19. 5-butyl-8-nitroquinoline (20)

mp 73 ºC; **FTIR** (v, cm^{-1}): 3079, 2954, 2927, 2868, 2359, 1574, 1515, 1468, 1397, 836, 797, 773, 740, 635, 613, 487; **^{1}H-NMR** ($CDCl_3$), δ: 0.98 (t, 3H, *J* = 7.6 Hz), 1.46 (m, 2H), 1.71 (m, 2H), 3.10 (t, 2H, *J* = 8.0 Hz), 7.42 (d, 1H, *J* = 7.6 Hz), 7.55 (dd, 1H, *J* = 8.4, 4.0 Hz), 7.94 (d, 1H, *J* = 7.6 Hz), 8.43 (dd, 1H, *J* = 8.8, 1.6 Hz), 9.05 (dd, 1H, *J* = 4.4, 1.6 Hz) ppm; **^{13}C-NMR** ($CDCl_3$), δ: 13.81, 22.62, 32.32, 32.94, 122.19, 123.49, 124.74, 132.44, 140.03, 144.90, 146.91, 151.91 ppm; **HRMS** (ESI): (m/z) calcd. for $C_{13}H_{15}N_2O_2$ $[M+H]^+$: 231.1134, found: 231.1126.

4.3.20. 5-butyl-6-nitroquinoline (19)

mp 62 ºC; **FTIR** (v, cm^{-1}): 2958, 2930, 2872, 1522, 1495, 1464, 1353, 1328, 877, 838, 812, 797, 770, 746, 542; **^{1}H-NMR** ($CDCl_3$), δ: 1.00 (t, 3H, *J* = 7.6 Hz), 1.55 (m, 2H), 1.75 (m, 2H), 3.18 (t, 2H, *J* = 8.0 Hz), 7.57 (dd, 1H, *J* = 8.4, 4.0 Hz), 7.99 (d, 1H, *J* = 9.2 Hz), 8.05 (d, 1H, *J* = 9.2 Hz), 8.50 (dd, 1H, *J* = 8.8, 0.8 Hz), 9.03 (dd, 1H, *J* = 4.4, 1.6 Hz) ppm; **^{13}C-NMR** ($CDCl_3$), δ: 13.75, 23.13, 27.76, 33.27, 122.34, 124.02, 127.00, 129.34, 133.97, 135.01, 149.26, 152.31 ppm; **HRMS** (ESI): (m/z) calcd. for $C_{13}H_{15}N_2O_2$ $[M+H]^+$: 231.1134, found: 231.1128.

4.3.21. 7-butyl-8-nitroquinoline (21)

mp 42 ºC; **FTIR** (v, cm^{-1}): 2957, 2930, 2872, 1598, 1529, 1497, 1457, 1376, 1354, 1315, 876, 838, 799, 642; **^{1}H-NMR** ($CDCl_3$), δ: 0.92 (t, 3H, *J* = 7.2 Hz), 1.39 (m, 2H), 1.68 (m, 2H), 2.75 (t, 2H, *J* = 7.6 Hz), 7.44 (d, 1H, *J* = 8.0 Hz), 7.46 (t, 1H, *J* = 8.0, 4.4 Hz), 7.84 (d, 1H, *J* = 8.8 Hz), 8.16 (dd, 1H, *J* = 8.8, 1.6 Hz), 8.93 (dd, 1H, *J* = 4.4, 1.6 Hz) ppm; **^{13}C-NMR** ($CDCl_3$), δ: 13.77, 22.53, 31.34, 32.67, 122.11, 126.91, 127.91, 129.24, 134.76, 135.62, 139.67, 148.10, 152.06 ppm; **HRMS** (ESI): (m/z) calcd. for $C_{13}H_{15}N_2O_2$ $[M+H]^+$: 231.1134, found: 231.1106.

4.3.22. 8-amino-5-butylquinoline (22)

This experiment was carried out by Turan Gul. The procedure of this experiment is the same as **4** (96.4%); **FTIR** (v, cm^{-1}): 3465, 3353, 2953, 2927, 2857, 1610, 1587, 1506, 1477, 1365, 1336, 821, 785; **^{1}H-NMR** ($CDCl_3$), δ: 0.97 (t, 3H, *J* = 7.6 Hz), 1.44 (m, 2H), 1.66 (m, 2H), 2.92 (t, 2H, *J* = 7.6 Hz), 4.87 (bs, 2H) 6.86 (d, 1H, *J* = 7.6 Hz), 7.16 (d, 1H, *J* = 7.6 Hz), 7.35 (dd, 1H, *J* = 8.8, 4.4 Hz), 8.26 (dd, 1H, *J* = 8.8, 1.6 Hz), 8.78 (dd, 1H, *J* = 4.4, 1.6 Hz) ppm; **^{13}C-NMR** ($CDCl_3$), δ: 14.06, 22.73, 31.54, 33.45, 109.89, 120.77, 126.90, 127.28, 132.43, 138.97, 142.28, 146.82 ppm; **HRMS** (ESI): (m/z) calcd. for $C_{13}H_{17}N_2$ $[M+H]^+$: 201.1392, found: 201.1376.

4.3.23. 8-amino-7-butylquinoline (23)

This experiment was carried out by Turan Gul. The procedure of this experiment is the same as **4** (75%); **FTIR** (v, cm^{-1}): 3478, 3370, 3050, 2954, 2927, 2858, 1586, 1558, 1504, 1456, 1371, 1105, 822, 798, 673; **^{1}H-NMR** ($CDCl_3$), δ: 1.00 (t, 3H, *J* = 7.6 Hz), 1.47 (m, 2H), 1.71 (m, 2H), 2.71 (t, 2H, *J* = 7.2 Hz), 5.02 (bs, 2H), 7.13 (d, 1H, *J* = 8.4 Hz), 7.28 (d, 1H, *J* = 8.4 Hz), 7.30 (t, 1H, *J* = 8.0, 4.0 Hz), 8.01 (d, 1H, *J* = 8.4 Hz), 8.77 (d, 1H, *J* = 4.0 Hz) ppm; **^{13}C-NMR** ($CDCl_3$), δ: 14.10, 22.85, 31.01, 31.44, 115.44, 120.44, 122.74, 127.15, 129.16, 135.82, 138.43, 140.71, 147.37 ppm; **HRMS** (ESI): (m/z) calcd. for $C_{13}H_{17}N_2$ $[M+H]^+$: 201.1392, found: 201.1367.

4.3.24. 6-butylquinoline (24)

The procedure of this experiment is the same as with **17** and **18** (59%); **FTIR** (v, cm^{-1}): 3013, 2955, 2927, 2856, 1499, 1464, 1377, 1118, 833, 796, 770, 615, 478; **^{1}H-NMR** ($CDCl_3$), δ: 0.86 (t, 3H, *J* = 7.2 Hz), 1.31 (m, 2H), 1.60 (m, 2H), 2.69 (t, 2H, *J* = 7.6 Hz), 7.23 (dd, 1H, *J* = 8.4, 4.4 Hz), 7.46 (m, 2H), 7.93 (d, 1H, *J* = 9.2 Hz), 7.95 (d, 1H, *J* = 8.4 Hz), 8.74 (dd, 1H, *J* = 4.4, 1.6 Hz) ppm; **^{13}C-NMR** ($CDCl_3$), δ: 12.89, 21.32, 32.33, 34.55, 119.96, 124.96, 127.30, 128.13, 130.03, 134.48, 140.27, 146.07, 148.47 ppm; **HRMS** (ESI): (m/z) calcd. for $C_{13}H_{16}N$ $[M+H]^+$: 186.1283, found: 186.1278.

4.3.25. 6-butyl-5-nitroquinoline (25)

The procedure of this experiment is the same as with **3**. Brown viscous liquid (62%); **FTIR** (v, cm^{-1}): 2958, 2931, 2872, 1522, 1495, 1464, 1353, 1328, 877, 838, 812, 797, 770, 746, 542; **^{1}H-NMR** ($CDCl_3$), δ: 0.83 (t, 3H, *J* = 7.2 Hz), 1.29 (m, 2H), 1.59 (m, 2H), 2.67 (t, 2H, *J* = 7.6 Hz), 7.42 (dd, 1H, *J* = 8.0, 4.4, 1.6 Hz), 7.52 (d, 1H, *J* = 8.8 Hz), 7.93 (d, 1H, *J* = 8.8 Hz), 8.06 (d, 1H, *J* = 8.8 Hz), 8.84 (dd, 1H, *J* = 4.4, 1.6 Hz) ppm; **^{13}C-NMR** ($CDCl_3$), δ: 13.75, 22.52, 31.54, 32.75, 120.22, 123.05, 130.00, 130.79, 132.18, 133.25, 146.36, 146.54, 150.93 ppm; **HRMS** (ESI): (m/z) calcd. for $C_{13}H_{15}N_2O_2$ $[M+H]^+$: 231.1134, found: 231.1123.

4.3.26. 5-bromo-6-butylquinoline (27) [99]

24 (3.42 g, 18.4 mmol) was slowly added to 18.4 mL conc. H_2SO_4 drop wise. The exothermic reaction was kept below 30 ^{o}C, then the solution was cooled to -40 ^{o}C and N-bromosuccinimide (NBS) (3.83 g, 21.5 mmol) was slowly added to this solution piecewise while the temperature was kept around -40 ^{o}C. The suspension was stirred at 0 ^{o}C for 1 h. Then the mixture was poured onto 100 g of crushed ice and 25% aqueous NH_3 was added until pH = 9 while the temperature was kept under 25 ^{o}C. The mixture was then extracted with diethyl ether. The organic phase was washed first with 15% aqueous NaOH and then twice with distilled water and dried over Na_2SO_4. Resulting mixture was filtered and evaporated. The crude product was purified first by crystallization where it was initially dissolved in 3-4 mL dichloromethane and then 100 mL of petroleum ether was added and the resulting solution was placed in a refrigerator. After crystallization, the product was separated by a column chromatography on silica gel using dichloromethane / hexane (1:3) as eluent to afford pure orange-yellow solid **27**, 4.47 g (92%) mp 51-54 ^{o}C; **FTIR** (v, cm^{-1}): 2955, 2927, 2859, 1522, 1492, 1456, 962, 906, 832, 804, 767; **^{1}H-NMR** ($CDCl_3$), δ: 0.75 (t, 3H, *J* = 7.6 Hz), 1.19 (m, 2H), 1.39 (m, 2H), 2.67 (t, 2H, *J* = 8.0 Hz), 7.12 (dd, 1H, *J* = 8.8, 4.4 Hz), 7.26 (d, 1H, *J* = 8.8 Hz), 7.76 (d, 1H, *J* = 8.8 Hz), 8.26 (dq, 1H, *J* = 8.8, 1.6 Hz), 8.60 (dd, 1H, *J* = 4.4, 1.6 Hz) ppm; **^{13}C-NMR** ($CDCl_3$), δ:13.92, 22.51, 32.08, 36.74, 121.90, 122.35, 127.97, 128.71, 131.39, 135.40, 140.91, 147.57, 149.82 ppm; **HRMS** (ESI): (m/z) calcd. for $C_{13}H_{15}{}^{79}BrN$ $[M+H]^+$: 264.0388, found: 264.0352.

4.3.27. 5-bromo-6-butyl-8-nitroquinoline (29)

The procedure of this experiment is the same as **3**. Yellowish solid (85%); **FTIR** (v, cm^{-1}): 3069, 2953, 2931, 2869, 1552, 1525, 1493, 1456, 1371, 1340, 1020, 966, 909, 891, 780, 729; **^{1}H-NMR** ($CDCl_3$), δ: 0.99 (t, 3H, *J* = 7.2 Hz), 1.46 (m, 2H), 1.71 (m, 2H), 3.03 (t, 2H, *J* = 8.0 Hz), 7.63 (dd, 1H, *J* = 8.8, 4.0 Hz), 7.94 (s, 1H), 8.70 (dd, 1H, *J* = 8.8, 1.6 Hz), 9.02 (dd, 1H, *J* = 4.0, 1.6 Hz) ppm; **^{13}C-NMR** ($CDCl_3$), δ: 13.86, 22.50, 31.82, 36.77, 123.71, 125.23, 126.58, 128.85, 136.01, 138.66, 140.75, 147.33, 152.05 ppm; **HRMS** (ESI): (m/z) calcd. for $C_{13}H_{14}{}^{79}BrN_2O_2$ $[M+H]^+$: 309.0239, found: 309.0251.

4.3.28. 8-amino-6-butylquinoline (30)

The procedure of this experiment is the same as **5**. Dark green liquid (77%); **FTIR** (v, cm^{-1}): 3467, 3347, 3030, 2954, 2927, 2857, 1618, 1588, 1502, 1431, 1380, 841, 785; **^{1}H-NMR** ($CDCl_3$), δ: 0.96 (t, 3H, *J* = 7.6 Hz), 1.41 (m, 2H), 1.68 (m, 2H), 2.68 (t, 2H, *J* = 8.0 Hz), 4.60 (bs, 2H) 6.80 (d, 1H, *J* = 1.6 Hz), 6.95 (s, 1H), 7.32 (dd, 1H, *J* = 8.8, 4.4 Hz), 7.97 (dd, 1H, *J* = 8.4, 1.6 Hz), 8.70 (d, 1H, *J* = 4.0, 1.2 Hz) ppm; **^{13}C-NMR** ($CDCl_3$), δ: 13.97, 22.40, 33.36, 36.02, 111.57, 114.84, 121.30, 128.88, 135.49, 142.31, 143.49, 146.59 ppm; **HRMS** (ESI): (m/z) calcd. for $C_{13}H_{16}N_2$ $[M+H]^+$: 201.1392, found: 201.1149.

4.4. General Procedures for the Coupling Reactions of Aromatic Amines and Aromatic Carboxylic Acids: Method A, Method B, and Method C

4.4.1. Method A

This coupling reaction is done according to the literature procedure [100]. The experiment is done under nitrogen by using dry CH_2Cl_2. Aromatic acid (0.5 mmol) is dissolved in 3 mL dry CH_2Cl_2 under N_2. To this solution, PBr_3 (0.07 mL, 0.75 mmol) is dropwise added at 0°C and the reaction mixture is stirred for 3 hours at room temperature. After 3 hours, triethylamine (0.21 mL, 1.5 mmol) is dropwise added. Aromatic amine (0.5 mmol) is dissolved in 2 mL dry CH_2Cl_2 and it is added to the reaction mixture. The reaction is stirred at room temperature and monitored by TLC. When the reaction is complete (app. 1 hour), the reaction mixture is diluted with CH_2Cl_2 (10 mL) and washed with H_2O. The organic layer

is dried over Na_2SO_4, filtered and concentrated under reduced pressure. The crude product is purified by column chromatography using silica gel.

4.4.2. Method B

In this method, two literature procedures for forming acid chloride and coupling it with aromatic amine were utilized [101, 102]. In a two-neck 25 ml round bottom flask aromatic acid (1.1 mmol) was added TFT (3 ml) under nitrogen. The mixture was cooled to 0^{o}C and added oxalyl chloride (0.10 ml, 1.21 mmol). The resulting mixture was stirred for 15 min and was added 2 drops of DMF (gas evolution!). The mixture was allowed to warm to room temperature and more oxalyl chloride (0.2 ml, 2.42 mmol) and 3 drops of DMF was added. After the resulting mixture was stirred at room temperature for 2 hours, the solvent was removed by rotavap. The resulting crude acid chloride was dissolved in TFT (3 ml) and DCM (1 ml; dry) and was dropwise added into a mixture of Et_3N (0.87 ml) and aromatic amine (1 mmol) (gas evolution!), and the resulting mixture was stirred at room temperature for 16 hours. The solvent was removed by rotavap, the crude product was washed with hexane and purified by column chromatography using silica.

4.4.3. Method C

The procedure was applied from a literature work [103]. EDC·HCl (156 mg, 0.81 mmol)) and BtOH (110 mg, 0.81 mmol)) were added sequentially to a stirred solution of aromatic acid (0.81 mmol) in dichloromethane/dimethylformamide (1/1) at room temperature. The reaction mixture was left under stirring for 30 min, and then aromatic amine (0.54mmol) dissolved in dichloromethane/dimethylformamide (1/1) was added dropwise. The solution was stirred for 22 h and then diluted with dichloromethane and washed with a saturated aqueous solution of $NaHCO_3$ and brine and then dried over Na_2SO_4. The solution was concentrated under reduced pressure and the crude material was purified by column chromatography using silica.

4.5. Synthesis of 8-amino-2-butylquinoline Derivatives

All the coupling reactions of 8-amino-2-butylquinolines were done by Method A as described above. The characterization of these compounds were done by ^{1}H-NMR, ^{13}C-NMR, and HRMS.

4.5.1. N-(2-butylquinolin-8-yl)benzamide (31)

^{1}H NMR ($CDCl_3$), δ: 0.93 (t, 3H, CH_2CH_3), 1.40 (m, 2H, $CH_2CH_2CH_3$), 1.83 (m, 2H, $CH_2CH_2CH_2$), 2.95 (t, 2H, $ArCH_2$), 7.27 (d, 1H, ArH), 7.47 (m, 5H, ArH), 7.99 (d, 1H, ArH), 8.01 (d, 1H, ArH), 8.03 (d, 1H, ArH), 8.82 (dd, 1H, ArH), 10.82 (s, 1H, NH) ppm. **^{13}C NMR** ($CDCl_3$), δ: 13.04 (CH_3), 21.39 (CH_2), 30.16 (CH_2), 37.10 (CH_2), 120.52 (ArC), 121.09 (ArC), 125.35 (ArC), 125.55 (ArC), 126.29 (ArC), 127.78 (ArC), 130.77 (ArC), 132.98 (ArC), 134.26 (ArC), 135.77 (ArC), 159.99 (C=O) ppm.

4.5.2. N-(2-butylquinolin-8-yl)-6-fluoro-2-naphthamide (32)

^{1}H NMR ($CDCl_3$), δ: 0.96 (t, 3H, CH_2CH_3), 1.44 (m, 2H, $CH_2CH_2CH_3$), 1.89 (m, 2H, $CH_2CH_2CH_2$), 3.00 (t, 2H, $ArCH_2$), 7.31 (m, 2H, ArH), 7.47 (m, 3H, ArH), 7.89 (d, 1H, ArH), 7.95 (dd, 1H, ArH), 8.03 (d, 1H, ArH), 8.10 (d, 1H, ArH), 8.55 (s, 1H, ArH), 8.85 (dd, 1H, ArH), 11.00 (s, 1H, NH) ppm.

4.5.3. N-(2-butylquinolin-8-yl)-2-naphthamide (33)

^{1}H NMR ($CDCl_3$), δ: 0.94 (t, 3H, CH_2CH_3), 1.41 (m, 2H, $CH_2CH_2CH_3$), 1.86 (m, 2H, $CH_2CH_2CH_2$), 2.95 (t, 2H, $ArCH_2$), 7.24 (d, 2H, ArH), 7.45 (m, 4H, ArH), 7.82 (m, 1H, ArH), 7.94 (m, 3H, ArH), 8.05 (d, 1H, ArH), 8.52 (s, 1H, ArH), 8.85 (s, 1H, ArH), 10.99 (s, 1H, NH) ppm. **^{13}C NMR** ($CDCl_3$), δ: 14.08 (CH_3), 22.42 (CH_2), 31.07 (CH_2), 38.24 (CH_2), 116.44 (ArC), 121.45 (ArC), 122.16 (ArC), 123.69 (ArC), 126.33 (ArC), 126.50 (ArC), 126.83 (ArC), 127.80 (ArC), 127.84 (ArC), 127.95 (ArC), 128.68 (ArC), 129.16 (ArC), 132.52 (ArC), 132.81 (ArC), 134.13 (ArC), 134.92 (ArC), 136.50 (ArC), 138.07 (ArC), 160.95 (ArC), 165.197 (C=O) ppm.

4.5.4. N-(2-butylquinolin-8-yl)-3-methoxy-2-naphthamide (34)

^{1}H NMR ($CDCl_3$), δ: 0.99 (t, 3H, CH_2CH_3), 1.45 (m, 2H, $CH_2CH_2CH_3$), 1.86 (m, 2H, $CH_2CH_2CH_2$), 3.45 (t, 2H, $ArCH_2$), 4.28 (s, 3H, OCH_3), 7.34 (m, 2H, Ar*H*), 7.41 (m, 1H, Ar*H*), 7.52 (m, 3H, Ar*H*), 7.78 (d, 1H, Ar*H*), 7.95 (d, 1H, Ar*H*), 8.07 (d, 1H, Ar*H*), 7.78 (d, 1H, Ar*H*), 7.95 (d, 1H, Ar*H*), 8.07 (d, 1H, Ar*H*), 8.90 (s, 1H, Ar*H*), 9.11 (s, 1H, N*H*) ppm. **^{13}C NMR** ($CDCl_3$), δ: 13.99 (CH_3), 22.67 (CH_2), 32.31 (CH_2), 39.14 (CH_2), 56.03 (OCH_3), 106.55 (Ar*C*), 111.86 (Ar*C*), 117.82 (Ar*C*), 121.55 (Ar*C*), 121.61 (Ar*C*), 123.69 (Ar*C*), 124.52 (Ar*C*), 126.22 (Ar*C*), 126.51 (Ar*C*), 126.57 (Ar*C*), 128.32 (Ar*C*), 129.27 (Ar*C*), 134.18 (Ar*C*), 135.14 (Ar*C*), 135.90 (Ar*C*), 136.59 (Ar*C*), 154.92 (Ar*C*), 161.03 (Ar*C*), 163.58 (*C*=O) ppm.

4.5.5. N-(2-butylquinolin-8-il))-6-methoxy-2-naphthamide (35)

^{1}H NMR ($CDCl_3$), δ: 0.95 (t, 3H, CH_2CH_3), 1.43 (m, 2H, $CH_2CH_2CH_3$), 1.87 (m, 2H, $CH_2CH_2CH_2$), 2.97 (t, 2H, $ArCH_2$), 3.88 (s, 3H, OCH_3), 7.15 (m, 2H, Ar*H*), 7.27 (d, 1H, Ar*H*), 7.44 (m, 2H, Ar*H*), 7.81 (t, 2H, Ar*H*), 7.99 (d, 1H, Ar*H*), 8.04 (dd, 1H, Ar*H*), 8.47 (s, 1H, Ar*H*), 8.85 (dd, 1H, Ar*H*), 10.80 (s, 1H, N*H*) ppm. **^{13}C NMR** ($CDCl_3$), δ: 13.92 (CH_3), 22.25 (CH_2), 32.86 (CH_2), 33.30 (CH_2), 104.69 (Ar*C*), 118.76 (Ar*C*), 121.10 (Ar*C*), 123.52 (Ar*C*), 124.37 (Ar*C*), 125.54 (Ar*C*), 126.30 (Ar*C*), 127.19 (Ar*C*), 129.77 (Ar*C*), 135.53 (Ar*C*), 158.27 (Ar*C*), 160.03 (*C*=O) ppm.

4.5.6. N-(2-butylquinolin-8-yl)-3,5-dimethoxy-2-naphthamide (36)

^{1}H NMR ($CDCl_3$), δ: 0.91 (t, 3H, CH_2CH_3), 1.39 (m, 2H, $CH_2CH_2CH_3$), 1.79 (m, 2H, $CH_2CH_2CH_2$), 2.98 (t, 2H, $ArCH_2$), 3.96 (s, 3H, OCH_3), 4.23 (s, 3H, OCH_3), 6.81 (d, 1H, Ar*H*), 7.27 (m, 2H, Ar*H*), 7.45 (m, 3H, Ar*H*), 7.65 (s, 1H, Ar*H*), 8.00 (d, 1H, Ar*H*), 8.78 (s, 1H, Ar*H*), 9.02 (d, 1H, Ar*H*), 12.19 (s, 1H, N*H*) ppm. **^{13}C NMR** ($CDCl_3$), δ: 13.99 (CH_3), 22.68 (CH_2), 32.34 (CH_2), 39.14 (CH_2), 55.57 (OCH_3), 56.10 (OCH_3), 101.36 (Ar*C*), 105.87 (Ar*C*), 117.87 (Ar*C*), 121.41 (Ar*C*), 121.57 (Ar*C*), 121.62 (Ar*C*), 123.80 (Ar*C*), 124.36 (Ar*C*), 126.49 (Ar*C*), 126.56 (Ar*C*), 127.89 (Ar*C*), 129.27 (Ar*C*), 130.16 (Ar*C*), 133.71 (Ar*C*), 135.13 (Ar*C*), 136.59 (Ar*C*), 138.63 (Ar*C*), 154.10 (Ar*C*), 154.66 (Ar*C*), 161.06 (Ar*C*), 163.69 (*C*=O) ppm.

4.6. Syntheses of 2-benzofuran and 2-benzothiophene Left-Hand Side Derivatives

All the benzofuran and benzothiophene derivatives were synthesized by using coupling Method A except N-(4-heptilfenil)benzofuran-2-karboksamit which was synthesized by Method C.

4.6.1. N-(4-butphenyl)benzofuran-2-carboxamide (37)

^{1}H NMR ($CDCl_3$), δ: 0.94 (t, 3H, CH_2CH_3), 1.37 (m, 2H, $CH_2CH_2CH_3$), 1.61 (m, 2H, $CH_2CH_2CH_2$), 2.60 (t, 2H, $ArCH_2$), 7.19 (m, 2H, Ar*H*), 7.31 (m, 1H, Ar*H*), 7.43 (m, 1H, $ArCH_2$), 7.55 (m, 2H, Ar*H*), 7.65 (m, 3H, Ar*H*), 8.39 (s, 1H, N*H*) ppm.**^{13}C NMR** ($CDCl_3$), δ: 13.95 (CH_3), 22.30 (CH_2), 33.62 (CH_2), 35.10 (CH_2), 111.23 (Ar*C*), 111.78 (Ar*C*), 120.08 (Ar*C*), 122.81 (Ar*C*), 123.86 (Ar*C*), 127.14 (Ar*C*), 127.73 (Ar*C*), 129.02 (Ar*C*), 134.83 (Ar*C*), 139.60 (Ar*C*),), 148.63 (Ar*C*), 154.78 (Ar*C*) 156.51 (*C*=O) ppm. **M (+1):** 294.14.

4.6.2. N-(4-pentylphenyl)benzofuran-2-carboxamide (38)

^{1}H NMR ($CDCl_3$), δ: 0.89 (t, 3H, CH_2CH_3), 1.33 (m, 4H, $CH_2CH_2CH_3$), 1.62 (m, 2H, $CH_2CH_2CH_2$), 2.60 (t, 2H, $ArCH_2$), 7.20 (m, 2H, Ar*H*), 7.33 (m, 1H, Ar*H*), 7.46 (m, 1H, Ar*H*), 7.59 (m, 4H, Ar*H*), 7.70 (m, 1H, Ar*H*), 8.32 (s, 1H, N*H*) ppm. **^{13}C NMR** ($CDCl_3$), δ: 14.08 (CH_3), 22.57 (CH_2), 31.19 (CH_2), 31.46 (CH_2), 35.40 (CH_2), 111.26 (Ar*C*), 111.80 (Ar*C*), 120.06 (Ar*C*), 122.83 (Ar*C*), 123.88 (Ar*C*), 127.15 (Ar*C*), 127.73 (Ar*C*), 129.03 (Ar*C*), 134.82 (Ar*C*), 139.64 (Ar*C*),), 148.60 (Ar*C*), 154.77 (Ar*C*) 156.52 (*C*=O) ppm.

4.6.3. N-(4-heptylphenyl)benzofuran-2-carboxamide (39)

^{1}H NMR ($CDCl_3$), δ: 0.89 (t, 3H, CH_2CH_3), 1.32 (m, 8H, $CH_2(CH_2)_4CH_3$), 1.61 (m, 2H, $CH_2CH_2(CH_2)_4$), 2.60 (t, 2H, $ArCH_2$), 7.19 (m, 2H, Ar*H*), 7.31 (m, 1H, Ar*H*), 7.44 (m, 1H, $ArCH_2$), 7.56 (m, 2H, Ar*H*), 7.63 (m, 2H, Ar*H*), 7.68 (m, 1H, Ar*H*), 8.35 (s, 1H, N*H*) ppm.

4.6.4. N-(4-butylphenyl)benzo[b]thiophene-2-carboxamide (40)

^{1}H NMR ($CDCl_3$), δ: 0.86 (t, 3H, CH_2CH_3), 1.28 (m, 2H, $CH_2CH_2CH_3$), 1.52 (m, 2H, $CH_2CH_2CH_2$), 2.52 (t, 2H, $ArCH_2$), 7.10 (d, 2H, ArH), 7.35 (m, 2H, ArH), 7.47 (d, 2H, ArH), 7.78 (m, 4H, ArH, NH). **^{13}C NMR** ($CDCl_3$), δ: 13.94 (CH_3), 22.28 (CH_2), 33.62 (CH_2), 35.09 (CH_2), 120.32 (ArC), 122.74 (ArC), 125.04 (ArC), 125.14 (ArC), 125.55 (ArC), 126.54 (ArC), 129.03 (ArC), 135.03 (ArC), 138.80 (ArC), 139.08 (ArC), 139.67 (ArC), 141.03 (ArC), 160.25 (C=O) ppm.

4.6.5. N-(4-hexylphenyl)benzo[b]thiophene-2-carboxamide (41)

^{1}H NMR ($CDCl_3$), δ: 0.82 (t, 3H, CH_2CH_3), 1.24 (m, 4H, $CH_2CH_2CH_2CH_3$), 1.50 (m, 4H, $CH_2CH_2CH_2CH_2$), 2.53 (t, 2H, $ArCH_2$), 7.12 (d, 2H, ArH), 7.37 (m, 2H, ArH), 7.47 (d, 2H, ArH), 7.70 (s, 1H, NH), 7.80 (m, 3H, ArH). **^{13}C NMR** ($CDCl_3$), δ: 14.09 (CH_3), 22.60 (CH_2), 28.90 (CH_2), 31.44 (CH_2), 31.71 (CH_2), 35.40 (CH_2), 120.26 (ArC), 122.76 (ArC), 125.07 (ArC), 125.14 (ArC), 125.55 (ArC), 126.56 (ArC), 129.04 (ArC), 135.01 (ArC), 138.77 (ArC), 139.07 (ArC), 139.71 (ArC), 141.02 (ArC), 160.17 (C=O) ppm.

4.7. Synthesis of Derivatives Obtained by Replacing Left-Hand Side with Various Aromatic Groups

4.7.1. N-(4-butylphenyl)-2-(2-methoxyphenoxy)acetamide (42)

Method C was used for the synthesis of this compound. **^{1}H NMR** ($CDCl_3$), δ: 0.94 (t, 3H, CH_2CH_3), 1.36 (m, 2H, $CH_2CH_2CH_3$), 1.59 (m, 2H, $CH_2CH_2CH_2$), 2.59 (t, 2H, $ArCH_2$), 3.91 (s, 3H, OCH_3), 4.63 (s, 2H, OCH_2CO), 6.95 (m, 3H, ArH), 7.04 (m, 1H, ArH), 7.16 (m, 2H, ArH), 7.52 (m, 2H, ArH), 8.97 (s, 1H, NH) ppm. **^{13}C NMR** ($CDCl_3$), δ: 13.95 (CH_3), 22.27 (CH_2), 33.65 (CH_2), 35.07 (CH_2), 55.90 (OCH_3), 70.51 (OCH_2Ar), 112.17 (ArC), 116.61 (ArC), 119.93(ArC), 121.36 (ArC), 123.60 (ArC), 128.92 (ArC), 134.90 (ArC), 139.30 (ArC), 147.37 (ArC), 149.90 (ArC), 166.78 (C=O) ppm. **M (+1):** 314.17.

4.7.2. N-(4-butylphenyl)-3-phenoxypropanamide (43)

Method B was used for the synthesis of this compound. **^{1}H NMR** ($CDCl_3$), δ: 0.91 (t, 3H, CH_2CH_3), 1.33 (m, 2H, $CH_2CH_2CH_3$), 1.56 (m, 2H, $CH_2CH_2CH_2$), 2.56 (t, 2H, $ArCH_2$), 2.83 (t, 2H, *CH2*CO),4.33 (t, 2H, $ArOCH_2$), 6.97 (m, 3H, Ar*H*), 7.12 (d, 2H, Ar*H*), 7.31 (m, 2H, Ar*H*), 7.41 (d, 2H, Ar*H*), 7.80 (s, 1H, N*H*) ppm.**^{13}C NMR** ($CDCl_3$), δ: 13.92 (CH_3), 22.25 (CH_2), 33.63 (CH_2), 35.03 (CH_2), 37.66 (*CH2*CO), 64.15 ($ArOCH_2$), 114.61 (2C, Ar*C*), 120.00 (2C, Ar*C*), 121.47 (Ar*C*), 128.85 (2C, Ar*C*), 129.63 (2C, Ar*C*), 135.34 (Ar*C*), 139.10 (Ar*C*), 158.07 (Ar*C*), 168.73 (*C*=O) ppm. **M (+1):** 298.17.

4.7.3. N-(4-butylphenyl)biphenyl-3-carboxamide (44)

Method C was used for the synthesis of this compound. **^{1}H NMR** ($CDCl_3$), δ: 0.93 (t, 3H, CH_2CH_3), 1.36 (m, 2H, $CH_2CH_2CH_3$), 1.59 (m, 2H, $CH_2CH_2CH_2$), 2.60 (t, 2H, $ArCH_2$), 7.19 (d, 2H, Ar*H*), 7.39 (m, 1H, Ar*H*), 7.47 (m, 2H, $ArCH_2$), 7.55 (t, 3H, Ar*H*), 7.63 (dd, 2H, Ar*H*), 7.60 (m, 2H, Ar*H*), 7.78 (m, 2H, Ar*H*), 7.86 (s, 1H, N*H*), 8.07 (t, 1H, Ar*H*) ppm. **^{13}C NMR** ($CDCl_3$), δ: 13.93 (CH_3), 22.27 (CH_2), 33.64 (CH_2), 35.08 (CH_2), 120.22 (Ar*C*), 125.59 (Ar*C*), 125.87 (Ar*C*), 127.20 (2C, Ar*C*), 127.84 (2C, Ar*C*), 128.92 (2C, Ar*C*), 128.98 (2C,Ar*C*), 129.20 (Ar*C*), 130.40 (Ar*C*), 135.45 (Ar*C*), 135.72 (Ar*C*), 139.40 (Ar*C*), 140.122 (Ar*C*), 141.96 (Ar*C*), 159.93 (*C*=O) ppm. **M (+1):** 330.18

4.7.4. N-(4-butylphenyl)-2-naphthamide (45)

Method A was used for the synthesis of this compound. **^{1}H NMR** ($CDCl_3$), δ: 8.31 (s, 1H, N*H*), 7.86 (m, 5H, Ar*H*), 7.51 (m, 4H, Ar*H*), 7.14 (d, 2H, Ar*H*), 2.55 (t, 2H, CH_2), 1.54 (m, 2H, CH_2), 1.30 (m, 2H, CH_2), 0.87 (t, 3H, CH_3) ppm. **^{13}C NMR ($CDCl_3$),** δ: 13.95 (CH_3), 22.29 (CH_2CH_3), 33.66 ($CH_2CH_2CH_3$), 35.09 (OCH_2), 120.29 (Ar*C*), 123.56 (Ar*C*), 126.90 (Ar*C*), 127.45 (Ar*C*), 127.80 (Ar*C*), 127.83 (Ar*C*), 128.71 (Ar*C*), 128.95 (Ar*C*), 129.00 (Ar*C*), 132.31 (Ar*C*), 132.62 (Ar*C*), 134.82 (Ar*C*), 135.57 (Ar*C*), 139.38 (Ar*C*), 165.71 (*C*=O) ppm. **M (+1):** 304.16.

4.7.5. N-(4-butylphenyl)-6-methoxy-2-naphthamide (46)

The design, the synthesis and the characterization of this compound were done by Selda Erkoc and experimental details can be found in her PhD thesis [59].

4.7.6. N-(4-butylphenyl)quinoline-2-carboxamide (47)

Method C was used for the synthesis of this compound. **^{1}H NMR** ($CDCl_3$), δ: 0.94 (t, 3H, CH_2CH_3), 1.37 (m, 2H, $CH_2CH_2CH_3$), 1.61 (m, 2H, $CH_2CH_2CH_2$), 2.62 (t, 2H, $ArCH_2$), 7.24 (d, 2H, ArH), 7.65 (m, 1H, ArH), 7.79 (m, 3H, $ArCH_2$), 7.91 (d, 1H, ArH), 8.21 (d, 1H, ArH), 8.38 (dd, 2H, ArH), 10.19 (s, 1H, NH) ppm. **M (+1):** 305.16.

4.7.7. N-(4-butylphenyl)quinoline-3-carboxamide (48)

Method A was used for the synthesis of this compound. **1H NMR** (CD_3OD), δ: 0.93 (t, 3H, CH_2CH_3), 1.35 (m, 2H, $CH_2CH_2CH_3$), 1.59 (m, 2H, $CH_2CH_2CH_2$), 2.56 (t, 2H, $ArCH_2$), 7.1 (d, 2H, ArH), 7.59 (m, 3H, ArH), 7.79 (t, 1H, ArH), 7.86 (d, 1H, ArH), 8.12 (d, 1H, ArH), 8.25 (s, 1H, ArH) 8.63 (d, 1H, ArH), 9.33(s, 1H, NH) ppm. **M(+1):** 305.16

4.7.8. N-(4-butylphenyl)isoquinoline-3-carboxamide (49)

Method C was used for the synthesis of this compound. **^{1}H NMR** ($CDCl_3$), δ: 0.86 (t, 3H, CH_2CH_3), 1.29 (m, 2H, $CH_2CH_2CH_3$), 1.55 (m, 2H, $CH_2CH_2CH_2$), 2.54 (t, 2H, $ArCH_2$), 7.15 (t, 2H, ArH), 7.67 (m, 4H, ArH), 7.96 (q, 2H, $ArCH_2$), 8.63 (s, 1H, ArH), 9.12 (s, 1H, ArH), 10.103 (s, 1H, NH) ppm. **^{13}C-NMR** ($CDCl_3$), δ: 13.95 (CH_3), 22.31 (CH_2), 33.68 (CH_2), 35.13 (CH_2), 119.71 (2C,ArC), 120.60 (ArC), 127.70 (ArC), 128.19 (ArC), 128.94 (2C,ArC), 128.98 (ArC), 129.73 (ArC), 131.16 (2C, ArC), 135.58 (ArC), 136.13 (ArC), 138.94 (ArC), 143.66 (ArC), 150.94 (ArC), 162.39 (C=O) ppm.

4.7.9. 3-((4-butylphenyl)carbamoyl)isoquinoline 2-oxide (50)

A modified procedure of a literature work was used to synthesize this compound [104]. A solution of **49** (75 mg; 0.25 mmol) in dry DCM (3ml) was added 3-chloroperoxybenzoic

acid (92 mg, 0.37 mmol) and the resulting mixture was stirred at room temperature overnight. Solvent was removed by rotavap and the resulting crude product was purified by column chromatography using silica. **^{1}H NMR** ($CDCl_3$), δ: 0.86 (t, 3H, CH_2CH_3), 1.30 (m, 2H, $CH_2CH_2CH_3$), 1.54 (m, 2H, $CH_2CH_2CH_2$), 2.54 (t, 2H, $ArCH_2$), 7.13 (d, 1H, ArH), 7.63 (m, 4H, ArH), 7.75 (d, 1H, ArH), 7.92 (d, 1H, ArH) , 8.82 (s, 1H, ArH) , 8.95 (s, 1H, ArH), 13.59 (s, 1H, NH) ppm. **^{13}C NMR** ($CDCl_3$), δ: 13.69 (CH_3), 22.07 (CH_2), 33.39 (CH_2), 34.93 (CH_2), 120.75 (ArC), 124.61 (ArC), 128.68 (ArC), 130.06 (ArC), 130.88 (ArC), 135.14 (ArC), 136.74 (ArC), 137.85 (ArC), 139.32 (ArC), 157.16 (ArC), 199.40 (C=O) ppm.
M (+1): 321.15.

4.8. Synthesis of (R)- and (S)- Stereoisomers of the Lead Compound

(R)- and (S)- enantiomers of the lead compound were synthesized by coupling the corresponding commercially available chiral acids with 4-butylaniline using Method C.

4.8.1. (R)-N-(4-butylphenyl)-2,3-dihydrobenzo[b][1,4]dioxine-2-carboxamide (51)

^{1}H NMR ($CDCl_3$), δ: 0.85 (t, 3H, CH_2CH_3), 1.27 (m, 2H, $CH_2CH_2CH_3$), 1.49 (m, 2H, $CH_2CH_2CH_2$), 2.52 (t, 2H, $ArCH_2$), 4.19 (m, 1H, O-CH_aH_b-CH), 4.52 (d, 1H, O-CH_aH_b-CH), 4.72 (d, 1H, O-CH-CONH-), 6.86 (m, 3H, ArH), 6.97 (m, 1H, ArH), 7.09 (d, 2H, ArH), 7.39 (d, 2H, ArH), 8.12 (s, 1H, NH) ppm. **^{13}C NMR** ($CDCl_3$), δ: 12.91 (CH_3), 21.24 (CH_2), 32.60 (CH_2), 34.04 (CH_2), 64.38 (O-CH_2-), 72.29 (O-CH-CONH-), 116.13 (ArC), 116.78 (ArC), 119.08 (ArC), 121.01 (ArC), 121.68 (ArC), 127.95 (ArC), 127.97 (ArC), 133.13 (ArC), 138.89 (ArC), 138.91 (ArC), 140.41 (ArC), 142.28 (ArC), 163.91 (C=O) ppm.

4.8.2. (S)-N-(2,3-dihydrobenzo[b][1,4]dioxin-2-yl)-2-naphthamide (52)

^{1}H NMR ($CDCl_3$), δ: 0.85 (t, 3H, CH_2CH_3), 1.27 (m, 2H, $CH_2CH_2CH_3$), 1.51 (m, 2H, $CH_2CH_2CH_2$), 2.51 (t, 2H, $ArCH_2$), 4.19 (m, 1H, O-CH_aH_b-CH), 4.55 (d, 1H, O-CH_aH_b-CH), 4.72 (d, 1H, O-CH-CONH-), 6.86 (m, 3H, ArH), 6.97 (m, 1H, ArH), 7.09 (d, 2H, ArH), 7.39 (d, 2H, ArH), 8.13 (s, 1H, NH) ppm. **^{13}C NMR** ($CDCl_3$), δ: 12.91 (CH_3), 21.24 (CH_2), 32.60 (CH_2), 34.04 (CH_2), 64.38 (O-CH_2-), 72.29 (O-CH-CONH-), 116.13 (ArC), 116.78 (ArC),

119.08 (Ar*C*), 121.01 (Ar*C*), 121.68 (Ar*C*), 127.95 (Ar*C*), 127.97 (Ar*C*), 133.13 (Ar*C*), 138.89 (Ar*C*), 138.91 (Ar*C*), 140.41 (Ar*C*), 142.28 (Ar*C*), 163.91 (*C*=O) ppm.

4.9. Miscellaneous Derivatives of the Lead Compound

4.9.1. N-(4-butylphenyl)naphthalene-2-carbothioamide (53)

The reaction was done according to the literature procedure [105]. Compound **45** and Lawesson's reagent were dissolved in toluene and the reaction mixture was refluxed at 120^{o}C for 24 hours. The solution was then concentrated under reduced pressure. The crude product was purified by column chromatography using silica. **^{1}H NMR** ($CDCl_3$), δ: 0.86 (t, 3H, CH_2CH_3), 1.29 (m, 2H, $CH_2CH_2CH_3$), 1.53 (m, 2H, $CH_2CH_2CH_3$), 2.55 (t, 2H, $ArCH_2$), 7.16 (m, 2H, Ar*H*), 7.45 (m, 2H, Ar*H*), 7.60 (d, 2H, $ArCH_2$), 7.80 (m, 4H, Ar*H*), 8.14 (s, 1H, Ar*H*), 9.08 (s, 1H, N*H*) ppm.

4.9.2. N-(3-butylphenyl)-2-naphthamide (54)

Method A was used for the synthesis of this compound. **^{1}H NMR** ($CDCl_3$), δ: 0.94 (t, 3H, CH_2CH_3), 1.39 (m, 2H, $CH_2CH_2CH_3$), 1.64 (m, 2H, $CH_2CH_2CH_2$), 2.65 (t, 2H, $ArCH_2$), 7.00 (d, 1H, Ar*H*), 7.30 (t, 1H, Ar*H*), 7.50 (d, 1H, Ar*H*), 7.59 (m, 3H, Ar*H*),7.94 (m, 5H, Ar*H*) 8.38 (s, 1H, N*H*)ppm. **^{13}C NMR** ($CDCl_3$), δ: 13.97 (CH_3), 22.38 (CH_2), 33.56 (CH_2), 35.67 (CH_2), 117.56 (Ar*C*), 120.25 (Ar*C*), 123.57 (Ar*C*), 124.78 (Ar*C*), 126.89 (Ar*C*), 127.47 (Ar*C*), 127.79 (Ar*C*), 127.85 (Ar*C*), 128.69 (Ar*C*), 128.91 (Ar*C*), 128.95 (Ar*C*), 132.27 (Ar*C*), 132.59 (Ar*C*), 134.81 (Ar*C*), 137.93 (Ar*C*), 144.10 (Ar*C*), 165.79 (*C*=O) ppm. **M (+1):** 304.16.

4.9.3. N-(4-butylphenyl)benzamide (55)

Method B was used for the synthesis of this compound. **^{1}H NMR** ($CDCl_3$), δ: 0.86 (t, 3H, CH_2CH_3), 1.29 (m, 2H, $CH_2CH_2CH_3$), 1.53 (m, 2H, $CH_2CH_2CH_2$), 2.53 (t, 2H, $ArCH_2$), 7.12 (m, 2H, Ar*H*), 7.45 (m, 5H, Ar*H*), 7.68 (s, 1H, N*H*), 7.80 (m, 2H, Ar*H*) ppm. **M (+1):** 254.15.

4.9.4. 4-butyl-N-phenylbenzamide (56)

Method A was used for the synthesis of this compound. **^{1}H NMR** ($CDCl_3$), δ: 0.94 (t, 3H, CH_2CH_3), 1.37 (m, 2H, $CH_2CH_2CH_3$), 1.63 (m, 2H, $CH_2CH_2CH_2$), 2.68 (t, 2H, $ArCH_2$), 7.15 (m, 1H, Ar*H*), 7.30 (d, 2H, Ar*H*), 7.37 (m, 2H, Ar*H*), 7.63 (dd, 2H, Ar*H*), 7.76 (s, 1H, N*H*), 7.84 (m, 2H, Ar*H*) ppm. **M (+1):** 254.15.

4.10. Attempts to Synthesize O(8)-Heterocycle Substituted Derivatives of Compound 42 and N-Heterocycle Substituted Derivatives of Compound 45

4.10.1. N-(4-butylphenyl)-2-(2-hydroxyphenoxy)acetamide (58)

The synthesis was done according to the literature procedure. (2-hydroxyphenoxy)acetic acid (336 mg, 2 mmol) was added to 1 mL of acetic anhydride. Concentrated H_2SO_4 (2 drops) was added, at which point the reaction mixture became homogeneous. After stirring for 20 min at room temperature, the reaction was quenched by pouring into 4 mL of H_2O. After stirring for 5 min to destroy excess Ac_2O, the reaction was cooled to 0^oC. The precipitate that formed was collected and dried, giving 230 mg (55 %) of white crystalline 57. An analytical sample was prepared by recrystallization from EtOAc. The resulting product was used for the coupling reaction using Method C. However, the product obtained was not the desired compound but the deprotected compound N-(4-butylphenyl)-2-(2-hydroxyphenoxy)acetamide instead. **^{1}H NMR** ($CDCl_3$), δ: 0.89 (t, 3H, CH_2CH_3), 1.31 (m, 2H, $CH_2CH_2CH_3$), 1.54 (m, 2H, $CH_2CH_2CH_2$), 2.54 (t, 2H, $ArCH_2$), 4.64 (s, 2H, O-CH_2), 6.87 (m, 2H, Ar*H*), 6.96 (m, 2H, s), 7.10 (d, 2H, Ar*H*), 7.41 (d, 2H, Ar*H*), 8.293 (s, 1H, N*H*) ppm.

4.10.2. Attempt to Synthesize 2-(2-(6-methoxypyrazin-2yloxy)phenoxy)acetic Acid

To a solution of 2-(2-hydroxyphenoxy)acetic acid (200 mg, 1.19 mmol) in methanol (15 mL) was added 1 N NaOH (2.3 mL, 2.27 mmol). After 5 min the solution was concentrated to dryness and dried well in a vacuum oven to leave the disodium salt of acid, which was used for the next step without further purification.

In a flame dried 25-ml round bottom flask 2-iodo-1-methoxypyrazine is dissolved in dioxane (2 ml) under nitrogen atmosphere. Disodium salt of acid (80 mg, 0.38 mmol), TMEDA (3.6 mg, 0.03 mmol), and CuCl (19 mg, 0.19 mmol) were added respectively and the mixture was refluxed under nitrogen for 16 h. The solvent was removed in vacuo, and the residue was dissolved in 1 N NaOH and filtered. The filtrate was acidified with concentrated HCl, and the solution was extracted with ethyl acetate. The solvent was concentrated in vacuo and poured onto petroleum ether to give the crude product. According to TLC using EA as eluent, the starting materials were recovered.

4.10.3. Attempts to Synthesize N-(4-butylphenyl)-N-(1-methyl-1H-pyrazol-5-yl)-2-naphthamide (60)

4.10.3.1. 1st Method. A procedure from literature was applied [87]. In a 25-ml round bottom flask with a reflux condenser was mixed N-(4-butylphenyl)-2-naphthamide (50 mg, 0.165 mmol), 5-iodo-1-methylimidazole (39 mg, 0.13 mmol), K_3PO_4 (59 mg, 0.276 mmol), and 1ml toluene under N_2. A solution of $Cu(TMHD)_2$ (3mg, 0.007mmol) in 1ml dry toluene was added to the reaction mixture dropwise. The reaction mixture was then stirred and heated to 130°C for 24 h. The solvent was evaporated and the residue was dissolved in dichloromethane. The resulting solution was washed with water twice. The aqueous phases were combined and extracted with dichloromethane. The organic phases were combined, dried over Na_2SO_4 and the solvent was evaporated. The reaction was unsuccessful as the starting material was recovered.

4.10.3.1. 2nd Method. A procedure from literature was applied [88]. In a 25-ml round bottom flask with a reflux condenser was placed N-(4-butylphenyl)-2-naphthamide (60 mg, 0.198 mmol), K_2CO_3 (36.5 mg, 0.264 mmol), CuI (2.5 mg, 0.013 mmol), and L-proline (3.1 mg, 0.026 mmol) under N_2. The mixture was dissolved in dry DMSO at room temperature. The resulting mixture was refluxed at 150°C for 28 h. The mixture was cooled to room temperature and hydrolyzed with water. Ethyl acetate was added and the organic phase was separated. The organic phase was washed with brine, dried over Na_2SO_4, and the solvent was evaporated under reduced pressure. The crude product was purified by column chromatography but compound 60 wasn't obtained.

4.10.4. Attempt to Synthesize N-(4-butylphenyl)-1-methyl-1H-imidazol-5-amine Buchwald-Hartwig Coupling

The synthesis of N-(4-butylphenyl)-1-methyl-1H-imidazol-5-amine was planned according to the literature method [89]. In a 2-neck round bottom flask 4-butylaniline (17.9 mg, 0.12 mmol), 5-iodo-1-methyl-1H-pyrazole (100 mg, 0.48 mmol), Cu(II)TMHD (10.3 mg, 20 mol % with respect to amine) and KOtBu (40.5 mg, 0.36 mmol) in toluene (2 ml) were mixed at room temperature under nitrogen atmosphere. The reaction mixture was then heated in an oil bath at 120^{o}C for 40 h. The reaction mixture was cooled to room temperature and the solvent was removed under reduced pressure. The residue obtained was subjected to column chromatography but, the product wasn't obtained.

4.11. Synthesis of Isoquinoline Derivatives as Quinoline Bioisosteres

4.11.1. N-(isoquinolin-5-yl)-2-(2-methoxyphenoxy)acetamide (64)

Method C was used for the synthesis of this compound. **^{1}H NMR** ($CDCl_3$), δ: 3.86 (s, 3H, O-C*H*$_3$), 4.71 (s, 2H, O-C*H*$_2$-CO), 7.02 (m, 4H, Ar*H*), 7.59 (t, 1H, Ar*H*), 7.76 (m, 2H, Ar*H*), 8.40 (d, 1H, Ar*H*), 8.55 (br, 1H, Ar*H*), 9.24 (br, 1H, N*H*), 9.51 (s, 1H, Ar*H*). **^{13}C NMR** ($CDCl_3$), δ: 54.75 (O-*C*H$_3$), 69.04 (O-*C*H$_2$), 108.98 (Ar*C*), 110.99 (Ar*C*), 110.99 (Ar*C*), 114.86 (Ar*C*), 114.86 (Ar*C*), 120.32 (Ar*C*), 121.80 (Ar*C*), 122.60 (Ar*C*), 122.60 (Ar*C*), 123.65 (Ar*C*), 126.59 (Ar*C*), 127.83 (Ar*C*), 130.18 (Ar*C*), 146.04 (Ar*C*), 148.68 (Ar*C*), 166.19 (*C*=O) ppm.

4.11.2. N-(isoquinolin-5-yl)-1,2,3,4-tetrahydronaphthalene-2-carboxamide (65)

Method C was used for the synthesis of this compound. **^{1}H NMR** ($CDCl_3$), δ: 0.81 (br, 2H, CH$_2$C*H*$_2$CH), 2.07 (br; 1H, CH$_2$C*H*CH$_2$ and 2H, ArC-C*H*$_2$CH$_2$), 2.89 (s, 1H, ArC-CH*H*$_a$CH), 3.12 (s, 1H ArC-CH*H*$_b$CH), 7.12 (br, 2H, Ar*H*), 7.19 (br, 2H, Ar*H*), 7.34 (br, 1H, Ar*H*), 7.56 (s, 1H, Ar*H*), 7.75 (s, 1H, Ar*H*), 7.90 (s, 1H, Ar*H*), 8.19 (s, 1H, Ar*H*), 8.38 (br, 1H, Ar*H*), 9.16 (br, 1H, N*H*) ppm. **^{13}C NMR** ($CDCl_3$), δ: 25.73 (*C*H$_2$), 27.125 (*C*H$_2$), 28.51 (*C*H$_2$), 41.53 (*C*H), 124.10 (Ar*C*), 124.11 (Ar*C*), 125.16 (Ar*C*), 125.34 (Ar*C*), 125.37

(Ar*C*), 126.81 (Ar*C*), 126.90 (Ar*C*), 128.11 (Ar*C*), 128.21 (Ar*C*), 130.90 (Ar*C*), 130.92 (Ar*C*), 133.39 (Ar*C*), 133.43 (Ar*C*), 134.75 (Ar*C*), 134.80 (Ar*C*), 173.24 (*C*=O) ppm.

4.11.3. N-(isoquinolin-5-yl)-3-phenoxypropanamide (66)

Method C was used for the synthesis of this compound. **^{1}H NMR** ($CDCl_3$), δ: 2.96 (s, 2H, CH_2CH_2CO), 4.39 (s, 2H, CH_2CH_2OPh), 6.98 (m, 3H, Ar*H*), 7.30 (m, 2H, Ar*H*), 7.56 (m, 2H, Ar*H*), 7.74 (d, 1H, Ar*H*), 8.23 (d, 1H, Ar*H*), 8.42 (m, 2H, Ar*H*), 9.18 (s, 1H, N*H*) ppm. **^{13}C NMR** ($CDCl_3$), δ: 36.72 (CH_2CH_2CO), 63.27 (CH_2CH_2OPh), 112.70 (Ar*C*), 113.54 (Ar*C*), 113.61 (Ar*C*), 120.97 (Ar*C*), 122.84 (Ar*C*), 123.79 (Ar*C*), 126.38 (Ar*C*), 128.80 (Ar*C*), 128.83 (Ar*C*), 128.86 (Ar*C*), 128.92 (Ar*C*), 142.19 (Ar*C*), 151.94 (Ar*C*), 152.03 (Ar*C*), 152.79 (Ar*C*), 168.61 (*C*=O) ppm.

4.11.4. N-(4-butylphenyl)isoquinoline-6-carboxamide (67)

Method C was used for the synthesis of this compound. **^{1}H NMR** ($CDCl_3$), δ: 0.88 (t, 3H, CH_2CH_3), 1.24 (m, 2H, $CH_2CH_2CH_3$), 1.54 (m, 2H, $CH_2CH_2CH_2$), 2.55 (t, 2H, $ArCH_2$), 7.14 (d, 2H, Ar*H*), 7.52 (d, 2H, Ar*H*), 7.67 (s, 1H, Ar*H*), 8.01 (m, 3H, Ar*H*) , 8.25 (s, 1H, Ar*H*), 8.54 (s, 1H, Ar*H*), 9.25 (s, 1H, N*H*). **^{13}C NMR** ($CDCl_3$), δ: 12.93 (CH_3), 21.27 (CH_2), 32.61 (CH_2), 34.09 (CH_2), 119.41 (Ar*C*), 120.12 (Ar*C*), 124.19 (Ar*C*), 124.28 (Ar*C*), 124.82 (Ar*C*), 127.48 (Ar*C*), 128.03 (Ar*C*), 134.18 (Ar*C*), 134.22 (Ar*C*), 134.29 (Ar*C*), 135.70 (Ar*C*), 135.72 (Ar*C*), 138.91 (Ar*C*), 142.94 (Ar*C*), 151.43 (Ar*C*), 163.95 (*C*=O) ppm.

4.11.5. N-(2,3-dihydrobenzo[b][1,4]dioxin-6-yl)isoquinoline-6-carboxamide (68)

Method C was used for the synthesis of this compound. **^{1}H NMR** ($CDCl_3$), δ: 4.18 (s, broad, 4H, O-CH_2), 6.78 (d, 1H, Ar*H*), 7.00 (dd, 1H, Ar*H*), 7.24 (d, 1H, Ar*H*), 7.63 (d, 1H, Ar*H*) , 7.95 (m, 2H, Ar*H*), 8.08 (s, 1H, Ar*H*), 8.22 (s, 1H, Ar*H*), 8.51 (d, 1H, Ar*H*), 9.22 (s, 1H, N*H*). **^{13}C NMR** ($CDCl_3$), δ: 64.42 (OCH_2), 67.95 (OCH_2), 110.29 (Ar*C*), 114.05 (Ar*C*), 117.35 (Ar*C*), 121.16 (Ar*C*), 125.26 (Ar*C*), 125.84 (Ar*C*), 128.46 (Ar*C*), 131.28 (Ar*C*), 135.22 (Ar*C*), 136.66 (Ar*C*), 140.95 (Ar*C*), 143.59 (Ar*C*), 143.82 (Ar*C*), 152.37 (*C*=O) ppm.

4. CONCLUSION

In this work, the synthesis of new long chain alkyl substituted aromatic carboxamide derivatives as inhibitors of CYP17 were reported. Several potentially active heteroaromatic derivatives of the lead compound including quinoline, isoquinoline, benzothiophene, and benzofuran rings were designed and synthesized. Bioisosterism was employed as a tool for rational drug design approach. The characterization of the synthesized drug candidates were done by ^{1}H-NMR, ^{13}C-NMR , 2D NMR (COSY and NOESY), FT-IR, HRMS experiments.

A detailed SAR study was performed for *n*-butyl-8-aminoquinoline substituted derivatives. For this purpose, a systematic study on the synthesis of 8-aminoquinoline derivatives with an *n*-butyl group at each alternate position of the quinoline ring was carried out. Then, *n*-butyl substituted 8-aminoquinolines were coupled with several naphthoic acid derivatives to obtain candidate final products. However, none of the quinolines substituted derivatives were found to be active in *in vitro* tests.

Benzofuran and benzothiophene derivatives were proposed to bind even better to the heme Fe atom through their O and S atoms. Several benzofuran and benzothiophene derivatives with different alkyl chain lengths were designed, synthesized and their biological activities were tested *in vitro*. All these derivatives showed some activity in preliminary test at 5 μM. The IC_{50} values of *n*-butyl substituted benzofuran derivative 37 and *n*-butyl substituted benzothiophene derivative 40 were found to 25.5 μM and 15.4 μM, respectively indicating that it would be worth to focus on these derivatives in future work.

Bioisosteric transformations were performed by virtually breaking bonds on the lead compound to modify flexibility, so as to increase the potency. The bonds of the 2,3-dihydrobenzodioxine ring of the lead compound were virtually broken to get compound 42 whose IC_{50} was calculated to be 9.1 μM. Other derivatives of were designed by replacing 2,3-dihydrobenzodioxine ring with several other aromatic groups including phenyl, naphthyl, biphenyl, quinoline and isoquinoline rings. Within this group, the 6-methoxynaphthalene substituted derivative 46 was calculated to have an IC_{50} value of 27.1.

Compounds 42 and 46 can also be used as template in future work in search for more active molecules.

(R)- and (S)- enantiomers of the lead compound were synthesized by coupling the corresponding commercially available chiral acids with 4-butylaniline using Method C. Neither of the enantiomers were found to be potent in a preliminary screening done at 2.5 μM. More biological testing needs to be done at higher concentrations since the IC_{50} value of the racemate is 37.7 μM.

Various other miscellaneous derivatives of the lead compound were designed and synthesized by making bioisosteric replacements. A promising result of preliminary biological testing of 45 has led to several of its derivatives through a series of classical bioisosteric, non-classical bioisosteric, and retroisosteric transformations. The results of the biological tests for this series however were not promising since only the phenyl derivative 55 was found to have a mediocre result of 23.8 % inhibition at 5 μM.

A small series of isoquinoline carboxamide derivatives were proposed and synthesized as quinoline bioisosteres. The design concept includes a mimicry of the binding mode of the abiraterone to Fe of heme of CYP17 enzyme by using isoquinoline ring. The biological tests for these compounds will be done later on.

APPENDIX A: SPECTROSCOPY DATA

This section includes 1D NMR (^{1}H, ^{13}C NMR) and 2D NMR (COSY, NOESY) spectroscopy of the synthesized products. Expansions were made on the NMR data for easy interpretation.

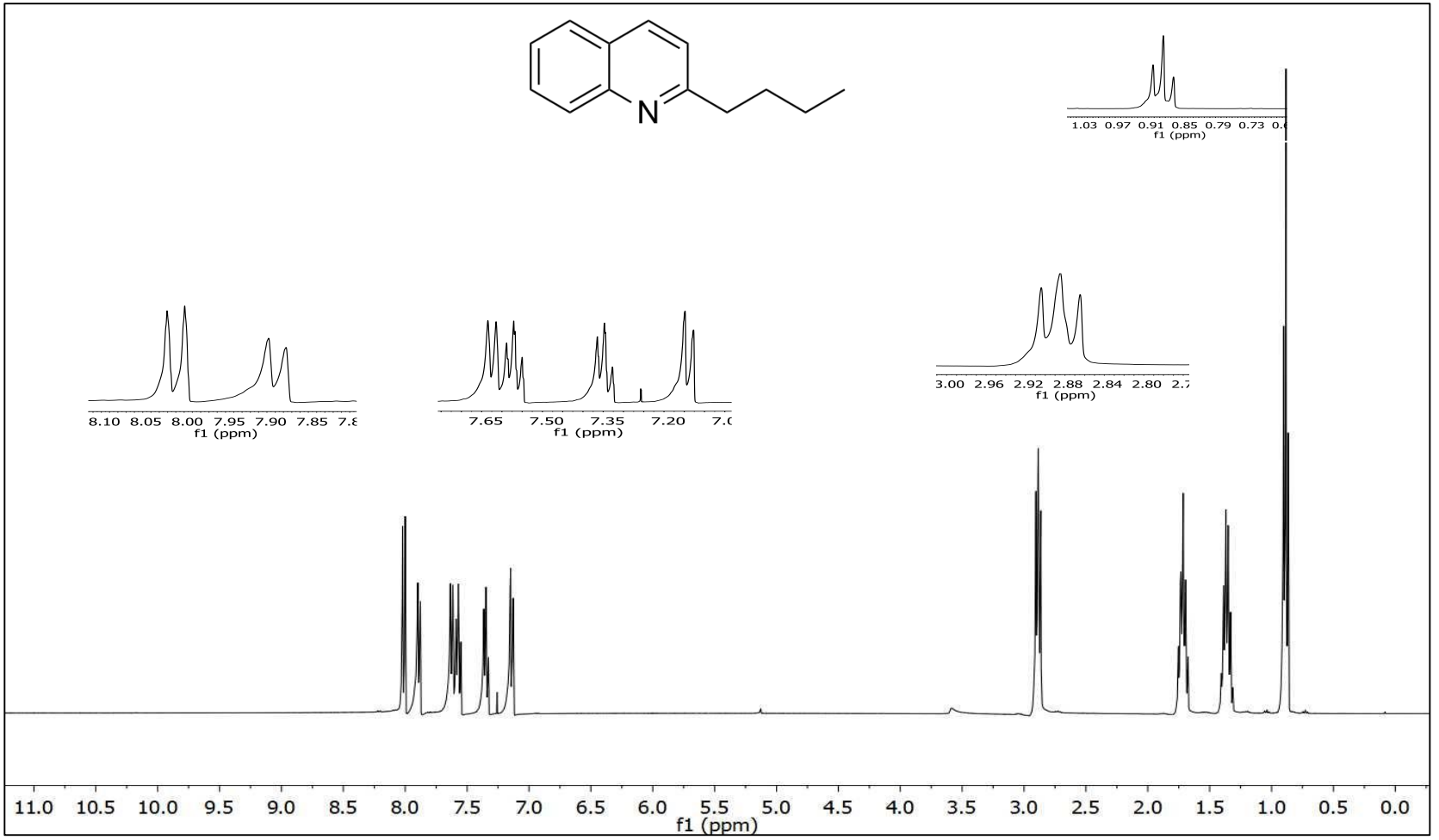

Figure A.1. ^{1}H-NMR Spectrum of 2-butylquinoline.

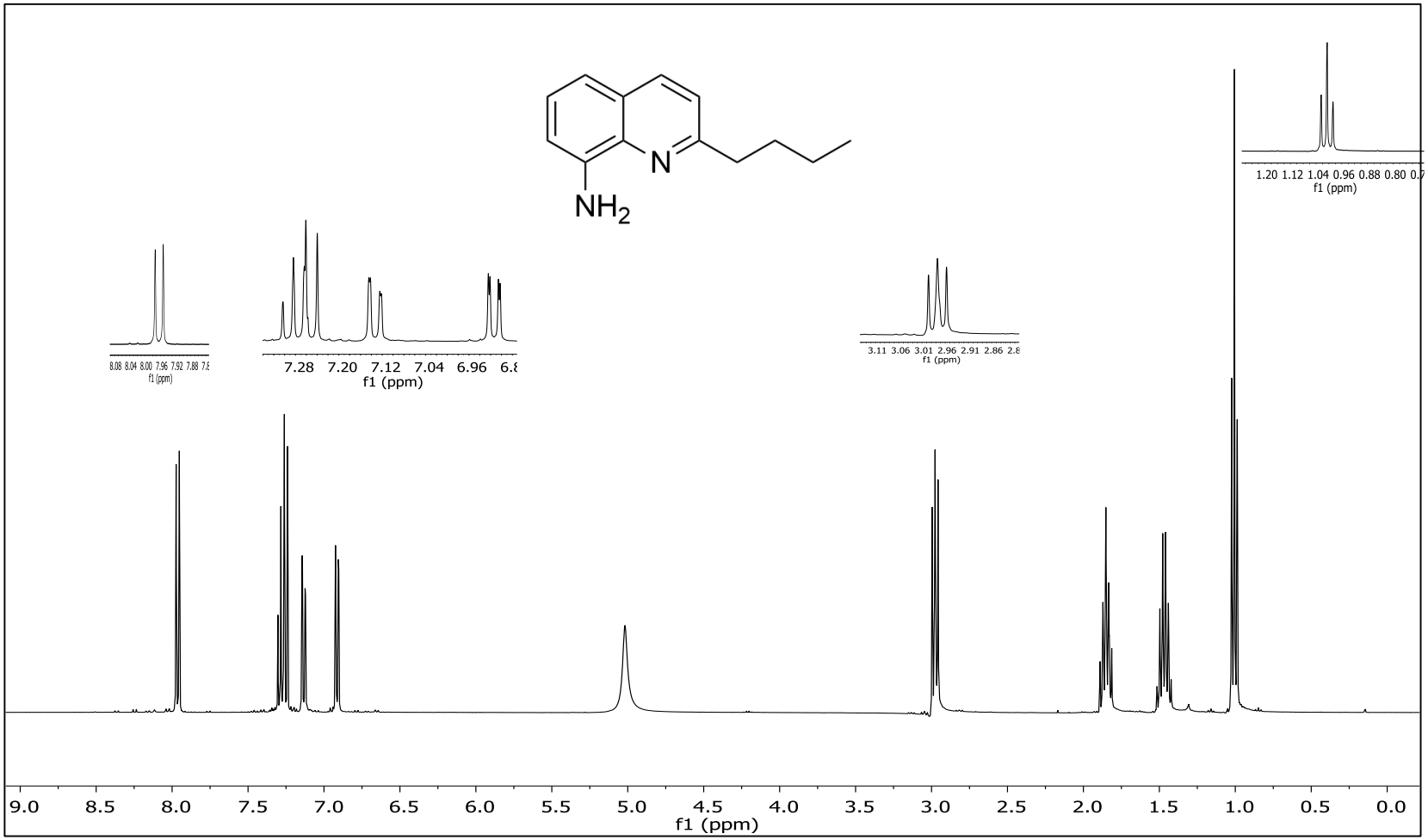

Figure A.2. ^{1}H-NMR Spectrum of 8-amino-2-butylquinoline.

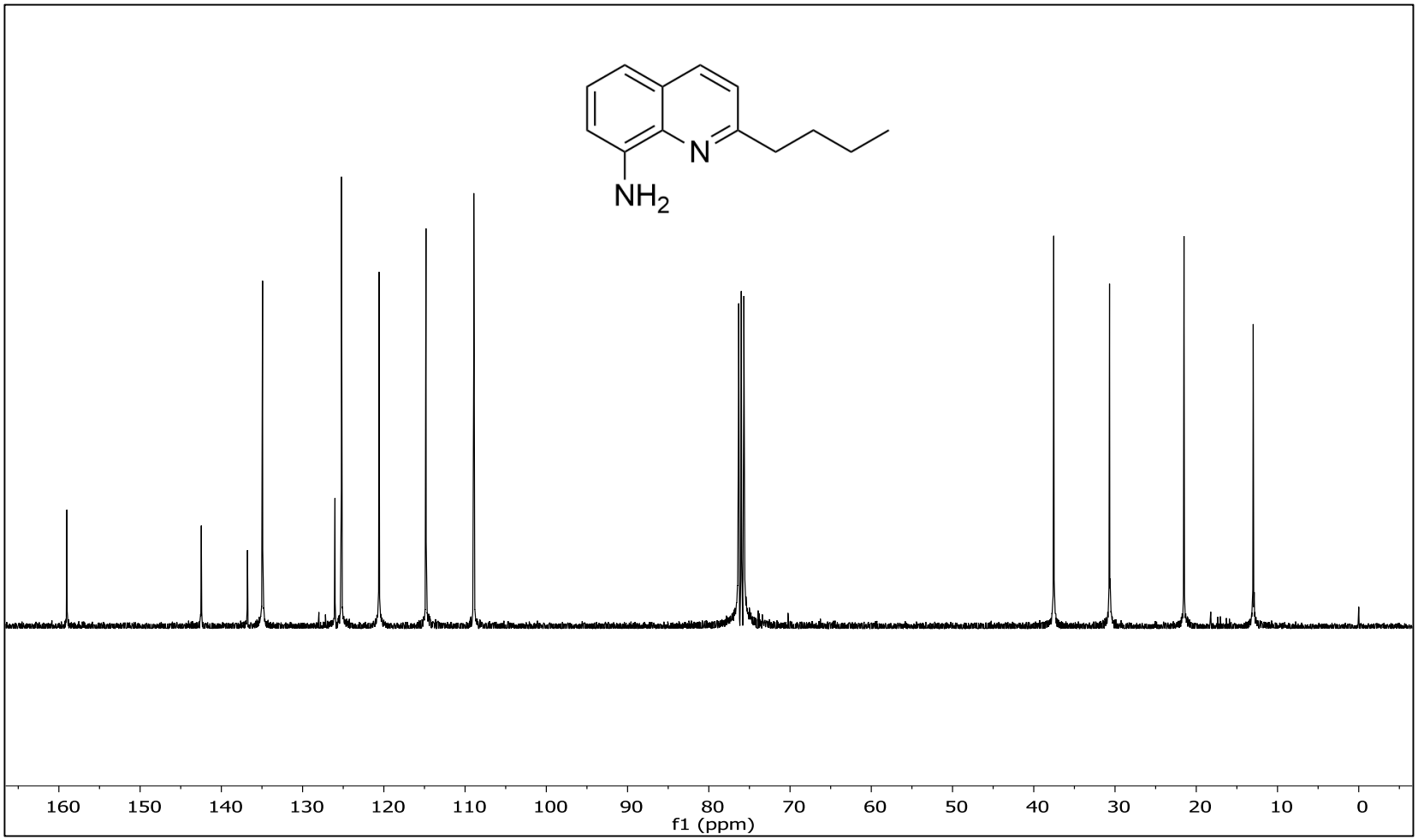

Figure A.3. ^{13}C-NMR Spectrum of 8-amino-2-butylquinoline.

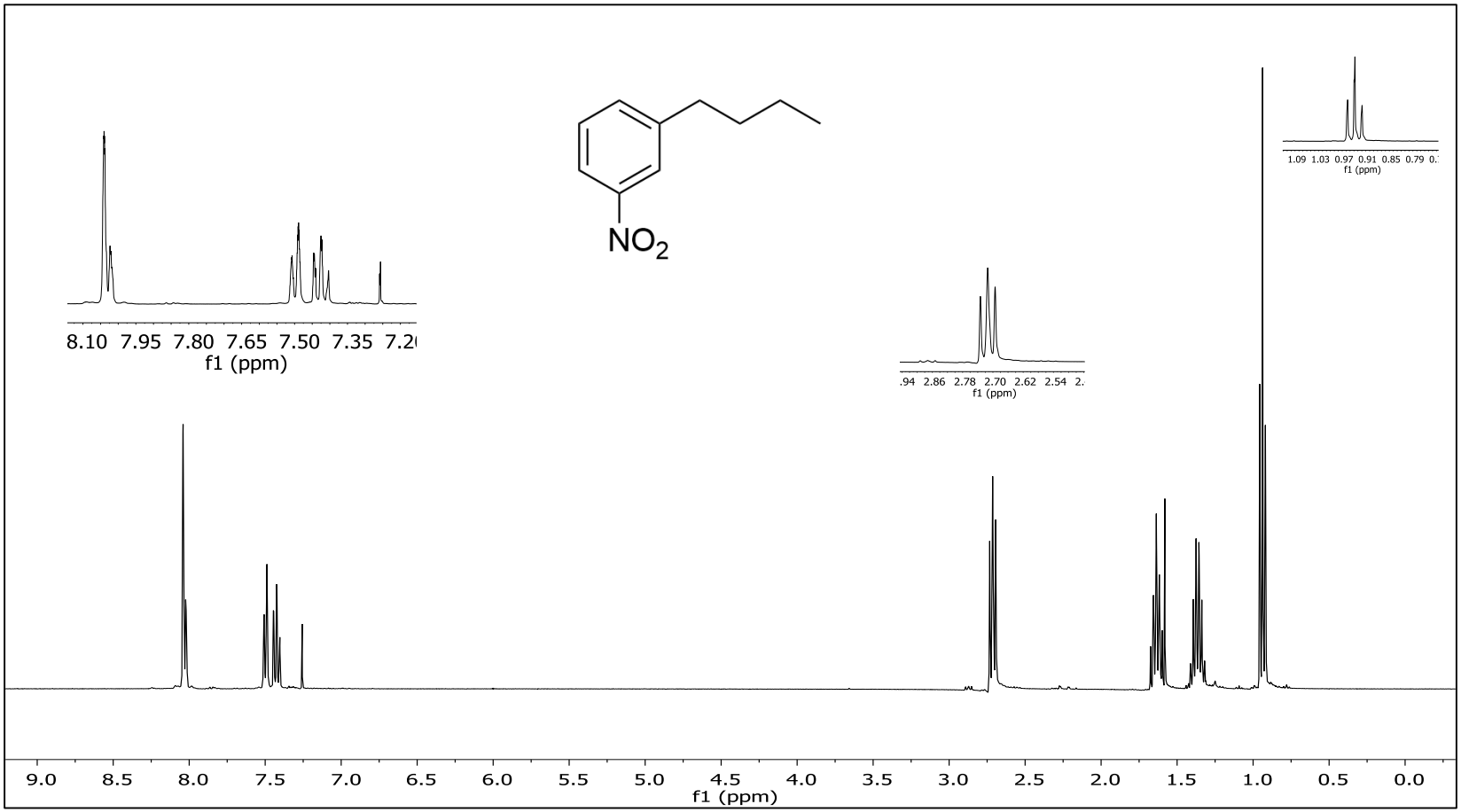

Figure A.4. ^{1}H-NMR Spectrum of 1-butyl-3-nitrobenzene.

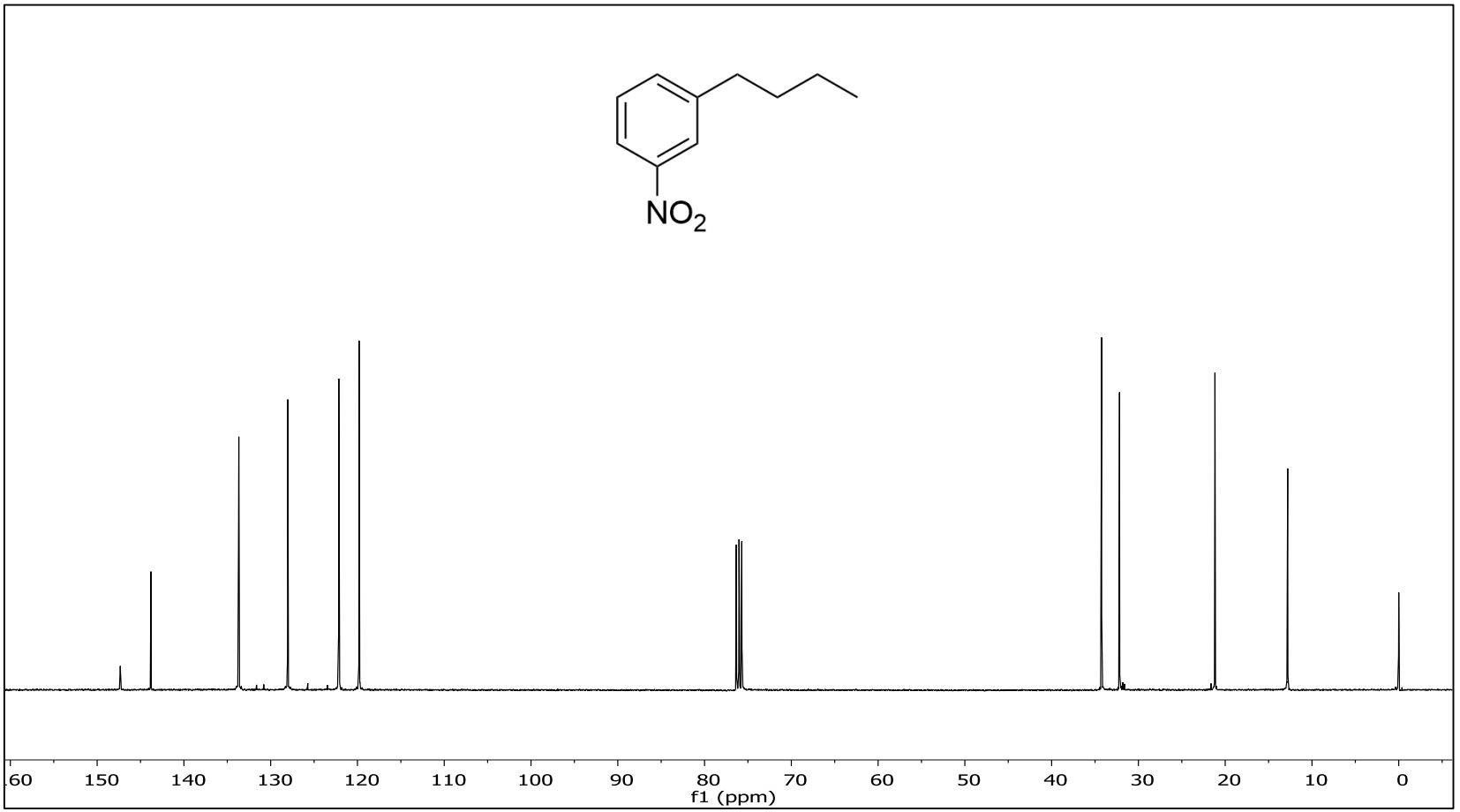

Figure A.5. ^{13}C-NMR Spectrum of 1-butyl-3-nitrobenzene.

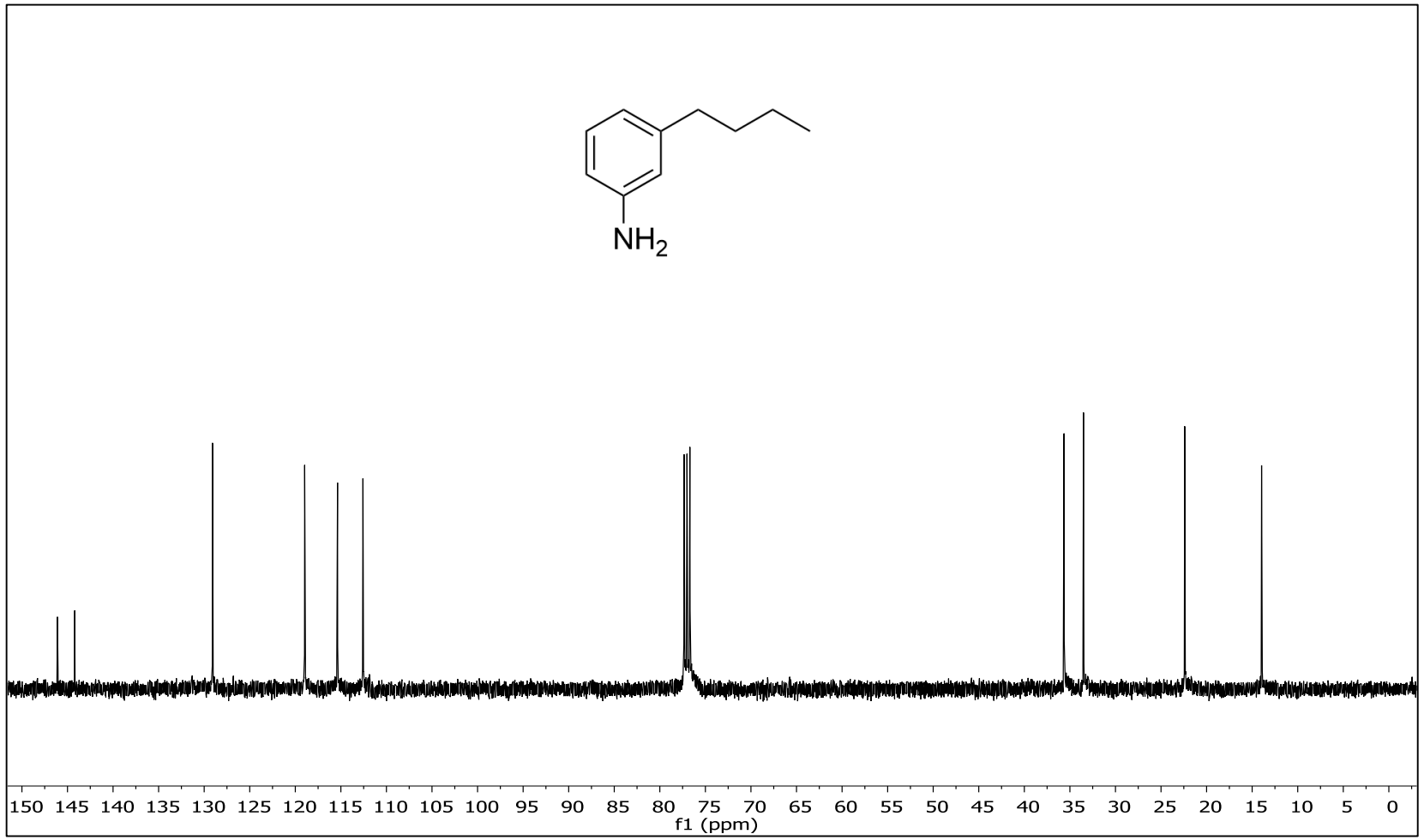

Figure A.6. ^{1}H-NMR Spectrum of 3-butylaniline.

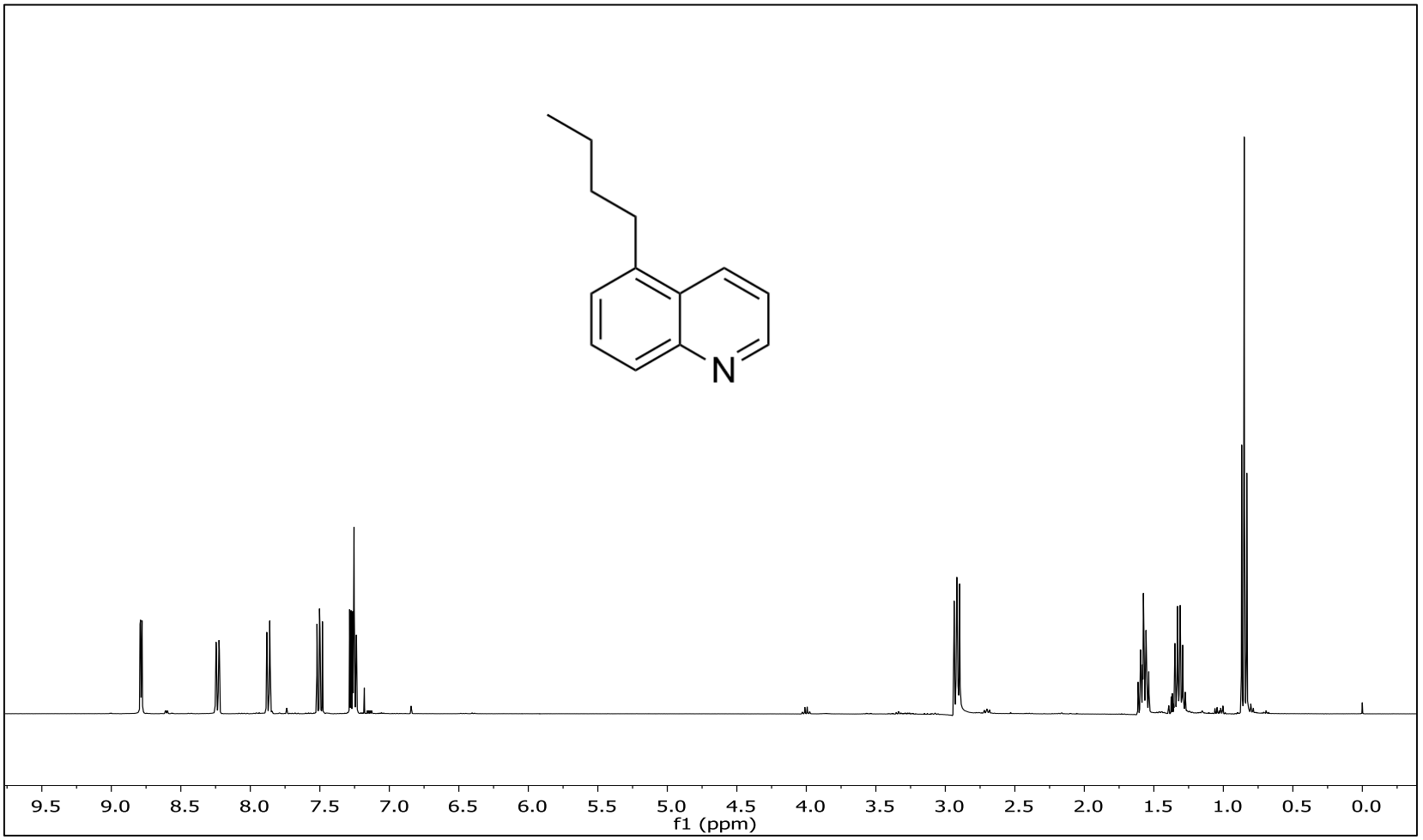

Figure A.7. ^{1}H-NMR Spectrum of 5-butylquinoline.

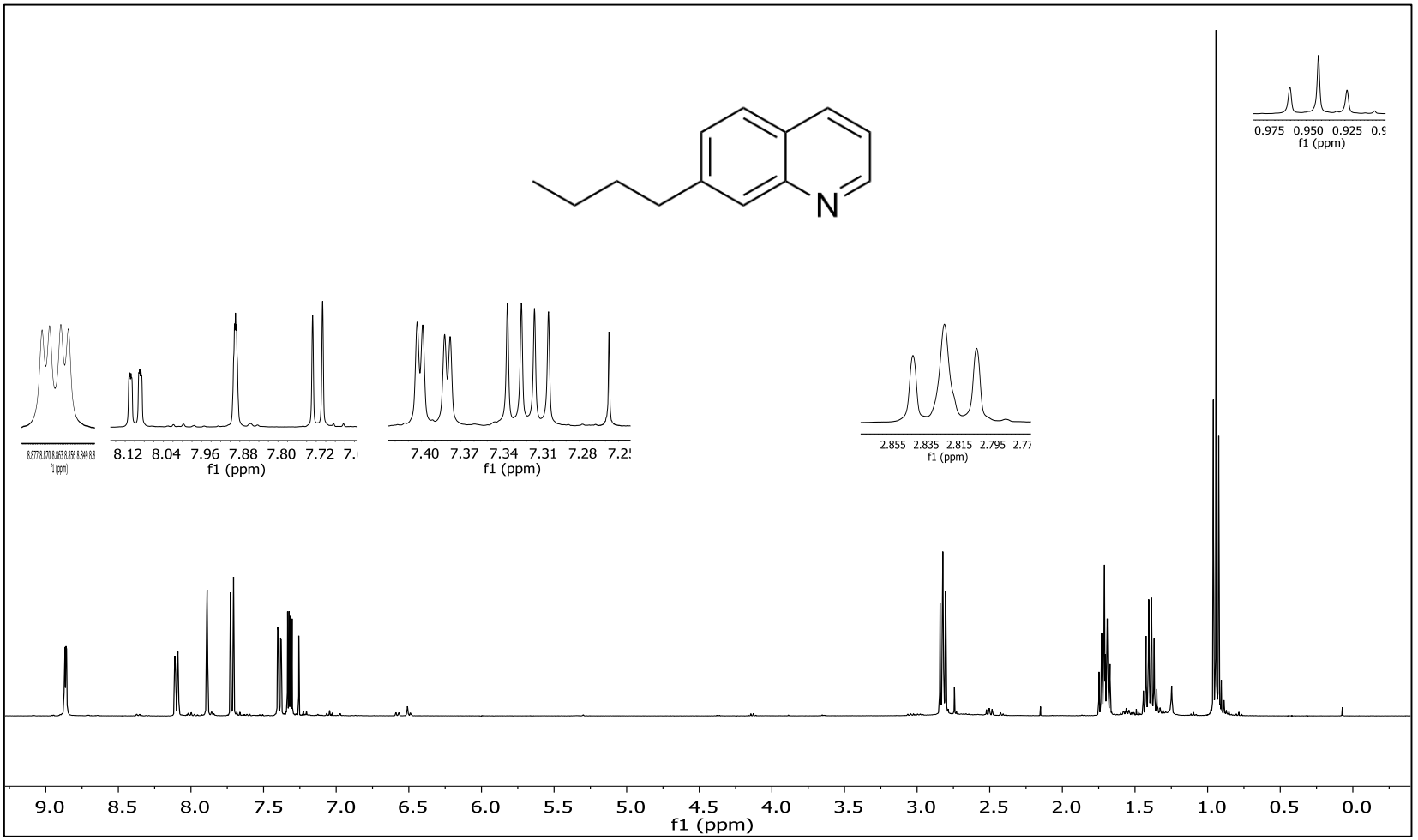

Figure A.8. ^{1}H-NMR Spectrum of 7-butylquinoline.

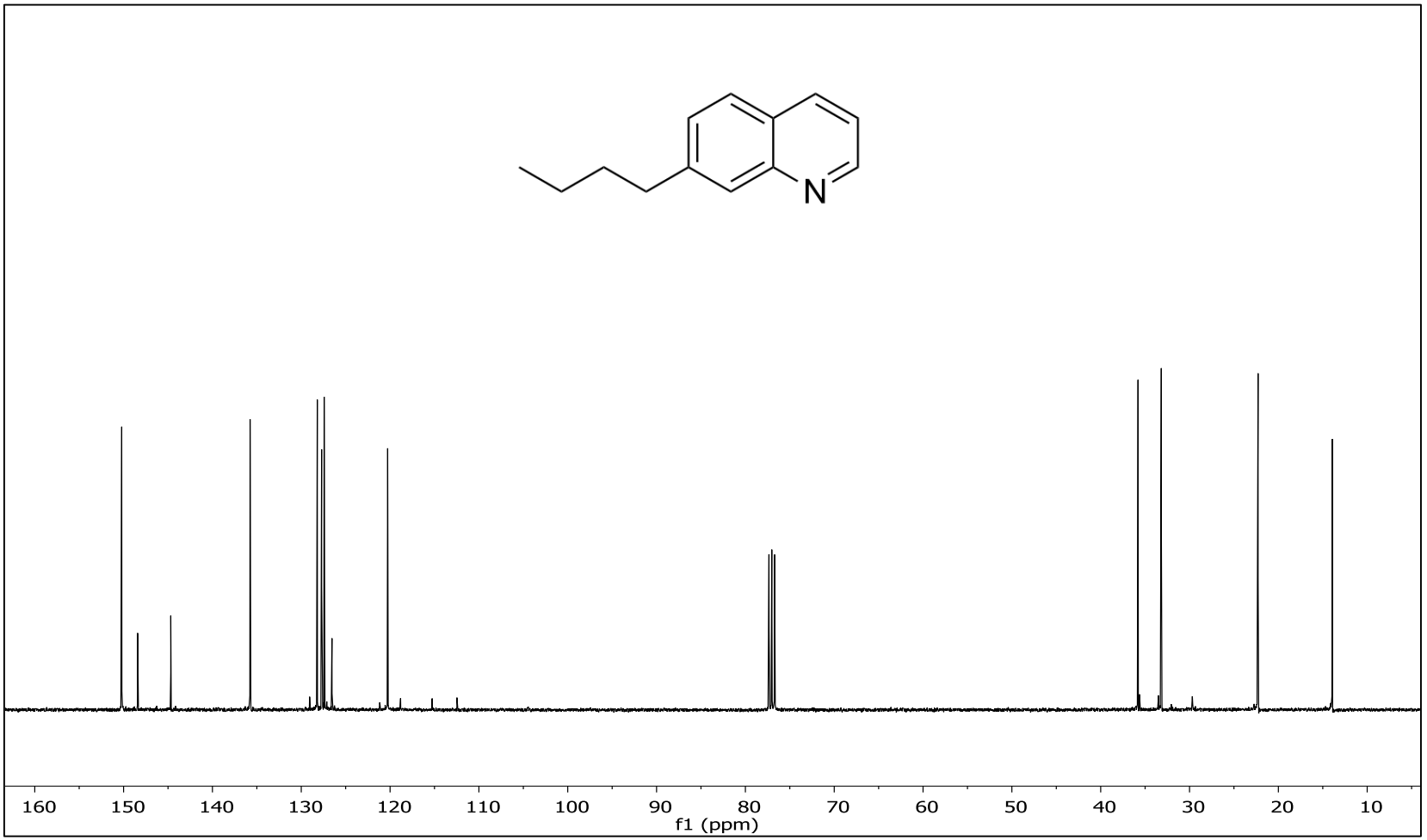

Figure A.9. ^{13}C-NMR Spectrum of 7-butylquinoline.

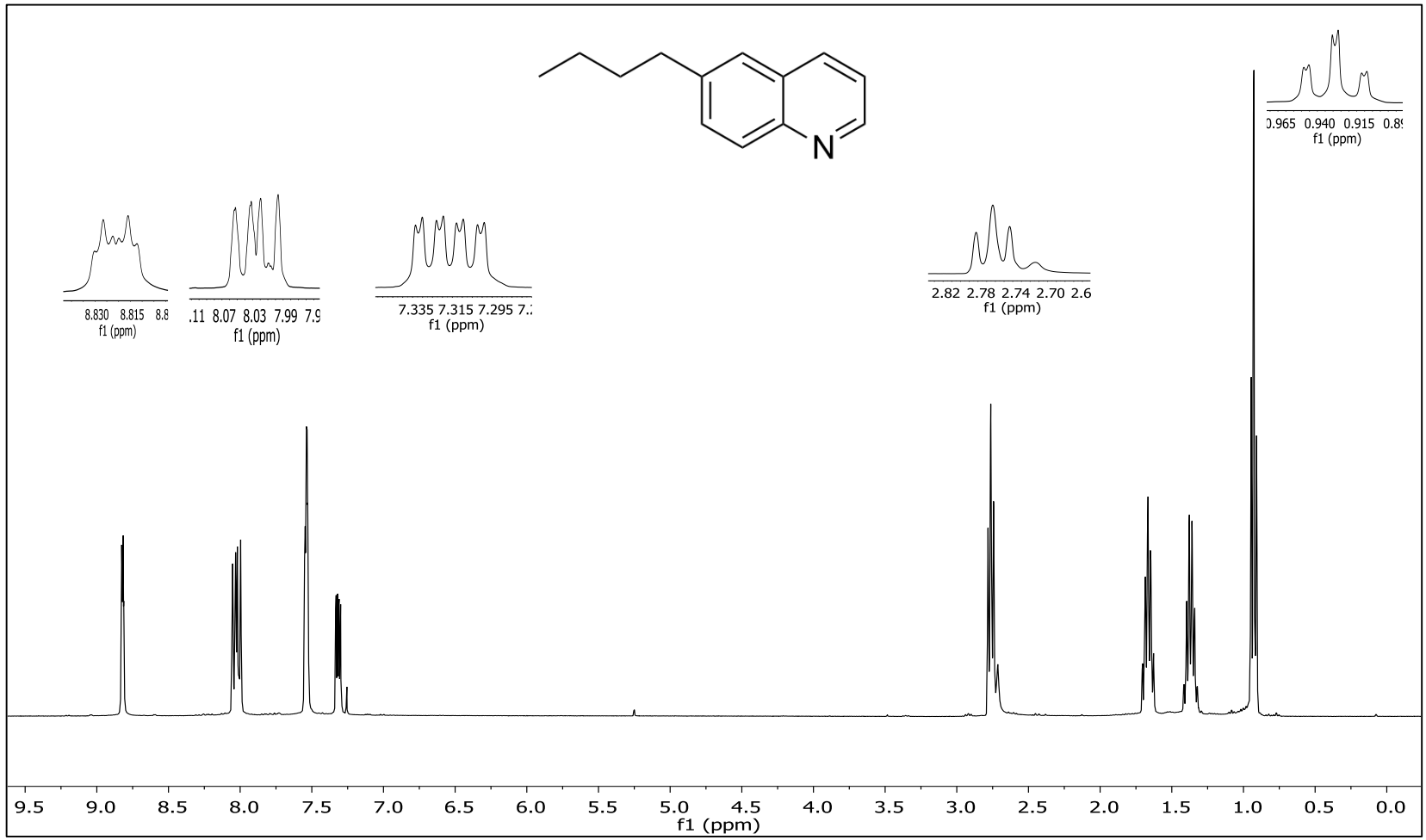

Figure A.10. ^{1}H-NMR Spectrum of 6-butylquinoline.

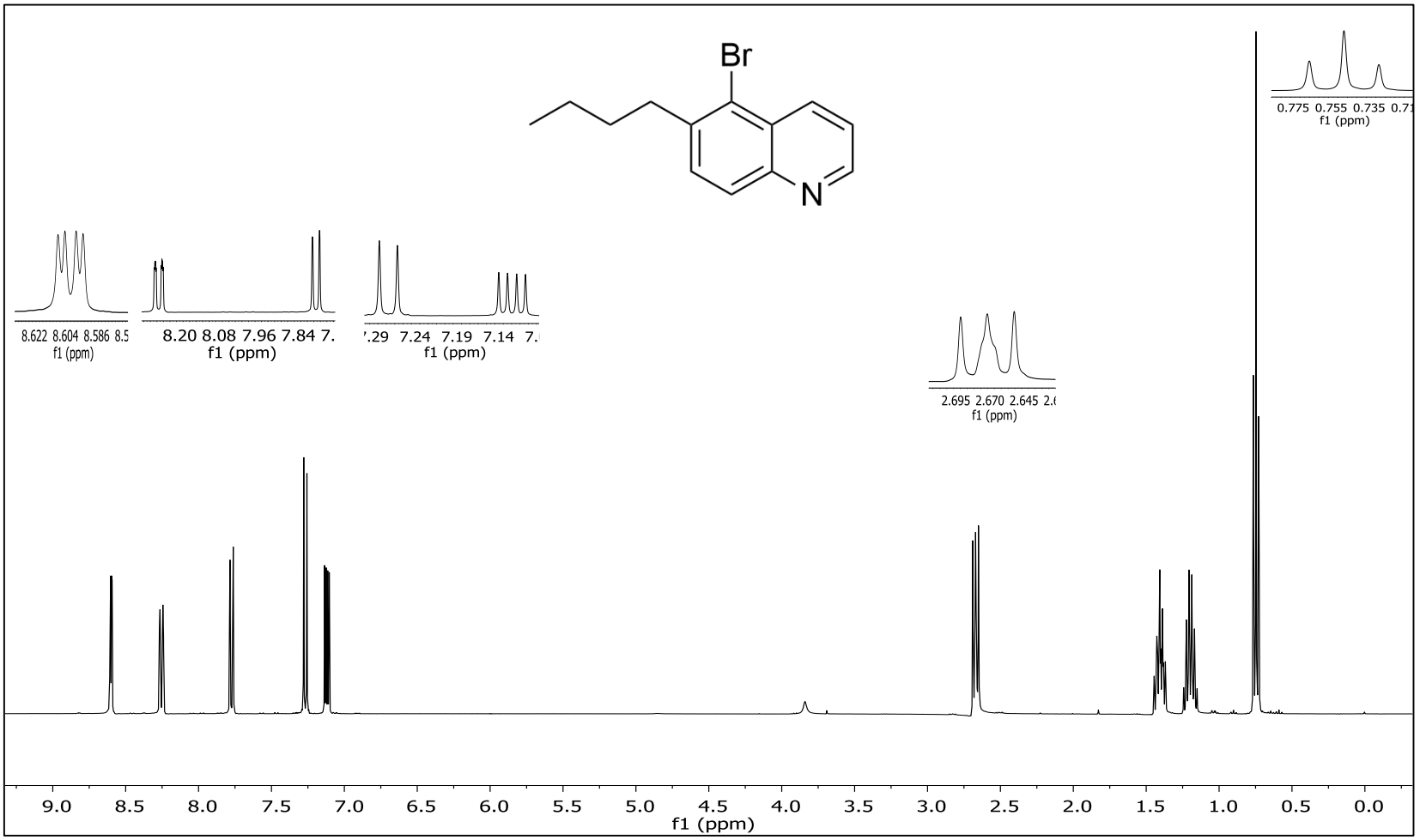

Figure A.11. ^{1}H-NMR Spectrum of 5-bromo-6-butylquinoline.

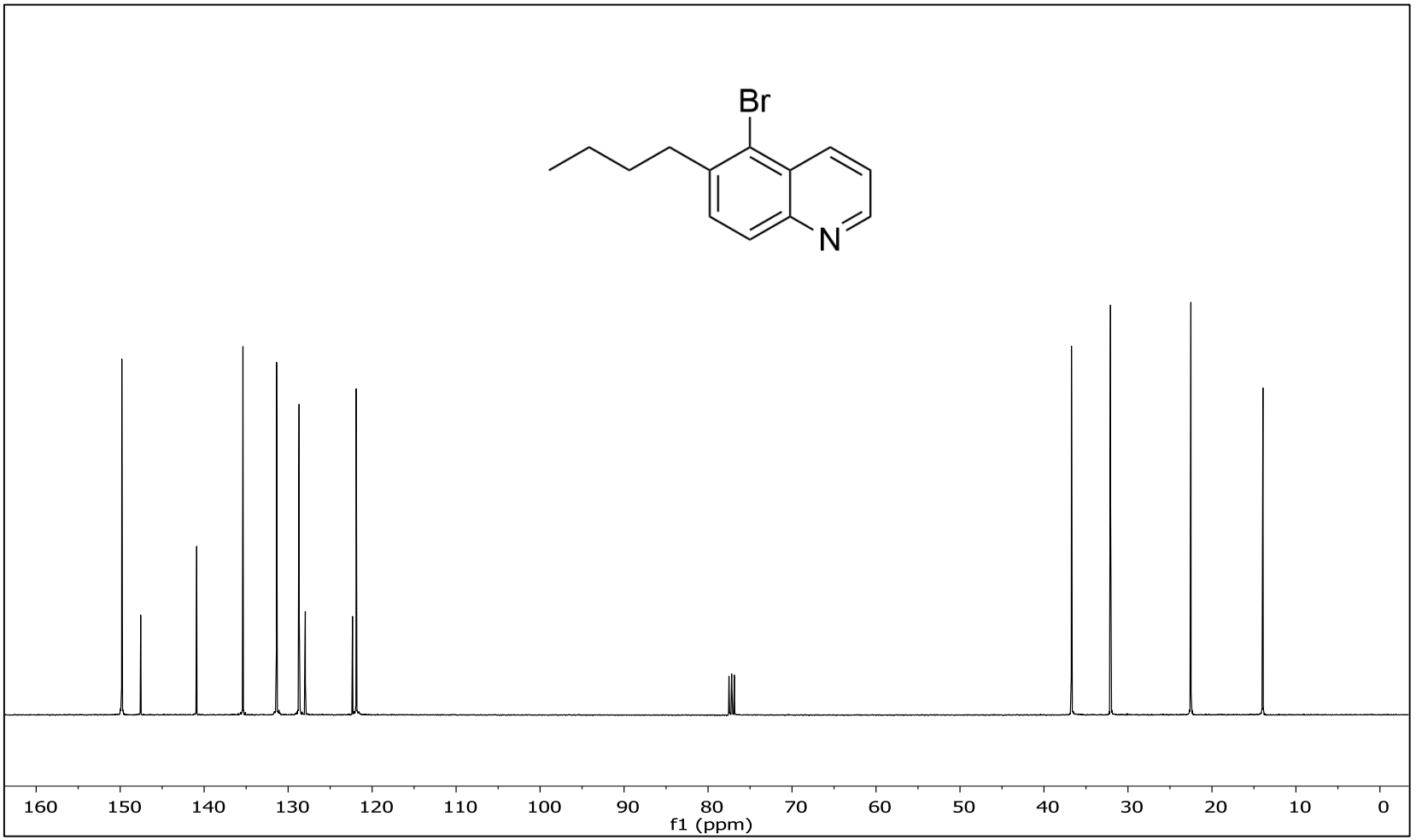

Figure A.12. ^{13}C-NMR Spectrum of 5-bromo-6-butylquinoline.

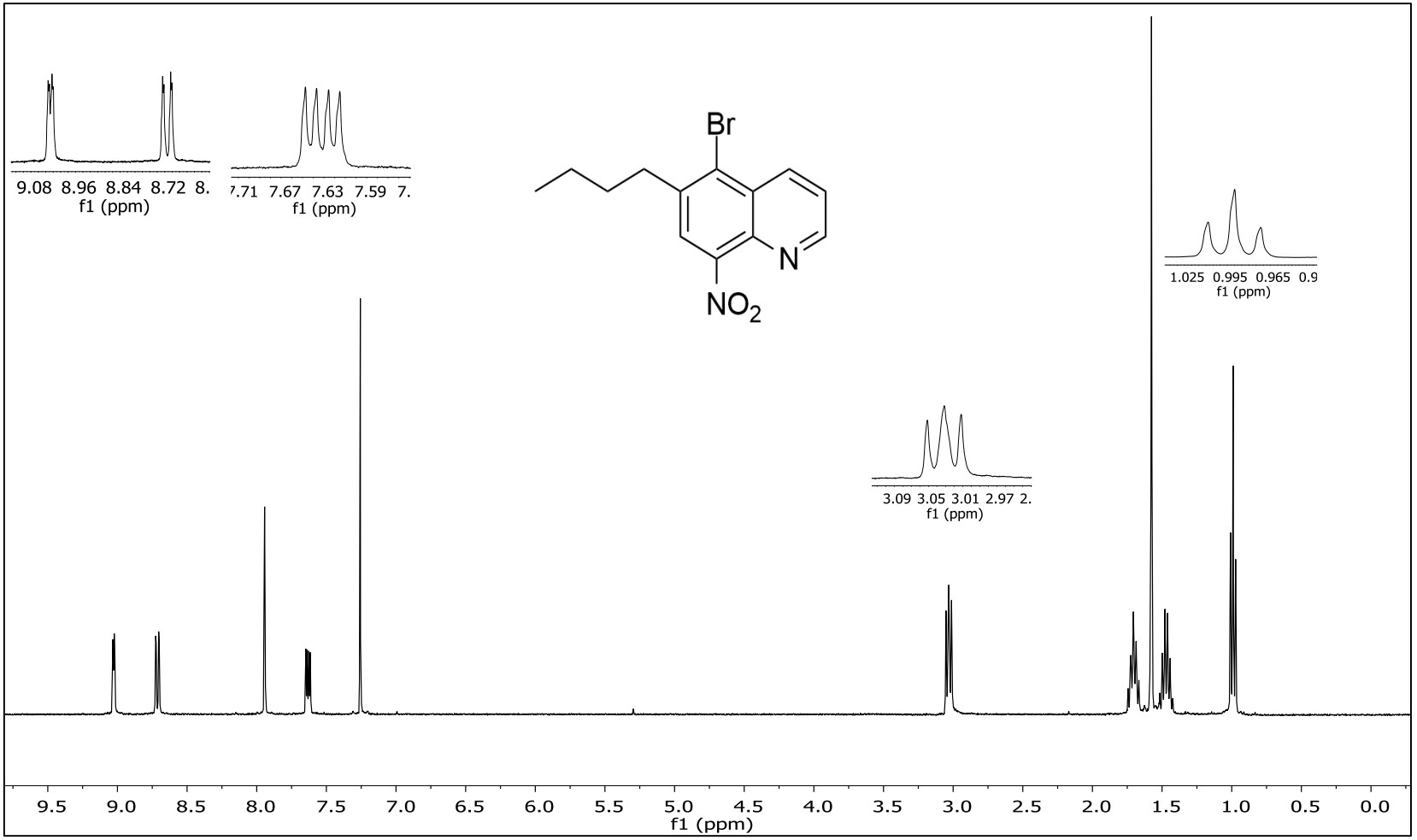

Figure A.13. ^{1}H-NMR Spectrum of 5-bromo-6-butyl-8-nitroquinoline.

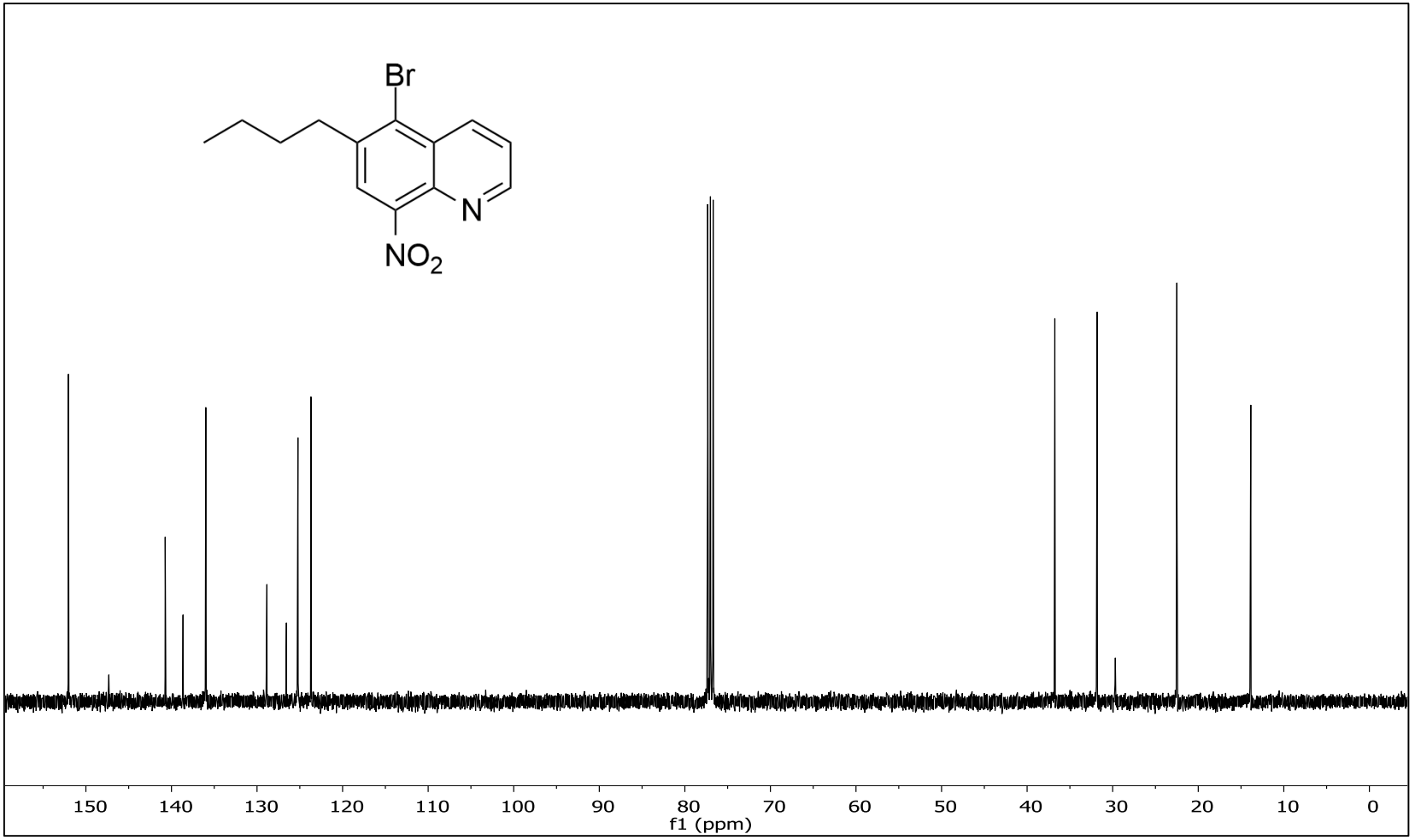

Figure A.14. ^{13}C-NMR Spectrum of 5-bromo-6-butyl-8-nitroquinoline.

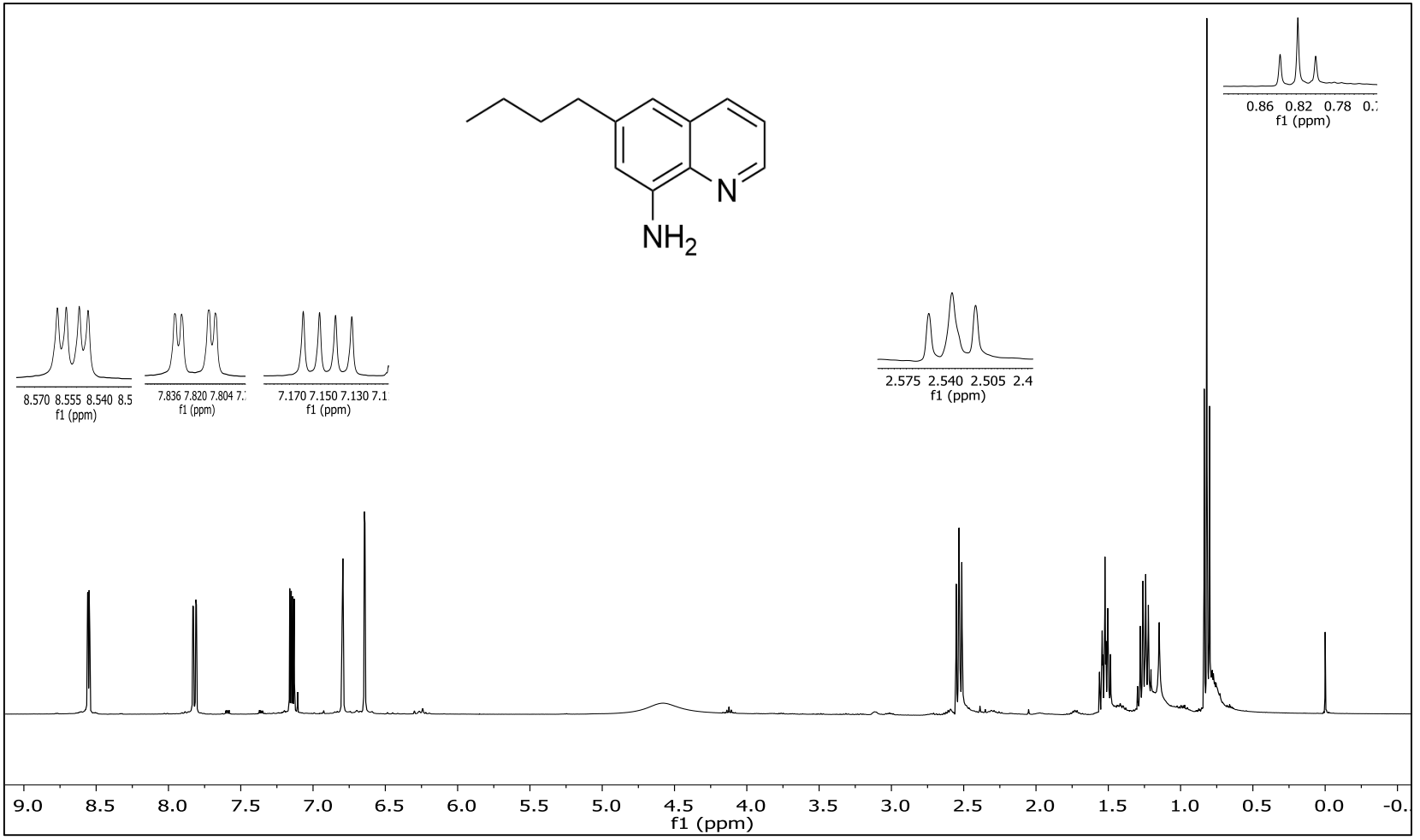

Figure A.15. ^{1}H-NMR Spectrum of 8-amino-6-butylquinoline.

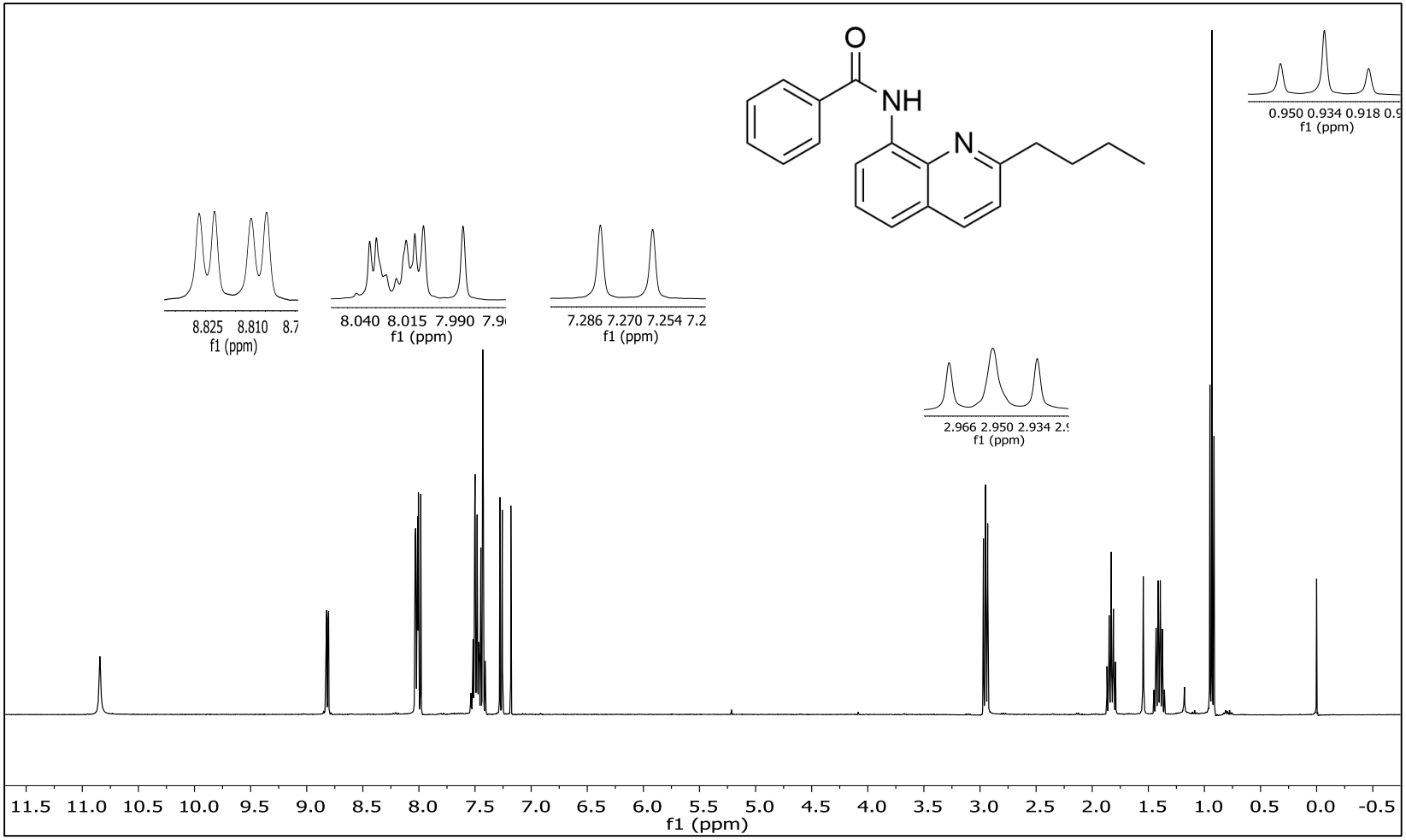

Figure A.16. ^{1}H-NMR Spectrum of N-(2-butylquinolin-8-yl)benzamide.

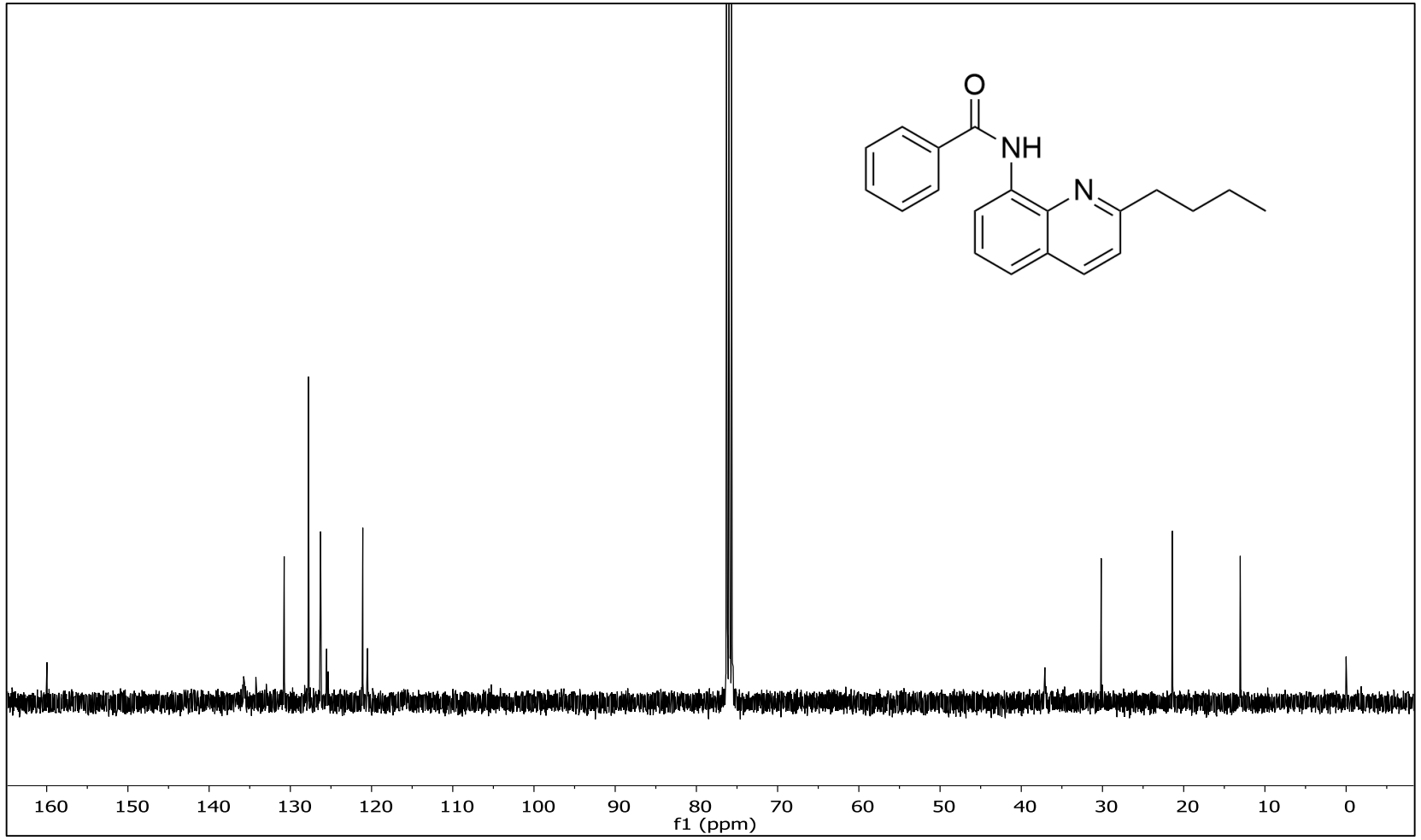

Figure A.17. ^{13}C-NMR Spectrum of N-(2-butylquinolin-8-yl)benzamide.

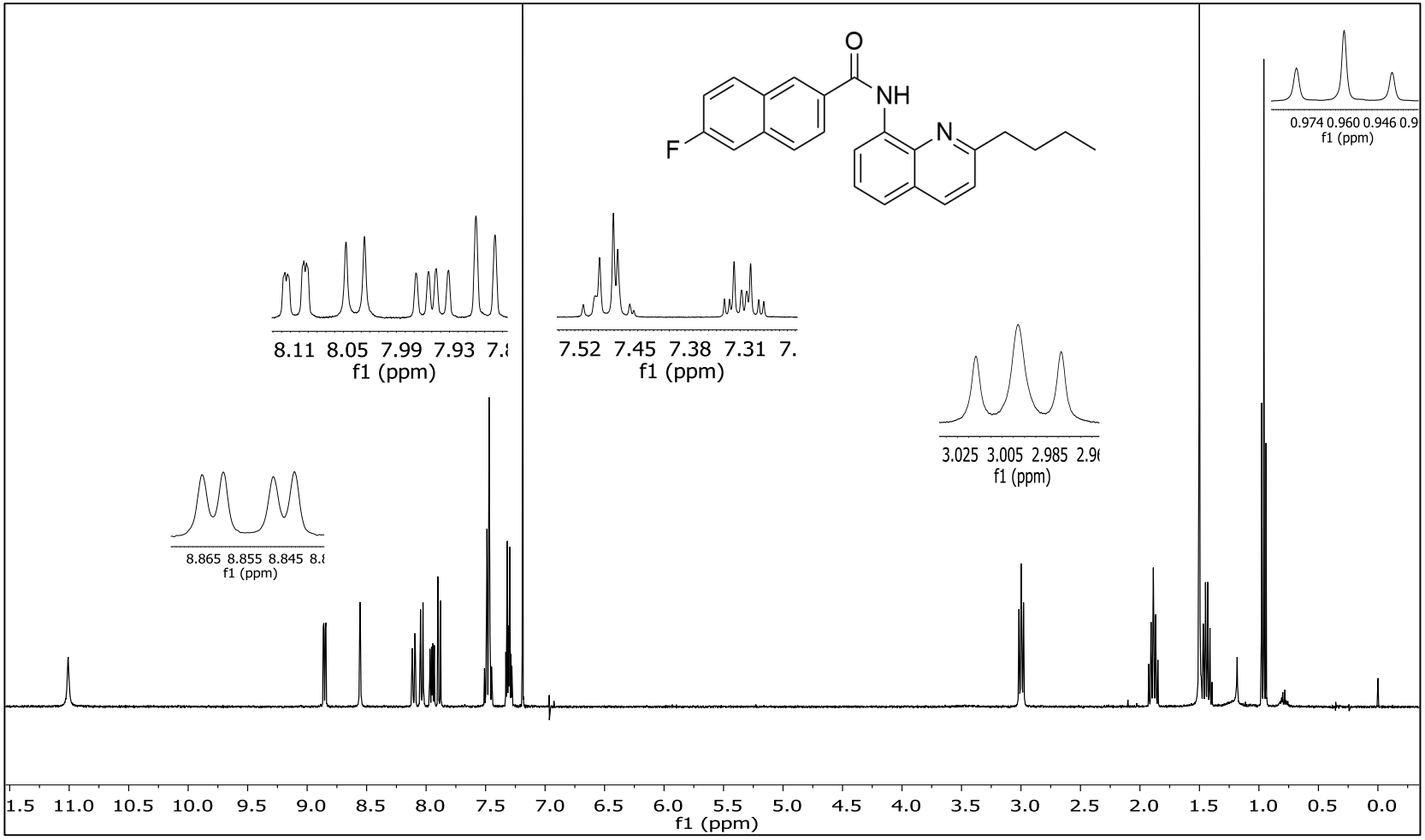

Figure A.18. ^{1}H-NMR Spectrum of N-(2-butylquinolin-8-yl)-6-fluoro-2-naphthamide.

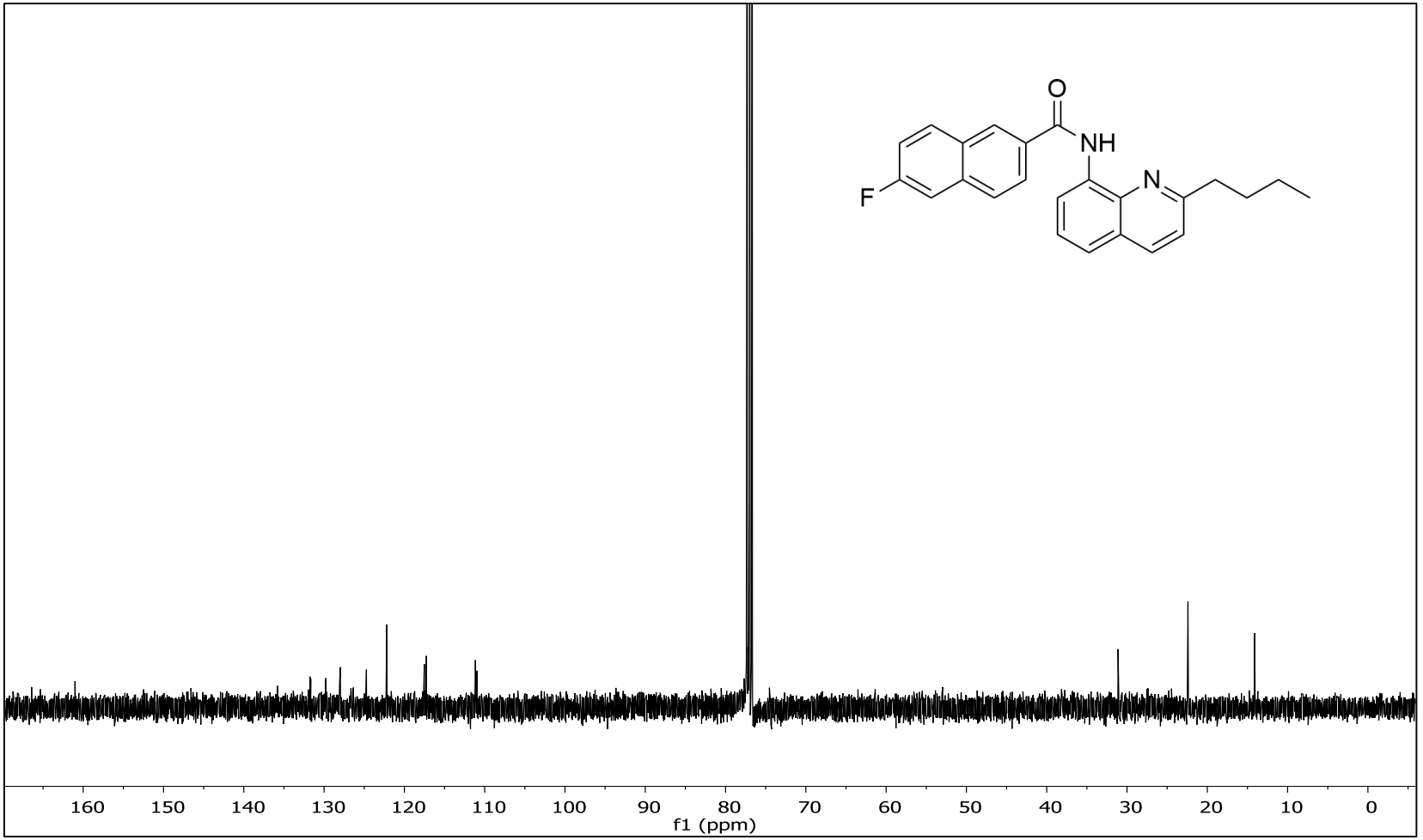

Figure A.19. ^{13}C-NMR Spectrum of N-(2-butylquinolin-8-yl)-6-fluoro-2-naphthamide.

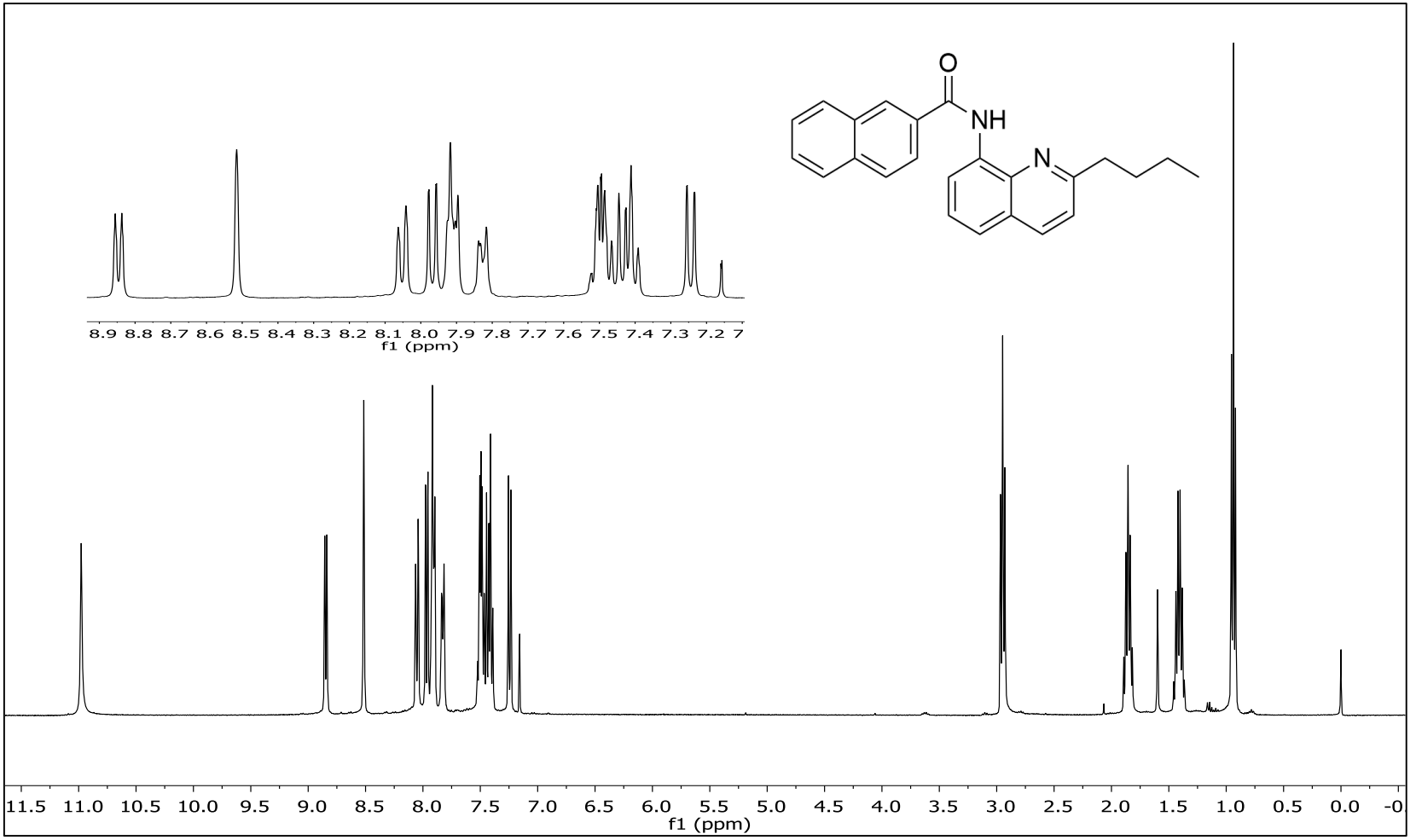

Figure A.20. ^{1}H-NMR Spectrum of N-(2-butylquinolin-8-yl)-2-naphthamide.

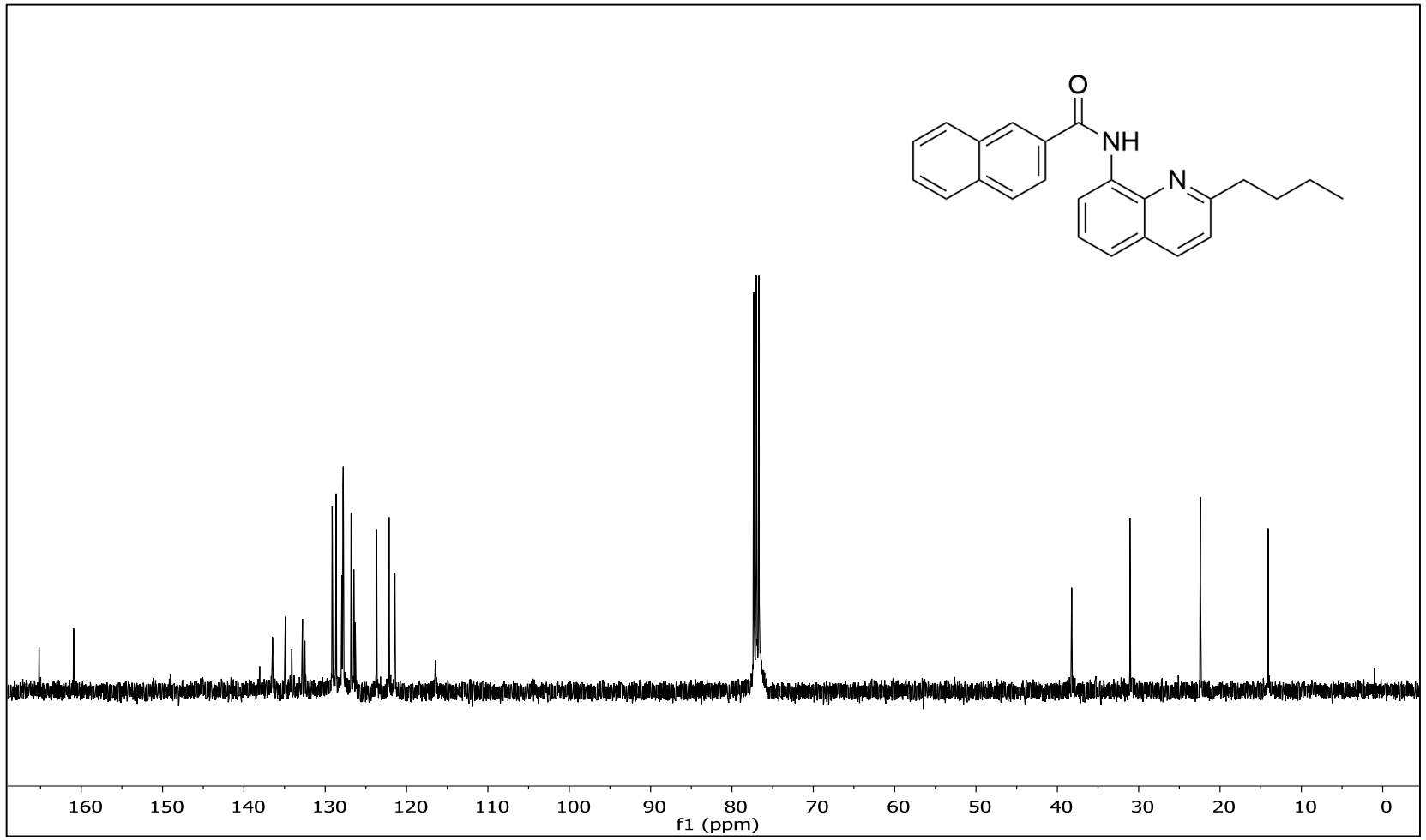

Figure A.21. ^{13}C-NMR Spectrum of N-(2-butylquinolin-8-yl)-2-naphthamide.

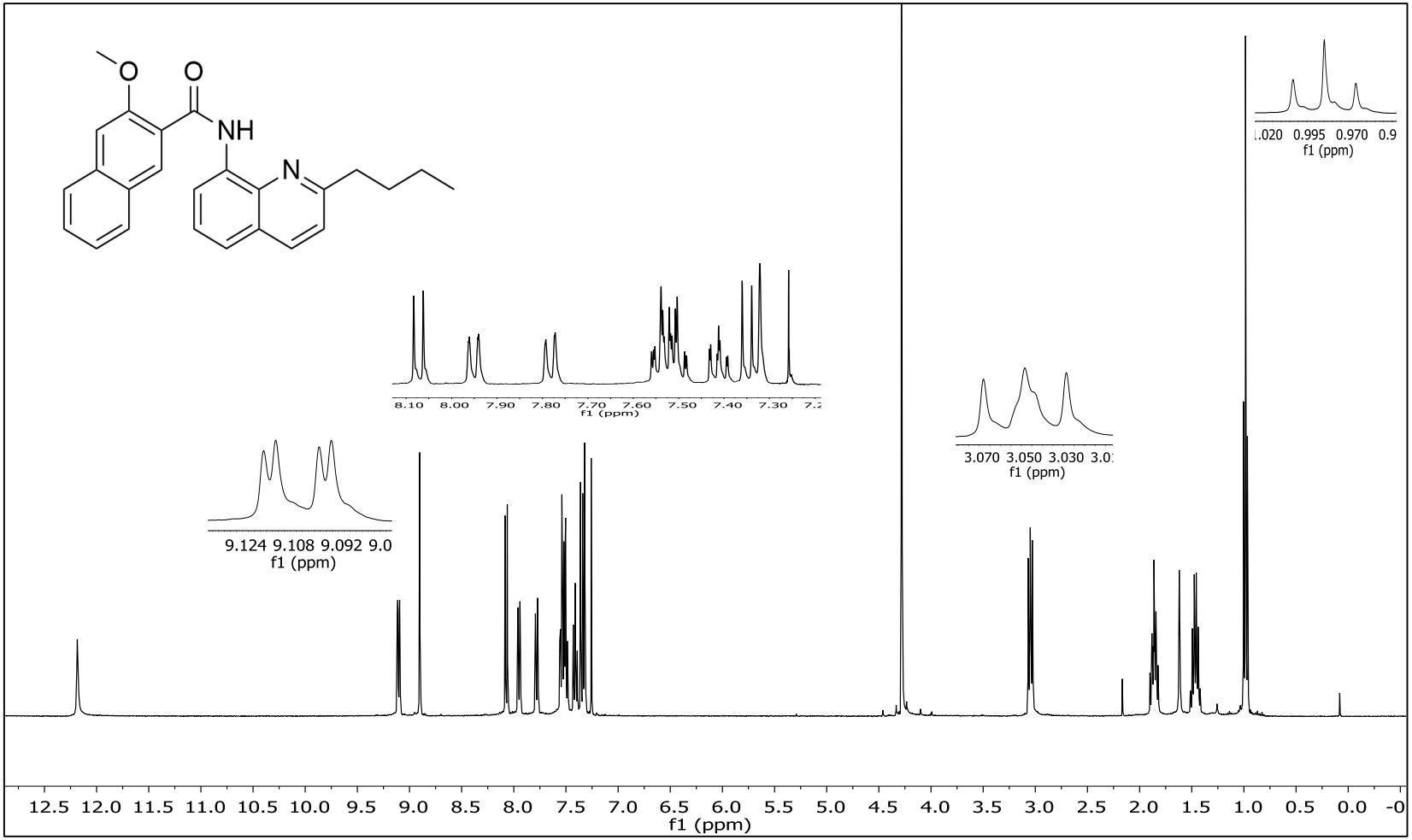

Figure A.22. ^{1}H-NMR Spectrum of N-(2-butylquinolin-8-yl)-3-methoxy-2-naphthamide.

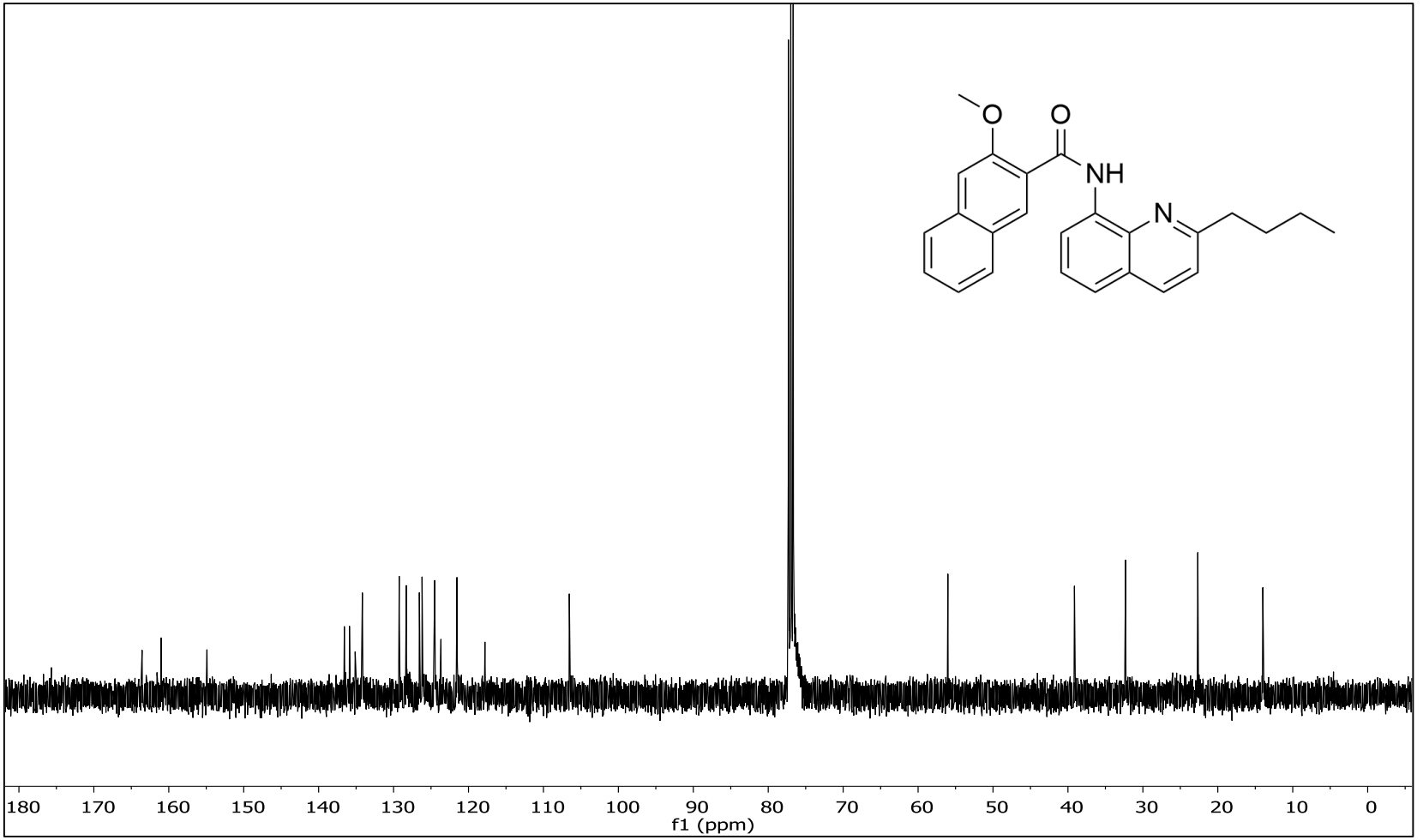

Figure A.23. ^{13}C-NMR Spectrum of N-(2-butylquinolin-8-yl)-3-methoxy-2-naphthamide.

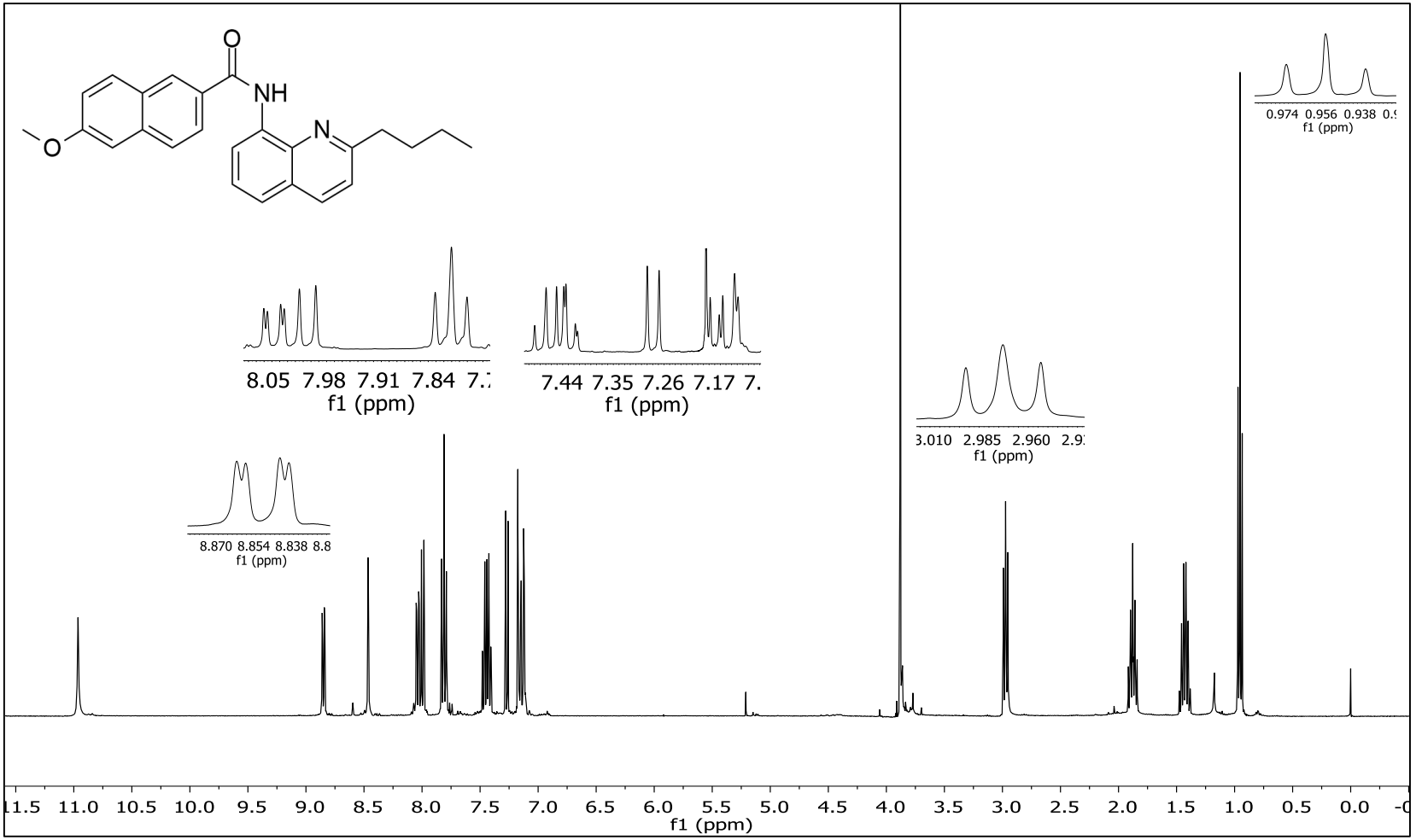

Figure A.24. ^{1}H-NMR Spectrum of N-(2-butylquinolin-8-yl)-6-methoxy-2-naphthamide.

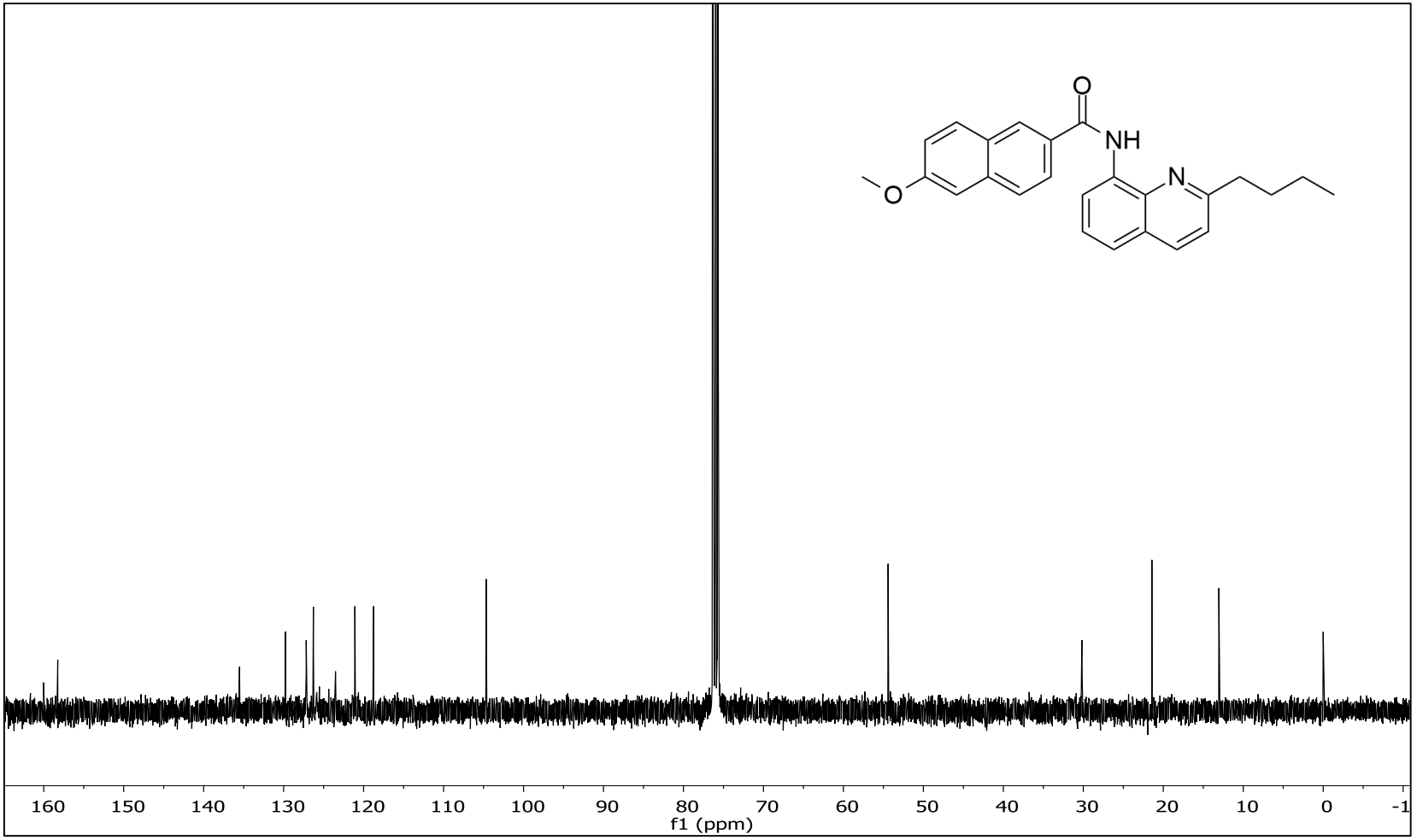

Figure A.25. ^{13}C-NMR Spectrum of N-(2-butylquinolin-8-yl)-6-methoxy-2-naphthamide.

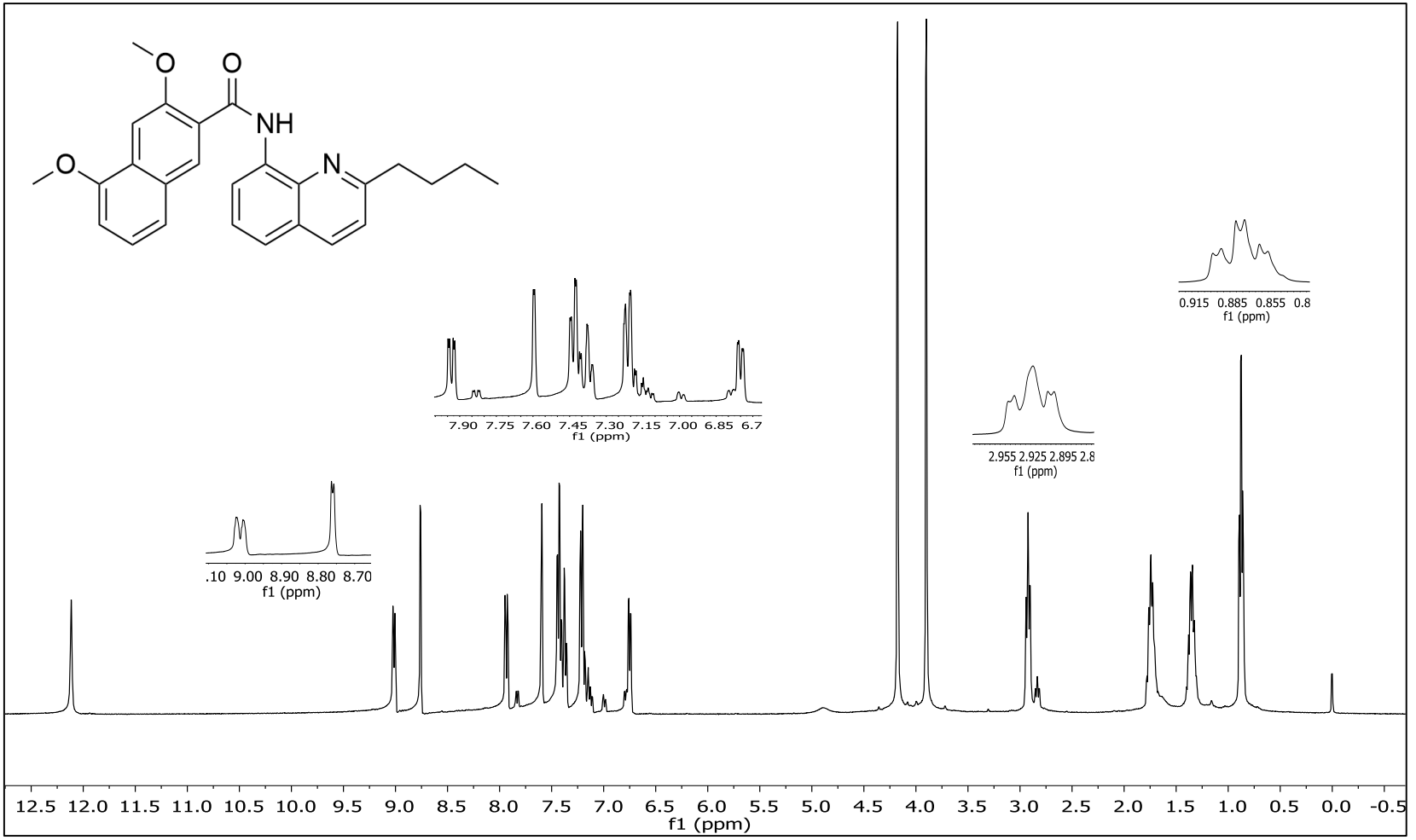

Figure A.26. ^{1}H-NMR Spectrum of N-(2-butylquinolin-8-yl)-3,5-dimethoxy-2-naphthamide.

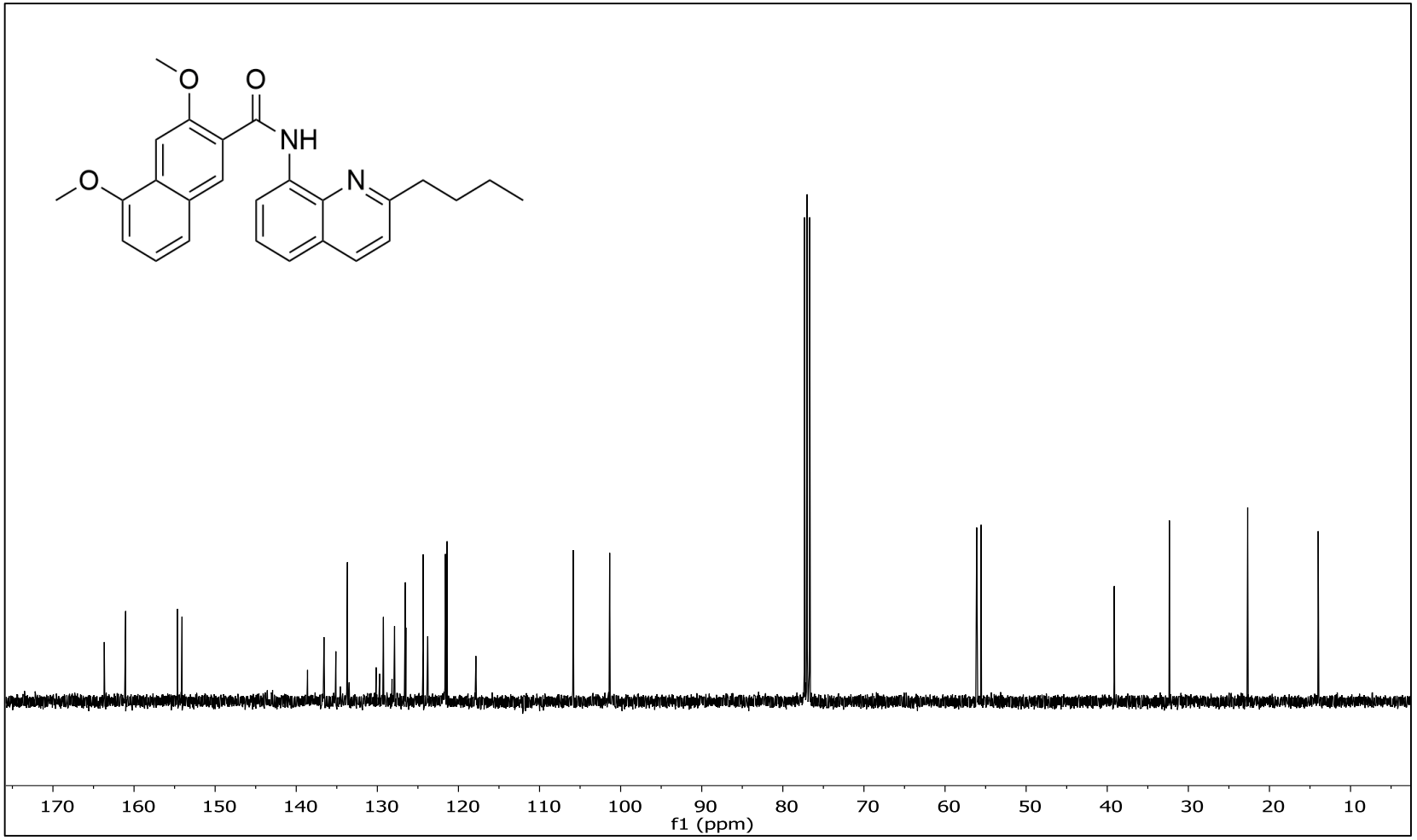

Figure A.27. ^{13}C-NMR Spectrum of N-(2-butylquinolin-8-yl)-3,5-dimethoxy-2-naphthamide.

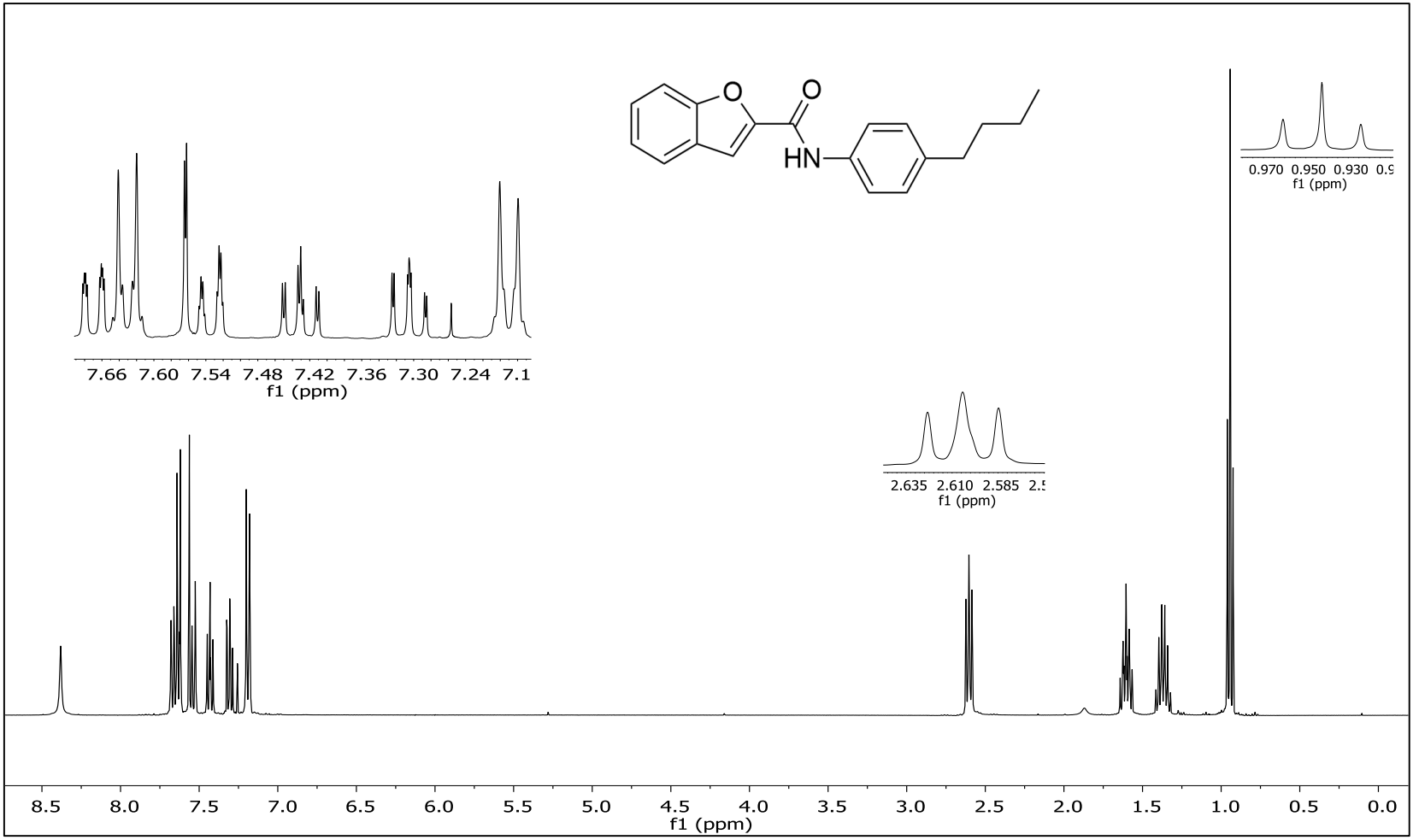

Figure A.28. ^{1}H-NMR Spectrum of N-(4-butylphenyl)benzofuran-2-carboxamide.

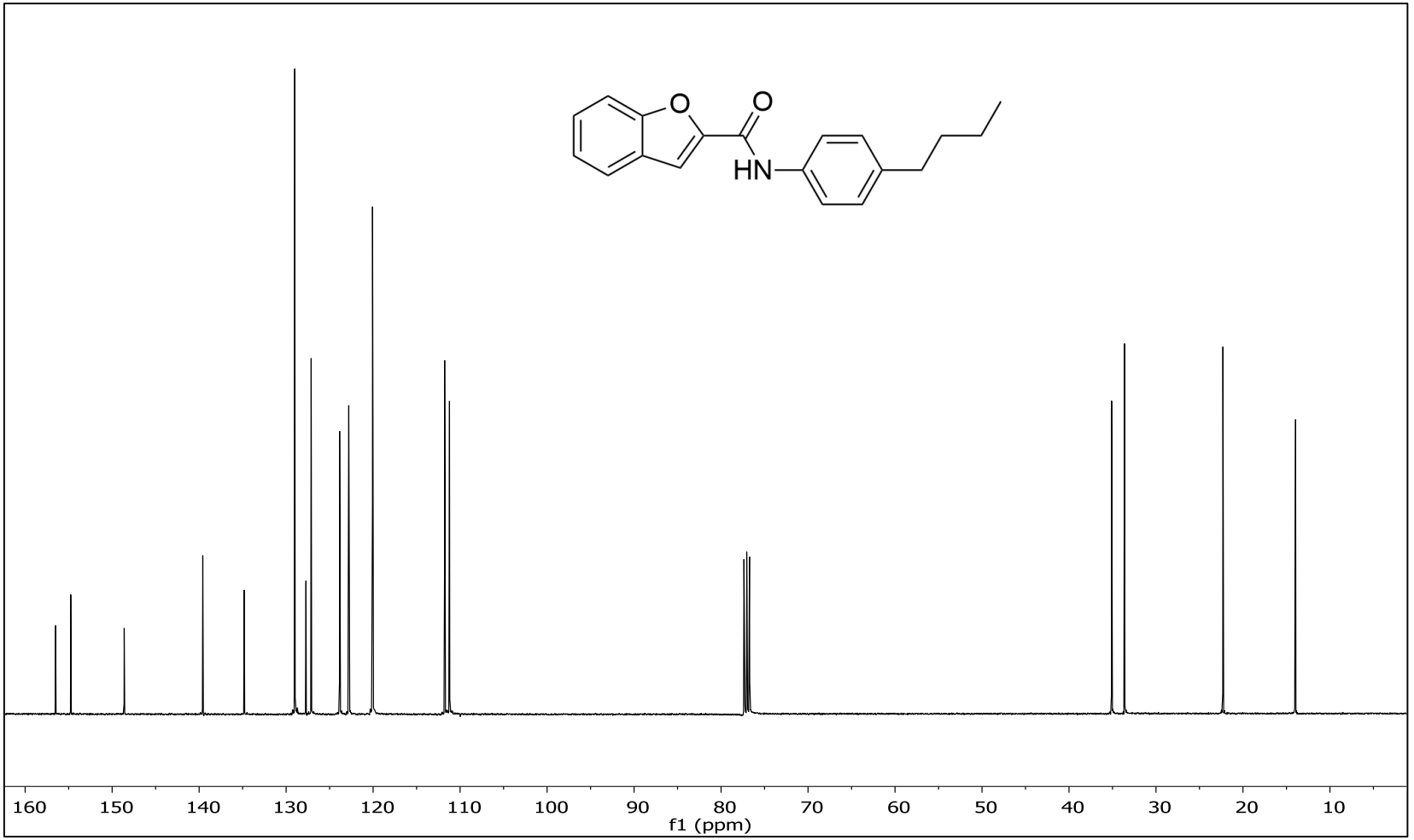

Figure A.29. ^{13}C-NMR Spectrum of N-(4-butylphenyl)benzofuran-2-carboxamide.

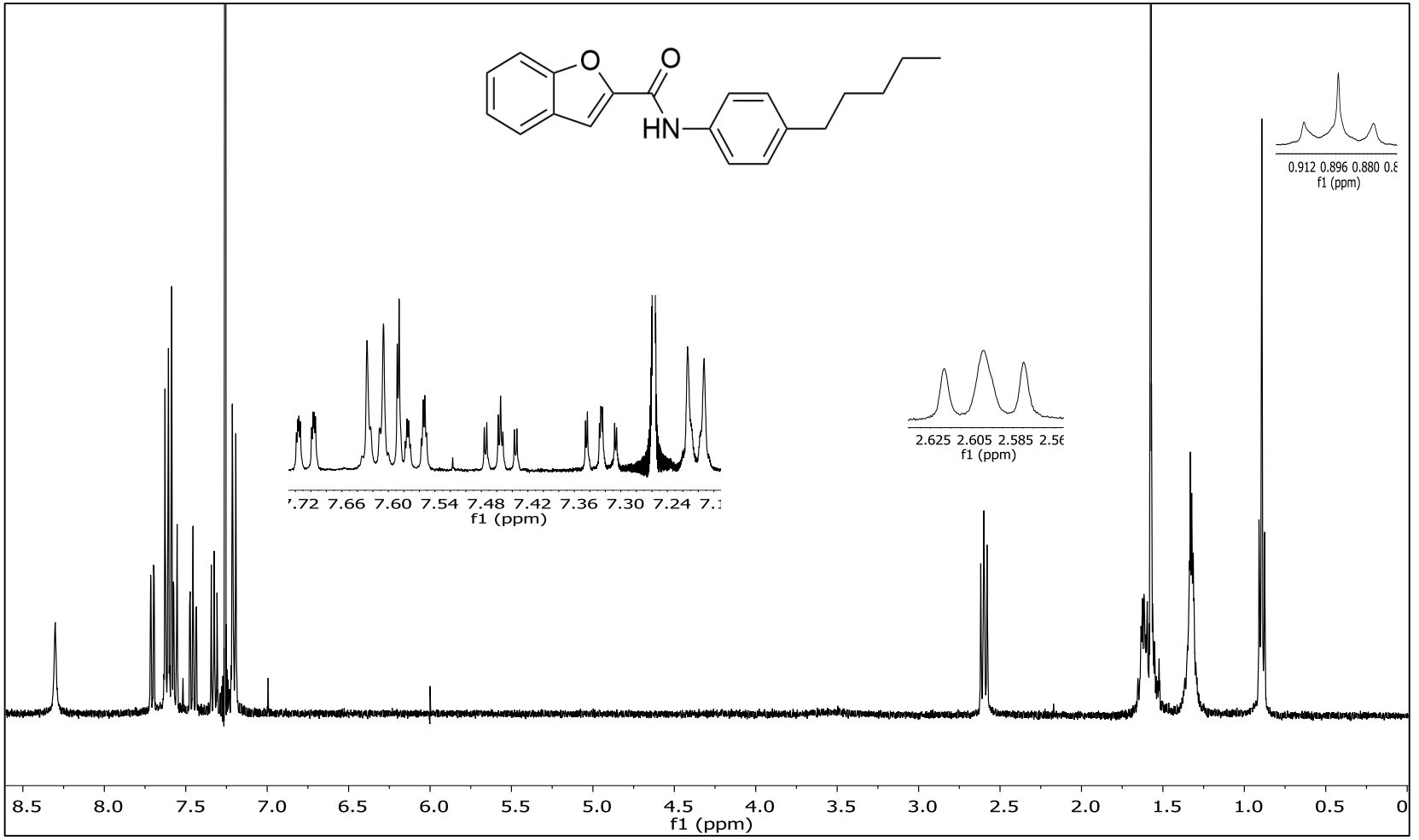

Figure A.30. ^{1}H-NMR Spectrum of N-(4-pentylphenyl)benzofuran-2-carboxamide.

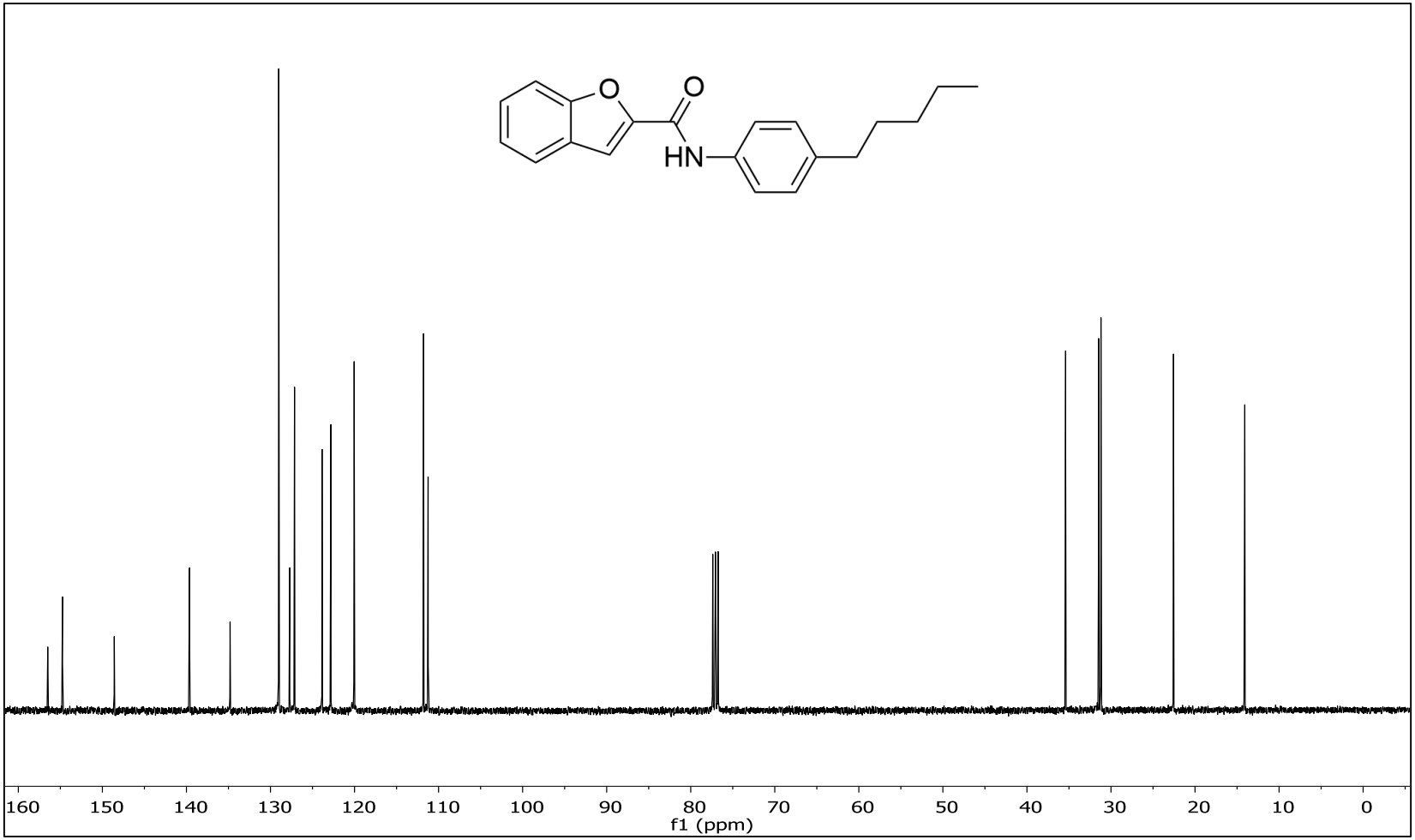

Figure A.31. ^{13}C-NMR Spectrum of N-(4-pentylphenyl)benzofuran-2-carboxamide.

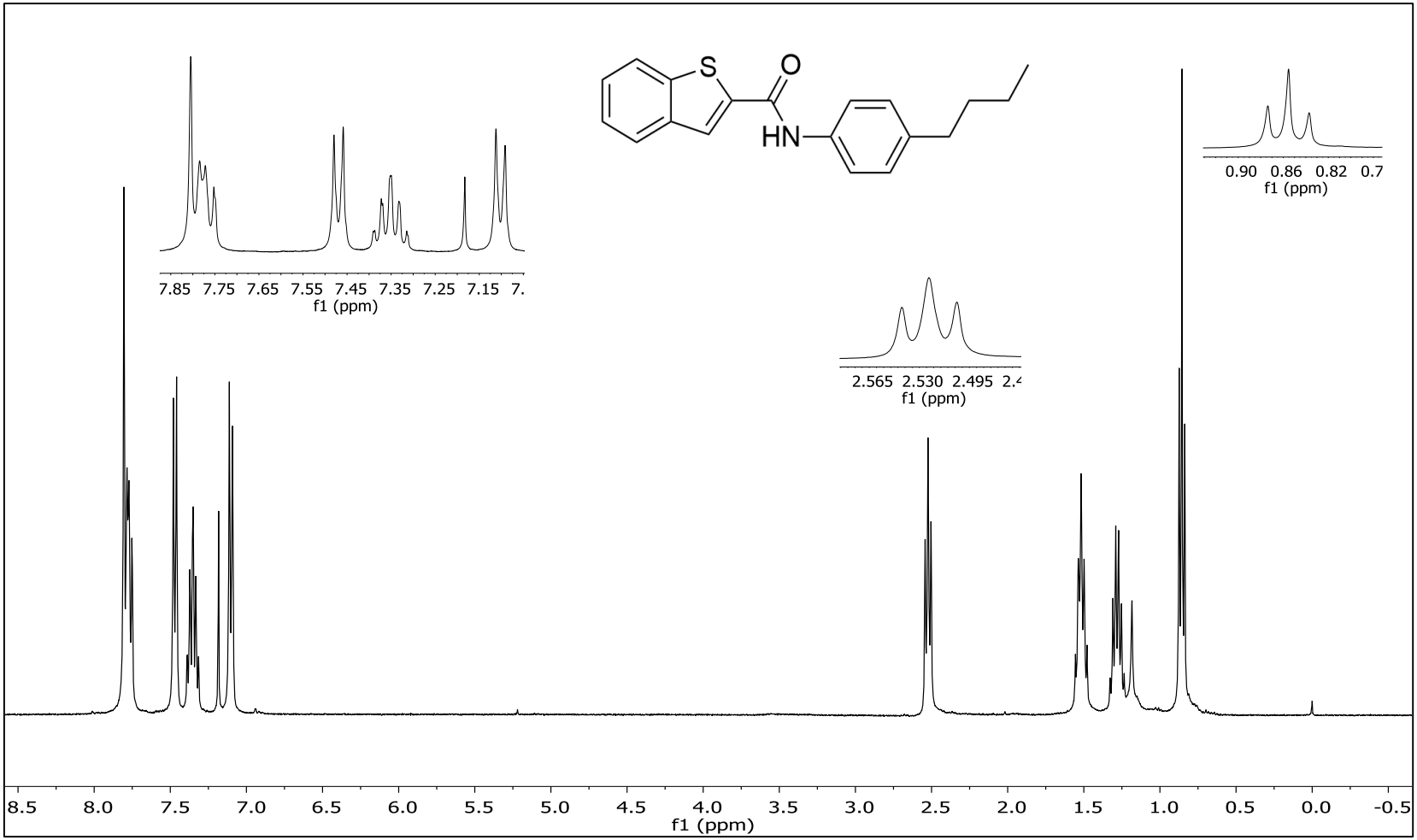

Figure A.32. ^{1}H-NMR Spectrum of N-(4-butylphenyl)benzo[b]thiophene-2-carboxamide.

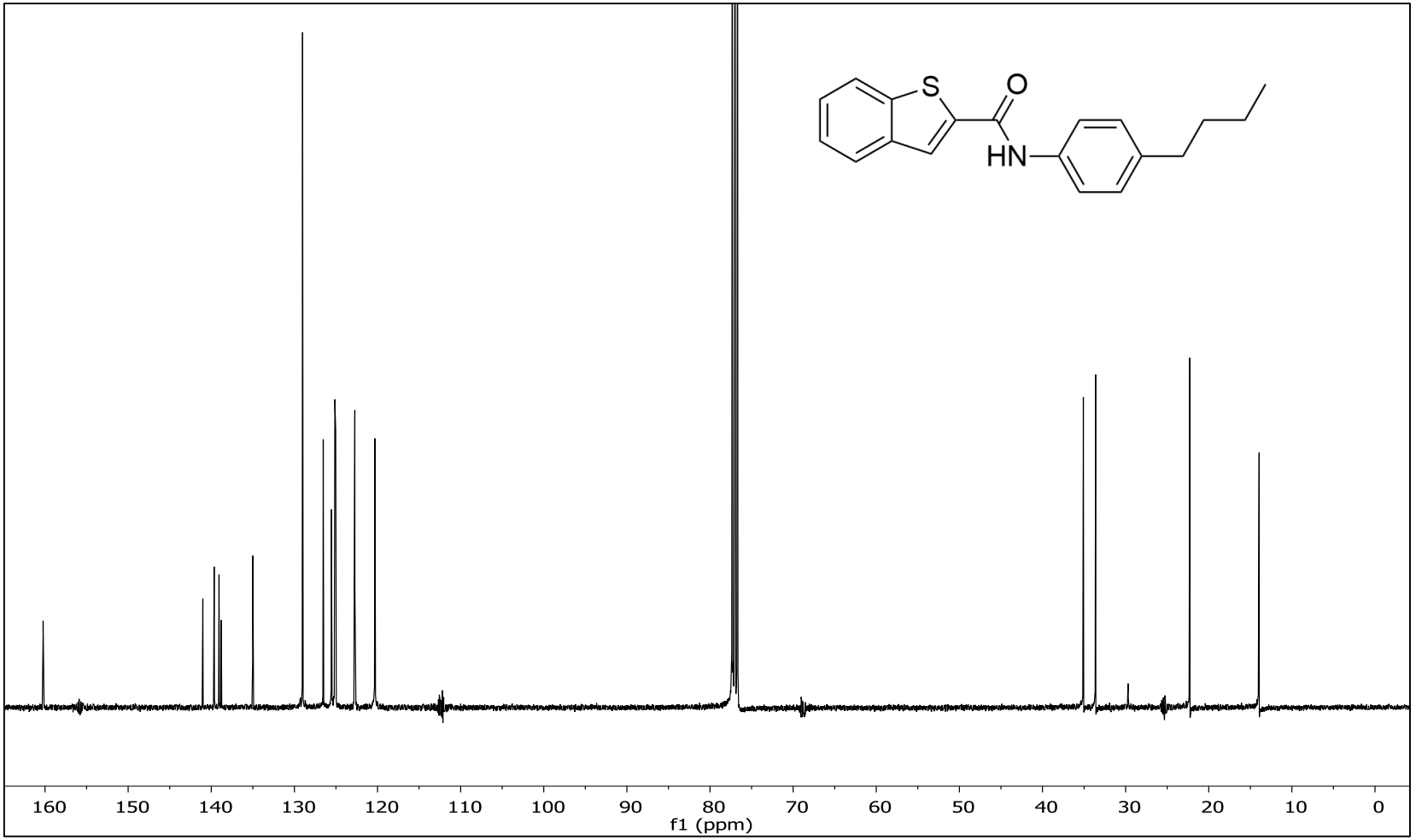

Figure A.33. ^{13}C-NMR Spectrum of N-(4-butylphenyl)benzo[b]thiophene-2-carboxamide.

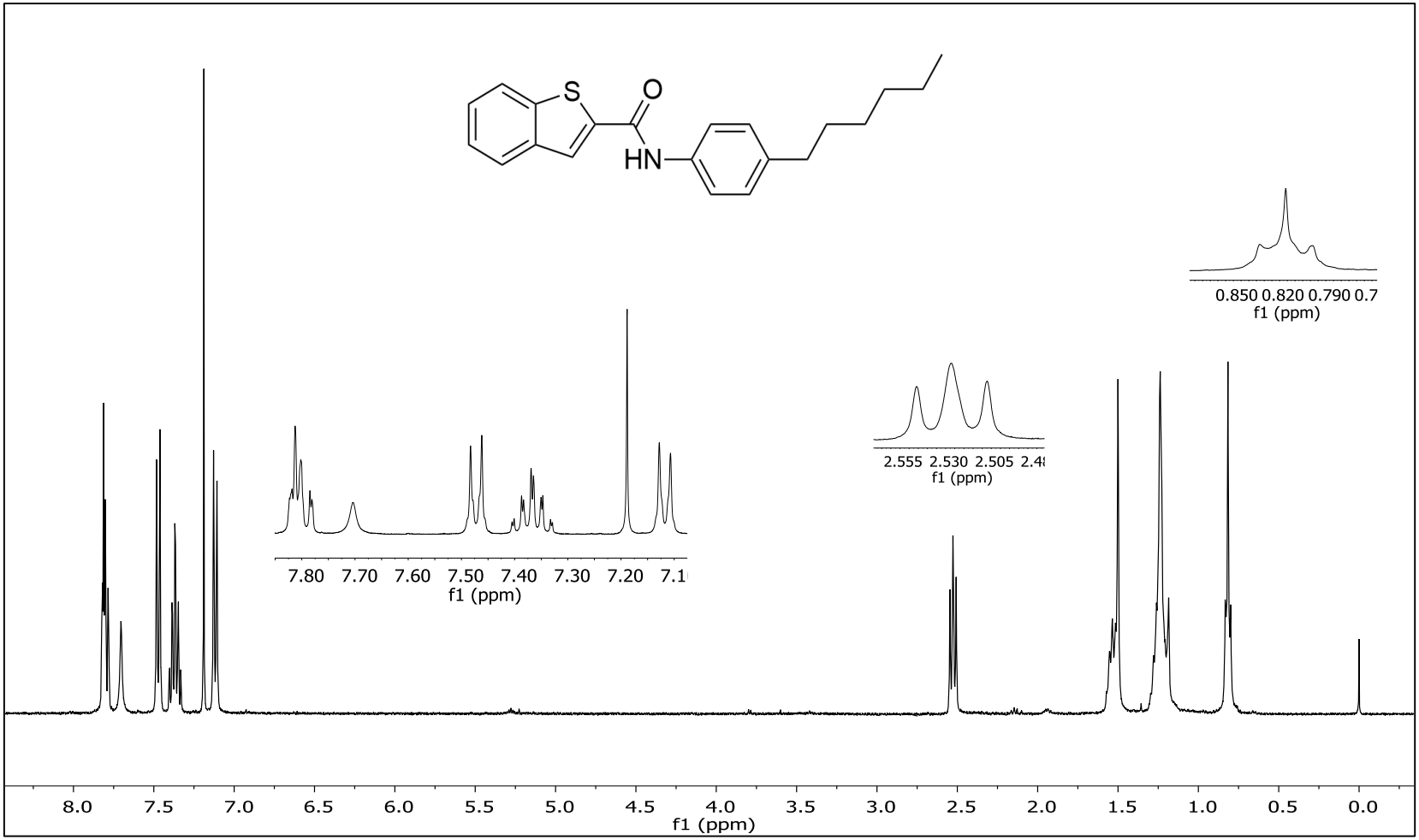

Figure A.34. ^{1}H-NMR Spectrum of N-(4-hexylphenyl)benzo[b]thiophene-2-carboxamide.

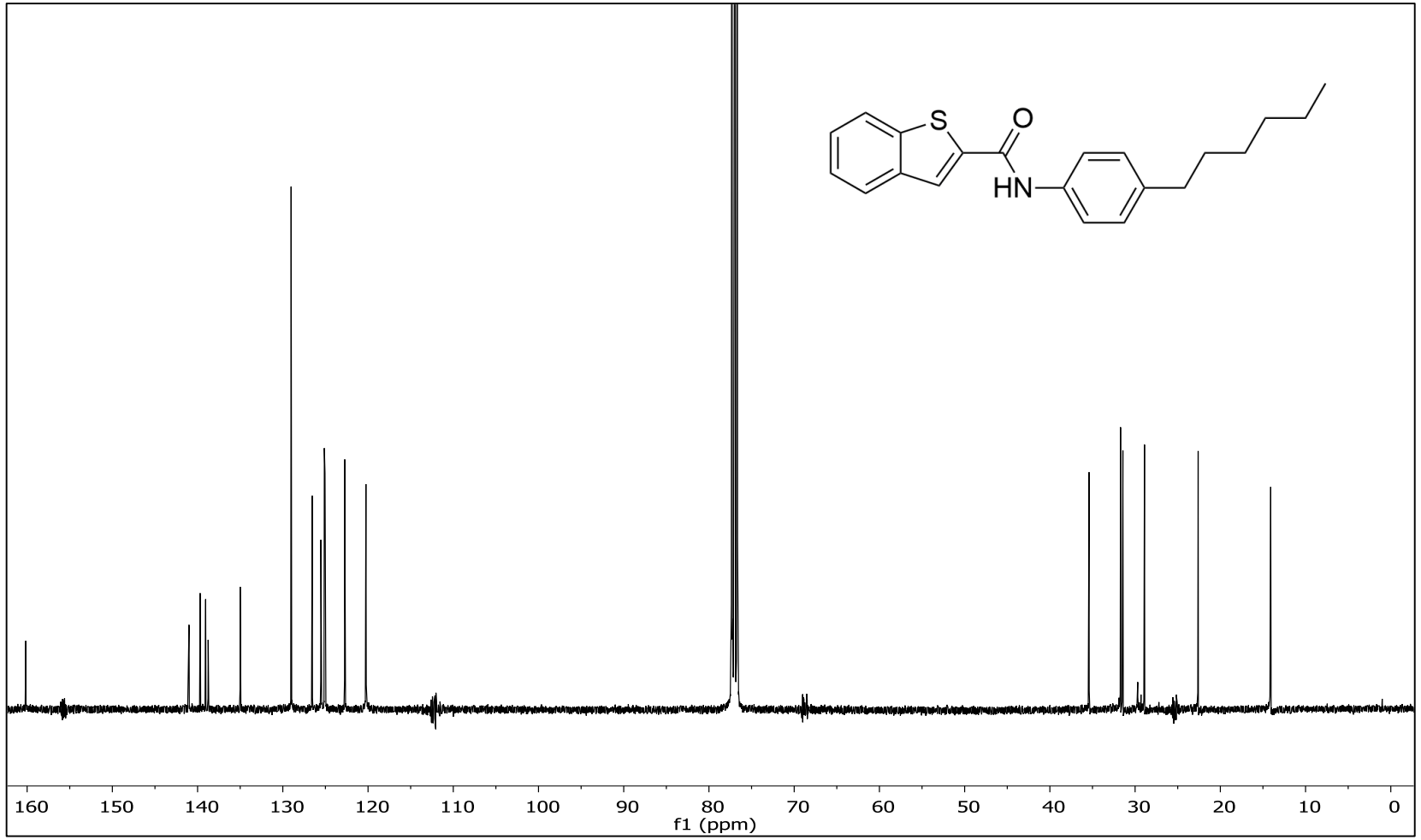

Figure A.35. ^{13}C-NMR Spectrum of N-(4-hexylphenyl)benzo[b]thiophene-2-carboxamide.

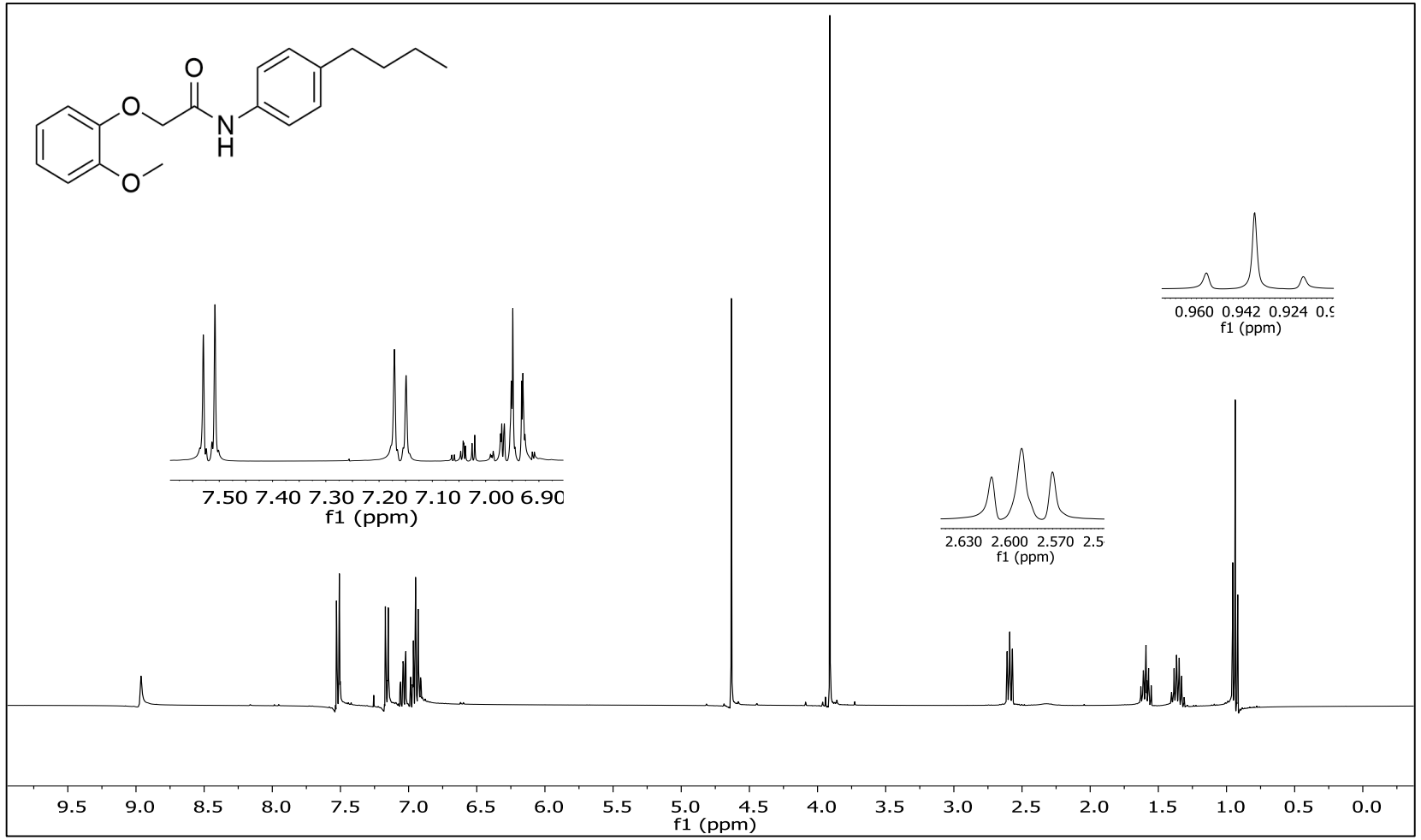

Figure A.36. ^{1}H-NMR Spectrum of N-(4-butylphenyl)-2-(2-methoxyphenoxy)acetamide.

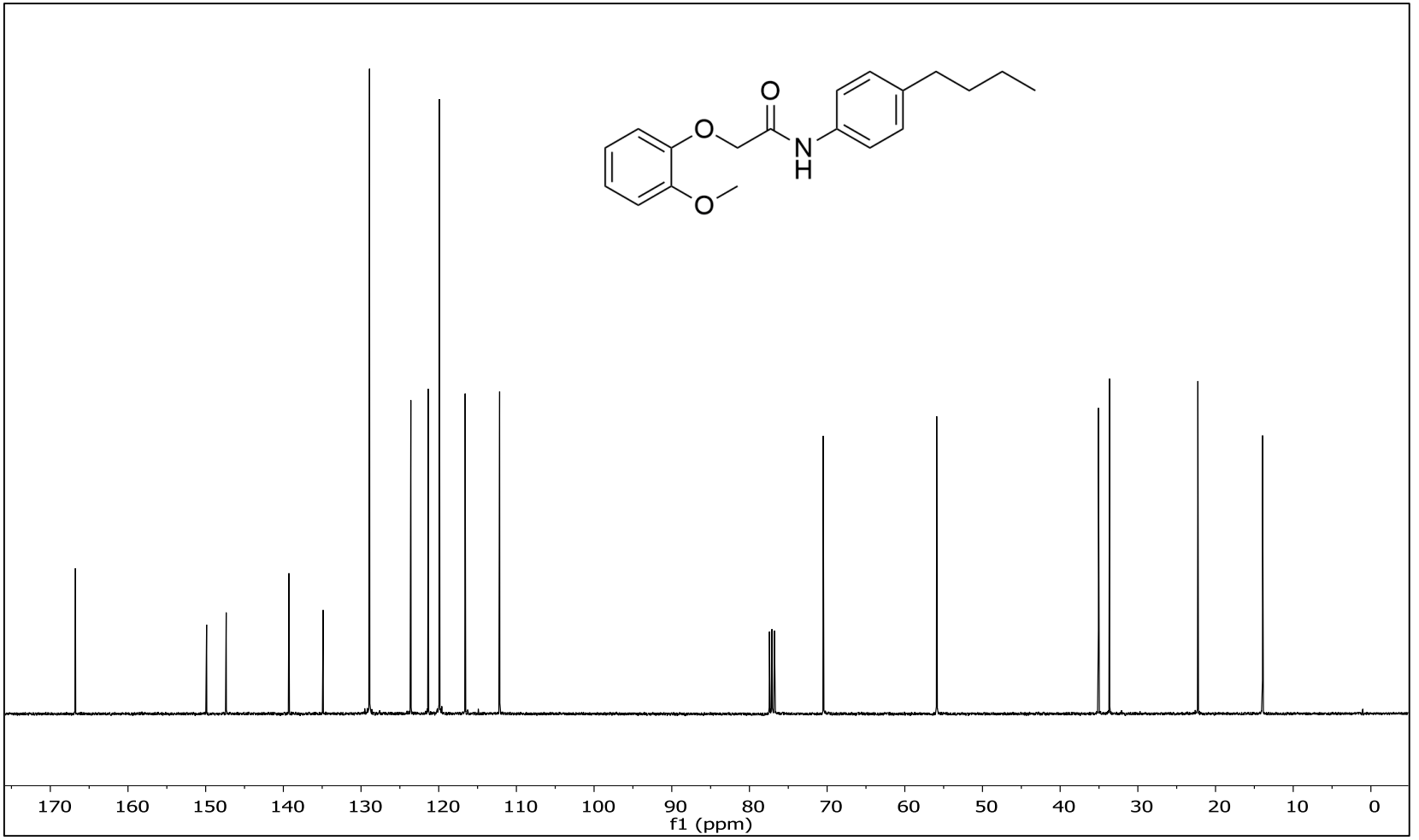

Figure A.37. ^{13}C-NMR Spectrum of N-(4-butylphenyl)-2-(2-methoxyphenoxy)acetamide.

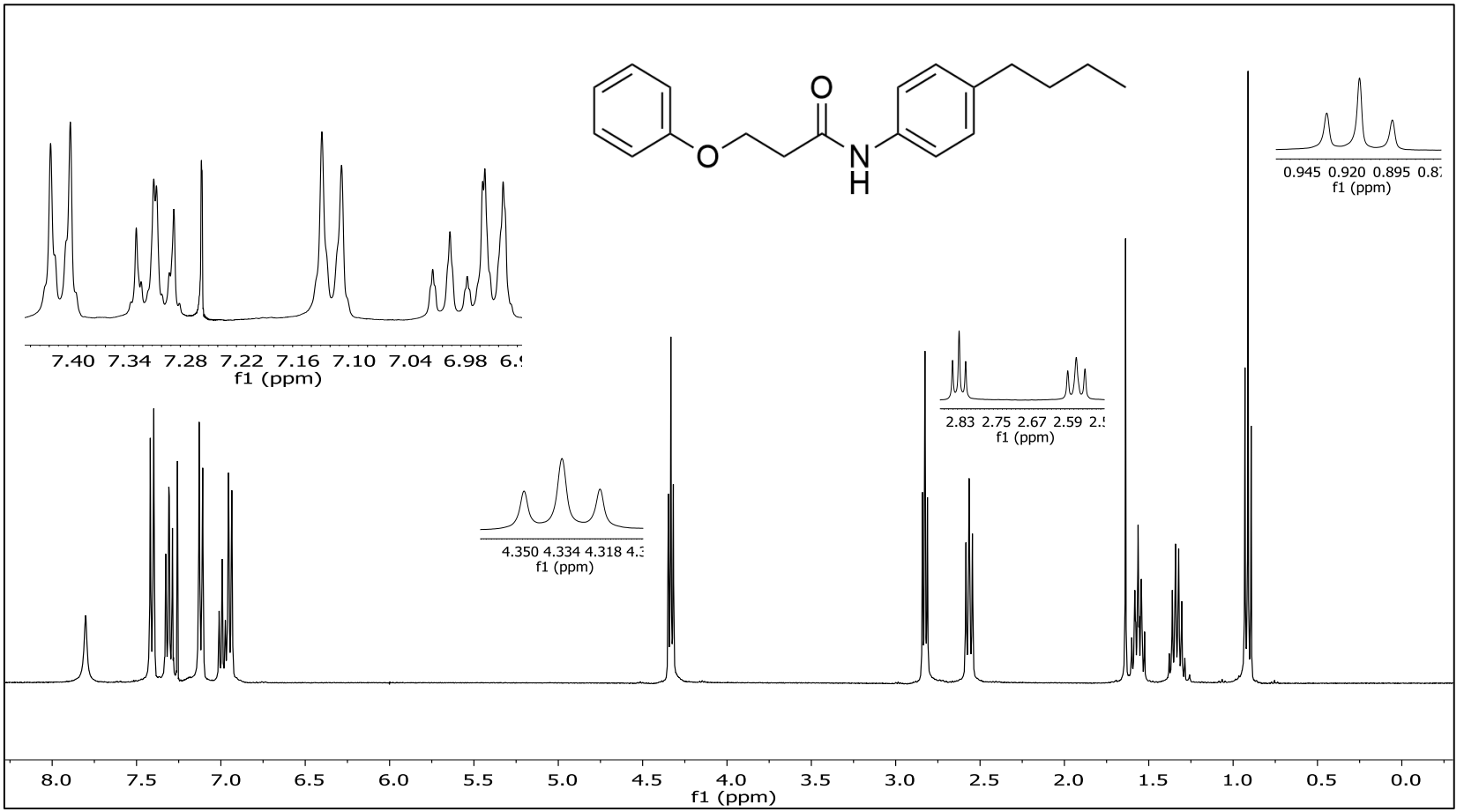

Figure A.38. ^{1}H-NMR Spectrum of N-(4-butylphenyl)-3-phenoxypropanamide.

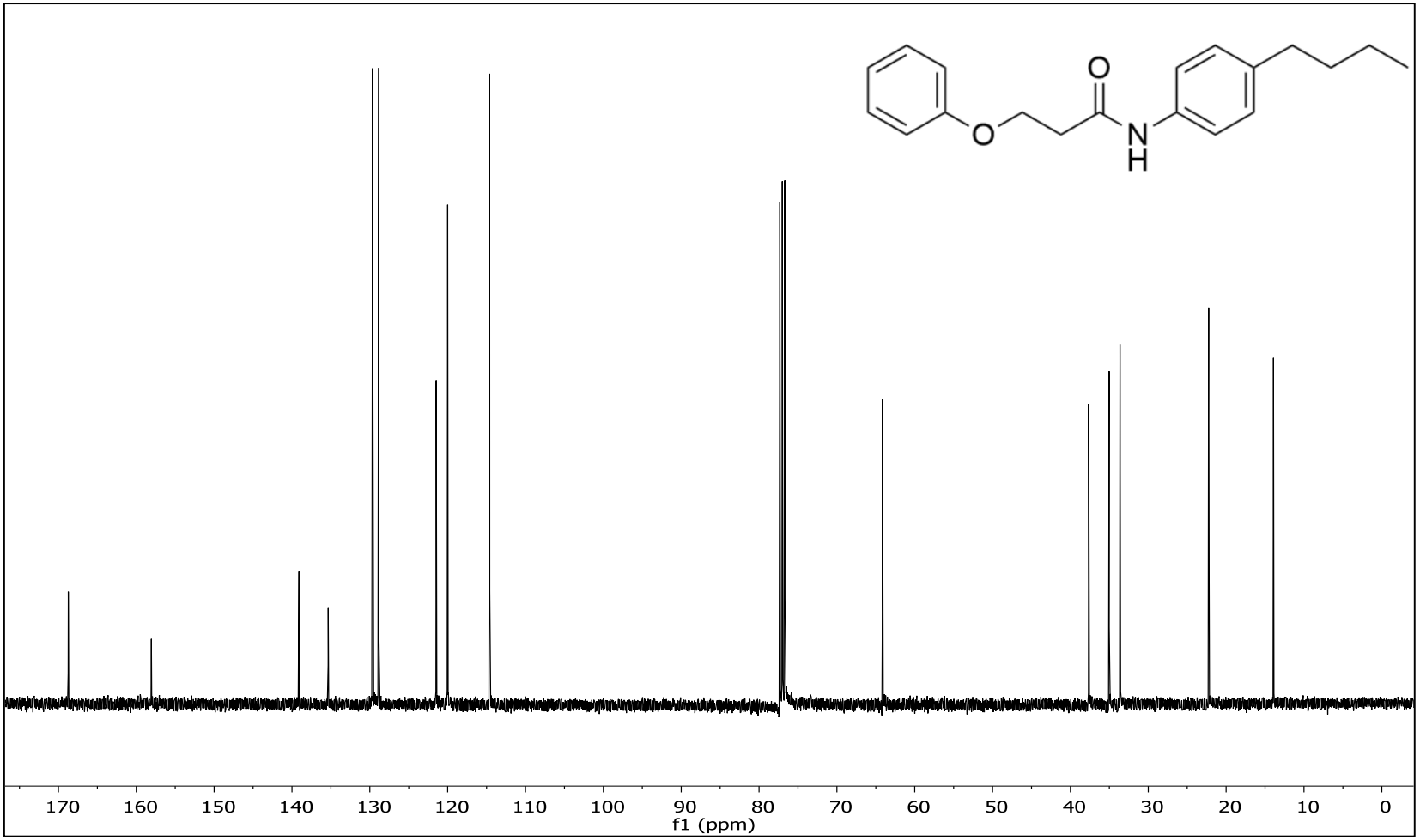

Figure A.39. ^{13}C-NMR Spectrum of N-(4-butylphenyl)-3-phenoxypropanamide.

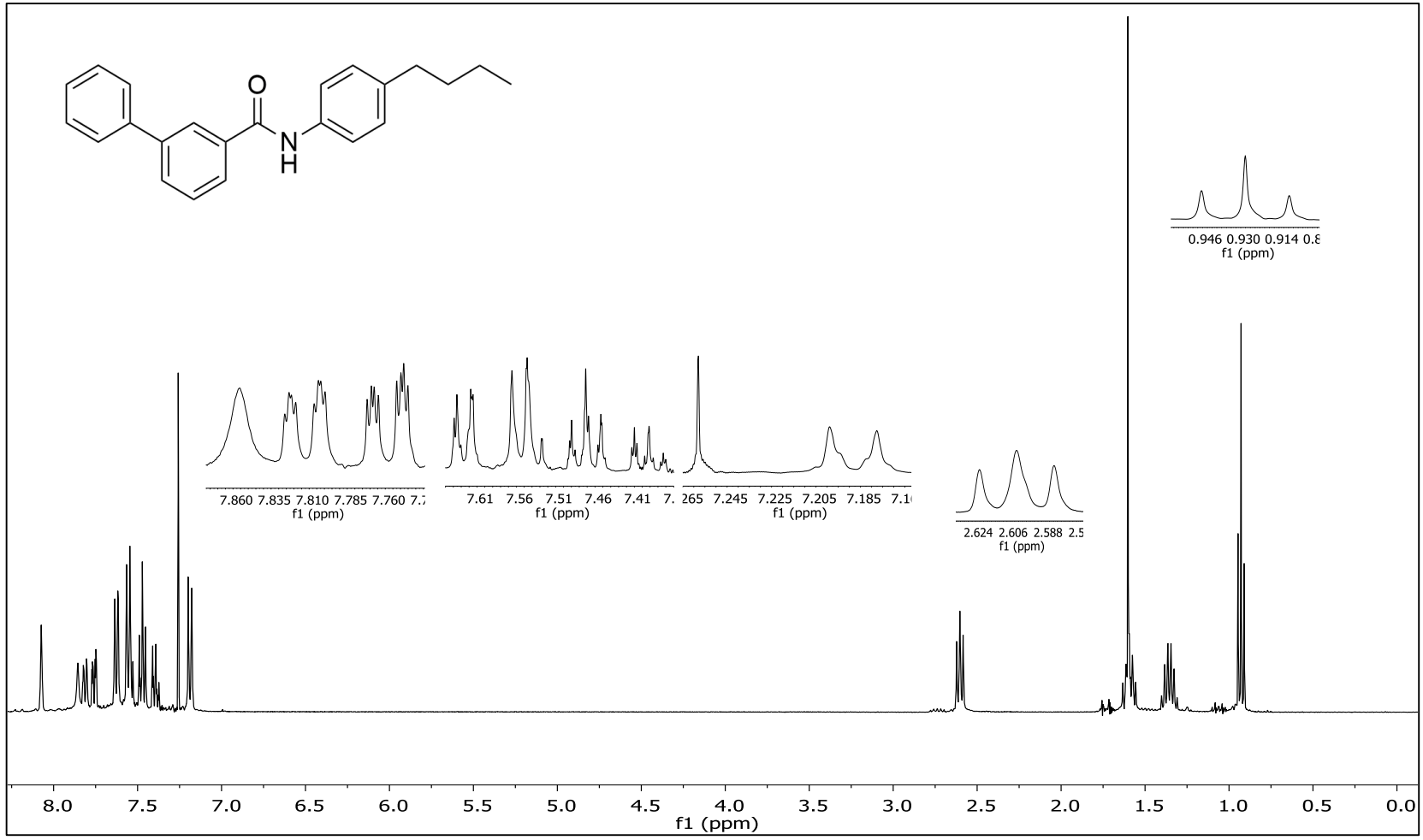

Figure A.40. ^{1}H-NMR Spectrum of N-(4-butylphenyl)biphenyl-3-carboxamide.

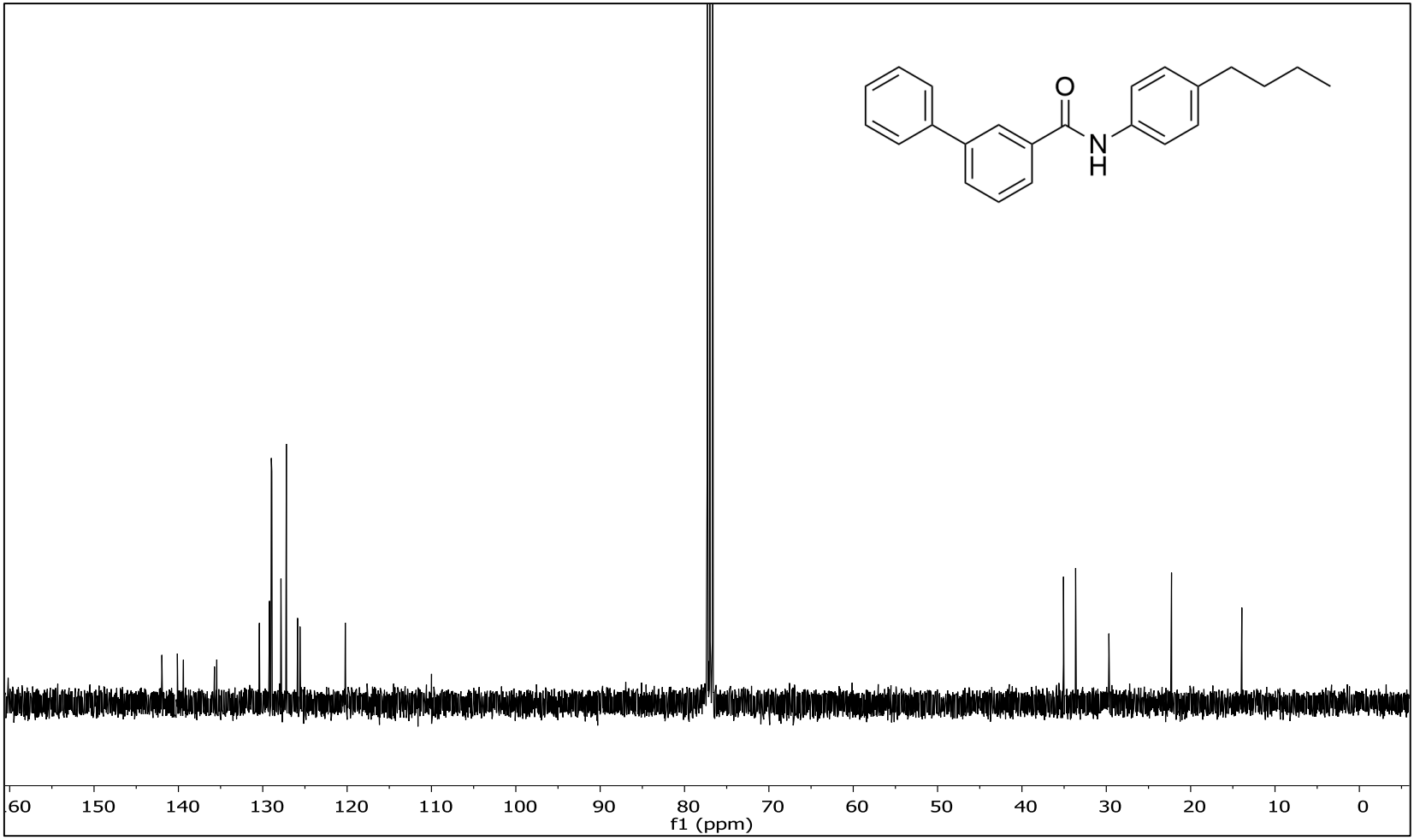

Figure A.41. ^{13}C-NMR Spectrum of N-(4-butylphenyl)biphenyl-3-carboxamide.

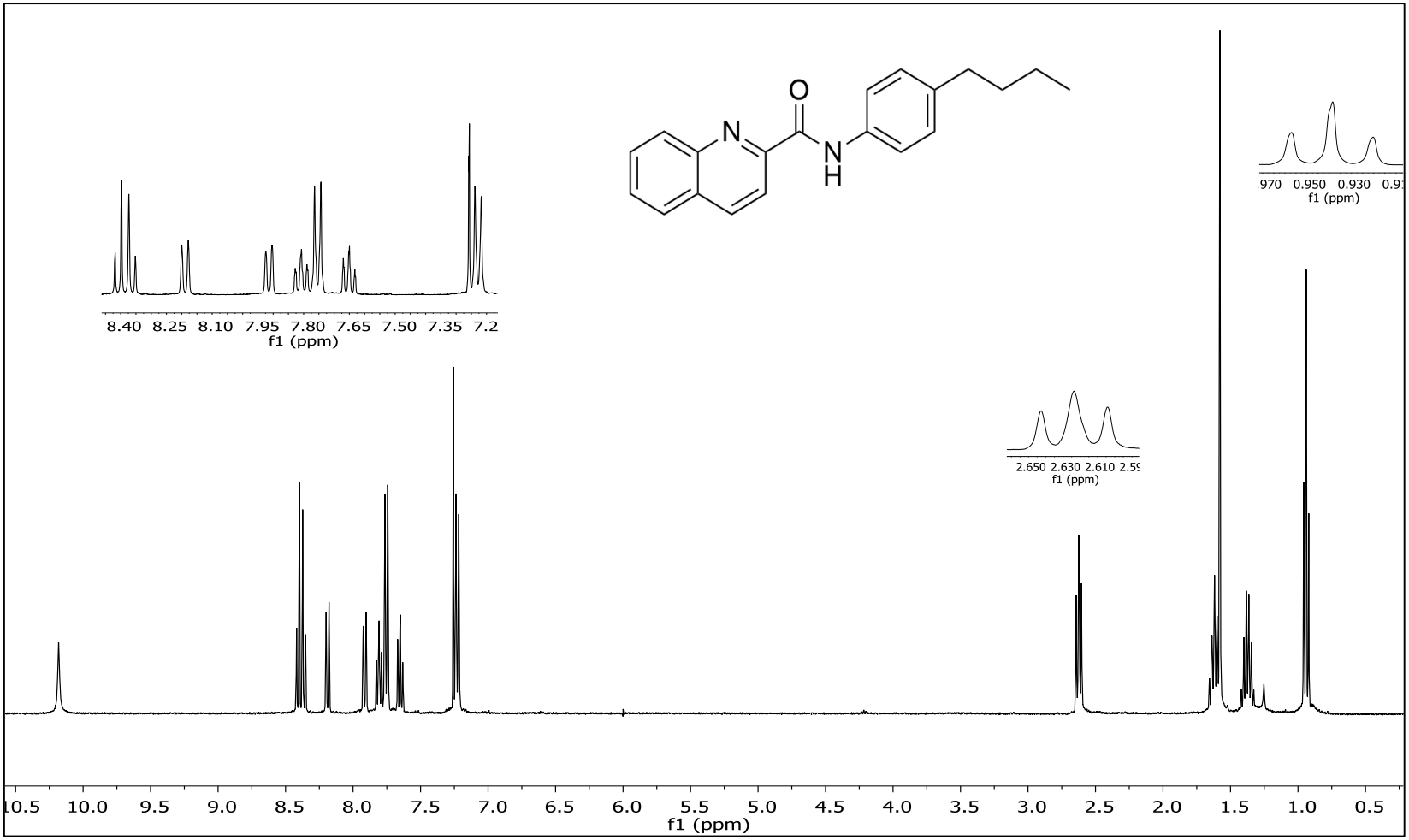

Figure A.42. ^{1}H-NMR Spectrum of N-(4-butylphenyl)quinoline-2-carboxamide.

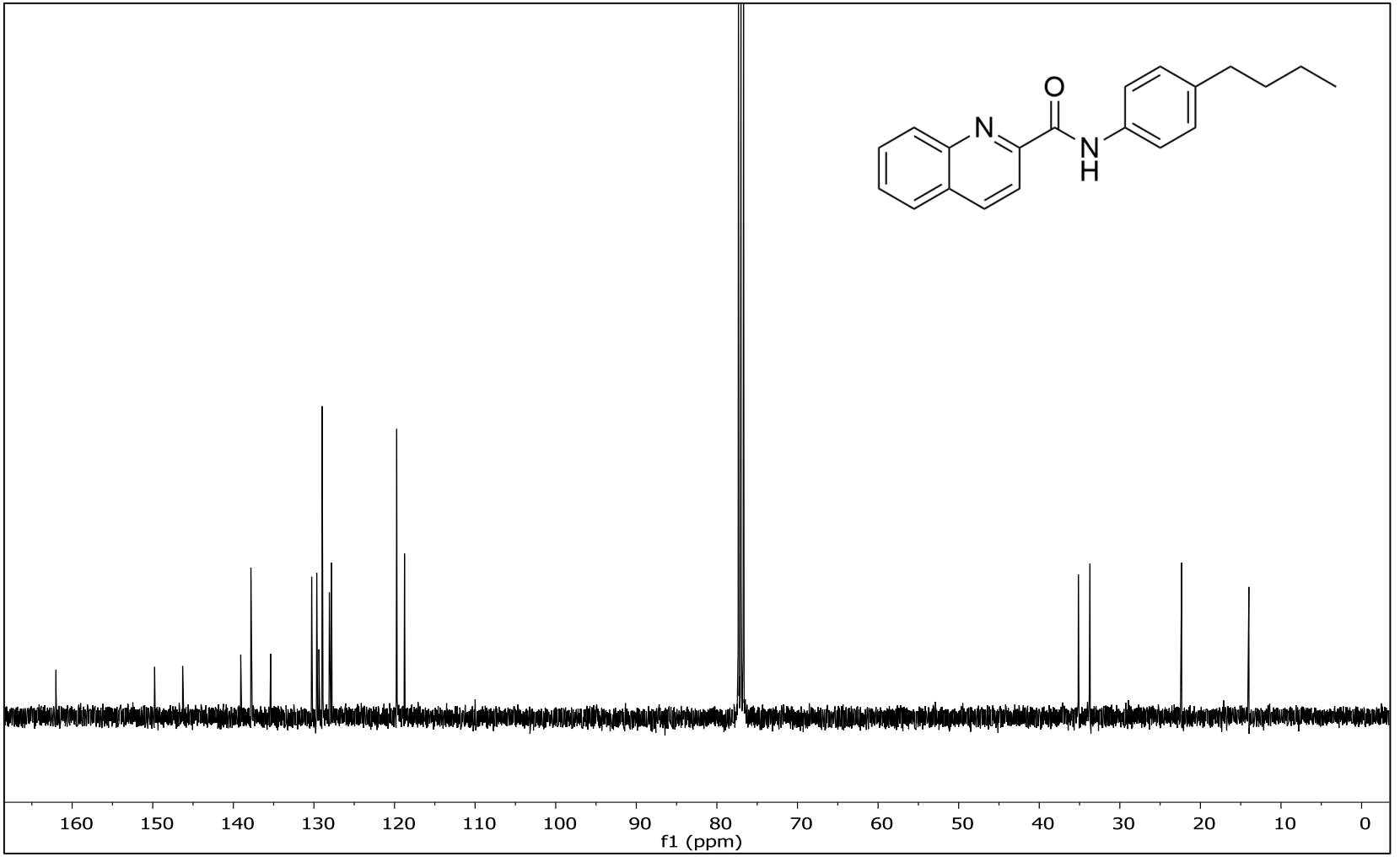

Figure A.43. ^{13}C-NMR Spectrum of N-(4-butylphenyl)quinoline-2-carboxamide.

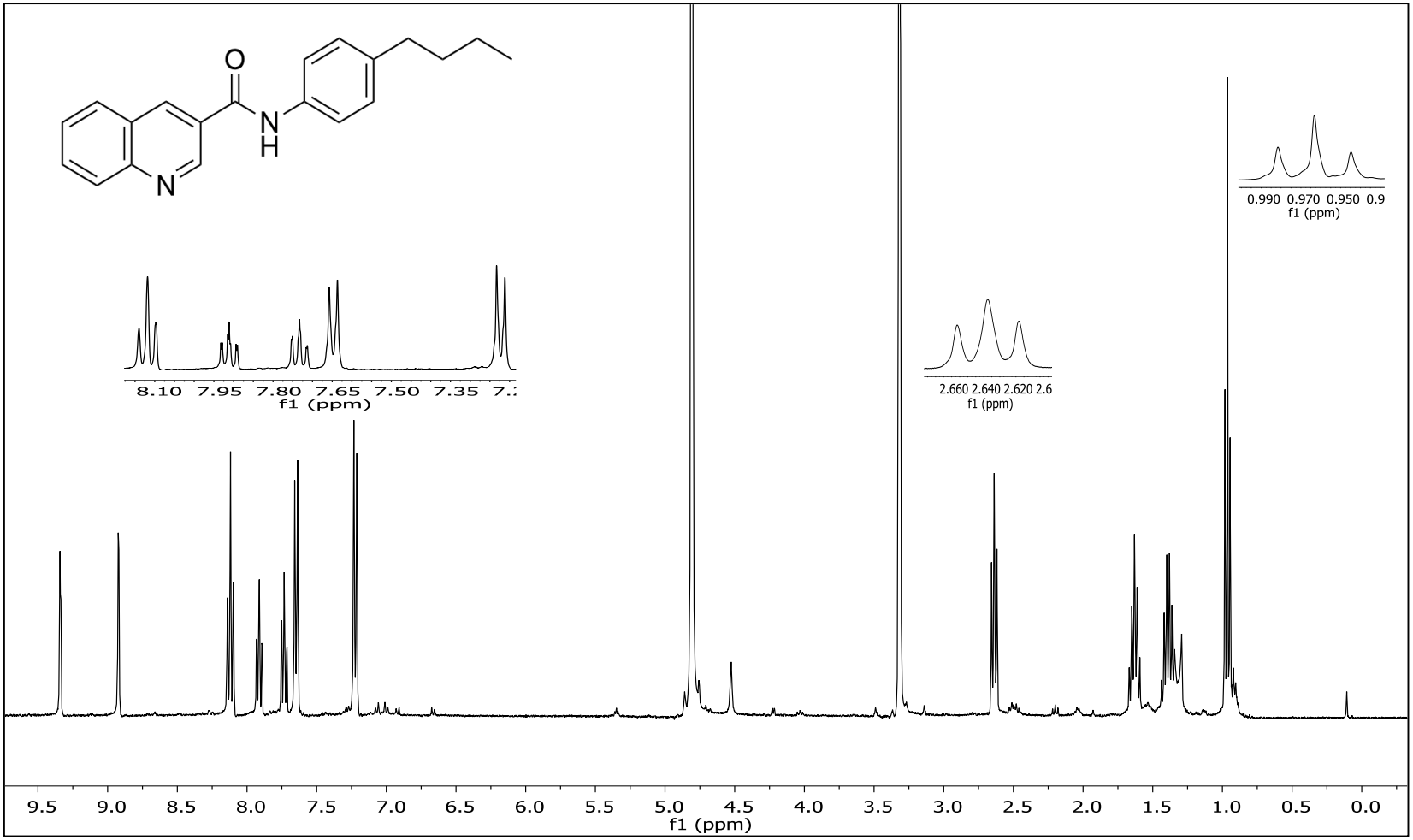

Figure A.44. ^{1}H-NMR Spectrum of N-(4-butylphenyl)quinoline-3-carboxamide.

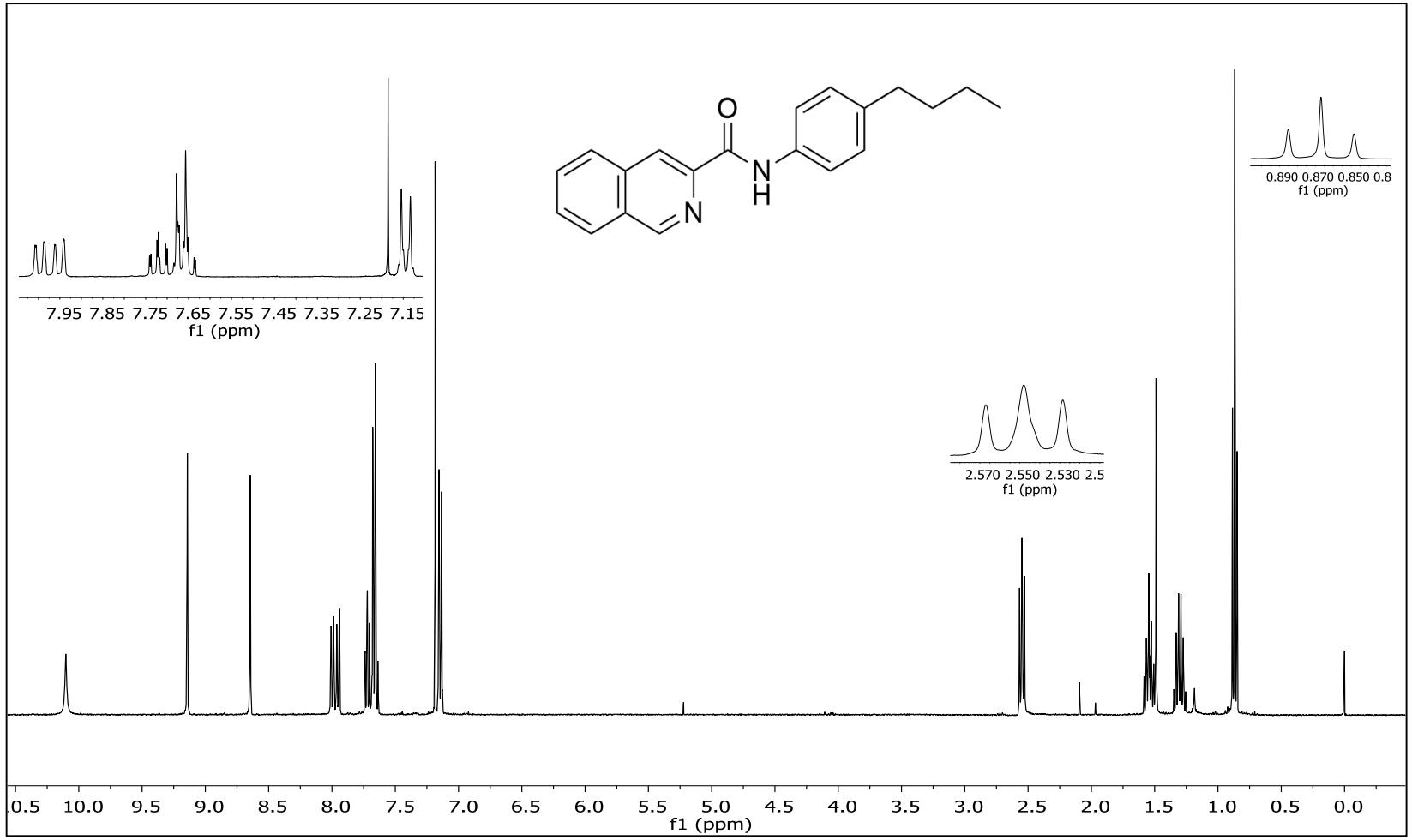

Figure A.45. ^{1}H-NMR Spectrum of N-(4-butylphenyl)isoquinoline-3-carboxamide.

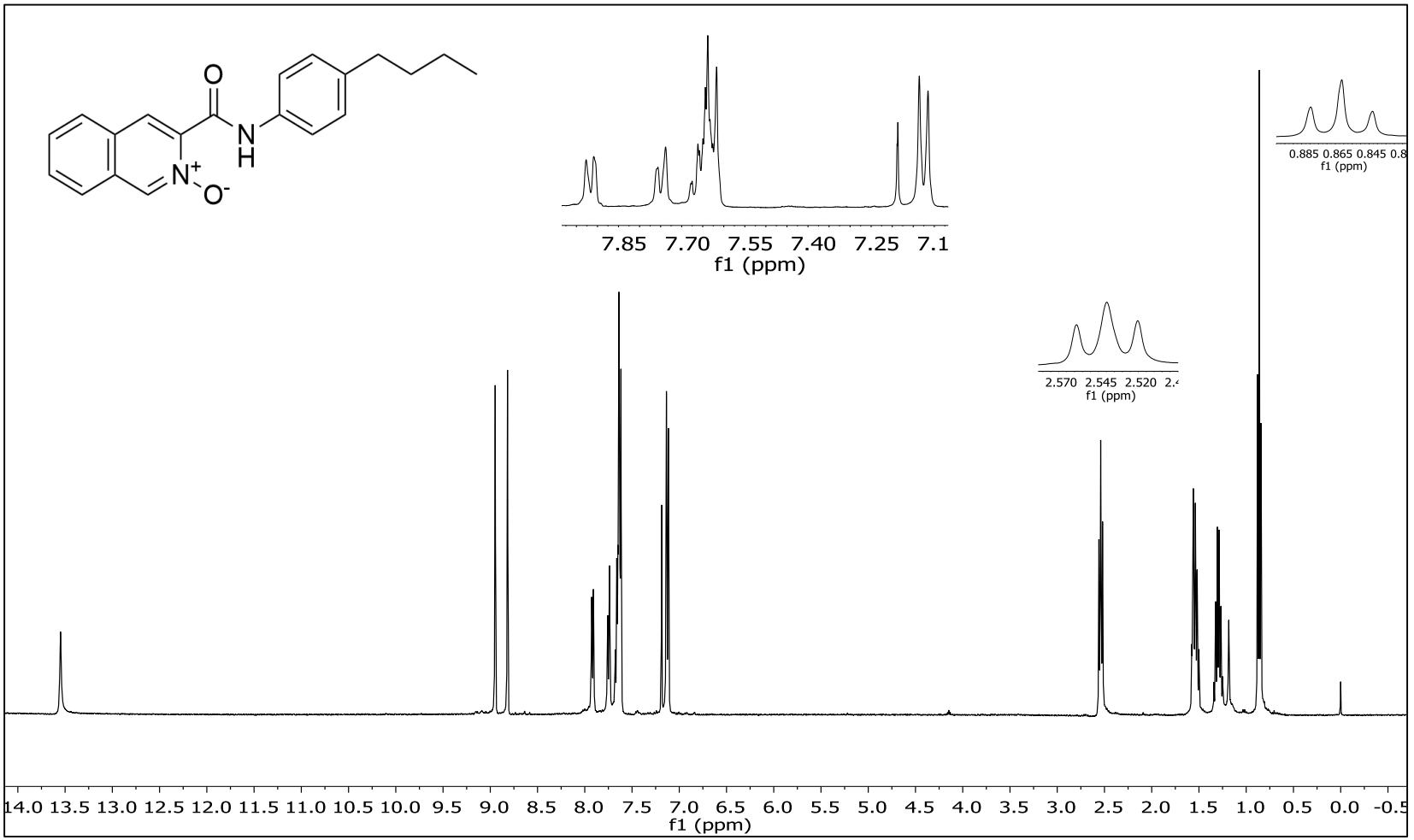

Figure A.46. ^{1}H-NMR Spectrum of 3-[(4-butylphenyl)carbamoyl]isoquinoline 2-oxide.

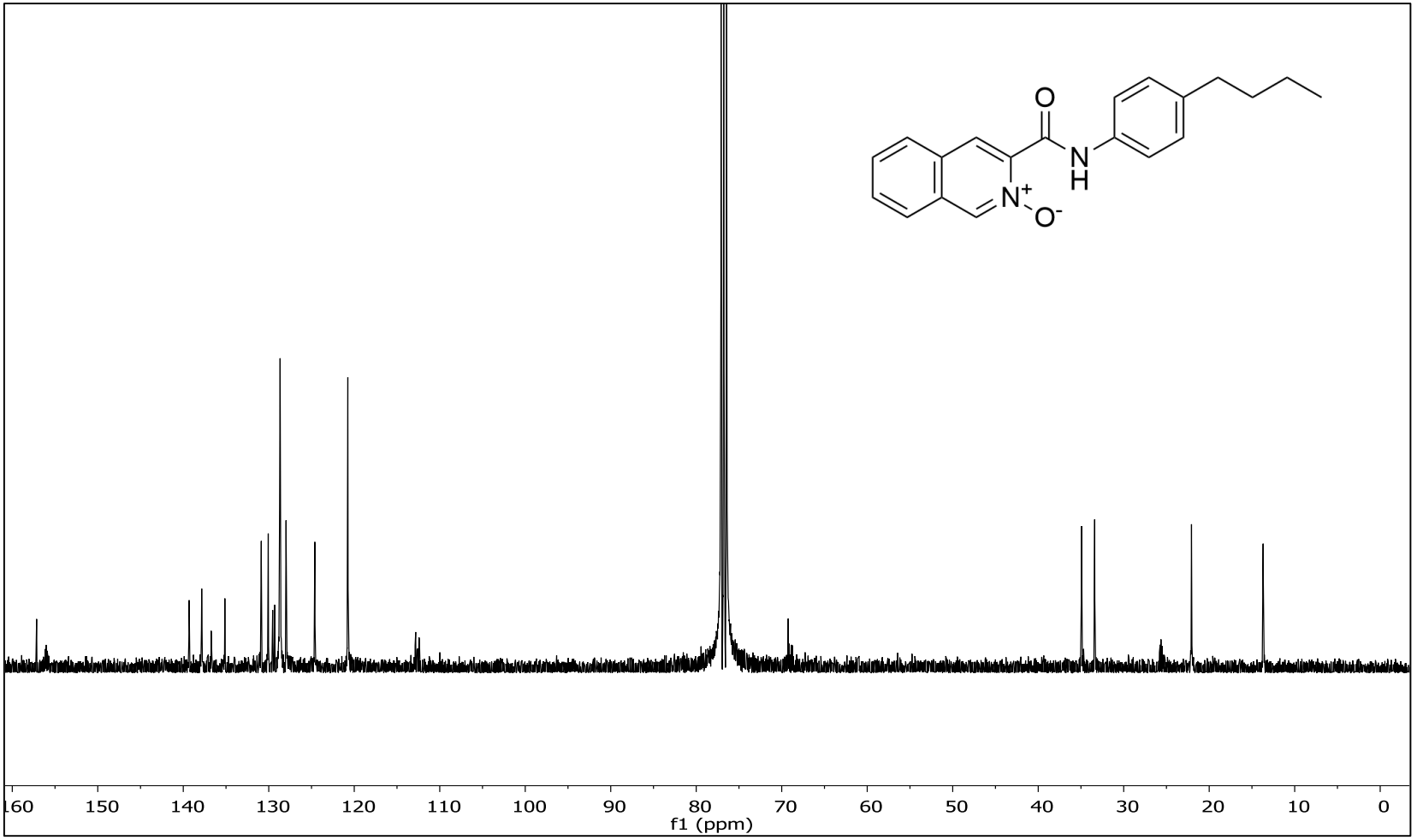

Figure A.47. ^{13}C-NMR Spectrum of 3-[(4-butylphenyl)carbamoyl]isoquinoline 2-oxide.

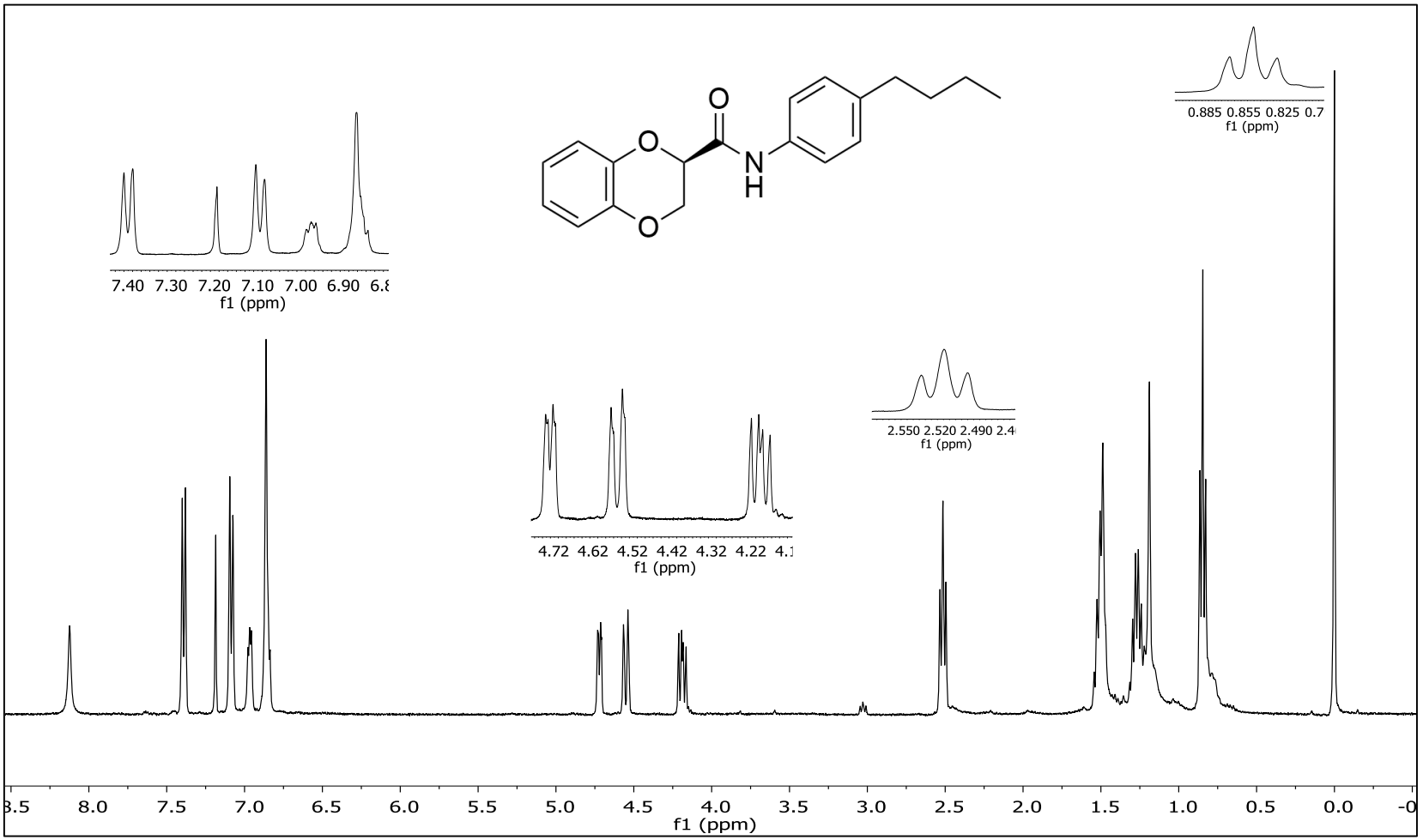

Figure A.48. ^{1}H-NMR Spectrum of (R)-N-(4-butylphenyl)-2,3-dihydrobenzo[b][1,4]dioxine-2-carboxamide.

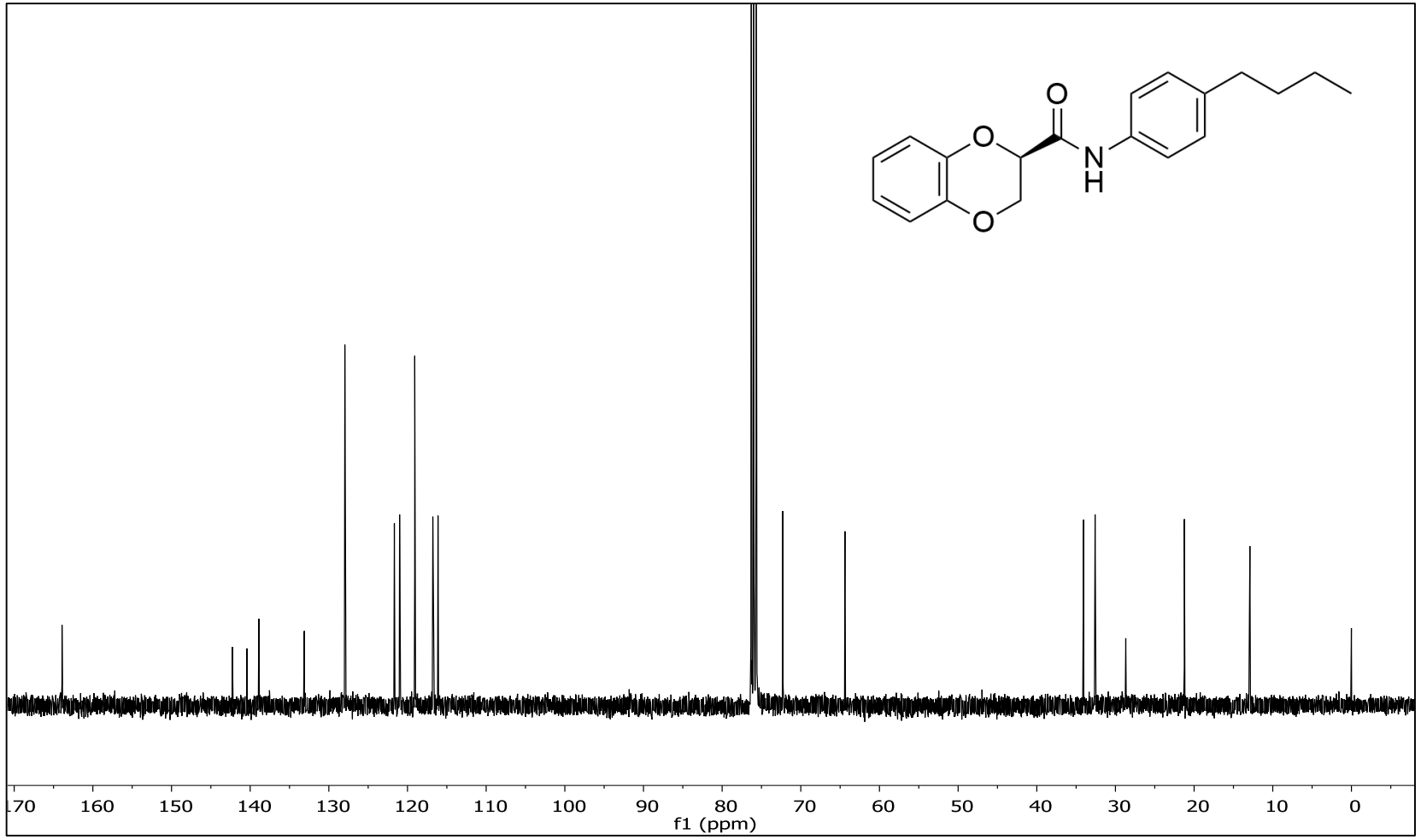

Figure A.49. ^{13}C-NMR Spectrum of (R)-N-(4-butylphenyl)-2,3-dihydrobenzo[b][1,4]dioxine-2-carboxamide.

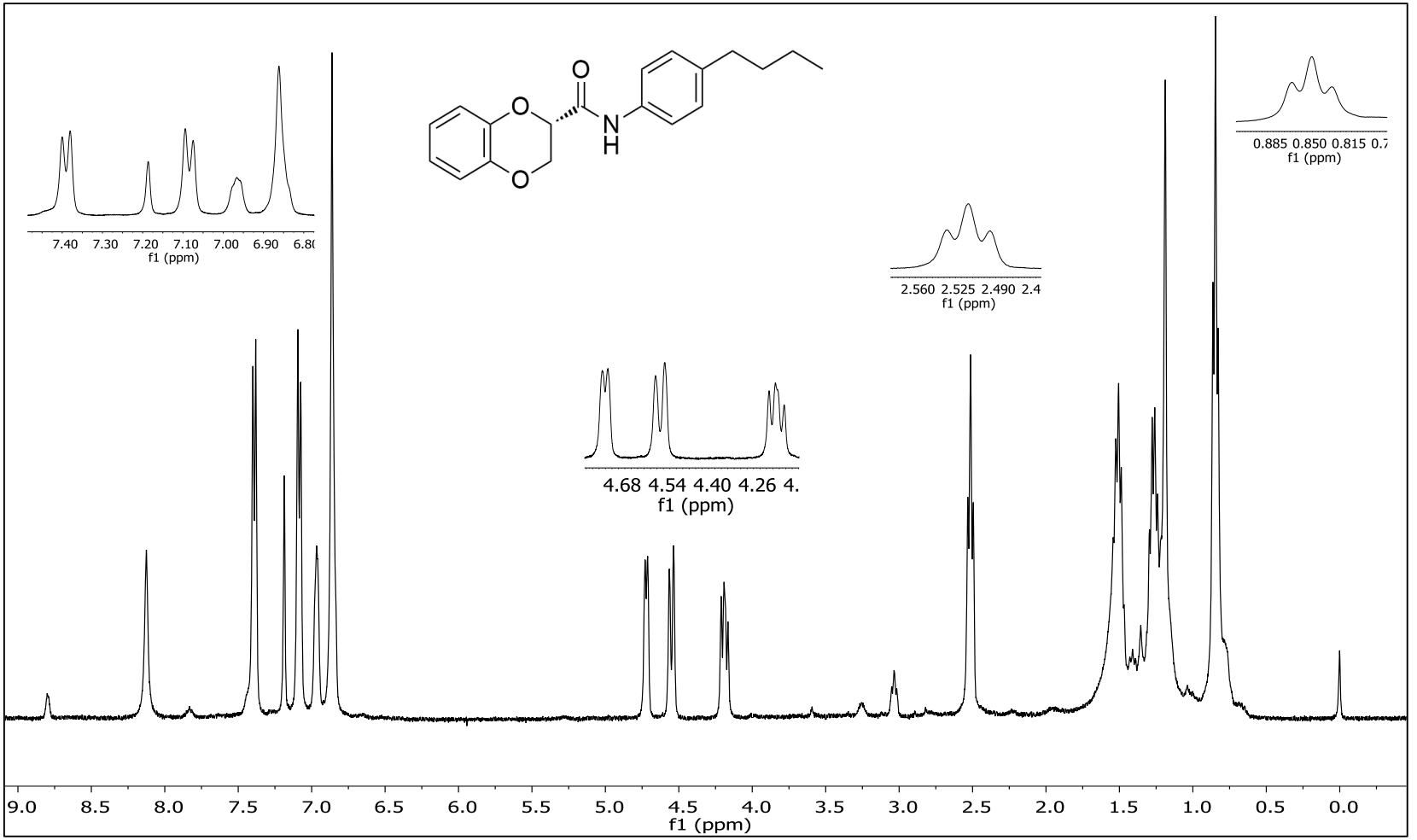

Figure A.50. ^{1}H-NMR Spectrum of (S)-N-(4-butylphenyl)-2,3-dihydrobenzo[b][1,4]dioxine-2-carboxamide.

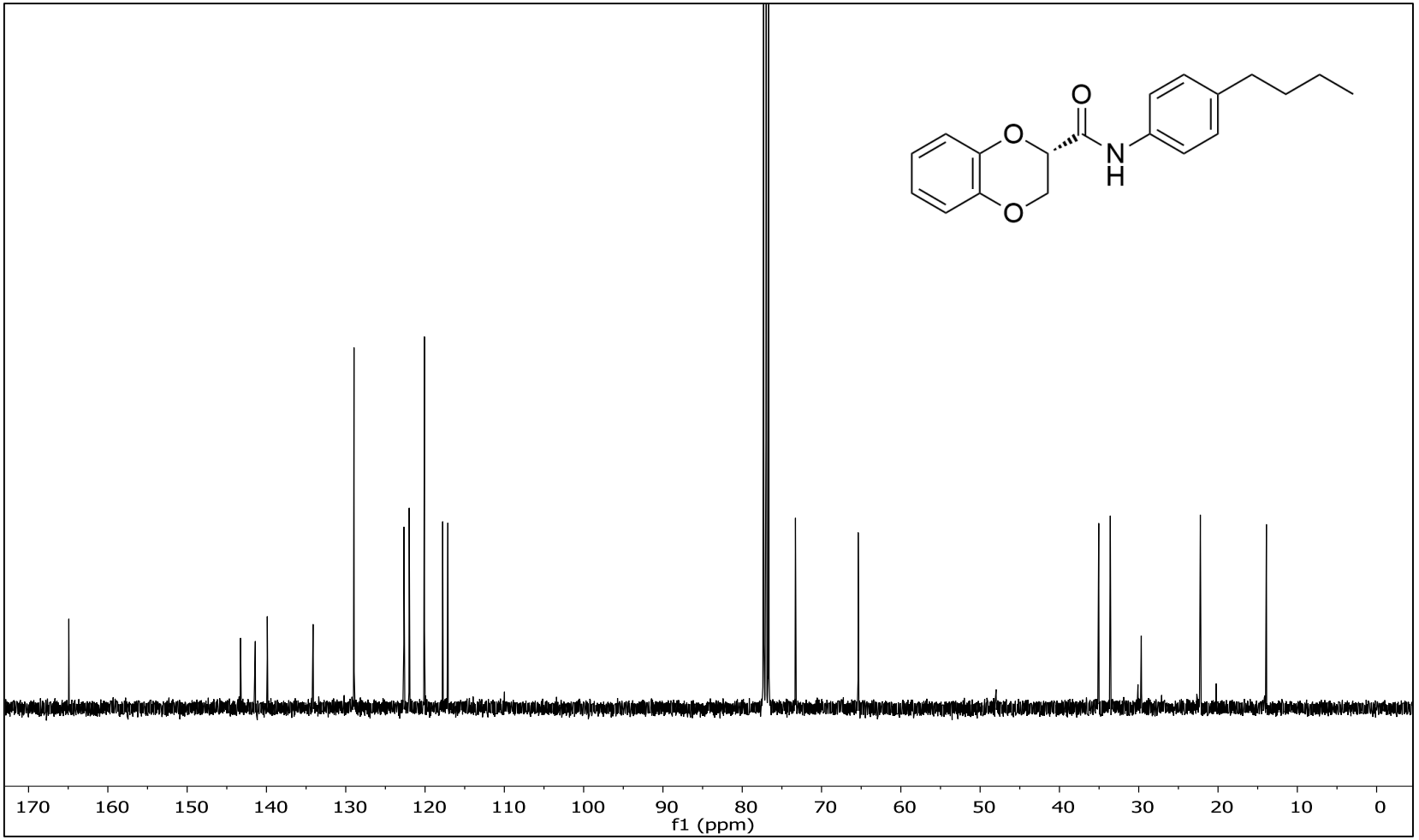

Figure A.51. ^{13}C-NMR Spectrum of (S)-N-(4-butylphenyl)-2,3-dihydrobenzo[b][1,4]dioxine-2-carboxamide.

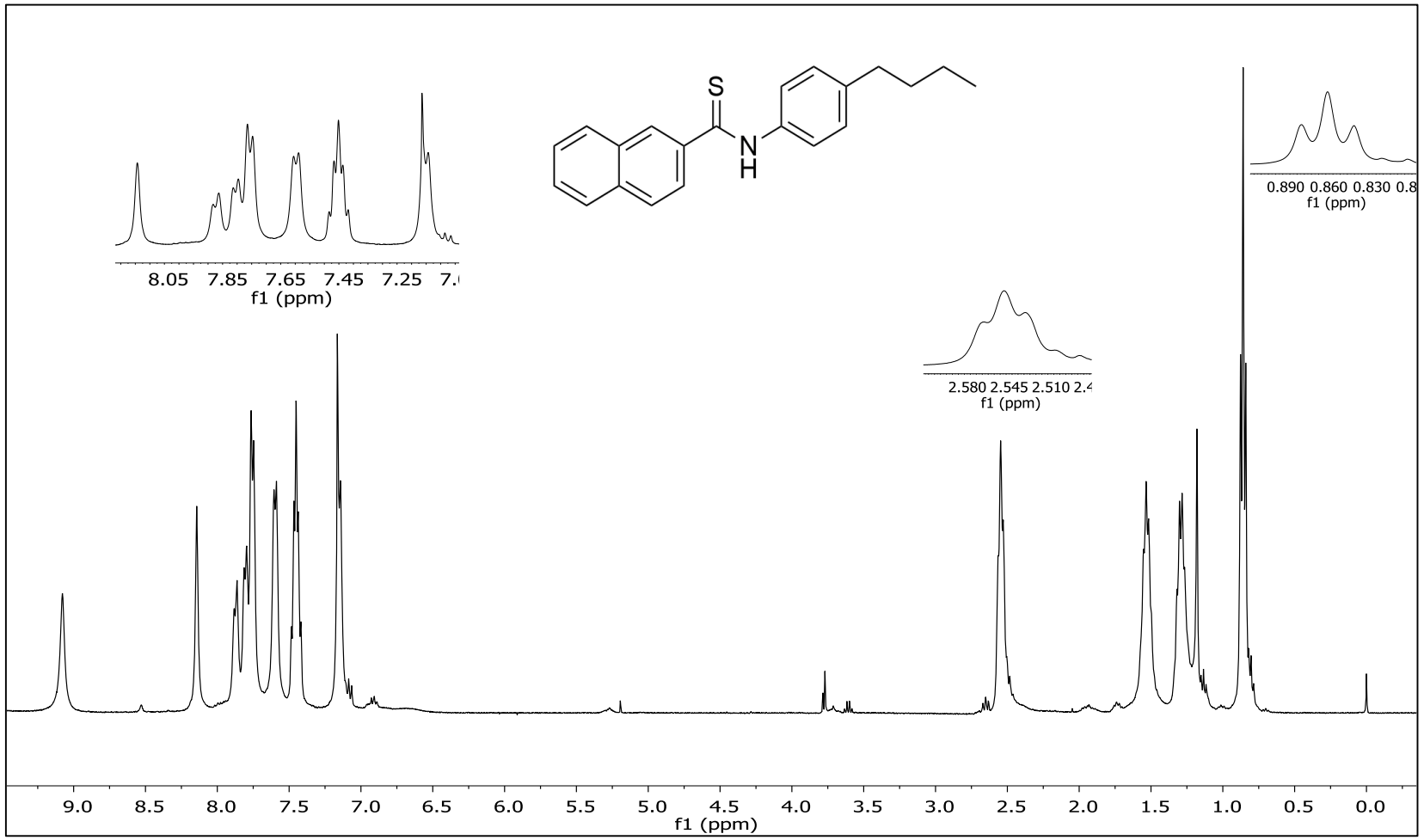

Figure A.52. ^{1}H-NMR Spectrum of N-(4-butylphenyl)naphthalene-2-carbothioamide.

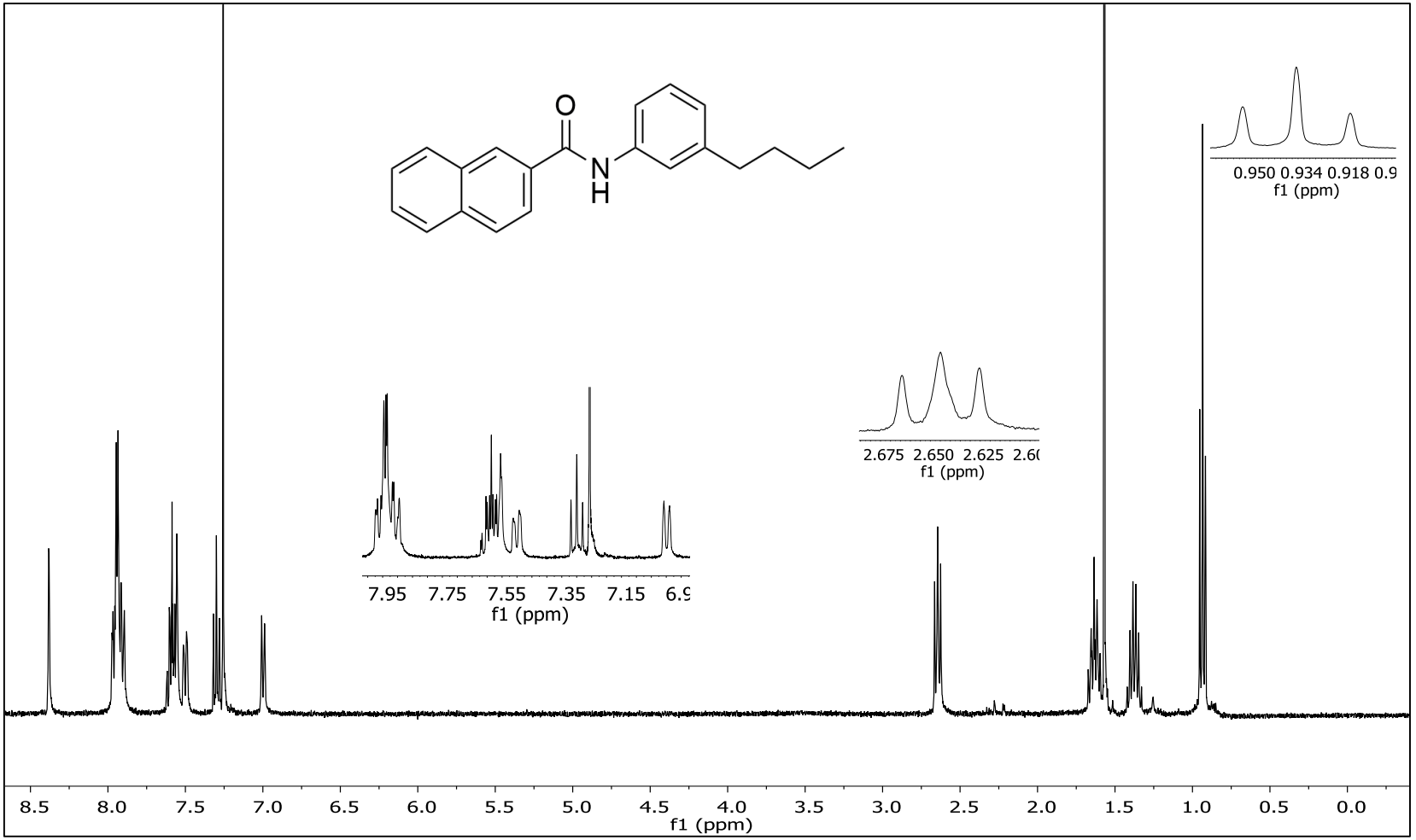

Figure A.53. ^{1}H-NMR Spectrum of N-(3-butylphenyl)-2-naphthamide.

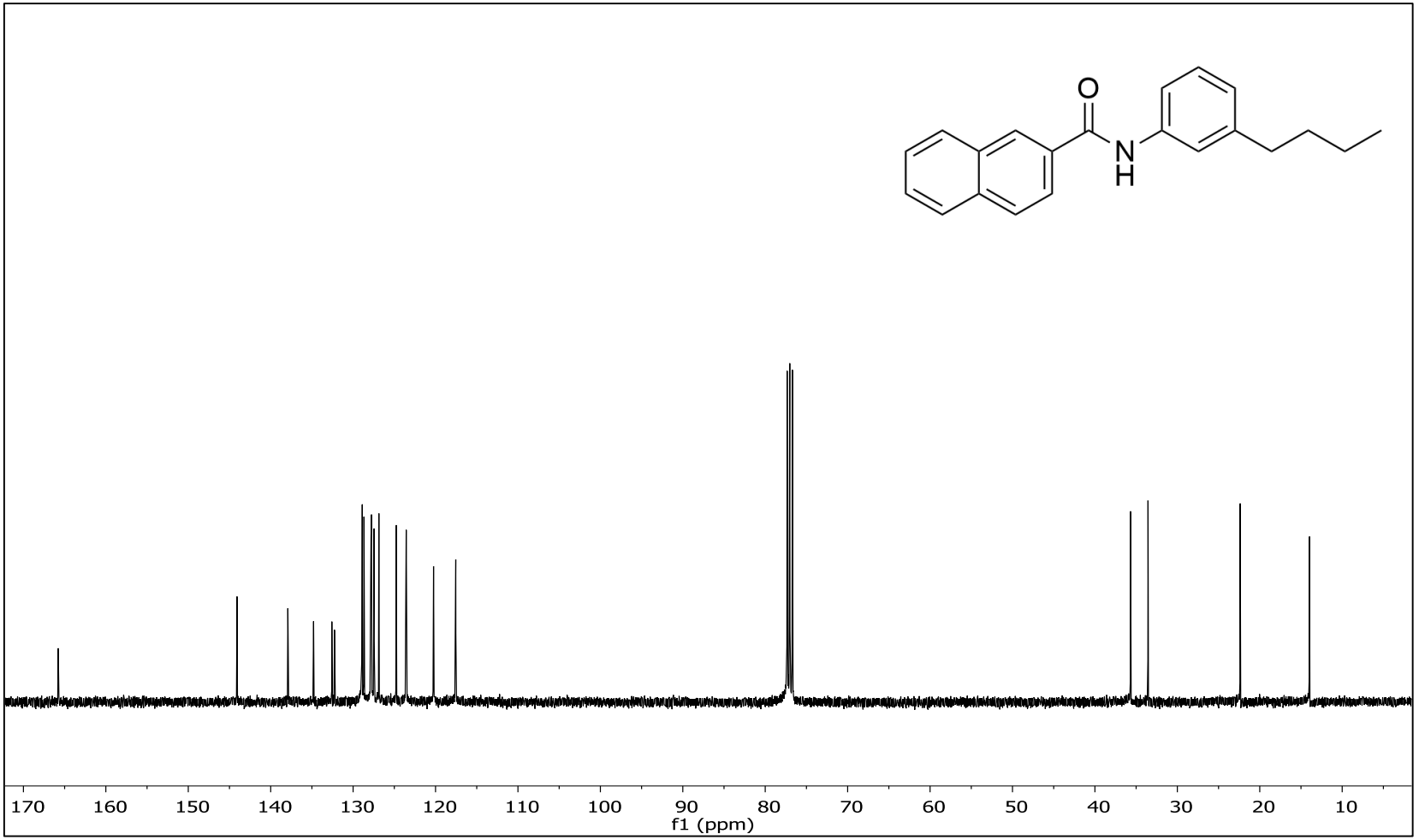

Figure A.54. ^{13}C-NMR Spectrum of N-(3-butylphenyl)-2-naphthamide.

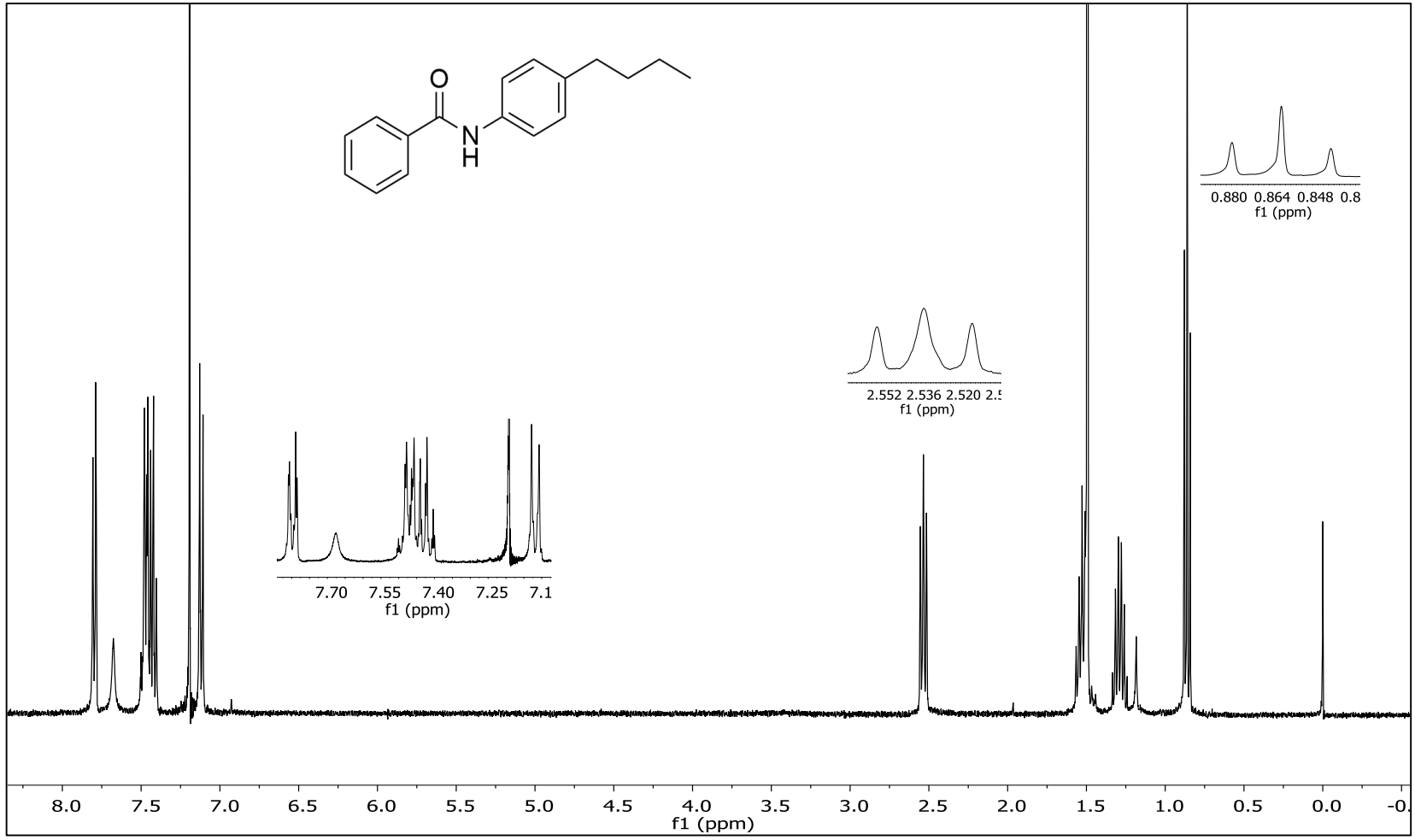

Figure A.55. ^{1}H-NMR Spectrum of N-(4-butylphenyl)benzamide.

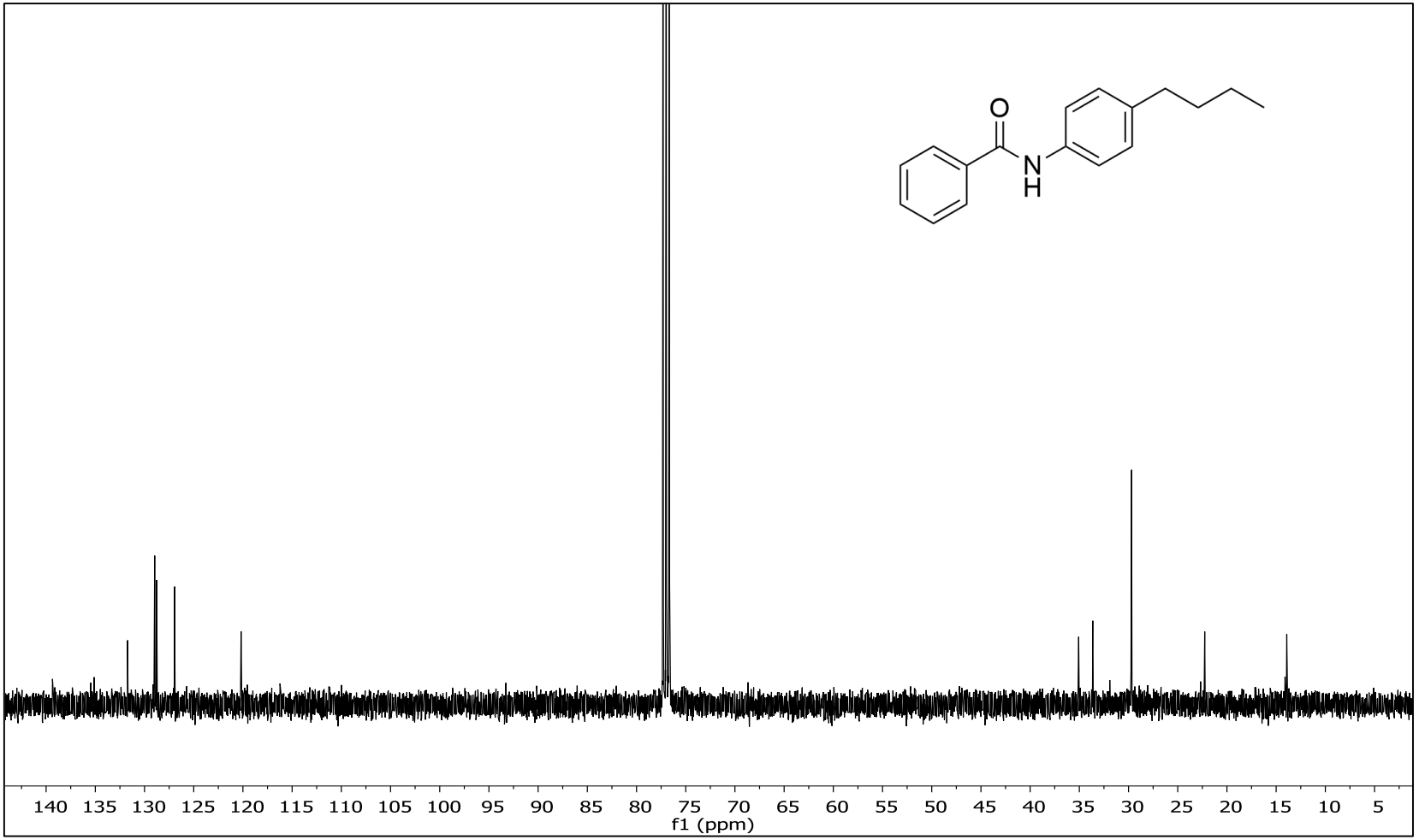

Figure A.56. ^{13}C-NMR Spectrum of N-(4-butylphenyl)benzamide.

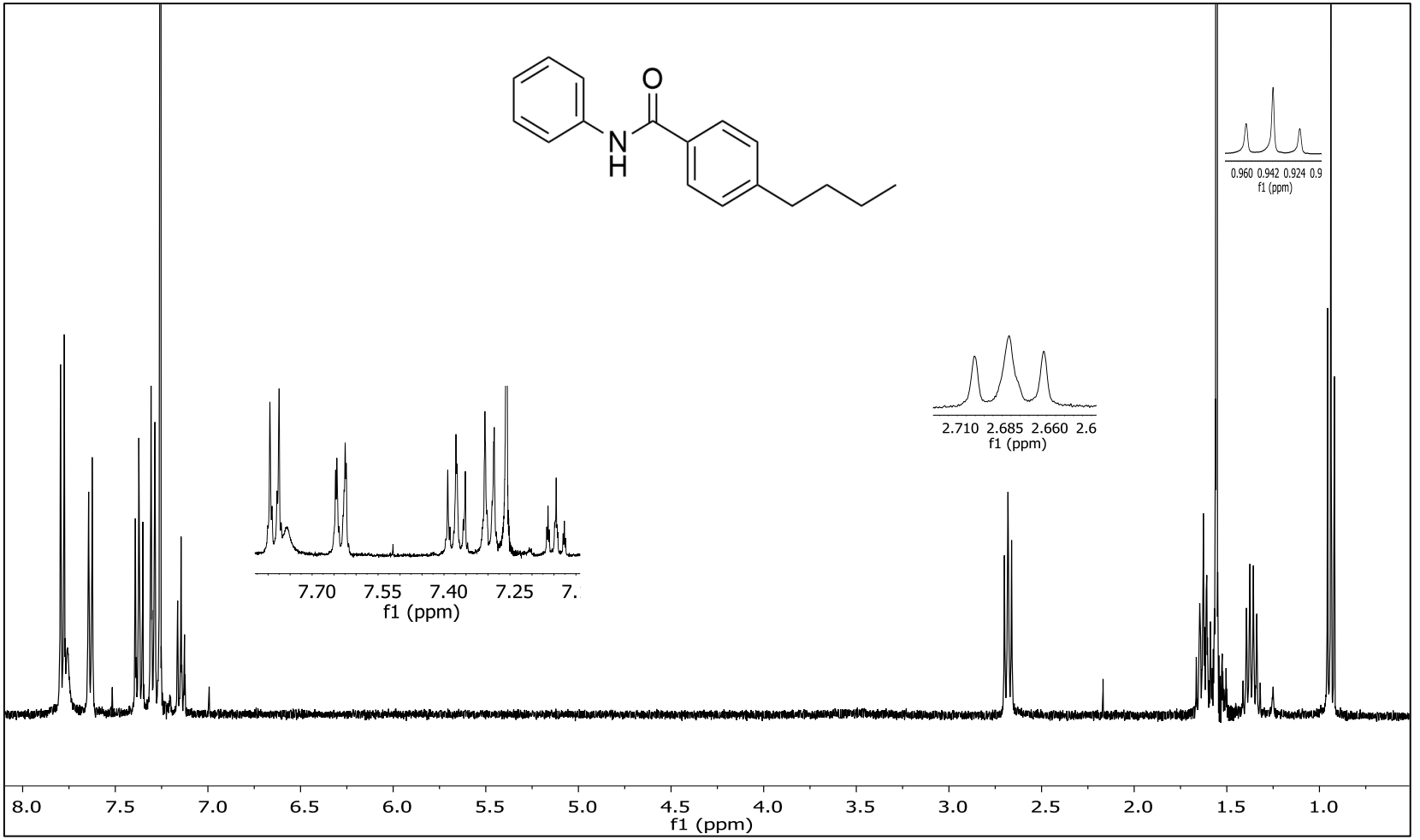

Figure A.57. ^{1}H-NMR Spectrum of 4-butyl-N-phenylbenzamide.

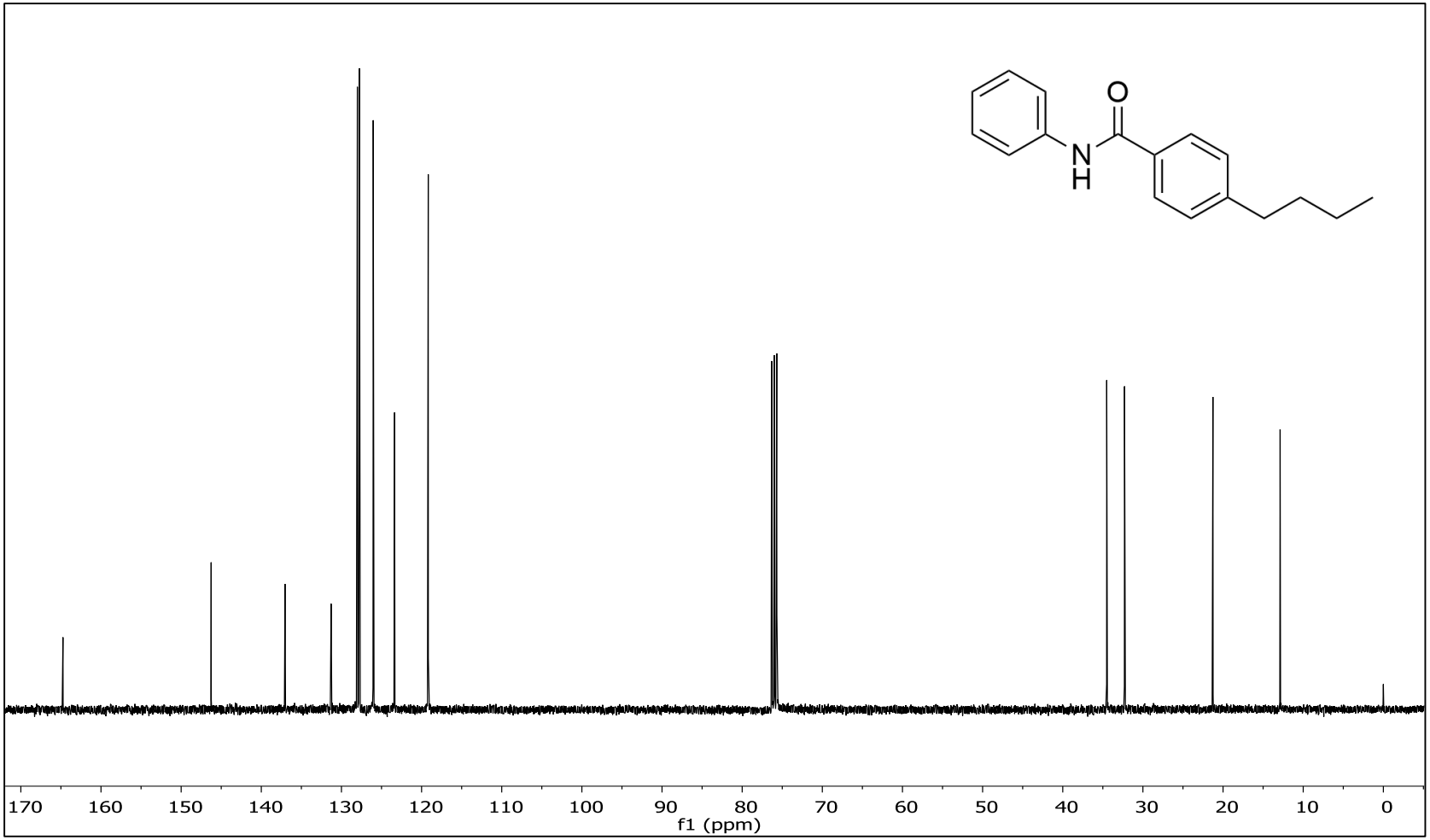

Figure A.58. ^{13}C-NMR Spectrum of 4-butyl-N-phenylbenzamide.

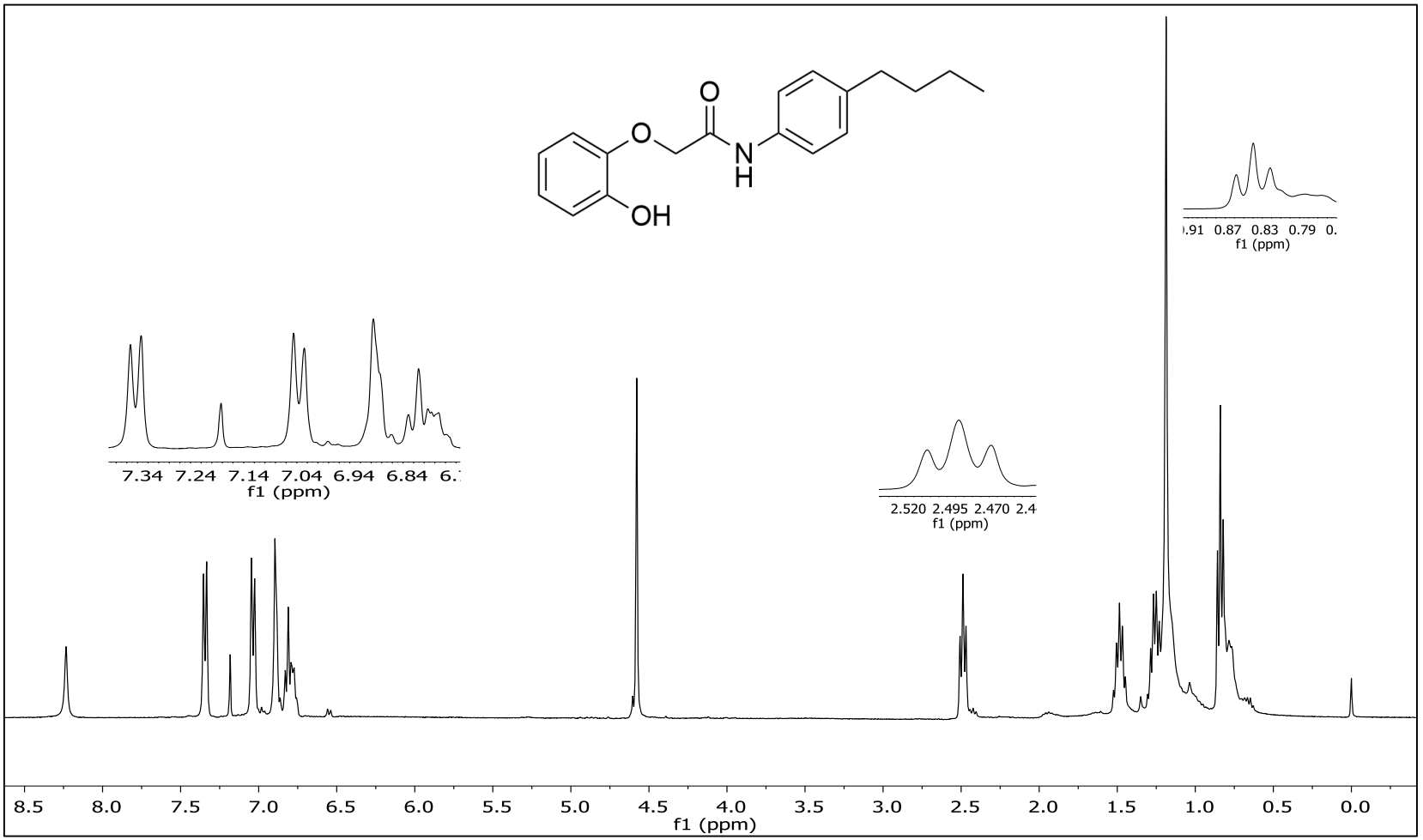

Figure A.59. ^{1}H-NMR Spectrum of N-(4-butylphenyl)-2-(2-hydroxyphenoxy)acetamide.

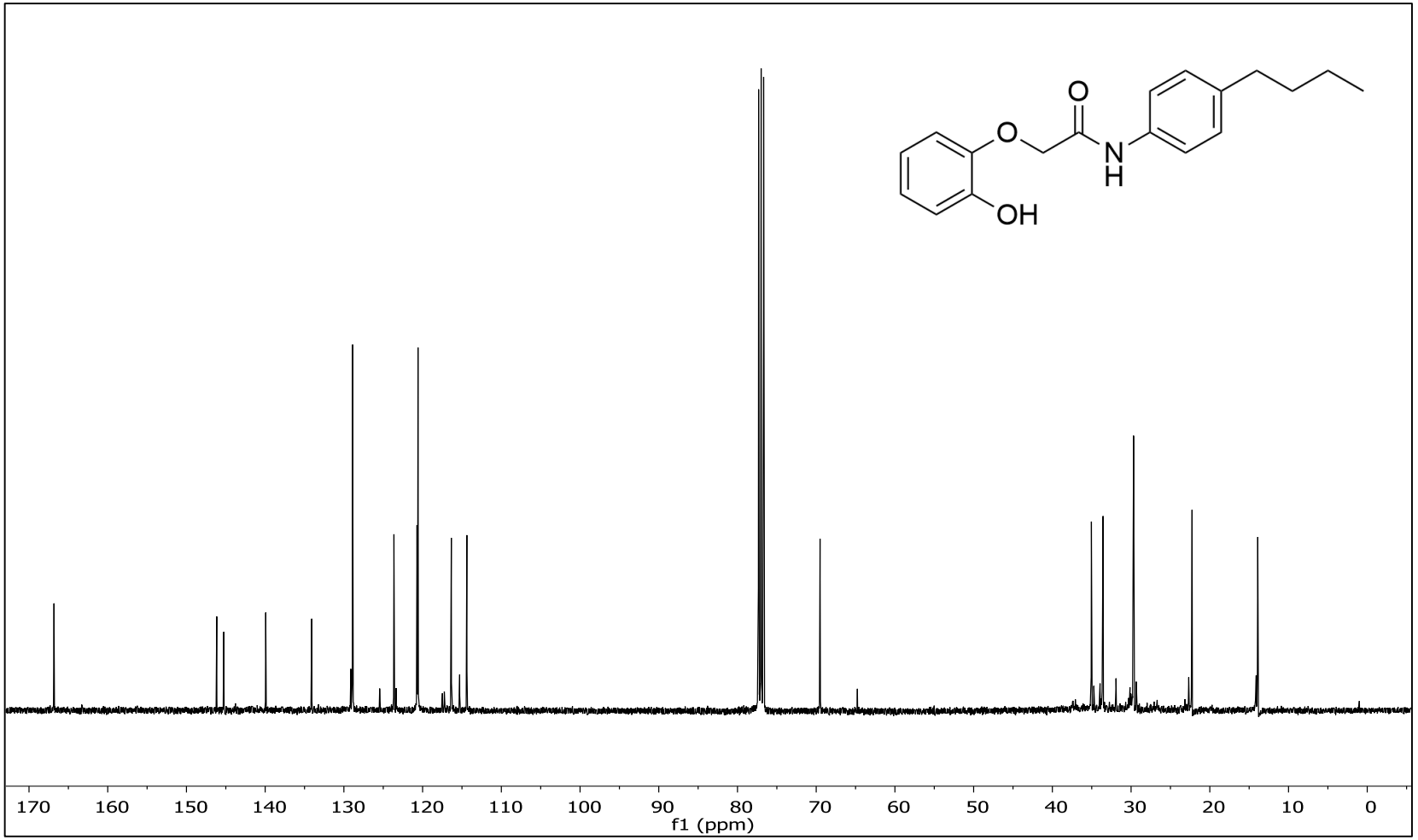

Figure A.60. ^{13}C-NMR Spectrum of N-(4-butylphenyl)-2-(2-hydroxyphenoxy)acetamide.

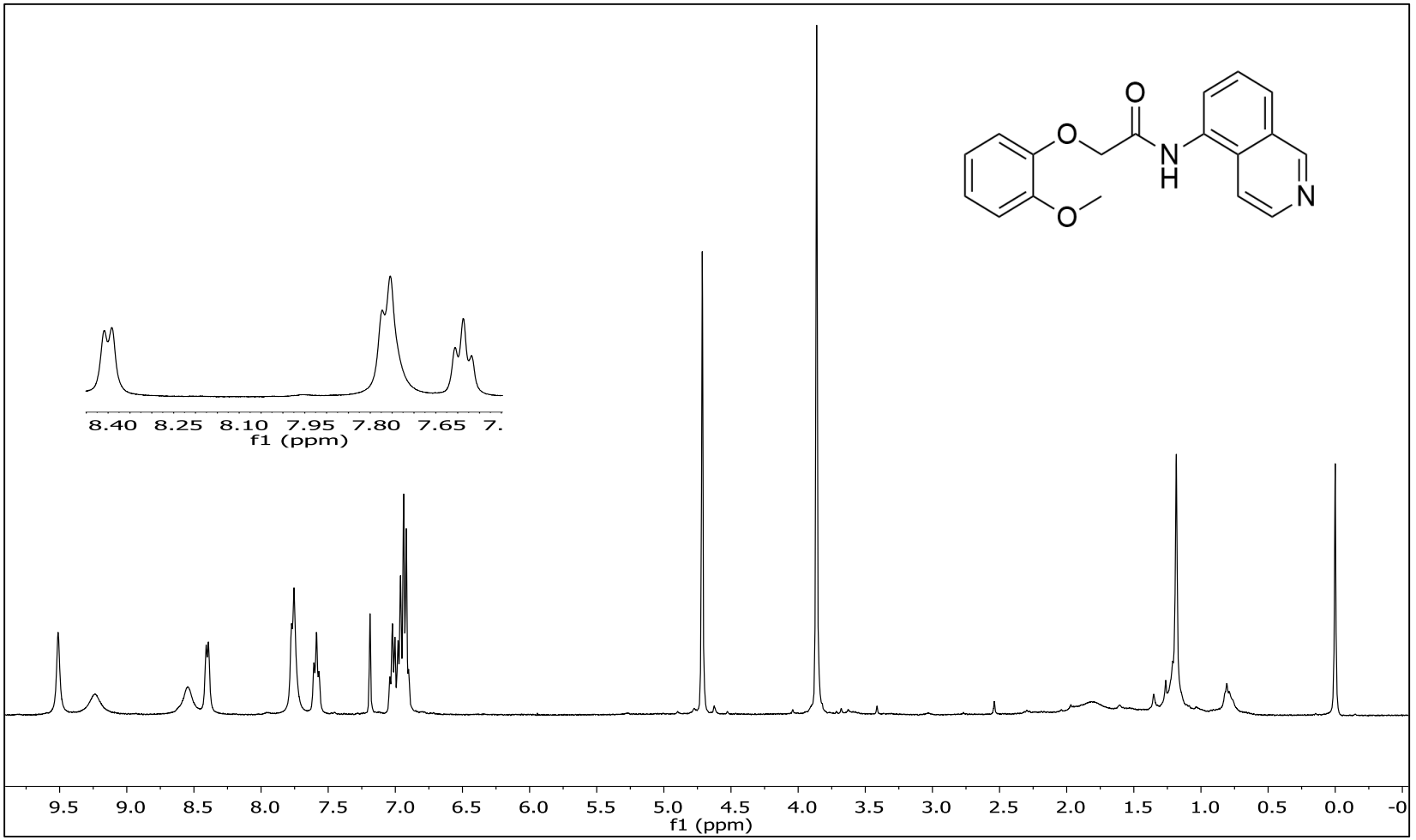

Figure A.61. ^{1}H-NMR Spectrum of N-(isoquinolin-5-yl)-2-(2-methoxyphenoxy)acetamide.

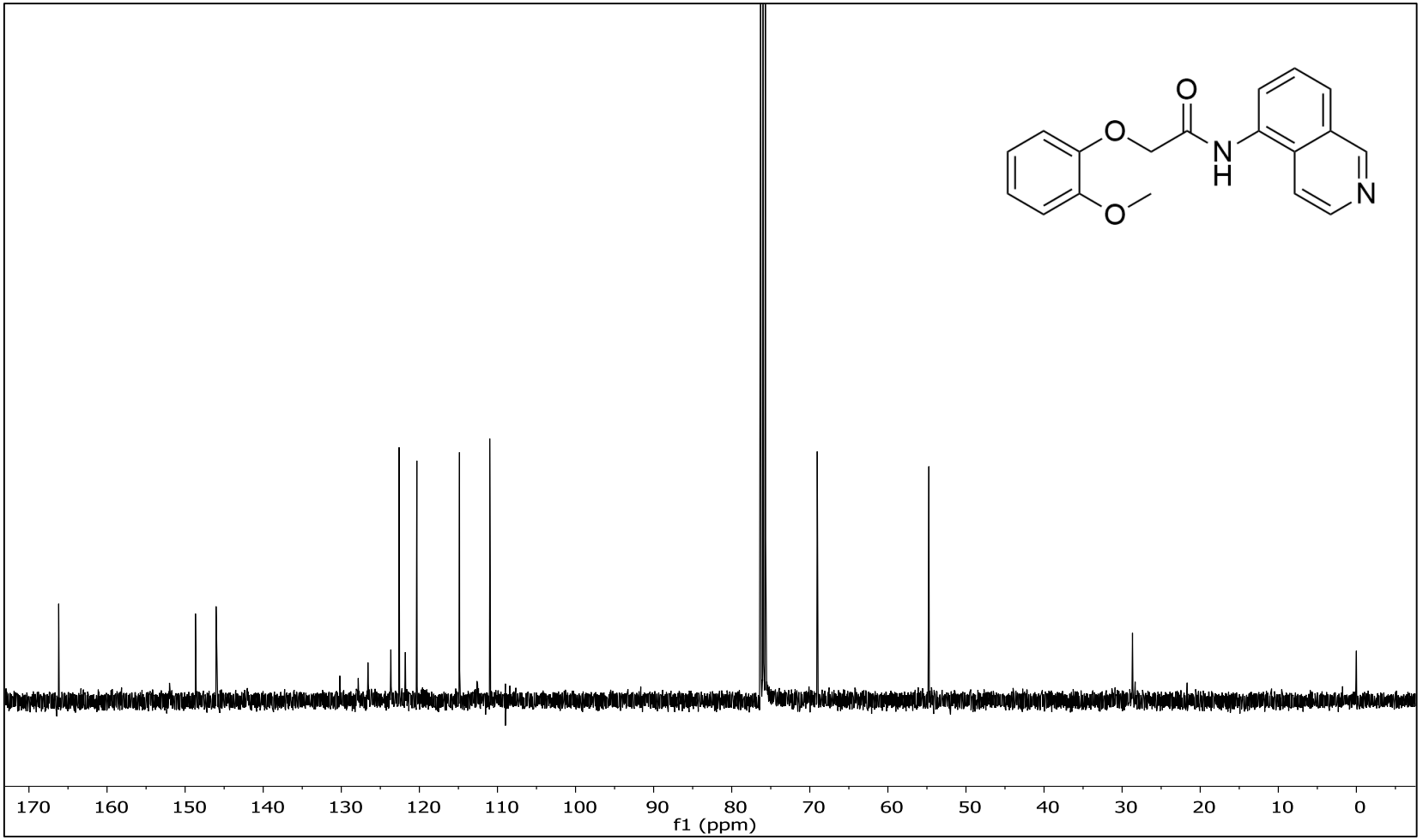

Figure A.62. ^{13}C-NMR Spectrum of N-(isoquinolin-5-yl)-2-(2-methoxyphenoxy)acetamide.

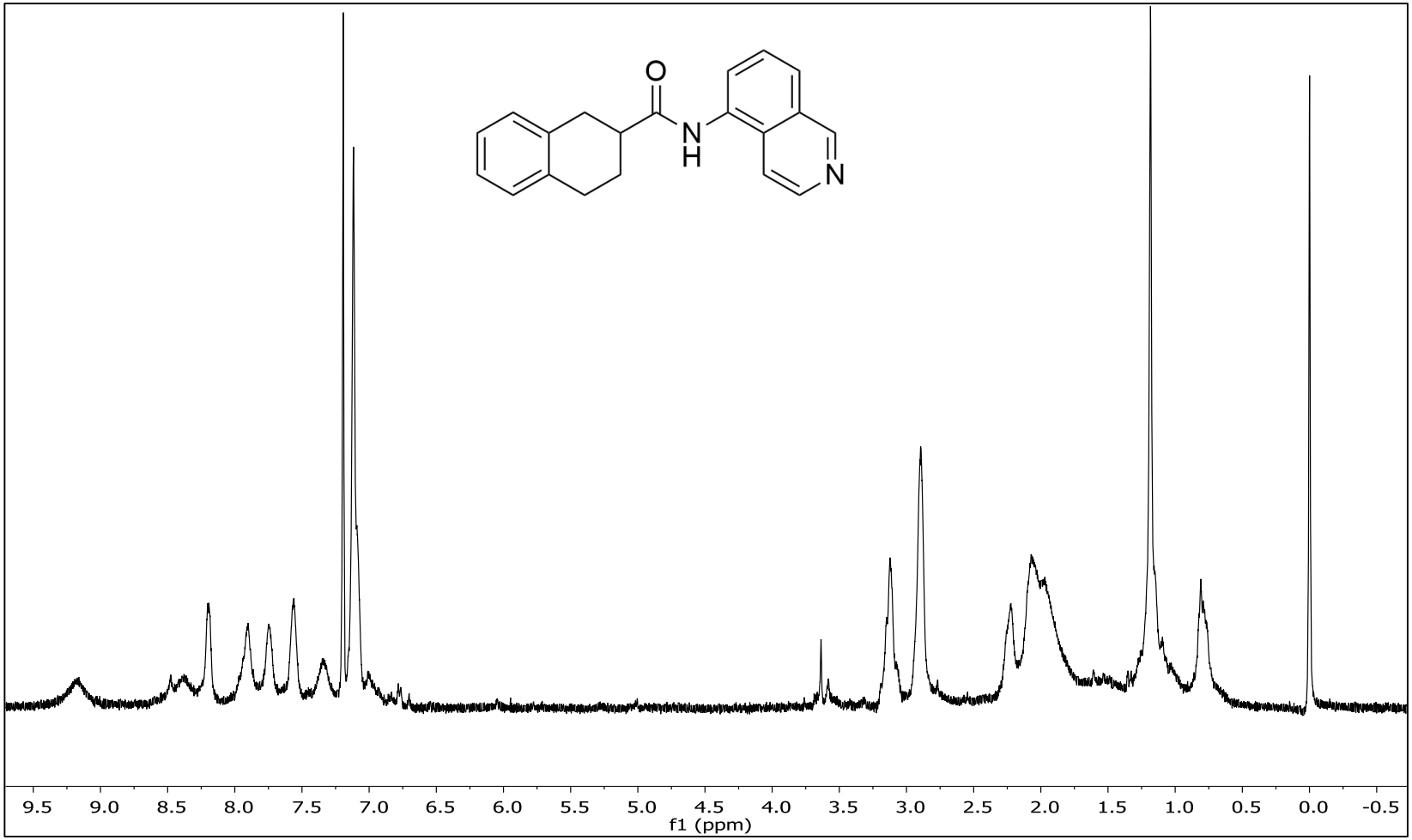

Figure A.63. ^{1}H-NMR Spectrum of N-(isoquinolin-5-yl)-1,2,3,4-tetrahydronaphthalene-2-carboxamide.

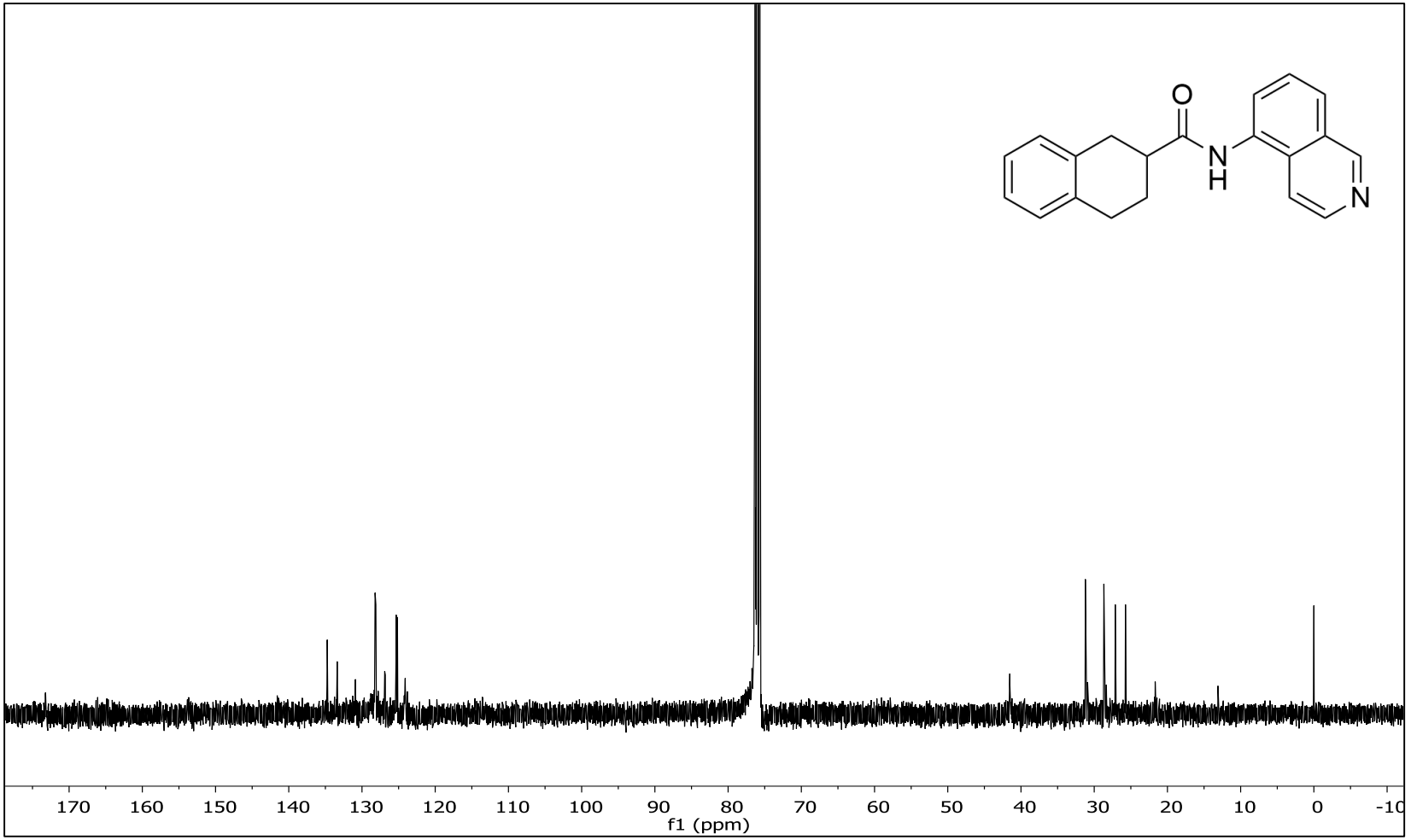

Figure A.64. ^{13}C-NMR Spectrum of N-(isoquinolin-5-yl)-1,2,3,4-tetrahydronaphthalene-2-carboxamide.

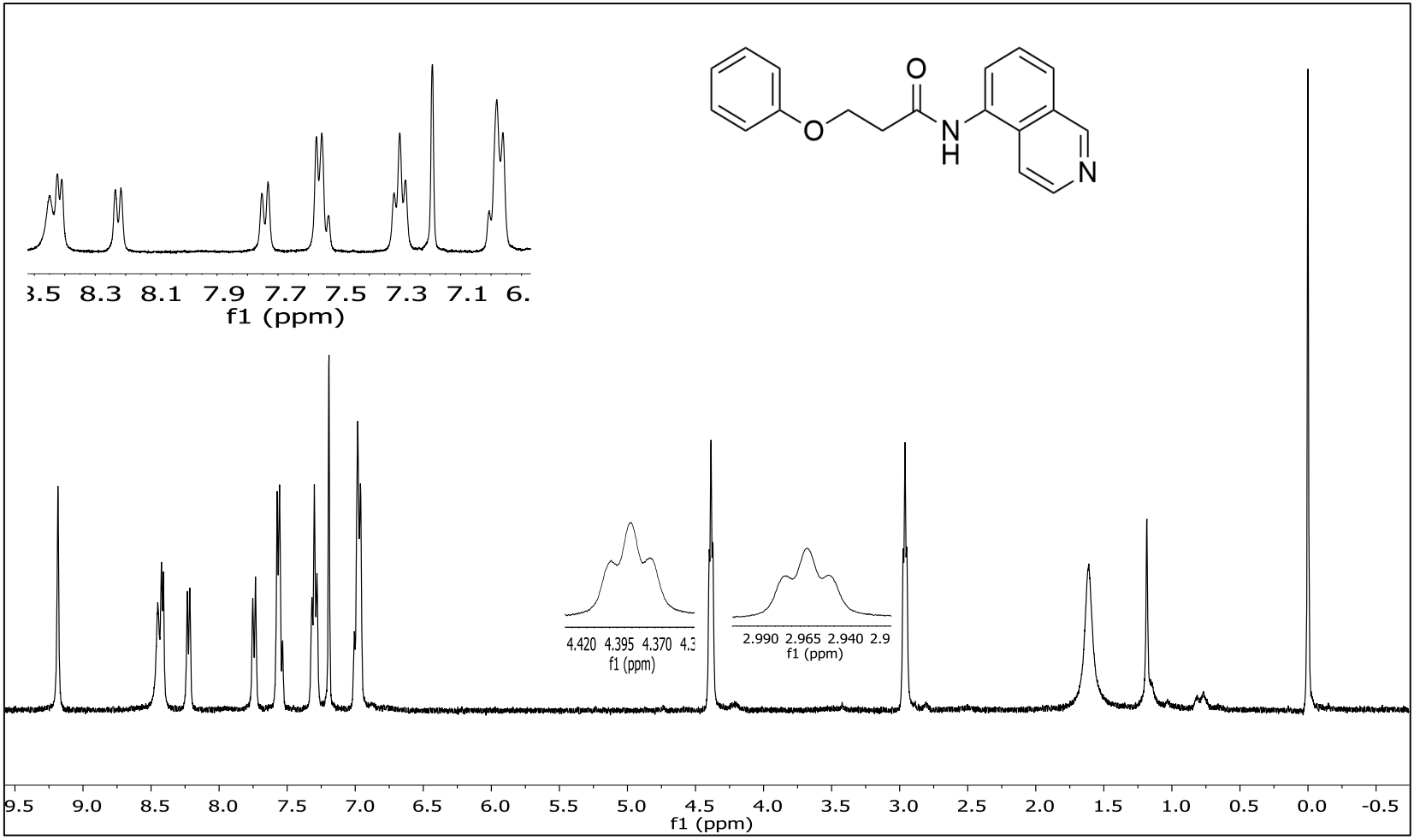

Figure A.65. ^{1}H-NMR Spectrum of N-(isoquinolin-5-yl)-3-phenoxypropanamide.

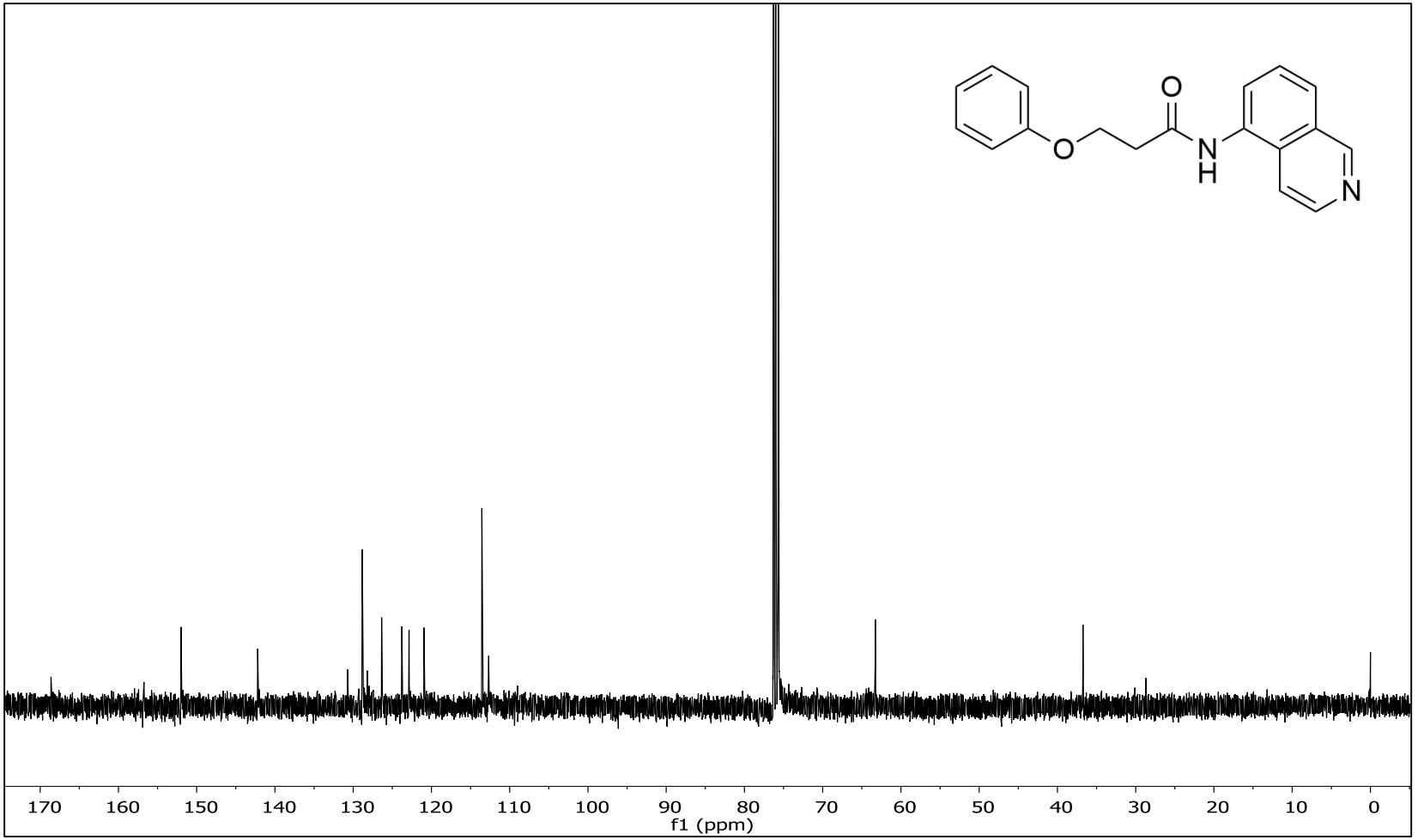

Figure A.66. ^{13}C-NMR Spectrum of N-(isoquinolin-5-yl)-3-phenoxypropanamide.

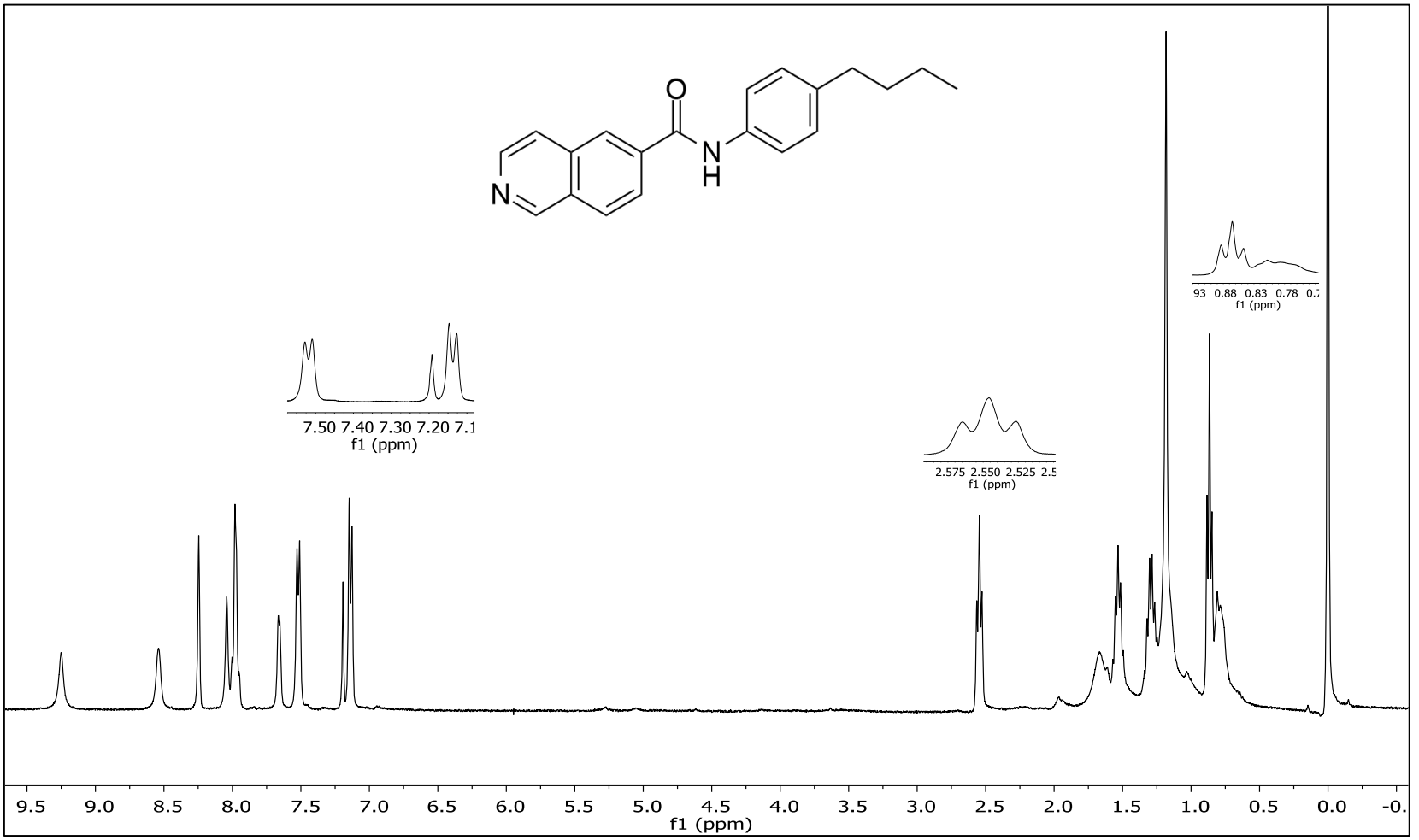

Figure A.67. ^{1}H-NMR Spectrum of N-(4-butylphenyl)isoquinoline-6-carboxamide.

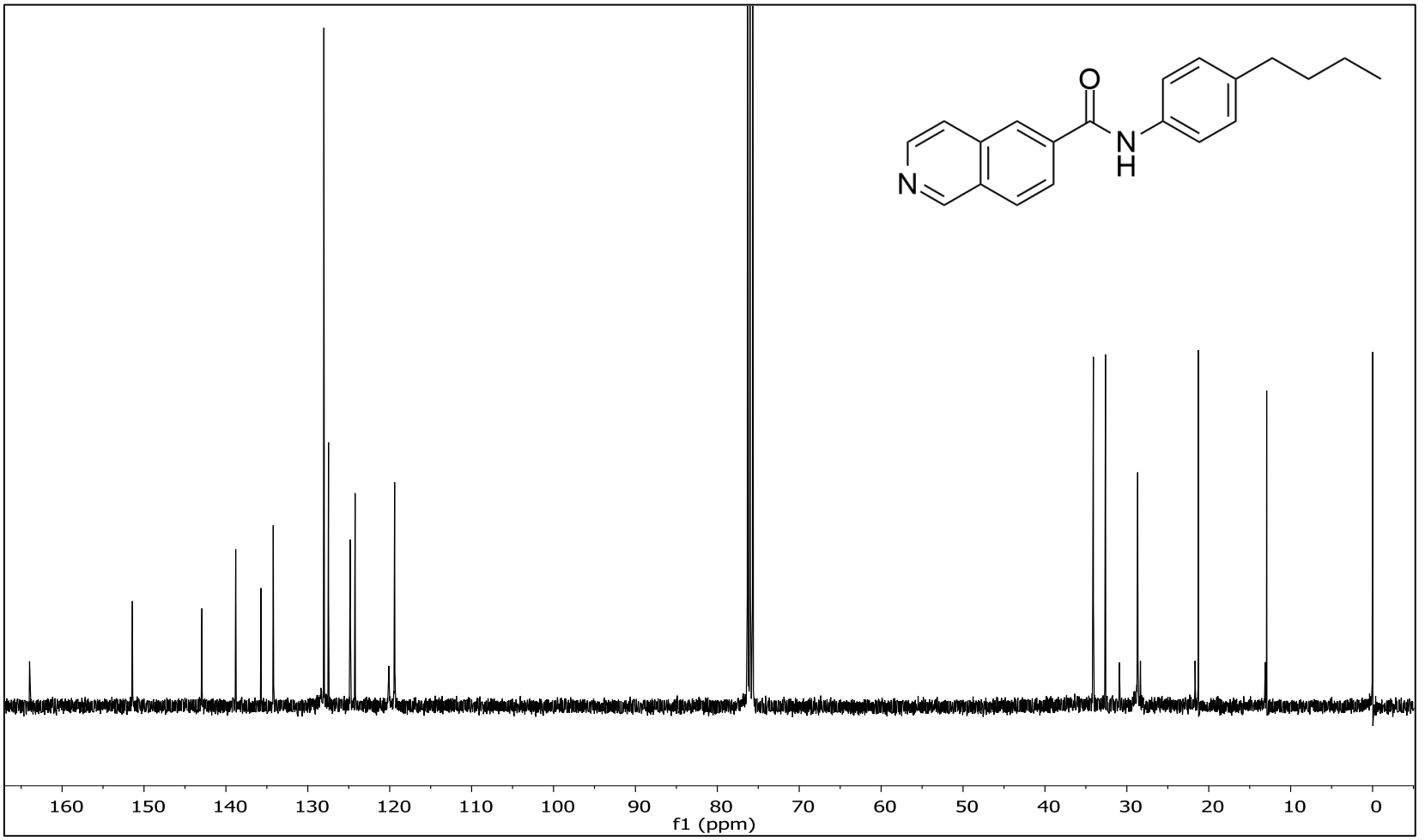

Figure A.68. ^{13}C-NMR Spectrum of N-(4-butylphenyl)isoquinoline-6-carboxamide.

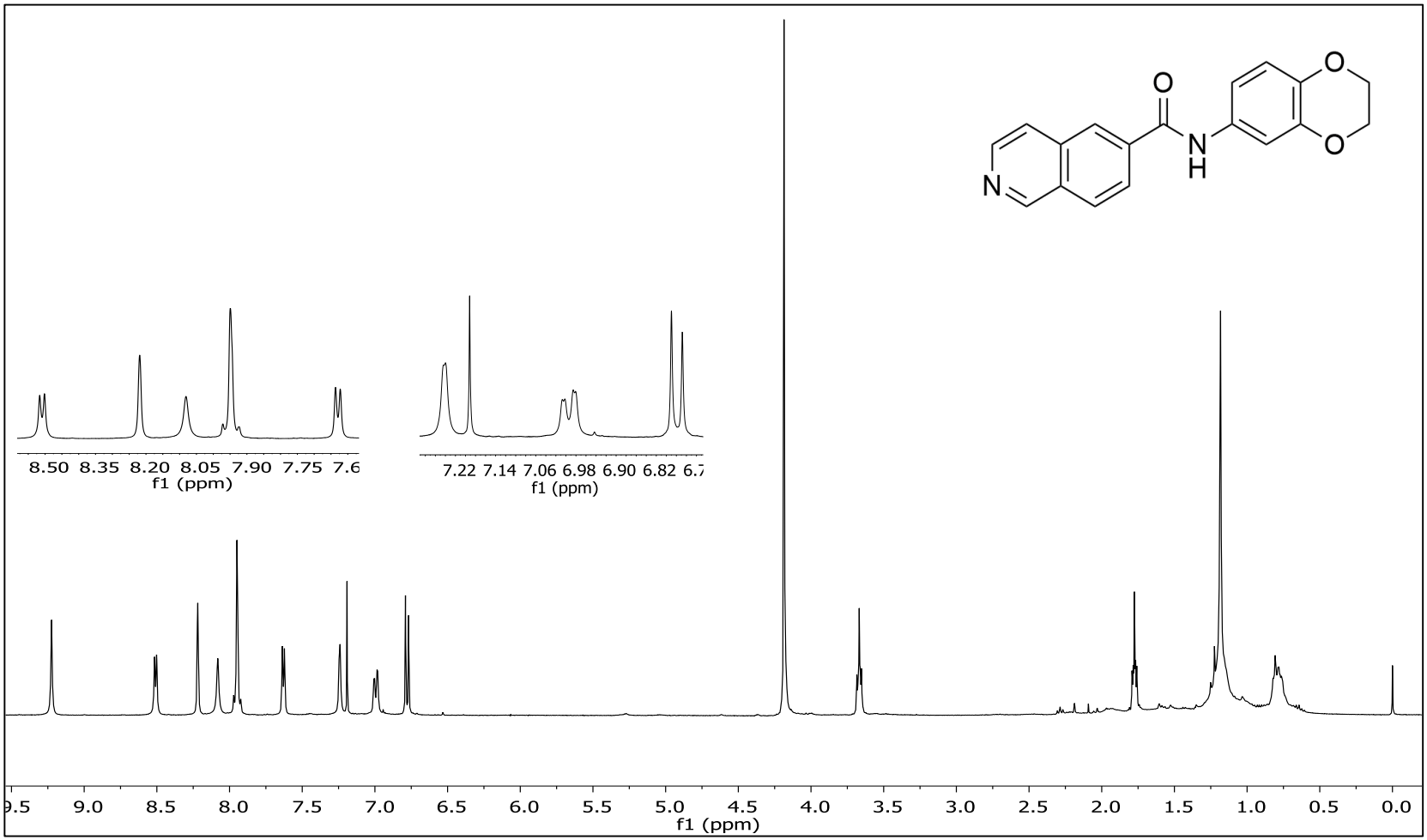

Figure A.69. ^{1}H-NMR Spectrum of N-(2,3-dihydrobenzo[b][1,4]dioxin-6-yl)isoquinoline-6-carboxamide.

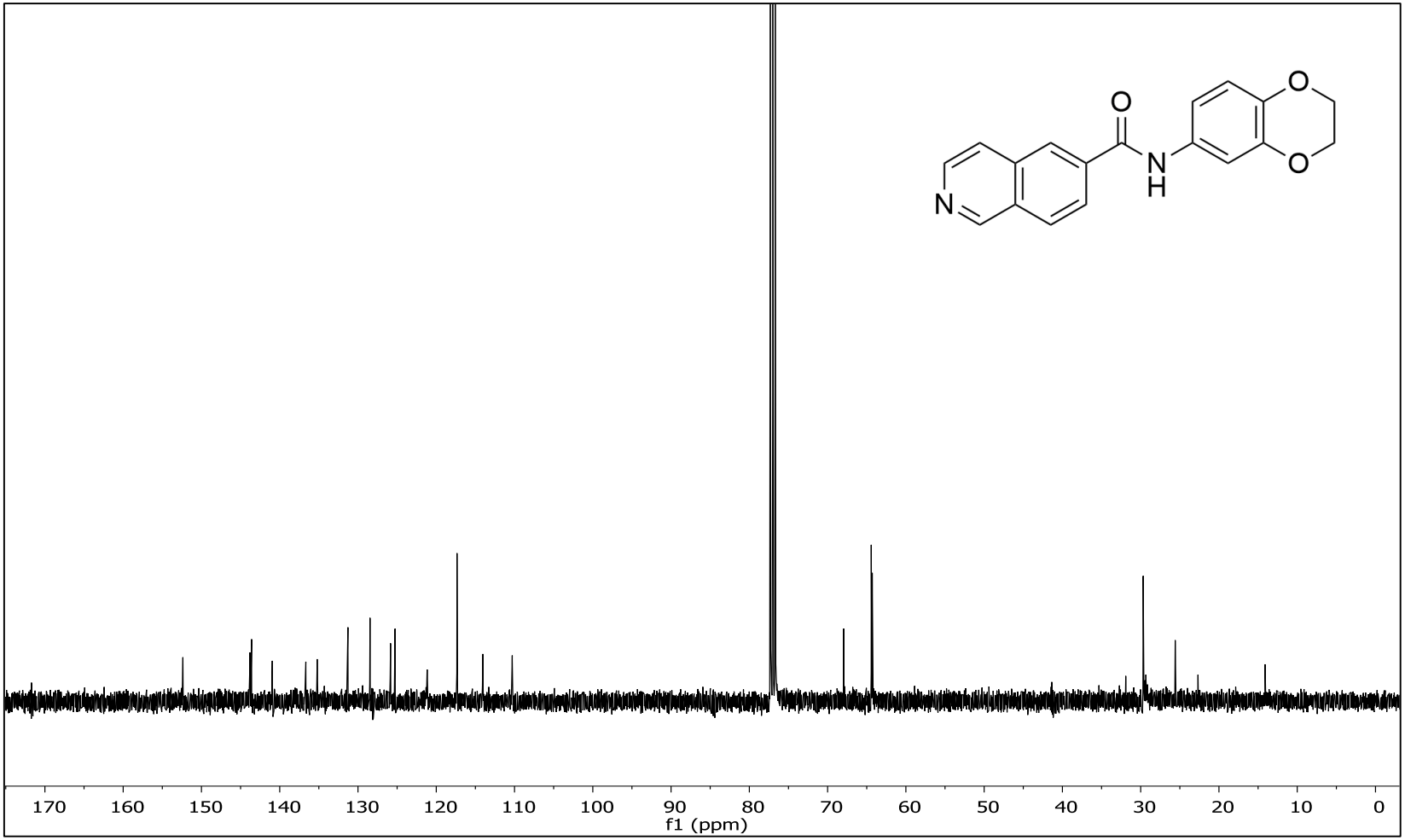

Figure A.70. ^{13}C-NMR Spectrum of N-(2,3-dihydrobenzo[b][1,4]dioxin-6-yl)isoquinoline-6-carboxamide.

REFERENCES

1. Mendieta, M. A. E., *Heme-iron Complexing Biphenyl and Naphthalene Derivatives as CYP17 Inhibitors for the Treatment of Prostate Cancer: Design, Synthesis and Evaluation*, Ph.D. Thesis, Saarland University, 2008.

2. National Cancer Institute, "Causes and Prevention", http://www.cancer.gov/cancertopics/causes, [Accessed April 2015].

3. Damber, J. E., G., Aus, "Prostate Cancer", *Lancet*, Vol. 371, pp. 1710-1721, 2008.

4. Isaacs, J. T., "Role of Androgens in Prostate Cancer", *Vitamins & Hormones*, Vol. 49, pp. 433-502, 1994.

5. Seruga, B., A., Ocana, I. F., Tannock, "Drug Resistance in Metastatic Castration Resistant Prostate Cancer", *Nature Reviews Clinical Oncology*, Vol. 8, pp. 12-23, 2011.

6. Lehmusvaara, S., *Traditional and Novel Treatments for Prostate Cancer*, Academic Dissertation, University of Tampere, 2012.

7. Wikipedia.com, "Prostate", http://en.wikipedia.org/wiki/Prostate, [Accessed April 2015].

8. Leissner, K. H., L. E., Tisell, "The Weight of the Human Prostate", *Scandinavian Journal of Urology and Nephrology*, Vol. 13, No. 2, pp. 137-142, 1979.

9. Wikipedia.com, "File:Illu Prostate Lobes", http://en.wikipedia.org/wiki/File:Illu_prostate_lobes.jpg, [Accessed April 2015].

10. Urologymatch.com, “Prostate Anatomy”, http://www.urologymatch.com/ProstateAnatomy.htm, [Accessed April 2015].

11. Prostate-cancer.com, “Prostate Cancer Treatment Overview”, http://www.prostate-cancer.com/prostate-cancer-treatment-overview/overview-prostate-anatomy.html, [Accessed April 2015].

12. SIU School of Medicine, http://www.siumed.edu/surgery/urology/images/bladder.jpg, [Accessed April 2015].

13. Krieger, J. N., L., Nyberg, J. C., Nickel, “NIH Consensus Definition and Classification of Prostatitis”, *The Journal of the American Medical Association*, Vol. 282, No. 3, pp. 236-237, 1999.

14. Oh, W. K., M., Hurwitz, A. V., D'Amico, J. P., Richie, P. W., Kantoff, “Neoplasms of the Prostate”. In: Kufe, D. W., R. E., Pollock, R. R., Weichselbaum, R. C., Bast, T. S., Gansler, J. F., Holland, E., Frei editors, *Holland-Frei Cancer Medicine*, 6th edition, Hamilton (ON): BC Decker; Chapter 111, 2003. Available from: http://www.ncbi.nlm.nih.gov/books/NBK13489/

15. American Cancer Society, “What are the Risk Factors for Prostate Cancer?”, http://www.cancer.org/cancer/prostatecancer/detailedguide/prostate-cancer-risk-factors, [Accessed April 2015].

16. American Cancer Society, “Can Prostate Cancer Be Prevented?”, http://www.cancer.org/cancer/prostatecancer/detailedguide/prostate-cancer-prevention, [Accessed April 2015].

17. Bonekamp, D., M. A., Jacobs, R., El-Khouli, D., Stoianovici, K. J., Macura, “Advancements in MR Imaging of the Prostate: From Diagnosis to Interventions”, *Radiographics*, Vol. 31, No. 3, pp. 677-703, 2011.

18. Barentsz, J. O., J., Richenberg, R., Clements, P. Choyke, S. Verma, G. Villeirs, O., Rouviere, V. Logager, J. J., Fütterer, "ESUR Prostate MR Guidelines 2012", *European Radiology*, Vol. 22, No. 4, pp. 746-757, 2012.

19. Natarajan, S., L. S., Marks, D., Margolis, J., Huang, M. L., Macairan, P., Lieu, A., Fenster, "Clinical Application of Ultrasound-Guided Prostate Biopsy System", *Urologic Oncology*, Vol. 29, No. 3, pp. 334-342, 2011.

20. Tan, N., D. J. A., Margolis, T. D., McClure, A., Thomas, D. S., Finley, R. E., Reiter, J. Huang, S. S., Raman, "Radical Prostatectomy: Value of Prostate MRI in Surgical Planning", *Abdominal Imagin*g, Vol. 37, pp. 664-674, 2012.

21. Essink-Bot, M., H. J., de Koning, H. G. T., Nijs, W. J., Kirkels, P. J., van der Maas, F. H., Schröder, "Short-Term Effects of Population-Based Screening for Prostate Cancer on Health-Related Quality of Life", *Journal of the National Cancer Institute*, Vol. 90, Issue. 12, pp. 925-931, 1998.

22. Figuerido, J. C., M. V., Grau, R. W., Haile, R. S., Sandler, R. W. Summers, R. S., Bresalier, C. A., Burke, G. E., McKeown-Eyssen, J. A., Baron, "Folic Acid and Risk of Prostate Cancer: Results from a Randomized Clinical Trial", *Journal of National Cancer Institute*, Vol. 101, No. 6, pp. 432-435, 2009.

23. Chuang, A., A. M., DeMarzo, R. W., Veltri, R. B., Sharma, C. J., Bieberich, J. I., Epstein, "Immunohistochemical Differentiation of High-Grade Prostate Carcinoma From Urothelial Carcinoma", *American Journal of Surgical Pathology*, Vol. 31, Issue 8., pp. 1246-1255, 2007.

24. Nutting, C., A., Horwich, C., Fisher, C., Parsons, D. P., Dearnaley, "Small-Cell Carcinoma of the Prostate", *Journal of the Royal Society of Medicine*, Vol. 90, No. 6, pp. 340-341, 1997.

25. Catz, S. D., J. L., Johnson, "BCL-2 in Prostate Cancer: A Minireview", *Apoptosis*, Vol. 8, pp. 29-37, 2003.

26. Chakravarthi, S., P., Thanikachalam, H. S., Nagaraja, D. L. W., Yang, N. I., Bukhari, "Assessment of Proliferative Index and Its Association with Ki-67 Antigen Molecule Expression in Nodular Hyperplasia of Prostate", *Indian Journal of Science & Technology*, Vol. 2, Issue 8., pp. 1-4, 2009.

27. American Cancer Society, "How is Prostate Cancer Staged?" http://www.cancer.org/cancer/prostatecancer/detailedguide/prostate-cancer-staging, [Accessed April 2015].

28. Wikipedia.com, "Prostate Cancer", http://en.wikipedia.org/wiki/Prostate_cancer, [Accessed April 2015].

29. Lu-Yao, G. L., P. C., Albertsen, D. F. Moore, W., Shih, Y., Lin, R. S., DiPaola, M. J. Barry, A., Zietman, M., O'Leary, E., Walker-Corkery, S. L., Yao, "Outcomes of Localized Prostate Cancer Following Conservative Management", *The Journal of the American Medical Association*, 1202-209, 2009.

30. Mohan, R., P. F., Schellhammer, "Treatment Options for Localized Prostate Cancer", *American Family Physician*, Vol. 84, No. 4, pp. 413–420, 2011.

31. Mouraviev, V., B., Evans, T. J., Polascik, "Salvage Prostate Cryoablation After Primary Interstitial Brachytherapy Failure: A Feasible Approach". *Prostate Cancer Prostatic Diseases*, Vol. 9, No. 1, pp. 99–101, 2006.

32. American Cancer Society, "Study: Active Surveillance OK for Some Men with Prostate Cancer", http://www.cancer.org/cancer/news/study-active-surveillance-ok-for-some-men-with- prostate-cancer, [Accessed April 2015].

33. Hong, H., Y., Zhang, J., Sun, W., Cai, "Positron Emission Tomography Imaging of Prostate Cancer", *Amino Acids*, Vol. 39, No. 1, pp. 11–27, 2009.

34. Fitzpatrick, J. M., "Management of Localized Prostate Cancer in Senior Adults: The Crucial Role of Comorbidity", *BJU International*, Vol. 101, Suppl. 2, pp. 16–22, 2008.

35. Thompson, J. C., J., Wood, D., Feuer, "Prostate Cancer: Palliative Care and Pain Relief", *British medical bulletin*, Vol. 83, pp. 341–354, 2007.

36. Hu, Q., R. W., Hartmann, "The Renaissance of CYP17 Inhibitors for the Treatment of Prostate Cancer", in *Cancer Drug Design and Discovery*, Nedel, S., Editor, 2nd Edition, pp. 319-356, 2014.

37. Krycer, J. R., A. J., Brown, "Cholesterol Accumulation in Prostate Cancer: A Classic Observation from a Modern Perspective", *Biochimica et Biophysica Acta*, Vol. 1835, pp. 219-229, 2013.

38. Wang, L. G., X. M., Liu, W., Kreis, D. R., Budman, "Phosphorylation Dephosphorylation of Androgen Receptor as a Determinant of Androgen Agonistic or Antagonistic Activity", *Biochemical and Biophysical Research Communications*, Vol. 259, pp. 21-28, 1999.

39. Masiello, D., S., Cheng, G. J., Bubley, M. L., Lu, S. P., Balk, "Bicalutamide Functions as an Androgen Receptor Antagonist by Assembly of a Transcriptionally Inactive Receptor", *The Journal of Biological Chemistry*, V. 277, pp. 26321-26326, 2002.

40. Migliaccio, A., G., Castoria, M. Di Domenico, A., de Falco, A., Bilancio, M., Lombardi, M. V., Barone, D., Ametrano, M. S., Zannini, C., Abbondanza, F., Auricchio, "Steroid-Induced Androgen Receptor-Oestradiol Receptor Beta-Src Complex Triggers Prostate Cancer Cell Proliferation", *The EMBO Journal*, Vol. 19, pp. 5406-5417, 2000.

41. Attard, G., A. H. M., Reid, T. A., Yap, F., Raynaud, M., Dowsett, S., Settatree, M., Barrett, C., Parker, V. Martins, E., Folkerd, J., Clark, C. S., Cooper, S. B., Kaye, D., Dearnaley, G., Lee, J. S., de Bono, "Phase I Clinical Trial of a Selective Inhibitor of CYP17, Abiraterone Acetate, Confirms That Castration-Resistant Prostate Cancer Commonly Remains Hormone Driven", *Journal of Clinical Oncology*, Vol. 26, pp. 4563–4571, 2008.

42. Titus, M. A., M. J., Schell, F. B., Lih, K. B., Tomer, J. L., Mohler, "Testosterone and Dihydrotestosterone Tissue Levels in Recurrent Prostate Cancer", *Clinical Cancer Research*, Vol. 11, pp. 4653–4657, 2005.

43. Stanbrough, M., G. J., Bubley, K., Ross, T. R., Golub, M. A., Rubin, T. M., Penning, P. G., Febbo, S. P., Balk, "Increased Expression of Genes Converting Adrenal Androgens to Testosterone in Androgen-Independent Prostate Cancer", *Cancer Research*, Vol. 66, pp. 2815–2825, 2006.

44. Suzuki, H., K., Akakura, A., Komiya, S., Aida, S., Akimoto, J., Shimazaki, "Codon 877 Mutation in the Androgen Receptor Gene in Advanced Prostate Cancer: Relation to Antiandrogen Withdrawal Syndrome", *Prostate*, Vol. 29, pp.153–158, 1996.

45. Hara, T., J., Miyazaki, H. Araki, M., Yamaoka, N., Kanzaki, M., Kusaka, M., Miyamoto, "Novel Mutations of Androgen Receptor: A Possible Mechanism of Bicalutamide Withdrawal Syndrome", *Cancer Research*, Vol. 63, pp. 149–153, 2003.

46. Zhao, X. Y., P. J., Malloy, A. V. Krishnan, S., Swami, N. M., Navone, D. M., Deehl, D., Feldman, "Glucocorticoids Can Promote Androgen- Independent Growth of Prostate Cancer Cells Through a Mutated Androgen Receptor", *Nature Medicine*, Vol. 6, pp. 703–706, 2000.

47. Scher, H. I., K., Fizazi, F. Saad, M., Taplin, C. N., Sternberg, K., Miller, R., de Wit, P., Mulders, K. N., Chi, N. D., Shore, A., J., Armstrong, T. W., Flaig, A., Flechon, P., Mainwaring, M., Fleming, J. D., Hainsworth, M., Hirmand, B., Selby, L., Seely, , J. S., de Bono, "Increased Survival with Enzalutamide in Prostate Cancer After Chemotherapy", *The New England Journal of Medicine*, Vol. 367, pp. 1187–1197, 2012.

48. Yin, L., Q., Hu, "CYP17 Inhibitors – Abiraterone, C17,20-lyase Inhibitors and Multi-Targeting Agents", *Nature Reviews Urology*, Vol. 11, pp. 32–42, 2014.

49. Potter, G. A., S. E., Barrie, M., Jarman, M. G., Rowlands, "Novel Steroidal Inhibitors of Human Cytochrome $P450_{17\alpha}$ (l7α-hydroxylase-$C_{l7,20}$-lyase): Potential Agents for the Treatment of Prostatic Cancer", *Journal of Medicinal Chemistry*, Vol. 38, pp. 2463-2471, 1995.

50. Salvador, J. A., R. M., Pinto, S. M., Silvestre, "Steroidal 5α-reductase and 17α-hydroxylase/17,20-lyase (CYP17) Inhibitors Useful in the Treatment of Prostatic Diseases", *The Journal of Steroid Biochemistry and Molecular Biology*, Vol. 137, pp. 199-222, 2013.

51. Tokai Pharmaceuticals, "About Galeterone", http://www.tokaipharma.com/programs.php, [Accessed April 2015]

52. Hu, Q., C., Jagusch, U. E., Hille, J., Haupenthal, R. W., Hartmann, "Replacement of Imidazolyl by Pyridyl in Biphenylmethylenes Results in Selective CYP17 and Dual CYP17 / CYP11B1 Inhibitors for the Treatment of Prostate Cancer", *Journal of Medicinal Chemistry*, Vol. 53, 5749-5758, 2010.

53. Krug, S. J., Q., Hu, R. W., Hartmann, "Hits Identified in Library Screening Demonstrate Selective CYP17A1 Lyase Inhibition", *Journal of Steroid Biochemistry & Molecular Biology*, Vol. 134, pp. 74-79, 2013.

54. Viamet Pharmaceuticals, "Viamet Pharmaceutıcals to Present at the 32nd Annual J.P. Morgan Healthcare Conference", http://www.viamet.com/sites/default/files/news-file-uploads/news-events_51_2756080874.pdf, [Accessed April 15]

55. ClinicalTrials.gov, "A Study to Evaluate Oral VT-464 in Patients with Castration-Resistant Prostate Cancer", https://clinicaltrials.gov/ct2/show/NCT02012920, [Accessed April 15].

56. Armutlu, P., M. E., Ozdemir, S., Ozdas, I. H., Kavakli, M., Turkay, " Discovery of Novel CYP17 Inhibitors for the Treatment of Prostate Cancer with Structure-Based Drug Design", *Letters in Drug Design & Discovery*, Vol. 6, pp. 337-344, 2009.

57. DeVore, N. M., E. E., Scott, "Structures of Cytochrome P450 17A1 with Prostate Cancer Drugs Abiraterone and TOK-001", *Nature*, Vol. 482, pp. 116-120, 2012.

58. Petrunak, E. M., N. M., DeVore, P. R., Porubsky, E. E., Scott, "Structures of Human Steroidogenic Cytochrome P450 17A1 with Substrates", *The Journal of Biological Chemistry*, Vol. 289, No. 47, pp. 32952-32964, 2014.

59. Erkoc, S., *Synthesis of Novel Potent Drug Molecules Active Against Prostate Cancer and Investigation of Bioactive Properties of Cyclopolymers Obtained by RAFT Polymerization*, Ph.D. Thesis, Bogazici University, 2011.

60. Ozdemir, M. E., *Structure-Based Drug Design for Prostate Cancer*, M.S. Thesis, Koc University, 2008.

61. Grigoryev, D. N., B. J., Long, I. P. Nnane, V. C. O., Njar, Y., Liu, A. M. H., Brodie, "Effects of New 17 Alpha-hydroxylase/C-17,C-20-lyase Inhibitors on LNCaP Prostate Cancer Cell Growth *in Vitro* and *in Vivo*", *British Journal of Cancer*, Vol. 81, pp. 622-630, 1999.

62. Lima, L. M., E. J., Barreiro, "Bioisosterism: a Useful Strategy for Molecular Modification and Drug Design", *Current Medicinal Chemistry*, Vol. 12, pp. 23-49, 2005.

63. Meanwell, N. A., Synopsis of Some Recent Tactical Application of Bioisosteres in Drug Design", *Journal of Medicinal Chemistry*, Vol. 54, pp. 2529-2591, 2011.

64. Gaikwad, P. L., P. S., Gandhi, D. M., Jagdale, V. J., Kadam, "The Use of Bioisosterism in Drug Design and Molecular Modification", *American Journal of Pharmatech Research*, Vol. 2, No. 4, pp. 1-23, 2012.

65. Burger, A., "Isosterism and Bioisosterism in Drug Design", *Progress in Drug Research*, Vol. 37, pp. 287-371, 1991.

66. Langmuir, I., "Isomorphism, Isosterism and Covalence", *Journal of the American Chemical Society*, Vol. 41, pp. 1543-1559, 1919.

67. Grimm, H. G., "On the Systematic Arrangement of Chemical Compounds from the Perspective of Research on Atomic Composition; and on Some Challenges in Experimental Chemistry", *Naturwissenschaften*, Vol. 17, pp. 557-564, 1928.

68. Friedman, H. L., *Influence of Isosteric Replacements upon Biological Activity*, NAS-NRS Publication No. 206; NAS-NRS: Washington, DC, Vol. 206, pp. 295-358, 1951.

69. Fox, R.I., "Mechanism of Action of Hydroxychloroquine as an Antirheumatic Drug", *Seminars in Arthritis Rheumatism*, Vol. 23, pp. 82-91, 1993.

70. Tilley, L., P., Loria, M., Foley, *Antimalarial Chemotherapy*, Rosenthal, P. J., Ed.; Humana Press: Totowa, New Jersey, Vol. 47, pp. 87-121, 2001.

71. Savarino, A., L., Gennero, H. C., Chen, D., Serrano, F., Malavasi, J. R., Boelaert, K., Sperber, "Anti-HIV Effects of Chloroquine: Mechanisms of Inhibition and Spectrum of Activity", *AIDS*, Vol. 15, pp. 2221-2229, 2001.

72. Finley, K. T., *Kirk-Othmer Encyclopedia of Chemical Technology*, 5th ed., Seidel A., Ed., Wiley: New Jersey, Vol. 21, pp. 182–214, 2001.

73. Economopoulos, S. P., C. L., Chochos, V. G., Gregoriou, J. K., Kallitsis, S., Barrau, G., Hadziioannou, "Novel Brush-Type Copolymers Bearing Thiophene Backbone and Side Chain Quinoline Blocks. Synthesis and Their Use as a Compatibilizer in Thiophene-Quinoline Polymer Blends", *Macromolecules*, Vol. 40, pp. 921-927, 2007.

74. Ma, Z., J., Ding, Y., Cheng, Z., Xie, L., Wang, X., Jing, F., Wang, "Synthesis and Characterization of Red Light-Emitting Electrophosphorescent Polymers with Different Triplet Energy Main Chain", *Polymer*, Vol. 52, No. 10, pp. 2189-2197, 2011.

75. Xue, G., J. S., Bradshaw, N. K., Dalley, P. B., Savage, K. E., Krakowiak, R. M., Izatt, L., Prodi, M. Montalti, N., Zaccheroni, "Convenient Synthesis and Preliminary Photophysical Properties of Novel 8-aminoquinoline Appended Diaza-18-crown-6 Ligands", *Tetrahedron*, Vol. 57, pp. 7623-7628. 2001.

76. Foley, M., N., Tilley, "Quinoline Antimalarials: Mechanisms of Action and Resistance and Prospects for New Agents", *Pharmacology & Therapeutics*, Vol. 79, No. 1, pp. 55-87, 1998.

77. Gryzło, B., K. Kulig, "Quinoline – A Promising Fragment in the Search for New Antimalarials", *Mini-Reviews in Medicinal Chemistry*, Vol. 14, No. 4, pp. 332-344, 2014.

78. Solomon, V. R., H., Lee, "Quinoline as a Privileged Scaffold in Cancer Drug Discovery", *Current Medicinal Chemistry*, Vol. 18, pp. 1488-1508, 2011.

79. Koseoglu, A., T., Gul, A. E., Acar, "A Systematic Study on the Synthesis of *n*-Butyl Substituted 8-Aminoquinolines", *Journal of Heterocyclic Chemistry*, doi: 10.1002/jhet.2399, 2015.

80. Gul, T., *Synthesis of Potentially Active Quinoline Derivatives Against Prostate Cancer*, M.Sc. Thesis, Bogazici University, 2011.

81. McConathy, J., M. J., Owens, "Stereochemistry in Drug Action", *The Primary Care Companion to the Journal of Clinical Psychiatry*, Vol. 5, pp. 70-73, 2003.

82. Agranat, I., H., Caner, J., Caldwell, "Putting Chirality to Work: The Strategy of Chiral Switches", *Nature Review Drug Discovery*, Vol. 1, No. 10, pp. 753-768, 2002.

83. Li, X. Q., L., Weidolf, R., Simonsson, T. B., Andersson, "Enantiomer/Enantiomer Interactions Between the S- and R- Isomers of Omeprazole in Human Cytochrome P450 Enzymes: Major Role of CYP2C19 and CYP3A4", *Journal of Pharmacology and Experimental Therapeutics*, Vol. 315, No. 2, pp. 777-787, 2005.

84. Lages, A. S., K. C. M., Silva, A. L. P., Miranda, C. A., Fraga, E. J., Barriero, "Synthesis and Pharmacological Evaluation of New Flosulide Analogues, Synthesized from Natural Safrole", *Bioorganic & Medicinal Chemistry Letters*, Vol. 8, pp. 183-188, 1998.

85. Summers, J. B., B. P., Gunn, H., Mazdiyasni, "In Vivo Characterization of Hydroxamic Acid Inhibitors of 5-lipoxygenase", *Journal of Medicinal Chemistry*, Vol. 30, No. 11, pp. 2121-2126, 1987.

86. Sumers, J. B., B. P., Gunn, J. G., Martin, "Structure-Activity Analysis of a Class of Orally Active Hydroxamic Acid Inhibitors of Leukotriene Biosynthesis", *Journal of Medicinal Chemistry*, Vol. 31, No. 10, pp. 1960-1964, 1988.

87. Racine, E., F., Monnier, J. P., Vors, M., Taillefer, "A Simple Copper-Catalyzed Synthesis of Tertiary Acyclic Amides", *Organic Letters*, Vol. 13, No. 11, pp. 2818-2821, 2011.

88. Dalton, J. T., C., Barret, D. D., Miller, S., Hong, Y., He, M. L., Mohler, R., Narayanan, Z., Wu, *Nuclear Receptor Binding Agents*, U.S. Patent 20120157539, 2012.

89. Nandurkar, N. S., M. J., Bhanushali, M. D., Bhor, B. M., Bhanage, "N-Arylation of Aliphatic, Aromatic and Heteroaromatic Amines Catalyzed by Copper Bis(2,2,6,6-tetramethyl-3,5-heptanedionate)", *Tetrahedron Letters*, Vol. 48, Issue 37, pp. 6573-6576, 2007.

90. Hamann, L. G., N. S., Mani, R. L., Davis, X., Wang, "Discovery of a Potent, Orally Active, Nonsteroidal Androgen Receptor Agonist: 4-Ethyl-1,2,3,4 tetrahydro-6-(trifluoromethyl)-8-pyridono[5,6-*g*]-quinoline (LG121071)", *Journal of Medicinal Chemistry*, Vol. 42, pp. 210-212, 1999.

91. Doherty, S., E. G., Robins, I., Pál, C. R., Newman, C., Hardacre, D., Rooney, D. A., Mooney, "Polymer-Supported Phosphoramidites: Highly Efficient and Recyclable

Catalysts for Asymmetric Hydrogenation of Dimethylitaconate and Dehydroamino Acids and Esters", *Tetrahedron: Asymmetry*, Vol. 14, pp. 1517-1527, 2003.

92. Ghosh, B., T., Antonio, J., Zhen, P., Kharkar, M. R. A., Reith, A. K., Dutta, "Development of (S)-N6-(2-(4-(Isoquinolin-1-yl)piperazin-1-yl)ethyl)-N6-propyl-4,5,6,7-tetrahydrobenzo[d]-thiazole-2,6-diamine and Its Analogue as a D3 Receptor Preferring Agonist: Potent in Vivo Activity in Parkinson's Disease Animal Models", *Journal of Medicinal Chemistry*, Vol. 53, pp. 1023-1037, 2010.

93. Ragoussis, V., A., Giannikopoulos, E., Skoka, P., Grivas, "Efficient Synthesis of (±)-4-methyloctanoic Acid, Aggregation Pheromone of Rhinoceros Beetles of the Genus Oryctes (Coleoptera: Dynastidae, Scarabaeidae)", *Journal of Agricultural and Food Chemistry*, Vol. 55, pp. 5050-5052, 2007.

94. Pomeranc, D., V., Heitz, J. C., Chambron, J. P., Sauvage, "Octahedral Fe(II) and Ru(II) Complexes Based on a New Bis 1,10-phenanthroline Ligand That Imposes a Well-Defined Axis", *Journal of the American Chemical Society*, Vol. 123, pp. 12215-12221, 2001.

95. Furniss, B. S., A. J., Hannaford, P. W. G., Smith, A. R., Tatchell, *Vogel's Textbook of Practical Organic Chemistry*, 5th Ed.; Longman: Harlow, 1989.

96. Bose, A. K., M. S., Manhas, S., Pednekar, S. N., Ganguly, H., He, W., Dang, A., Mandadi, "Large Scale Biginelli Reaction via Water-Based Biphasic Media: A Green Chemistry Strategy", *Tetrahedron Letters*, Vol. 46, pp. 1901-1903, 2005.

97. Buszek, K. R., N., Brown, D., Luo, "Concise Total Synthesis of (±)-cis-Trikentrin A and (±)-Herbindole A via Intermolecular Indole Aryne Cycloaddition", *Organic Letters*, Vol. 11, No. 1, pp. 201-204, 2009.

98. Malkov, A. V., M., Figlus, S., Stoncius, P., Kocovsky, "Organocatalysis with a Fluorous Tag: Asymmetric Reduction of Imines with Trichlorosilane Catalyzed by

Amino Acid-Derived Formamides", *Journal Organic Chemistry*, Vol. 72, pp. 1315-1325, 2007.

99. Offner, J. D., G., Schnakenburg, F., Rose-Munch, E., Rose, K. H., Dötz, "Dibenzo[f,h]quinoline $Cr(CO)_3$ Complexes: Synthesis by Chromium-Templated Benzannulation, Cyclomanganation and Haptotropic Chromium Migration", *Organometallics*, Vol. 29, pp. 3308-3317, 2010.

100. Kang, D. H., T. Y. Joo, E. H. Lee, S. Chaysripongkul, W. Chavasiri, D. O. Jang, "A Mild and Efficient Reaction for Conversion of Carboxylic Acids into Acid Bromides with Ethyl Tribromoacetate / Triphenylphosphine Under Acid-Free Conditions", *Tetrahedron Letters*, Vol. 47, pp. 5693, 2006.

101. Chan, J. C., G. A., Freeman, J. H. Tidwell, K. R., Romines, L. T., Schaller, J. R. Cowan, S. S., Gonzales, G. S., Lowell, C. W. 3rd., Andrews, D. J., Reynolds, M., St Clair, R. J., Hazen, R. G., Ferris, K. L., Creech, G. B., Roberts, S. A., Short, K., Weaver, G. W., Koszalka, L. R., Boone, "Novel Benzophenones as Non-Nucleoside Reverse Transcriptase Inhibitors of HIV-1", *Journal of Medicinal Chemistry*, Vol. 47, No.5, pp. 1175-1182, 2004.

102. Chang, Y., M., Hsu, S. Wang, L., Huang, K., Qian, S. L., Morris-Natschke, E., Hamel, S., Kuo, K., Lee, "Design and Synthesis of 2-(3-benzo[b]thienyl)-6,7-methylenedioxyquinolin-4-one Analogues as Potent Antitumor Agents That Inhibit Tubulin Assembly", *Journal of Medicinal Chemistry*, Vol. 52, pp. 4883-4891, 2009.

103. Leslie, C. P., M., Biagetti, S., Bison, S. M., Bromidge, R., Di Fabio, D., Donati, A., Falchi, M. J., Garnier, A., Jaxa-Chamiec, G., Manchee, G., Merlo, D. A., Pizzi, L. P., Stasi, J., Tibasco, A., Vong, S. E., Ward, L., Zonzini, "Discovery of 1-(3-{2-[4-(2-methyl-5-quinolinyl)-1-piperazinyl]ethyl}phenyl)-2-imidazolidinone (GSK163090), a Potent, Selective, and Orally Active 5-HT1A/B/D Receptor Antagonist", *Journal of Medicinal Chemistry*, Vol. 53, pp. 8228-8240, 2010.

104. Karthikeyan, P., A. M., Rani, R., Saiganesh, K. K., Balasubramanian, S., Kabilan, "Synthesis of 5,6-dihydrobenz[c]acridines: A Comparative Study", *Tetrahedron*, Vol. 65, pp. 811-821, 2009.

105. Hwang, J., M. G., Choi, S., Eor, S., Chang, "Fluorescence Signaling of Zr^{4+} by Hydrogen Peroxide Assisted Selective Desulfurization of Thioamide", *Inorganic Chemistry*, Vol. 51, No. 1634-1639, 2012.